UNIVERSIDADE
DE VIGO

Ciclo de la materia orgánica disuelta en un sistema de afloramiento costero

Dissolved Organic Matter Cycling in a Coastal Upwelling System

TESIS DOCTORAL

presentada en el
Departamento de Química Orgánica
Universidad de Vigo

Memoria presentada por María del Mar Nieto Cid para optar al título de Doctor en Química por la Universidad de Vigo

El Dr. **Xosé Antón Álvarez Salgado**, *Científico Titular*, y el Dr. **Félix Fernández Pérez**, *Profesor de Investigación*, del Consejo Superior de Investigaciones Científicas (CSIC),

HACEN CONSTAR: Que la presente memoria, titulada **"Ciclo de la materia orgánica disuelta en un sistema de afloramiento costero / *Dissolved Organic Matter Cycling in a Coastal Upwelling System*"**, presentada por la licenciada María del Mar Nieto Cid para optar al grado de Doctor en Química, ha sido realizada bajo nuestra dirección, cumpliendo las condiciones exigidas para su presentación, la cual autorizamos.

Y para que así conste y surta los efectos oportunos, firmamos la presente en Vigo, a 23 de junio de 2005.

Fdo.: X. A. Álvarez Salgado Fdo.: F. Fernández Pérez

UNIVERSIDADE
DE VIGO

D. **Antonio Ibáñez Paniello**, *Profesor Titular* del Departamento de Química Orgánica de la Universidad de Vigo, y Tutor de la presente memoria de Tesis Doctoral titulada: **"Ciclo de la materia orgánica disuelta en un sistema de afloramiento costero / *Dissolved Organic Matter Cycling in a Coastal Upwelling System*"**, de la que es autora María del Mar Nieto Cid y que ha sido dirigida por el Dr. Xosé Antón Álvarez Salgado, Científico Titular, y el Dr. Félix Fernández Pérez, Profesor de Investigación, del Consejo Superior de Investigaciones Científicas (CSIC),

AUTORIZA su presentación en la Universidad de Vigo para su lectura y defensa.

Y para que así conste y surta los efectos oportunos, firmo la presente en Vigo, a 23 de junio de 2005.

Fdo.: A. Ibáñez Paniello

Esta tesis fue realizada durante el disfrute de una beca de Formación de Personal Investigador del Ministerio de Educación y Ciencia y una beca de postgrado del programa I3P del Consejo Superior de Investigaciones Científicas.

Los trabajos que se recogen en esta memoria fueron financiados por los proyectos del Programa Nacional de Ciencias y Tecnologías Marinas: **DYBAGA** (CICYT-MAR99-1039-C02-01) y **REMODA** (CICYT-REN-2000-0800-C02-01)

Además, en el transcurso de la elaboración de esta tesis Doctoral, se realizó una estancia de dos meses en el Laboratoire de Microbiologie Marine (C.O.M.) en Marsella (Francia) financiada por el Ministerio de Educación y Ciencia.

A mi familia,
especialmente a mis padres,
a mis hermanos y a Kais

Agradecimientos -Remerciements - Acknowledgements

Pepe, yo no entiendo mucho de dirigir tesis (aún no he dirigido ninguna…), pero por lo que sé, por estar del otro lado, creo que te mereces la máxima puntuación. Muchas gracias, principalmente y entre muchas otras cosas, por hacerme vivir y entender la Oceanografía Química

Félix, gracias por darme la oportunidad de participar de todo este 'mundillo' de la Oceanografía

Fernando Fraga, sin duda de los pioneros en esto de la Oceanografía en España, siempre ha sido y siempre será un placer escuchar sus acertados comentarios y explicaciones

Antonio Paniello y Bea Iglesias, ha sido muy grato y tranquilizador poder contar con vuestro apoyo en la universidad

Marylo, gracias por ayudarme en mis primeros pasos por este nuevo 'mundo'. Trini, has sido una ayuda fundamental en los análisis de esta tesis, junto con Marta Penabad, Vane, y Rita, graciñas. Suso y Samanta, siempre un apoyo en los muestreos y fuera de ellos, un millón.

Paco, Aída, Carmen y Des, mis 'otros jefes'…, siempre prestos a echar una mano y a resolver dudas y problemas

Mis compañeros de fatigas, filtraciones y demás 'menesteres' en el laboratorio han sido siempre 'lo más del gallinero', a lo mejor me dejo algún nombre en el tintero (sorry!) pero todos os merecéis un huequecito en esta tesis y mi agradecimiento… Marylo, Luisa, Suso, Marta Álvarez, Vero, Vicki, Belén, Pili, Miguel Gilcoto, Paula, Sandra, Elisa, Iván, Trini, Samanta, Alcira, Kike, Roberta, Bibiana, Toni, Fernando, Isabel, Marta Penabad, Óscar 'Pere', Seila, Miguel (Ávila), Mónica, Vane, Rosa, Chús, Rita, Nicolás, Teri, Miguel Martís, Óscar, Marcos

…y también los que habéis pasado más fugazmente, Julien, Jonka, Pierre, Nacho, Merche, Enma, Itziar, Sara, María, Pablo, Sébastien, Mélanie…

Los chicos y chicas de nuestra unidad asociada (GOFUVI) son un encanto y siempre están (o estuvieron) ahí para echar una mano: Juan, Silvita (el electrón deslocalizado…), Ramiro, Gaby, Ángel, Pablito, Rocío, Belén, Silvia Torres, Carlos…

Merci a tous les bons gens de Luminy. Richard, merci pour me donner la opportunité de apprendre le HPLC à Marseille; Marc et Christos, très bon travaille avec vous!; et Raymond, gracias por ser tan MAJO (finalement, petit à petit l'oiseau fait son nid)

Durante un año, DYBAGA podría haber sido un infierno… pero los compis del 'Mytilus' lograron todo lo contrario, sois una 'tripu' genial: Jorge, Ricardo, Pirri, Apo y Waldo

Merci a tout le monde sur 'La Thalassa' et 'L'Atalante'. Il y a des très bons gents sur les bateaux françaises

Even in the Antarctic seas, in the Russian ship 'Akademic Sergey Vavilov', I was lucky to find nice and interesting people

En estos últimos meses, los proyectos ZOTRACOS e IMPRESIÓN me han brindado la oportunidad de colaborar con muy buenos profesionales y compañeros, gracias por los buenos ratos tanto en el 'Cornide Saavedra' como en los mesocosmos

El 'resto de los habitantes' del Instituto de Investigaciones Marinas, sois todos un valiosísimo apoyo, tanto operacional (de todos los departamentos… gracias por los préstamos de material), como logístico (los servicios de biblioteca, de informática, de mantenimiento, de almacén y de limpieza) y administrativo ('las chicas' de dirección, gerencia y administración). Y como no… nuestros vigilantes favoritos (no los de la playa…), siempre atentos a todo, y siempre con una sonrisa

Y… ¡no!, aún no se ha acabado… ya que, aunque no han hecho ningún análisis, ni muestreado en ningún barco, ni escrito ninguna letra de esta tesis (bueno… alguno sí ;P), sin el apoyo de los míos yo no llegaría hasta aquí, así que mi más sincero y cariñoso agradecimiento a…

A mami y a papi, por estar siempre, siempre ahí. A mis hermanos Óscar, Abel y Luis, bueno, si en el fondo… ¡nos encanta hacernos rabiar! A la abuela Pura y al abuelo Jesús, un besiño. Y tampoco me olvido de los pequeños habitantes de la casa, la alegría y el alboroto

A Kais, que nombre más bonito y original, a juego contigo. Gracias por muchísimas cosas… pero sobre todo por los ánimos y las ayuditas en esta recta final, gracias por creer en mí. ¡Eres genial! (K)

A toda mi familia, que como ya dije una vez, es muy numerosa y está muy dispersa en el espacio, pero… muy, muy juntita en el corazón. En especial a Cris y a Carmen, por tener más fe en mí que yo misma

A las recuas de amiguitos… a los de siempre (Gus, Vishal, Pablito y familias, un bikiño), a los de la carrera (Fer, Ruth, Santi, Emilio, Marcos, Juan…), a los del CUVI (Rupi, Rachel, Dieguito, Ferrín, Gato, Montse…), a la nueva pandilla (Richard, Víctor, Laura, Sonia, Geli, Tachi, Marta, Javi, Laura y Rafa) y a Paula, Fes, Ana, Eva, Amaya (aunque separadas espacialmente, juntas en los momentos importantes)

Abuelo Julio, abuela Basilisa, tío David. Una tesis es un largo camino, y hay trocitos de vida que se fueron quedando en ese camino…

Desde este rincón un agradecimiento especial también para los PRECARIOS, si poco a poco se van consiguiendo avances en la situación de los investigadores 'en formación' es gracias a vosotros. Todos empezamos con mucha ilusión, ojalá el incierto camino a recorrer no la apague

Y, por último… gracias a ti por leer este manuscrito (aunque solo sea por cotillear un poco…), porque creo que el fin último de una tesis, además de formar un nuevo doctor, es aportar un granito de arena a la playa del conocimiento

A veces sentimos que lo que hacemos es tan solo una gota en el mar, pero el mar sería menos si le faltara una gota

Sometimes we feel that what we do represents only one drop in the sea, but the sea would be less without the drop

Madre Teresa de Calcuta

TABLE OF CONTENTS

Chapter 1:

Introduction

INTRODUCTION

Since this Thesis is going to be presented in a Faculty of Chemistry, it would be convenient to start answering a simple question: What can do a Chemist in Oceanography? The study of the physical, biological and geochemical processes occurring in the oceans, and their interactions with the continents and the atmosphere, requires a multidisciplinary approach. Therefore, Oceanography is based on the need for the combination of all basic science to understand the marine environment. In this context, Chemical Oceanography consists on solving oceanographic problems by means of the concepts and methods of Chemistry. It should be noted that Chemical Oceanography (which consider the marine environment as a chemical reactor) is quite different from Marine Chemistry (which just uses suitable analytical techniques in the marine environment). It is remarkable the lack of Chemists devoted to Oceanography in Spain in particular, but in Europe in general.

The study of aquatic ecosystems is gaining more and more attention due to its implications for global climate change. The ocean can regulate climate controlling the exchange of water, heat and greenhouse gases with the atmosphere (Fig. 1.1). Therefore, the way these gases distribute between the atmosphere and the ocean is a remarkable scientific issue. In this sense, chemical oceanographers analyse the sequestration of anthropogenic CO_2 in the oceans by means of the solubility and the biological pumps. The solubility pump involves only physical processes. On the other hand, the biological pump promotes the flux of biogenic carbon towards deep waters. The role of dissolved (DOM) and particulate organic matter (POM) in the recycling and export of biogenic carbon is crucial to understand these processes. So, chemical oceanographers **1)** develop the adequate analytical methods to estimate the dissolved organic carbon, nitrogen and phosphorus pools, **2)** characterise the DOM (molecular weight, isotopic abundance, chemical

composition, optical properties) and **3)** study the biological, chemical and photochemical reactivity of organic matter.

Dissolved organic matter cycling in open ocean waters

Conceptually, DOM is the organic material that is not susceptible to sink. From an operative point of view, DOM is the organic matter that passes a 0.2-1.0 μm filter, and can include small bacteria and all viruses. This dissolved material constitutes the largest reservoir of organic matter in the oceans. The most recent estimations indicate that the DOM pool is 685-700 Gt-C (Schimel et al. 1996, Hansell & Carlson 1998a), equalling the CO_2 accumulated in the atmosphere (Falkowski et al. 2000). In comparison, the sum of detritus (20 Gt-C), phytoplankton (4 Gt-C) and zooplankton (0.1 Gt-C) only represents 3% of the total organic matter. Most of this dissolved material (~90%) has been formed *in situ* as a result of phytoplankton primary production (~50 Gt-C per year) and transformed into DOM throughout different biological (exudation, grazing, autolysis or virolysis) and photochemical processes (Fig. 1.1). The main function of DOM, from the point of view of the solubility and biological pumps, is the recycling and export of biogenic material. In addition, DOM takes part in other relevant processes (Sunda 1995):

1) DOM complexes trace metals operating like a buffer that controls the bioavailability of free metal ions, avoiding high concentrations and ensuring metal availability in the long-term.

2) DOM acts as electron-donor in Fe and Mn photo-reduction and solubilization processes, enhancing their availability and preventing their exportation to the deep ocean.

3) Some phytoplankton groups produce dimethysulphoniopropionate (DMSP) that is transformed in dimethyl sulphide (DMS). This organic compound is susceptible to exchange with the atmosphere, where it is oxidized to sulphuric acid, contributing to the regulation of the Earth climate.

4) Humic acids constitute a significant fraction of the organic matter in continental waters. Their anionic nature promotes their capability to regulate the pH between 3 and 5.

5) Humic substances are also coloured compounds that absorb visible radiation. Large concentrations of these compounds reduce the quantity and quality of light radiation available for phytoplankton, decreasing the total production.

6) Phytoplankton exudates organic compounds with surfactant properties, which diminish the gas exchange with the atmosphere.

7) The photolysis of some DOM compounds produces trace gases that exchange with the atmosphere.

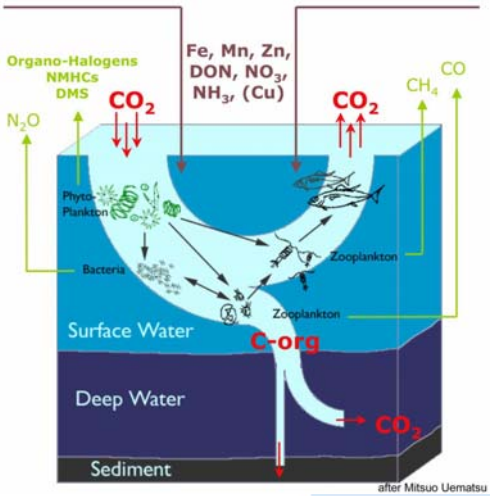

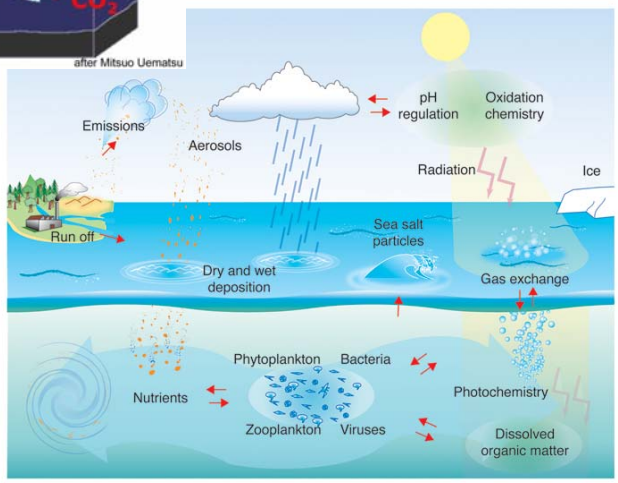

Figure 1.1 Below, scheme of the main processes that occur in the ocean and in the atmosphere-ocean interaction. Left, scheme of the biological pump: inorganic carbon (CO_2) exchanged between the ocean and the atmosphere is transformed into organic carbon (C-org), sequestered in the deep-ocean or, to a lesser extent, preserved in the sediments.
From http://www.uea.ac.uk/env/solas

The study of DOM was accentuated in the 1980s because of the development of suitable analytical techniques, as the high temperature catalytic oxidation (HTCO) method, which produced 5-10 times higher DOM concentrations than the classical wet oxidation methods (Suzuki et al. 1985, Sugimura & Suzuki 1988). Although these authors retracted from their results (Suzuki 1993), they contributed to focus the interest of marine scientists on DOM, developing new and better methods of analysis and promoting intercalibration exercises (Sharp et al. 2002, 2004). In parallel with the progress in the study of DOM, other concepts, such as the new (NP) and regenerated production (RP), were revisited. The NP of a given system is the production supported by external (either temporally or spatially) nutrients, whereas RP is maintained by nutrients recycled within the boundaries of the ecosystem. Both, inorganic and organic nutrients support NP and RP.

DOM comprises a myriad of compounds with recycling times ranging from hours to thousands of years, which are usually grouped in three different categories as a function of its lability:

1) labile DOM (l-DOM), with turnover times of minutes to days (Keil & Kirchman 1999). This pool supports the short-time-scale variability of DOM (Kirchman 2000) and it is recycled within the boundaries of the study ecosystem, *i.e.* it contributes to the RP of surface waters (Fig. 1.2).

2) semi-labile DOM (s-DOM), with turnover times of months to years, resists rapid microbial degradation (Cherrier et al. 1996). This material supports the seasonal variability of DOM and it is exported out of the boundaries of the study ecosystem, *i.e.* it contributes to the NP (Carlson 2002). An example is shown in Figure 1.3.

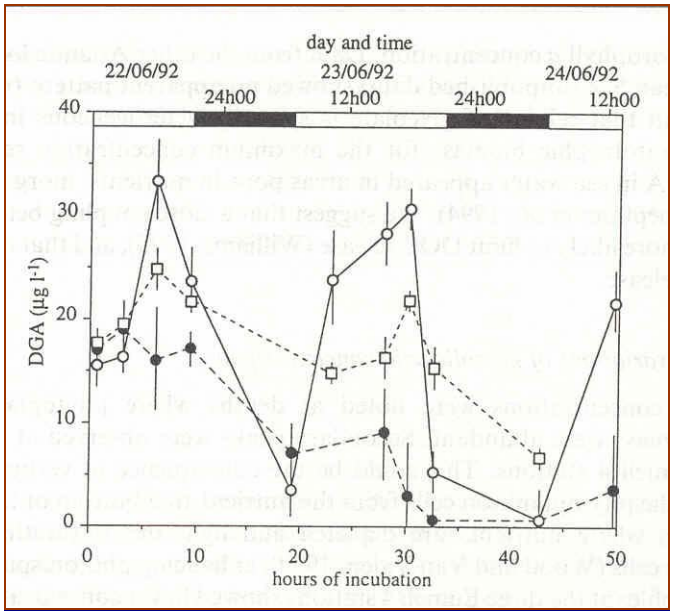

Figure 1.2 Short-time-scale variability of DOM by Leboulanger et al. (1997). They observed how the daily changes in the concentration of dissolved glycolic acid represents from 50% of the total primary production (1 g C m^{-2} d^{-1}) in eutrophic waters to 100% of the total primary production (0.5 g C m^{-2} d^{-1}) in oligotrophic waters of the North Atlantic, although this compound only represented <2% of the DOC pool

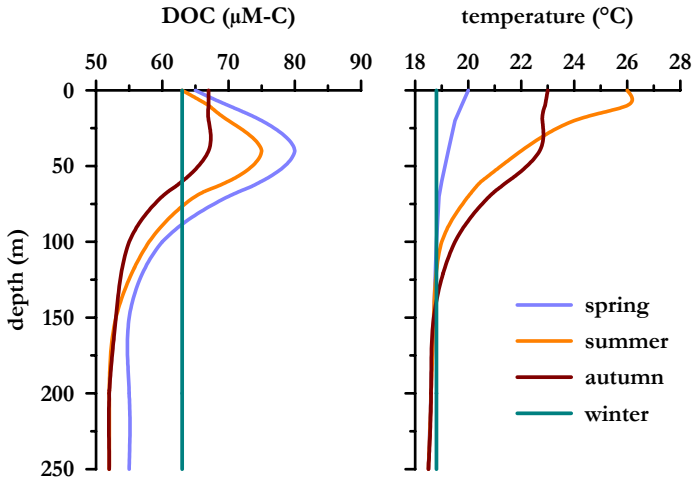

Figure 1.3 Carlson et al. (1994) showed an annual cycle of DOC at the BATS (Bermuda Atlantic Time Series) station where DOC accumulates after the spring bloom, it is partially consumed during summer and autumn and, finally, the remanent DOC accumulated in the surface layer (s-DOM) dilutes homogenously in the winter mixed layer to be consumed in deeper waters

3) refractory DOM (r-DOM), with turnover times of centuries to millennia (Williams & Druffel 1987), supports the long-term variability involved in the large-scale ocean circulation and contributes to the immobilisation of phytogenic materials, partially produced from anthropogenic CO_2. However, Hansell & Carlson (1998b; Fig. 1.4) demonstrated that refractory does not mean eternal: DOM in deep ocean waters decreases by 30% from the recently formed North Atlantic deep waters (48 μM C) to the 2 ky older North Pacific deep waters (34 μM C).

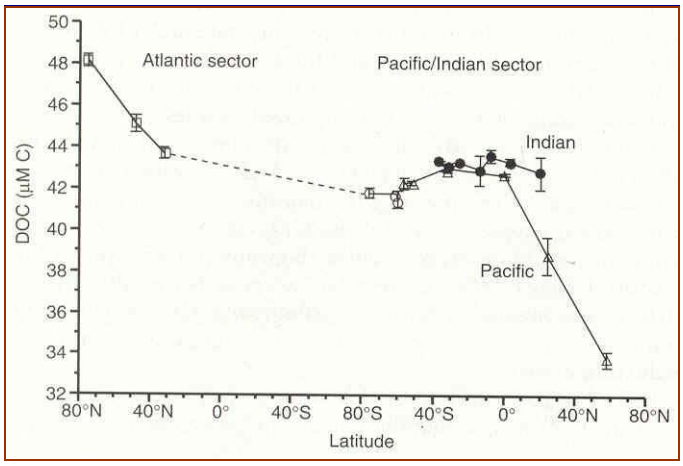

Figure 1.4 Hansell & Carlson (1998b) showed a DOM decrease in deep ocean waters from the North Atlantic to the North Pacific

The development of better analytical methods promoted the change in the conceptual model of the classical biological pump (Eppley & Peterson 1979) to introduce DOM. Traditionally, the biological pump (Fig. 1.5) was based only on the POM produced by phytoplankton from CO_2, which falls downwards (Knauer 1993). Fifty percent of this organic material was respired in the upper water column (100-300 m) and the corresponding CO_2 returned to the atmosphere in short time scales (10^0-10^1 years; Martin et al. 1987). The rest reached the bottom layers (>500 m) where it was transformed into CO_2, and sequestered for 10^2-10^3 years in the deep-ocean circulation (Wong & Hirai

1997). Only a minimal percentage of the primary production (~0.1%) is preserved in the sediments (Wollast 1998).

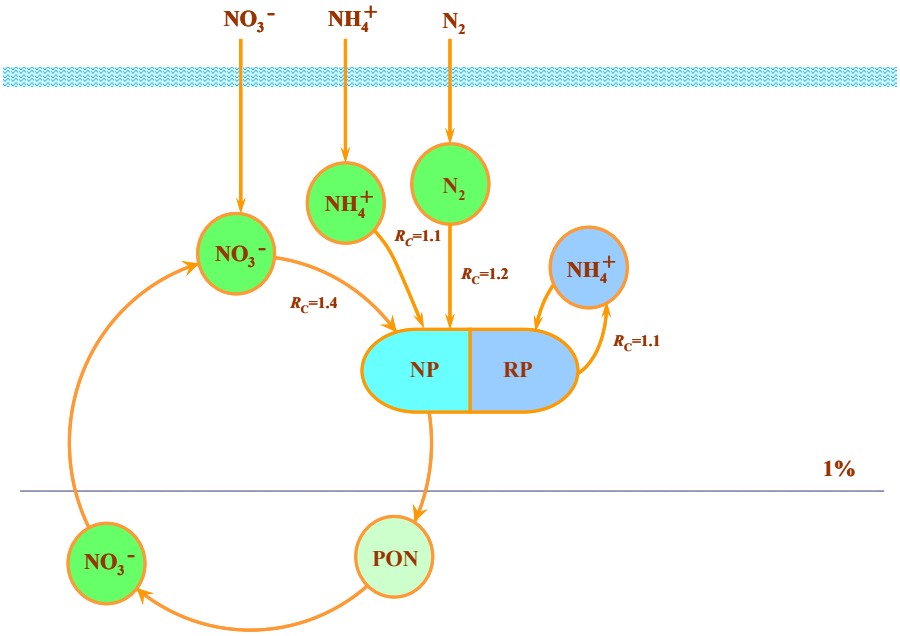

Figure 1.5 Classical scheme of the biological pump of nitrogen that was fuelled only by particulate organic matter (PON)

The l-DOM is the most reactive fraction and constitutes a primary nutrient and energy source to bacteria (Rich et al. 1997, Skoog et al. 1999). Thus, the extracellular release of l-DOM has to be considered as an intermediate step during nutrient recycling (Fig. 1.6). In this sense, phytoplankton cells are able to assimilate other regeneration products than NH_4^+, as urea, some amino acids and nitrogen bases (adenine and guanine). These products are present in seawater, for example, urea concentrations in surface open ocean waters are of the same order as NH_4^+ (Bronk 2002). Usually the contribution of l-DOM to the total pool is low; nevertheless, the l-DOM fluxes could be high. In average, 20-40% of the total production (TP = NP + RP) is recycled through DOM (Azam et al. 1983, Cole et al. 1988, Carlson 2002).

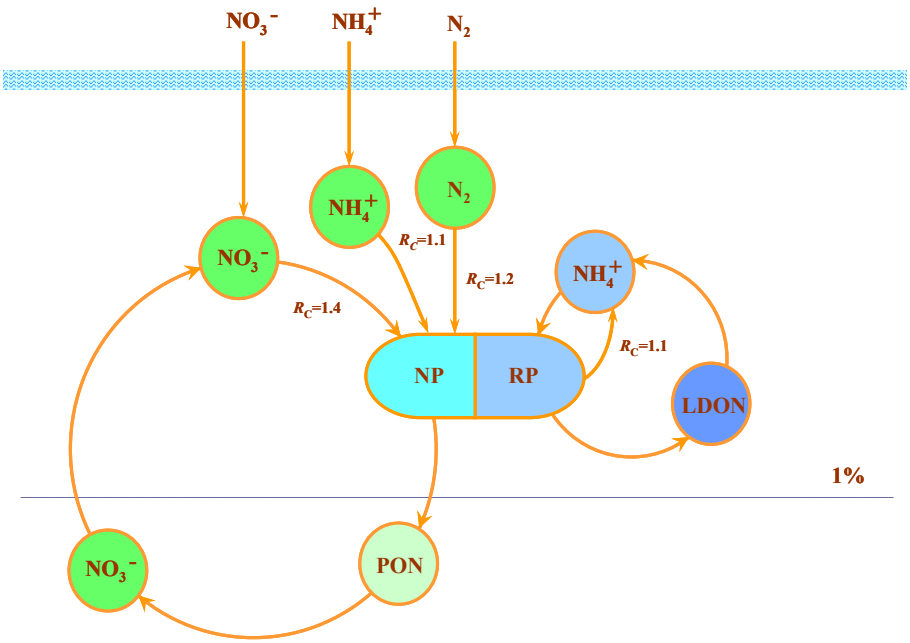

Figure 1.6 Scheme of the biological pump of nitrogen fuelled by particulate organic matter (PON) and labile DOM (LDON)

The s-DOM is accumulated or exported, especially after the end of a phytoplankton bloom. The downward transport of this phytogenic organic matter in the dissolved form becomes larger than the sedimentation in some areas, such as the Sargasso Sea and the NW Mediterranean, where winter mixing succeeds summer stratification (Copin-Montégut & Avril 1993, Hansell & Carlson 2001). Most of the organic matter export to deep waters in temperate ecosystems occurs at two well-defined periods: **1)** after the spring bloom, with the massive sedimentation of phytogenic materials; and **2)** during deep winter convection, when the DOM accumulated in the summer mixed layer is transported downwards. In addition, it is necessary to consider the partial solubilization of sinking organic matter, to be transformed into DOM. Therefore, the downward flux of DOM and the DOM which results from the solubilization of sinking particles have to be added to the organic material collected on sediment traps to calculate export rates properly, which have to be

equalled to the entry of new nutrients under the assumption of steady-state conditions of the biological pump (Carlson et al. 1994, Antia 2005; Fig. 1.7).

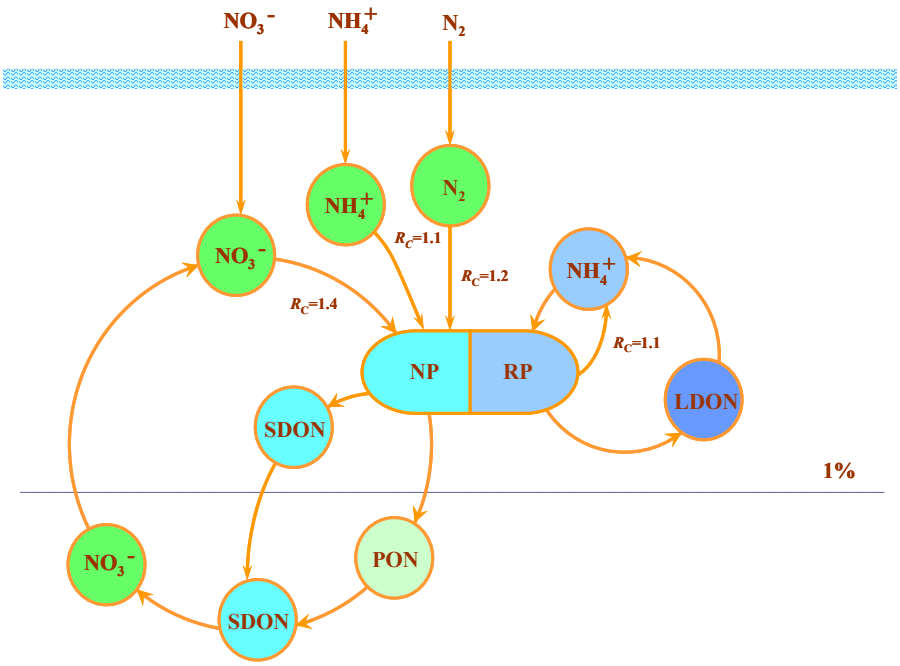

Figure 1.7 Scheme of the biological pump of nitrogen fuelled by particulate organic matter (PON), labile (LDON) and semilabile DOM (SDON)

On the other hand, the transformation of biogenic material into r-DOM in surface ocean waters reduces the bioavailability of C, N and P, contributing to sequestrate part of the anthropogenic CO_2 excess initially used by marine phytoplankton (Fig. 1.8). The r-DOM accumulated in surface waters can be exported *in situ* (10^1 km), as the s-DOM, towards deep waters during winter mixing (10^0 years) or horizontally by means of the oceanic circulation (10^4 km, 10^1-10^2 years; Legendre & Le Fèvre 1995). Some authors argued that r-DOM could be the sink of the missing fraction (20%) of anthropogenic CO_2 (1.3 ± 1.5 Gt-C y^{-1}; Schimel et al. 1996).

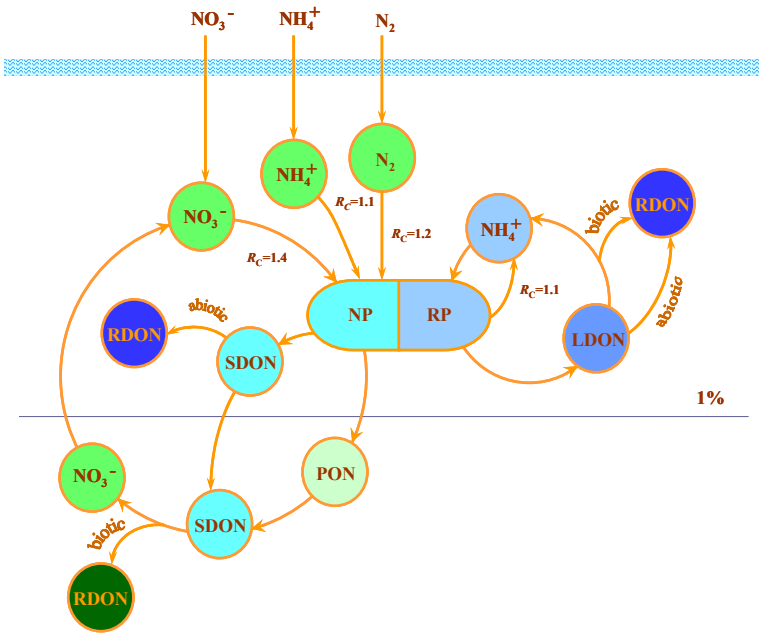

Figure 1.8 Scheme of the biological pump of nitrogen, fuelled by particulate organic matter (PON), labile (LDON), semilabile (SDON) and refractory DOM (RDON)

Chemical composition of DOM

DOM concentrations in the ocean are too low to perform a direct and complete characterisation. Actual knowledge about the composition of phytoplankton exudates (Myklestad 1995, Biddanda & Benner 1997, Nagata 2000) includes carbohydrates (mono-, poly- and oligosaccharides), nitrogen compounds (amino acids, polypeptides and proteins), fatty acids and other carboxylic acids (glycolate, tricarboxylic acids, vitamins…). The major advances have been achieved with the combination of ultrafiltration methods (Amon & Benner 1996) and nuclear magnetic resonance (NMR) techniques (Table 1.1). Thus, the ultrafiltrated DOM (UDOM, > 1nm = 10 Å, 1 kDa, 20-35% of DOM) is used to assess the chemical composition of DOM, despite its properties are not exactly the same as the bulk DOM pool. By ^{13}C-NMR studies, Benner et al. (1992) estimate that the contribution of carbohydrates to ultrafiltrated DOC vary from 50% at the surface to 25% at the bottom layers.

McCarthy et al. (1997) studied the UDOM composition by ^{15}N-NMR and observed contributions through the water column of 66-86% of amides, 8-10% of peptides and 6-25% of indols and pyrroles. On the other hand, Clark et al. (1998) pointed to a higher contribution of phosphoric esters (75%) compared to fosfonates (25%) using ^{32}P-NMR techniques.

Table 1.1 Relation of some NMR studies in ultrafiltered DOM

	ultrafiltered DOM (>1 kDa, 20-40% of DOM)	
technique	**compounds**	**references**
^{13}C NMR	polysaccharides (25-50% of C)	Benner et al. (1992)
^{15}N NMR	amides (66-86% of N) peptides (8-10% of N) indols and pirrols (6-25% of N)	McCarthy et al. (1996)
^{32}P NMR	phosphoric esters (75% of P) fosfonates (25% of P)	Clark et al. (1998)
^{1}H NMR	carbohydrate (60-80% of C) acetate (5-7% of C)	Aluwihare et al. (2005)

In addition, NMR spectroscopy allowed to distinguish between two different pools of organic nitrogen accumulated in the ocean, taken advantage of the change in the acid lability of the amide bonds (Aluwihare et al. 2005).

The coastal margins

Coastal margins represent less than 8% and 1% of the total surface and volume of sea, respectively, but there occurs between 20 and 50% of NP (Walsh 1991, Chavez & Toggweiler 1995, Wollast 1998), and its sediments retained 87% of the organic carbon preserved in the marine environment (Middelburg et al. 1993). In these areas, biogeochemical processes (production, respiration, vertical and horizontal export…) are intensified, enhancing,

consequently, the fluxes of anthropogenic CO_2 between the surface waters and the atmosphere.

Biogeochemical cycles in the coastal zone differ from those in the open ocean in four main issues:

1) Carbon and nutrient cycles in ocean margins are fuelled by the input of nutrients salts from the continents, the atmosphere, and the adjacent ocean. In the global coastal zone, 70% of the nitrogen input comes from the ocean, 22% from the continents and 8% from the atmosphere (Wollast 1998). However, the percentages are very variable from site to site. Continental inputs could become dominant in large drainage basins dedicated to intensive agriculture and farming, where rivers play a major role in the transference of materials from land to sea and influence significantly processes in coastal waters. Atmospheric inputs are especially relevant in high-industrialised coastal areas (Duce et al. 1991). Finally, the open ocean is the main source of external nutrient salts in the coastal upwelling areas associated to ocean eastern boundary currents (Walsh 1991).

2) The primary production (PP) per unit area is significantly higher than in the oceans due to the larger nutrient input. Coastal margins produce ~210 g C m^{-2} y^{-1}, almost twice than the open ocean.

3) The sediments receive ~30% of PP in opposition with ~0.1% in the open ocean. In addition, the mineralization in the sediments becomes more notable and operates as a source of nutrients for the water column. Nevertheless, whereas in the ocean sediments the mineralization is predominantly aerobic, in the coastal regions is usual to observe denitrification, sulphatereduction or, even, fermentation (Middelburg et al. 1993).

4) About 75% of the total organic N (Wollast 1993) or 87% of the total organic C (Middelburg et al. 1993) is preserved in the coastal sediments, so they constitute the most effective trap for anthropogenic carbon in the sea.

Coastal areas in Europe cover four main zones: the Baltic Sea, Mediterranean Sea, Black Sea and the European Atlantic coast including the North Sea, with high diversity of habitats and communities. The mean value of PP in these coastal waters is 180 g C m^{-2} y^{-1}, whereas, in average, benthic community respiration consumes approximately 40% of the pelagic organic matter production (Gazeau et al. 2004). The average PP in the European Atlantic / North Sea region was higher (224 g C m^{-2} y^{-1}) but the benthic community presented lower respiration rates (~30% of PP).

The importance of DOM for carbon and nutrient cycles is enhanced in coastal waters, where exudation by aquatic organisms and degradation of marine and terrestrial plant matter produce large amounts of DOM (Nagata 2000, Carlson 2002). DOM production is especially intense in coastal upwelling areas, where the shelf wind regimen supports a strong exchange with the adjacent ocean waters (Barber & Smith 1981, Walsh 1991), which promotes a high nutrient fertilisation (Hansell & Carlson 1998a, Doval et al. 1997, Álvarez-Salgado et al. 2001a). Organic matter produced in upwelling areas can experience extreme oxidising and reducing conditions (Gagosian et al. 1978).

DOM in the Iberian Upwelling System

The Iberian Upwelling System is located between 37º and 43ºN, in the northern boundary of the Iberian-NW Africa upwelling system (Fig. 1.9) and includes the Rías Baixas at 42-43ºN, four large (>2.5 km^3) V-shaped embayments, and the adjacent shelf. The rías are characterised by a 2-layered residual circulation pattern, with an ongoing bottom current and an outgoing surface current during upwelling events and a reversal of the flow during downwelling conditions. Therefore, these embayments respond to the influence of shelf winds despite that island protect them (Gilcoto et al. 2001). In addition, continental runoff modulates also the circulation of the rías, mainly at the innermost segment, which behaves as a partially mixed estuary

driven by tidal currents (average tidal range, 3 m) and river runoff. The circulation of shelf waters off the Rías Baixas is more complex; it is composed of a wind-driven along-shore current and an across-shore exchange with the adjacent ocean and the Rías Baixas. During the upwelling season, shelf surface waters are imported from the rías, and the bottom waters of the rías enter from the shelf. On the contrary, during the downwelling season, a convergence front between the shelf and the rías develops. The position of that front in the along-shore direction depends on the relative strength of coastal winds and continental runoff (Álvarez-Salgado et al. 2000; Fig. 1.10).

The NW Iberian Peninsula presents two conspicuous characteristics; first, the annual cycle is divided in an upwelling season, with short relaxation intervals that enhance the productivity (Álvarez-Salgado et al. 1999), and other season dominated by downwelling episodes, distinguished by low primary production. During upwelling events northerly winds cause the uplift of Eastern North Atlantic Central Water (ENACW) over the shelf, entering the bottom of the ría and enhancing the positive residual circulation pattern (Rosón et al. 1997). Another remarkable phenomenon in this region is the intrusion of the Iberian Poleward Current (IPC) along the slope during the winter, carrying subtropical waters to our latitudes (Haynes & Barton 1990, Álvarez-Salgado et al. 2003).

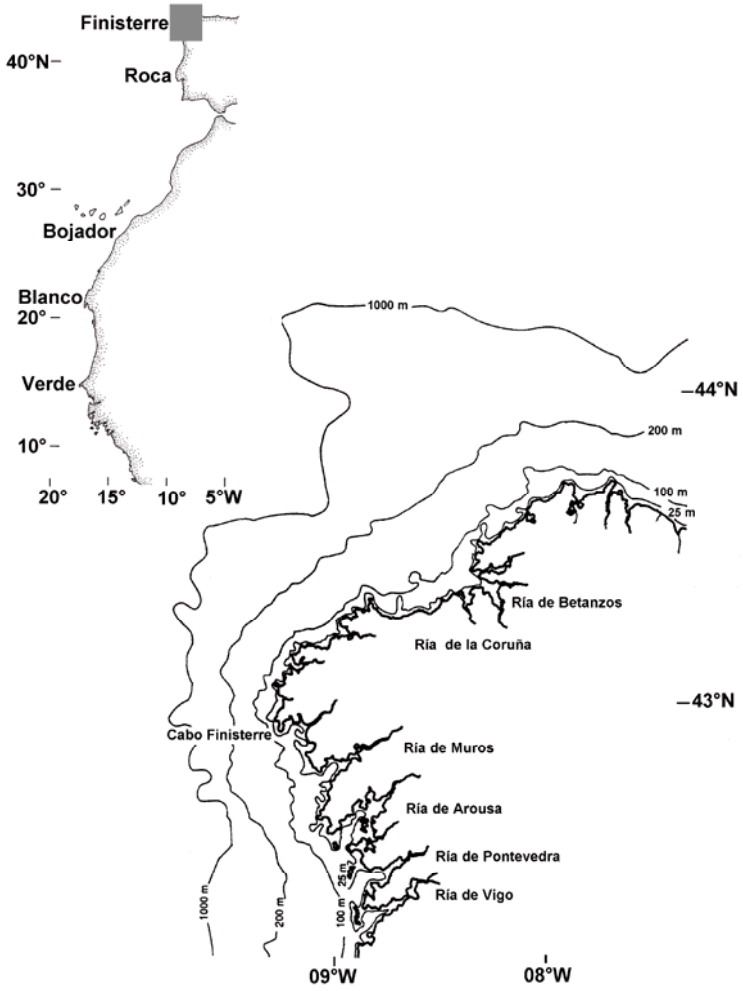

Figure 1.9 Localization of the NW Iberian upwelling system

The NW Iberian upwelling is an ideal system due to **1)** the large spatial and temporal variability at different scales, **2)** the knowledge about its circulation and C, N, P and Si cycles, and **3)** the economic significance of the area due to fishing and aquaculture resources.

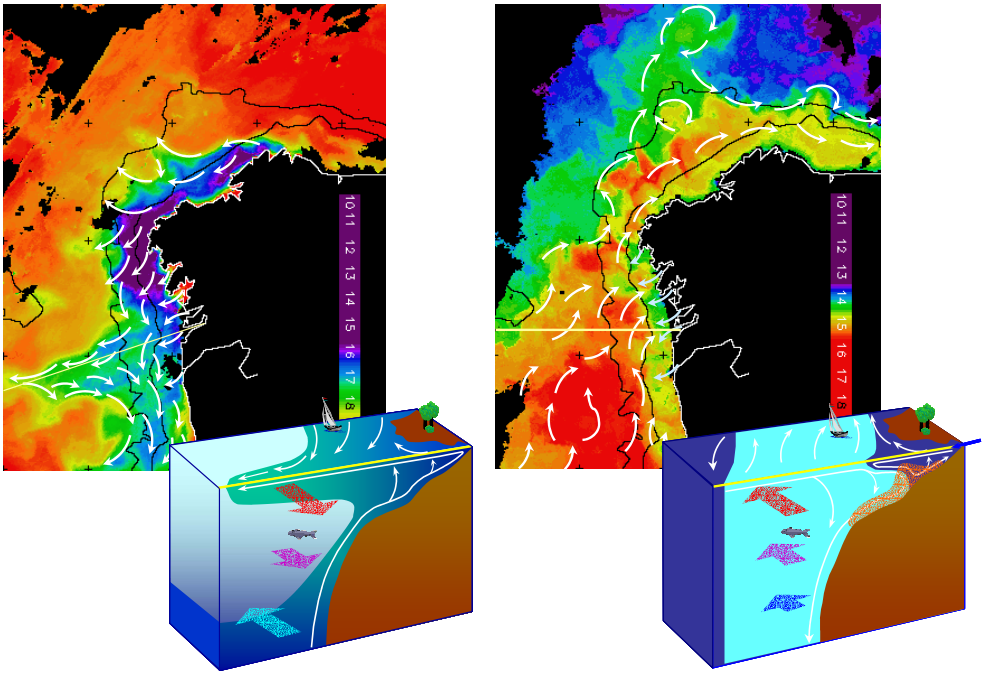

Figure 1.10 Water circulation patterns in the NW Iberian upwelling system during the upwelling and downwelling season

The interest in the role played by the DOM in the biogeochemical cycles in the NW Iberian upwelling system emerged in 1989, during a cruise in the Ría de Arousa (Fig. 1.9). The use of an inverse box model (Rosón et al. 1997) revealed, before the HTCO methods, that more of 40% of the inorganic C and N consumption during the upwelling season was probably transformed in DOM (Álvarez-Salgado et al. 1996a, 1996b, Rosón et al. 1999). The development of HTCO methods (Álvarez-Salgado & Miller 1998) made possible to go deeply in the study of the contribution of DOM to the biogeochemical cycles in this system. Thus, Doval et al. (1997) and Álvarez-Salgado et al. (1999) produced a complete dissolved and particulate organic carbon and nitrogen data collection in the middle Ría de Vigo and the adjacent shelf. A surface accumulation of DOM, in comparison with the concentration expected from the mixing between continental runoff waters and ENACW, was observed during the upwelling season. The C/N ratio of POM increased

significantly from the surface (6.3) to the bottom (8.8), due to the lability of N compounds in the water column and sediments (Copin-Montégut & Copin-Montégut 1983). Particulate organic carbon (POC) and nitrogen (PON) profiles presented two maxima, the largest at the surface and the second at the bottom layer. On the other hand, the concentrations of dissolved organic carbon (DOC) and nitrogen (DON) decrease monotonically from a surface maximum to a bottom minimum. The DOC/DON molar ratio did not change significantly with depth, ranging from 11 to 18. POM accumulates during upwelling 'spin down', when nutrient concentrations are still high and the horizontal transport is low (Zimmerman et al. 1987, Álvarez-Salgado et al. 1996b, Doval et al. 1997). However, DOM accumulation occurs several days after the upwelling relaxation, when phytoplankton growth is limited by nutrient depletion. Álvarez-Salgado et al. (1999) concluded that the Rías Baixas operate as sources of biodegradable DOM for the adjacent shelf waters. The probable fate of DOM produced in the rías is the dilution with ENACW (poor in DOM) with export to the adjacent ocean waters during upwelling events, and *in situ* consumption during relaxation-downwelling events (Álvarez-Salgado et al. 2001a). In addition, it was found that 50% of the material exported from the shelf to the ocean by a filament in August 1998 was DOM (Álvarez-Salgado et al. 2001b).

In March 1992, an extensive survey of nitrogen forms and phytoplankton of the euphotic zone on the northern Spanish shelf showed an accumulation of DON in relation with the mixing of continental runoff waters and ENACW (Bode et al. 2001). It was also found in this study an uncoupling between phytoplankton and DON production, which suggest the participation of microplanktonic grazers in the release of DON. Later research in the Ría de A Coruña (NW Spain; Fig. 1.9) achieved high rates of N regeneration, indicating that a large proportion of the organic matter produced after an upwelling pulse

was recycled in the water column through the microbial food web (Bode et al. 2004a). This behaviour was also suggested by Teira et al. (2003) in a cruise off this ría, indicating the autotrophic nature of this coastal system, which exported between 1 and 86% of total primary production from the euphotic layer in the form of POC. In addition, carbon and nitrogen fluxes pointed out that the release of carbon was produced preferentially at the surface, whereas the release of nitrogen occurred near the base of the euphotic zone (Bode et al. 2004b).

The relationship between phytoplankton size-structure and DOC production was also established in the NW Iberian upwelling system by Teira et al. (2001a, 2001b). Thus, picoplankton-dominated communities showed net heterotrophic or balanced metabolisms and relatively high rates of DOC production in relation to the total primary production. Nevertheless, during stratification or downwelling conditions, dominated by large-sized cells, a net autotrophic metabolism occurred and low rates of DOC production in relation to PP. In this sense, Teira et al. (2001a) found three different conditions: during summer upwelling they estimated that DOC production was 6% of PP with autotrophic conditions, during summer stratification DOC production increased up to 20% and the metabolism was balanced, and, finally, during autumn downwelling, DOC production reached the largest values (~33%) whereas the heterotrophic nature was dominant (Fig. 1.11). Moreover, DOC and POC production rates were linearly related during upwelling conditions, however, in oligotrophic relaxation and downwelling conditions they did not correlate, which suggests different DOC release processes in both situations (Teira et al. 2001b).

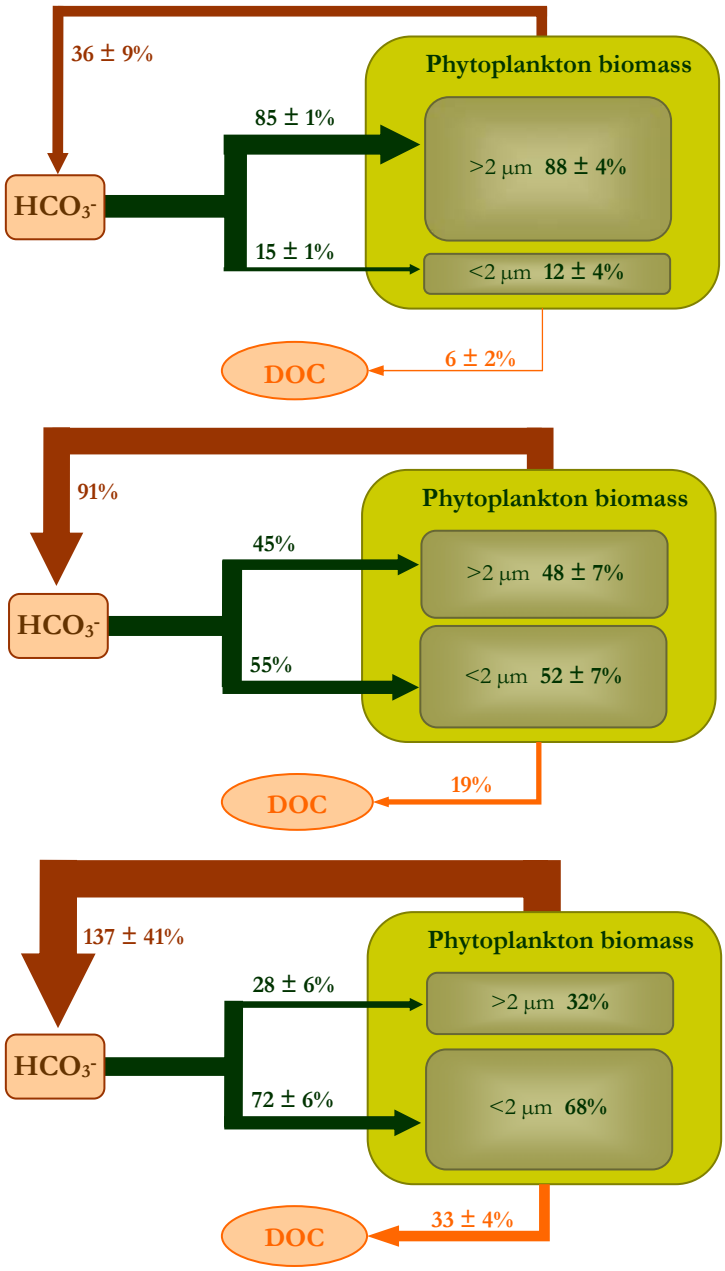

Figure 1.11 Carbon budgets for three contrasting environments studied in the coastal-transition zone off NW Iberian Peninsula (summer upwelling, summer stratification and autumn downwelling). Percentages represent the relative contribution of any given flux or phytoplankton size class with respect to total organic carbon production or total phytoplankton biomass, respectively (From Teira et al. 2001a)

Marañón et al. (2004) were the first to present concurrent DOC and POC production rates during a seasonal cycle in the Ría de Vigo. No marked seasonal patterns were detected and DOC production contributed 15-25% of PP, remaining constant or even increasing with depth. On the other hand, POC production decreased markedly below the surface. In this sense, the results of Marañón et al. (2004) argue against the view that the release of DOC is an overflow mechanism occurring preferentially under conditions of high irradiance and low nutrient concentration. In addition, Varela et al. (2003) suggested that physiological processes (such as carbohydrate exudation by diatoms) seem to be the cause of large DOC accumulation, whereas trophic processes (such as grazing) are more likely the cause of enhanced DON release.

Hypotheses and objectives

The general hypothesis of this work is:

The spatial (ría, shelf and slope systems) and temporal variability, either at the seasonal (upwelling, downwelling or transitional periods) or event (coastal wind stress/relaxation cycles) scale influences strongly the exchange of materials between the different systems and, consequently, the partition (dissolved and suspended phases), the chemical composition and the reactivity of the produced (or consumed) materials.

This general hypothesis has been divided into four specific objectives, that we will try to demonstrate in this work:

1) Fractionation during organic matter mineralization. The chemical composition (C/N/P stoichiometry) and the optical properties (fluorescent dissolved organic matter) of the produced, transported or consumed organic matter in these waters vary from the coast to the ocean and from surface to bottom layer.

2) Partitioning during organic matter mineralization. The contribution of dissolved, suspended and sinking organic matter to mineralization processes changes from the coast to the ocean and from the surface to the bottom layer.

3) Carbohydrates cycling in a coastal upwelling system. Carbohydrates are a major component of the biogenic organic carbon produced and accumulated in the upper layer of the NW Iberian upwelling system. The partition in mono- and polysaccharides allows to characterize labile and semilabile material, respectively.

4) DOM fluorescence as a suitable tracer for microbial and photochemical processes. The fluorescent fraction of DOM is biological and photochemically reactive, in such way that the spatio-temporal variability of certain fluorophores (humic- and protein-like materials) can be used as a tracer of labile material production-consumption, mineralization and photodegradation processes.

INTRODUCCIÓN (en castellano)

Pensando en el hecho de que esta Tesis va a ser presentada en una Facultad de Química es conveniente comenzarla contestando a una simple cuestión: ¿Qué puede hacer un Químico en Oceanografía? El estudio de los procesos físicos, biológicos y geoquímicos que ocurren en los océanos, y de sus interacciones con los continentes y la atmósfera, requiere un tratamiento multidisciplinar. Por tanto la Oceanografía está basada en la necesidad de combinar toda ciencia básica para así entender el medio marino. En este contexto, la Oceanografía Química consiste en resolver problemas oceanográficos mediante conceptos y métodos químicos. En este punto debe hacerse notar que existe una gran diferencia entre Oceanografía Química (la cual considera el ambiente marino como un reactor químico) y la Química Marina (la cual solamente aplica las técnicas analíticas adecuadas en el ambiente marino). Así, se observa que en España en particular, pero en toda Europa en general, existe una carencia de químicos dedicados a la Oceanografía.

Cada vez se concede más atención al estudio de los ecosistemas acuáticos debido a su implicación en el cambio climático global. El océano puede regular el clima controlando el intercambio con la atmósfera de agua, calor y gases invernadero (Fig. 1.1). En consecuencia, el modo en el que estos gases se distribuyen entre la atmósfera y el océano se convierte en una relevante cuestión para la ciencia. En este sentido, los oceanógrafos químicos analizan el secuestro de CO_2 antropogénico en los océanos mediante las bombas de solubilidad y biológica. La bomba de solubilidad involucra únicamente procesos físicos, mientras que la bomba biológica promueve el flujo de carbono biogénico hacia aguas más profundas. Para entender estos procesos es crucial conocer el papel de la materia orgánica disuelta y particulada en el reciclado y la exportación del carbono biogénico. Para ello, los oceanógrafos químicos **1)** desarrollan los métodos analíticos adecuados para estimar las

concentraciones de carbono, nitrógeno y fósforo orgánico disuelto, **2)** caracterizan la materia orgánica disuelta (peso molecular, riqueza isotópica, composición química, propiedades ópticas) y **3)** estudian su reactividad biológica, química y fotoquímica.

El ciclo de la materia orgánica disuelta en aguas oceánicas

Conceptualmente, la materia orgánica disuelta es el material orgánico que no es susceptible de sedimentar. Desde un punto de vista operativo, la materia orgánica disuelta es el material orgánico que pasa a través de filtros de 0.2-1.0 µm, e incluye pequeñas bacterias y todos los virus. Este material disuelto constituye la mayor reserva de materia orgánica en los océanos. Las estimaciones más recientes indican que el conjunto de la materia orgánica disuelta alcanza los 685-700 Gt-C (Schimel et al. 1996, Hansell & Carlson 1998a), igualando el CO_2 acumulado en la atmósfera (Falkowski et al. 2000). En comparación, la suma de detritus (20 Gt-C), fitoplancton (4 Gt-C) y zooplancton (0.1 Gt-C) solo representa el 3% de la materia orgánica total. La mayor parte de este material disuelto (~90%) ha siso formado *in situ* como resultado de la producción primaria del fitoplancton (~50 Gt-C por año) y transformado en materia orgánica disuelta a través de diferentes procesos tanto biológicos (exudación, herbivoría, autolisis o virolisis) como fotoquímicos (Fig. 1.1). La principal función de la materia orgánica disuelta, desde el punto de vista de las bombas biológica y de solubilidad, es el reciclado y la exportación del material biogénico. Además, este material participa en otros procesos relevantes (Sunda 1995):

1) La materia orgánica disuelta compleja metales traza, operando como un tampón que preserva los iones metálicos libres, evitando las altas concentraciones y asegurando su disponibilidad a largo plazo.

2) La materia orgánica disuelta actúa como dador de electrones en los procesos de foto-reducción y solubilización de Fe y Mn, aumentando su disponibilidad y previniendo su exportación hacia el océano profundo.

3) Algunos grupos fitoplanctónicos producen dimetilsulfoniopropionato (DMSP) el cual es transformado en dimetil sulfóxido (DMS). Este compuesto orgánico es susceptible de intercambiarse con la atmósfera, donde es oxidado a ácido sulfúrico, contribuyendo a la regulación del clima en la Tierra.

4) Los ácidos húmicos constituyen una fracción significante de la materia orgánica en las aguas continentales. Su naturaleza aniónica es la responsable de su capacidad de regular el pH entre 3 y 5.

5) Las sustancias húmicas son además compuestos coloreados que absorben radiación visible. Cuando se encuentran en grandes concentraciones provocan una reducción en la calidad y cantidad de la radiación luminosa disponible para el fitoplancton, disminuyendo así la producción total.

6) El fitoplancton exuda compuestos orgánicos con propiedades surfactantes, los cuales disminuyen el intercambio de gases con la atmósfera.

7) La fotolisis de algunos compuestos incluidos en la materia orgánica disuelta produce gases que pueden ser intercambiados con la atmósfera.

El estudio de la materia orgánica disuelta se acentúo en los años 80 debido al desarrollo de técnicas analíticas adecuadas como el método de la oxidación catalítica a alta temperatura (HTCO), que originó concentraciones de materia orgánica disuelta 5-10 veces mayores que los métodos clásicos de oxidación por vía húmeda (Suzuki et al. 1985, Sugimura & Suzuki 1988). Aunque estos autores acabaron retractándose de sus resultados (Suzuki 1993), los mismos contribuyeron a enfocar el interés de los científicos marinos en la materia orgánica disuelta, desarrollando nuevos y mejores métodos de análisis y promoviendo ejercicios de intercalibración (Sharp et al. 2002, 2004).

En paralelo con el progreso en el estudio de la materia orgánica disuelta, otros conceptos, como la producción nueva y regenerada, fueron revisados. La producción nueva de un sistema dado es la producción sostenida por nutrientes externos (tanto temporal como espacialmente), mientras que la producción regenerada es mantenida por nutrientes reciclados dentro de los límites del ecosistema. Ambas producciones son sostenidas tanto por nutrientes inorgánicos como orgánicos.

La materia orgánica disuelta abarca una miríada de compuestos con tiempos de reciclado comprendidos entre horas y miles de años, los cuales son normalmente agrupados en tres categorías diferentes en función de su labilidad:

1) materia orgánica disuelta LÁBIL (l-DOM), con tiempos de reciclado de minutos a días (Keil & Kirchman 1999). Estos compuestos sostienen la variabilidad de la materia orgánica disuelta a corta escala (Kirchman 2000) y son reciclados dentro de los límites del sistema de estudio, *i.e.*, contribuyen a la producción regenerada de las aguas superficiales (Fig. 1.2).

2) materia orgánica disuelta SEMILÁBIL (s-DOM), con tiempos de reciclado de meses a años, es resistente a la rápida degradación microbiana (Cherrier et al. 1996). Este material sostiene la variabilidad estacional de la materia orgánica disuelta y es exportado fuera de los límites del sistema de estudio, *i.e.*, contribuye a la producción nueva (Carlson 2002). Se muestra un ejemplo en la Figura 1.3.

3) materia orgánica disuelta REFRACTARIA (r-DOM), con tiempos de reciclado de cientos a miles de años (Williams & Druffel 1987), sostiene la variabilidad a largo plazo, implicada en la circulación oceánica de larga escala, y contribuye a la inmovilización de materiales fitogénicos, parcialmente producidos a partir de CO_2 antropogénico. De todas formas, Hansell & Carlson (1998b; Fig. 1.4) demostraron que refractario no significa eterno: la materia orgánica disuelta disminuye en un 30% desde las aguas profundas del

Atlántico Norte (recientemente formadas; 48 μM C) hasta las aguas profundas del Pacífico Norte (envejecidas durante 2 años; 34 μM C).

El desarrollo de mejores métodos analíticos promovió el cambio en el modelo conceptual de la bomba biológica clásica (Eppley & Peterson 1979) para introducir la materia orgánica disuelta. Tradicionalmente, la bomba biológica estaba basada solamente en la materia orgánica particulada producida por el fitoplancton a partir del CO_2 (Fig. 1.5; Knauer 1993). El 50% de este material era respirado en la parte superior de la columna de agua (100-300 m) y así, el correspondiente CO_2 regresaba a la atmósfera en escalas de tiempo pequeñas (10^0-10^1 años; Martin et al. 1987). El resto alcanzaba las capas inferiores (>500 m) donde era transformado en CO_2 y secuestrado durante 10^2-10^3 años en la circulación del océano profundo (Wong & Hirai 1997). En los sedimentos se preserva solamente un porcentaje mínimo de la producción primaria (~0.1%; Wollast 1998).

La materia orgánica lábil constituye la fracción más reactiva lo cual la convierte en un nutriente primario y una fuente de energía para las bacterias (Rich et al. 1997, Skoog et al. 1999). Esto provoca que la liberación extracelular de l-DOM sea considerada como un paso intermedio durante el reciclado de nutrientes (Fig. 1.6). En este sentido, las células fitoplanctónicas son capaces de asimilar productos regenerados que no sean NH_4^+, como por ejemplo urea, algunos aminoácidos y bases nitrogenadas (adenina y guanina). Estos productos están ampliamente presentes en el agua de mar, por ejemplo las concentraciones de urea en la superficie del océano abierto son del mismo orden que las de amonio (Bronk 2002). Generalmente la contribución de los flujos de l-DOM es alta: en promedio el 20-40% de la producción total se recicla a través de la materia orgánica disuelta (Azam et al. 1983, Cole et al. 1988, Carlson 2002).

La materia orgánica disuelta semilábil es acumulada o exportada, especialmente al final de un 'bloom' de fitoplancton. En ciertas áreas, como en mar de los Sargazos y en el NO del mar Mediterráneo donde la mezcla invernal sucede después de la estratificación estival, el transporte hacia el fondo de este material fitogénico en forma disuelta sobrepasa las tasas de sedimentación (Copin-Montégut & Avril 1993, Hansell & Carlson 2001). En los ecosistemas de la zona templada, la mayor parte de la materia orgánica se exporta a las aguas profundas en dos periodos muy bien definidos: **1)** después del 'bloom' primaveral, con una sedimentación masiva de materiales fitogénicos; y **2)** durante la convección invernal profunda, cuando la materia orgánica disuelta acumulada en la capa de mezcla durante el verano es transportada hacia el fondo. Como complemento, es necesario considerar la solubilización parcial de la materia orgánica que está sedimentando, que es así transformada en disuelta. De este modo, el nuevo material disuelto que es exportado hacia las capas inferiores debe añadirse al material recogido en las trampas de sedimentos para calcular apropiadamente tasas de exportación, las cuales deben ser igualadas a la entrada de nuevos nutrientes bajo la condición de estado-estacionario de la bomba biológica (Carlson et al. 1994, Antia 2005; Fig. 1.7).

Por otro lado, la transformación de material biogénico en r-DOM en las oceánicas superficiales reduce la biodisponibilidad de C, N y P, contribuyendo a secuestrar parte del exceso del CO_2 antropogénico usado inicialmente por el fitoplancton marino (Fig. 1.8). La r-DOM acumulada en las aguas superficiales puede ser exportada *in situ* (10^1 km), como la s-DOM, hacia las aguas profundas durante la mezcla invernal (10^0 años) u horizontalmente mediante la circulación oceánica (10^4 km, 10^1-10^2 años; Legendre & Le Fèvre 1995). Algunos autores argumentan que la r-DOM puede ser la fracción perdida (20%) del CO_2 antropogénico (1.3 ± 1.5 Gt-C por año; Schimel et al. 1996).

Composición química de la materia orgánica disuelta

La concentración de la materia orgánica disuelta en el océano es demasiado baja para llevar a cabo una caracterización directa y completa. El conocimiento actual sobre los exudados de fitoplancton (Myklestad 1995, Biddanda & Benner 1997, Nagata 2000) incluye carbohidratos (mono-, poli- y oligosacáridos), compuestos de nitrógeno (aminoácidos, polipéptidos y proteínas), ácidos grasos y otros ácidos carboxílicos (glicolato, ácidos tricarboxílicos, vitaminas…). Los mayores avances se han producido mediante la combinación de métodos de ultrafiltración (Amon & Benner 1996) y las técnicas de resonancia magnética nuclear (NMR; Tabla 1.1). Así, la materia orgánica disuelta ultrafiltrada (UDOM, >1nm = 10 Å, 1 kDa, constituye el 20-35% de la materia orgánica disuelta) es utilizada para discernir la composición química de la materia orgánica disuelta, a pesar de que sus propiedades no son exactamente las mismas que el conjunto global. Mediante estudios de resonancia magnética nuclear de ^{13}C, Benner et al. (1992) estimaron que la contribución de los carbohidratos al material ultrafiltrado varía desde el 50% en la superficie al 25% en las capas de fondo. McCarthy et al. (1997) estudiaron la composición de la UDOM mediante resonancia magnética nuclear de ^{15}N y observaron que las amidas constituyen en promedio, en la columna de agua, el 66-86%, los péptidos el 8-10% y los indoles y pirroles el 6-25% del material ultrafiltrado. Por otra banda, Clark et al. (1998) señalaron una mayor contribución a la materia orgánica disuelta ultrafiltrada de los ésteres fosfóricos (75%) en comparación con los fosfonatos (25%) utilizando técnicas de resonancia magnética nuclear de ^{32}P.

Además, la espectroscopia de resonancia magnética nuclear permite distinguir entre dos conjuntos diferentes de nitrógeno orgánico acumulado en el océano, aprovechando el cambio de labilidad de los enlaces amida (Aluwihare et al. 2005).

Los márgenes costeros

Los márgenes costeros representan menos de un 8% y un 1% de la superficie y el volumen total de los ecosistemas marinos, respectivamente, sin embargo, en ellos sucede entre el 20 y el 50% de la producción nueva (Walsh 1991, Chavez & Toggweiler 1995, Wollast 1998), y los sedimentos costeros retienen el 87% del carbono orgánico preservado en los ambientes marinos (Middelburg et al. 1993). Los procesos biogeoquímicos (producción, respiración, exportación vertical y horizontal…) están intensificados en estas áreas, aumentando, consecuentemente, los flujos de CO_2 antropogénico entre las aguas superficiales y la atmósfera.

Los ciclos biogeoquímicos de las zonas costeras se diferencian de los ciclos en océano abierto en cuatro aspectos:

1) Los ciclos de carbono y nutrientes en los márgenes oceánicos están mantenidos por el aporte de sales nutrientes desde los continentes, la atmósfera y el océano adyacente. Globalmente, en la zona costera el 70% de los aportes de nitrógeno provienen del océano, el 22% de los continentes y el 8% de la atmósfera (Wollast 1998). De todas formas, estos porcentajes son muy variables en función de la zona de estudio. Los aportes continentales se pueden convertir en dominantes en cuencas de elevado drenaje dedicadas a la agricultura y ganadería intensiva, donde los ríos juegan un papel principal en la transferencia de materiales desde la tierra al mar, e influencian procesos de gran importancia en las aguas costeras. Los aportes atmosféricos son especialmente relevantes en las áreas costeras altamente industrializadas (Duce et al. 1991). Por último, decir que el océano abierto es la principal fuente de nutrientes externos en los sistemas de afloramiento costero asociados a las corrientes de borde este (Walsh 1991).

2) La producción primaria por unidad de superficie es significativamente mayor que en los océanos debido la mayor entrada de nutrientes. Los márgenes costeros producen ~210 g C m^{-2} por año, casi el doble que en los océanos.

3) Los sedimentos reciben ~30% de la producción primaria, en contraposición con el ~0.1% en océano abierto. Además la mineralización en los sedimentos adquiere gran importancia, actuando como una valiosa fuente de nutrientes para la columna de agua. Sin embargo, mientras en los sedimentos oceánicos la mineralización es predominantemente aeróbica, en las regiones costeras es habitual observar la desnitrificación, sulfato-reducción e incluso la fermentación (Middelburg et al. 1993).

4) El 75% del nitrógeno orgánico total (Wollast 1993), o el 87% del carbono orgánico total (Middelburg et al. 1993), es preservado en los sedimentos costeros, por lo que constituyen la trampa más efectiva para el carbono antropogénico en el mar.

Las zonas costeras en Europa cubren cuatro regiones principales, el mar Báltico, el mar Mediterráneo, el mar Negro y la costa europea atlántica, incluyendo el mar del Norte, presentando una amplia diversidad de hábitats y comunidades. El valor promedio de la producción primaria en estas aguas es de 180 g C m^{-2} por año, mientras que, en promedio, la respiración de la comunidad bentónica consume aproximadamente el 40% de la producción pelágica de materia orgánica (Gazeau et al. 2004). La producción primaria media en la región que abarca la zona costera Atlántica y el mar del Norte es mayor (224 g C m^{-2} por año), sin embargo la comunidad bentónica presenta menores tasas de respiración (~30% de la producción primaria).

La importancia de la materia orgánica disuelta en los ciclos de carbono y nutrientes está intensificada en las aguas costeras, donde tanto la exudación producida por los organismos acuáticos como la degradación de la materia vegetal marina y terrestre produce grandes cantidades de materia orgánica

disuelta (Nagata 2000, Carlson 2002). La producción de este material disuelto es especialmente elevada en las áreas de afloramiento costero, donde el régimen de vientos en la plataforma sustenta un fuerte intercambio con las aguas del océano adyacente (Barber & Smith 1981, Walsh 1991), lo que provoca una elevada fertilización de nutrientes (Hansell & Carlson 1998a, Doval et al. 1997, Álvarez-Salgado et al. 2001a). Además, esta materia orgánica producida en las zonas de afloramiento es susceptible de experimentar unas condiciones extremas de oxidación y reducción (Gagosian et al. 1978).

La materia orgánica disuelta en el Sistema de Afloramiento Ibérico

El Sistema de Afloramiento Ibérico está localizado entre el 37º y el 43ºN, en el límite septentrional del sistema de afloramiento Ibérico-NO de África (Fig. 1.9) e incluye las Rías Baixas en la zona del 42-43ºN, cuatro largos (>2.5 km^3) entrantes de mar en forma de V, y la plataforma adyacente. Las rías están caracterizadas por un patrón de circulación residual en dos capas, con una corriente de fondo de entrada y una corriente superficial de salida durante los eventos de afloramiento; y con inversión de los flujos durante condiciones de hundimiento. Estas bahías responden a la influencia de los vientos de plataforma, aún a pesar de estar protegidas por islas (Gilcoto et al. 2001). Los aportes continentales modulan también la circulación de las rías, principalmente en el segmento más interior, el cual se comporta como un estuario parcialmente mezclado cuya circulación está dominada por las corrientes de marea (rango mareal medio, 3 m) y los aportes fluviales. La circulación de las aguas de plataforma fuera de las Rías Baixas es más compleja; está compuesta por una corriente a lo largo de la costa dirigida por el viento y un intercambio perpendicular a la costa con el océano adyacente y las Rías Baixas. Durante la estación de afloramiento, las aguas superficiales de la plataforma son importadas desde las rías, provocando así la entrada de agua de la plataforma por las capas más profundas hacia el interior de las rías. Por el

contrario, durante la estación de hundimiento, se desarrolla un frente de convergencia entre la plataforma y las rías. La posición de este frente a lo largo de la costa depende de la fuerza relativa de los vientos costeros y de los aportes continentales (Álvarez-Salgado et al. 2000; Fig. 1.10).

El noroeste de la Península Ibérica presenta dos notables características; la primera, el ciclo anual está dividido en una estación de afloramiento, con cortos intervalos de relajación que aumentan la productividad (Álvarez-Salgado et al. 1999), y otra estación dominada por episodios de hundimiento, que se distingue por una baja producción primaria. Durante los eventos de afloramiento los vientos del norte provocan la elevación del Agua Central del Atlántico Norte Oriental (ENACW) sobre la plataforma, entrando por el fondo de la ría e impulsando el modelo de circulación residual positiva (Rosón et al. 1997). Otro notable fenómeno de esta región es la intrusión de la Corriente Ibérica hacia el Polo (IPC) a lo largo de la costa durante el invierno, transportando aguas subtropicales hasta nuestras latitudes (Haynes & Barton 1990, Álvarez-Salgado et al. 2003).

El afloramiento del NO Ibérico es un sistema de estudio ideal debido a **1)** la amplia variabilidad espacial y temporal a diferentes escalas, **2)** el conocimiento existente acerca de su circulación y de los ciclos de C, N, P y Si, y **3)** la importancia económica de esta zona por sus recursos pesqueros y de acuicultura.

El interés en el papel jugado por la materia orgánica disuelta en los ciclos biogeoquímicos en el sistema de afloramiento del NO Ibérico emergió en 1989, durante una campaña en la Ría de Arousa (Fig. 1.9). El uso de un modelo inverso de cajas (Rosón et al. 1997) reveló, antes del uso de métodos HTCO, que más del 40% del consumo de carbono y nitrógeno inorgánico durante la estación de afloramiento era probablemente transformado en materia orgánica disuelta (Álvarez-Salgado et al. 1996a, 1996b, Rosón et al. 1999). El desarrollo

de las técnicas HTCO (Álvarez-Salgado & Miller 1998) hicieron posible profundizar en el estudio de la contribución de la materia orgánica disuelta a los ciclos biogeoquímicos en este sistema. Así, Doval et al. (1997) y Álvarez-Salgado et al. (1999) produjeron una completa colección de datos de carbono y nitrógeno orgánico disuelto y particulado en el segmento medio de la Ría de Vigo y en la plataforma adyacente. Durante la estación de afloramiento se observó una acumulación superficial de materia orgánica disuelta, en comparación con la concentración esperada por la mezcla entre aguas continentales y aguas centrales oceánicas. La relación C/N del material orgánico particulado presentó un aumento desde las capas superficiales (6.3) hasta las de fondo (8.8), debido a la labilidad de los compuestos de nitrógeno en la columna de agua y los sedimentos (Copin-Montégut & Copin-Montégut 1983). Los perfiles de carbono y nitrógeno orgánico particulado presentaron dos máximos, el mayor en la superficie y el secundario en la capa de fondo. Por otro lado, las concentraciones de carbono y nitrógeno orgánico disuelto decrecieron desde un máximo superficial a un mínimo en el fondo. La relación molar entre el carbono y el nitrógeno orgánico disuelto no cambia significativamente con la profundidad, oscilando entre 11 y 18. La materia orgánica particulada se acumula durante la relajación del afloramiento, cuando la concentración de nutrientes es aún alta y el transporte horizontal es bajo (Zimmerman et al. 1987, Álvarez-Salgado et al. 1996b, Doval et al. 1997). Sin embargo, la acumulación de materia orgánica disuelta ocurre varios días después de la relajación del afloramiento, cuando el crecimiento del fitoplancton está limitado por agotamiento de nutrientes. Álvarez-Salgado et al. (1999) concluyeron que las Rías Baixas operan como fuentes de materia orgánica disuelta biodegradable para las aguas de la plataforma adyacente. El probable destino de la materia orgánica disuelta producida en las rías es, durante los eventos de afloramiento, la dilución con las aguas centrales

atlánticas (pobres en esta materia orgánica) junto con la exportación hacia las aguas del océano adyacente, y consumo *in situ* durante los eventos de relajación-hundimiento (Álvarez-Salgado et al. 2001a). Asimismo, se ha observado que el 50% del material exportado desde la plataforma al océano por un filamento en agosto de 1998 era materia orgánica disuelta (Álvarez-Salgado et al. 2001b).

En marzo de 1992, un exhaustivo estudio de las formas nitrogenadas y del fitoplancton de la zona eufótica de la plataforma del norte de España mostró una acumulación de nitrógeno orgánico disuelto, en comparación con la mezcla de las aguas de los aportes continentales y las aguas centrales (Bode et al. 2001). También se observó en este estudio un desacoplamiento entre el fitoplancton y la producción de nitrógeno orgánico disuelto, lo que sugiere la participación de herbívoros microplanctónicos en la liberación de nitrógeno orgánico disuelto. Un posterior trabajo en la Ría de La Coruña (NO España; Fig. 1.9) encontró altas tasas de regeneración de nitrógeno, indicando que una amplia proporción de la materia orgánica producida después del pulso de afloramiento fue reciclada en la columna de agua a través del bucle microbiano (Bode et al. 2004a). Teira et al. (2003) sugirieron un comportamiento similar en una campaña llevada a cabo en el exterior de esta ría, indicando la naturaleza autotrófica de este sistema costero, el cual exporta desde la capa eufótica entre el 1 y el 86% de la producción primaria total en forma de carbono orgánico particulado. Del mismo modo, los flujos de carbono y nitrógeno señalaron que la liberación de carbono se producía preferentemente en la superficie, mientras que la liberación de nitrógeno ocurría cerca de la base de la zona eufótica (Bode et al. 2004b).

La relación existente entre la estructura de tamaños del fitoplancton y la producción de carbono orgánico disuelto fue también establecida en el sistema de afloramiento del NO Ibérico por Teira et al. (2001a, 2001b). De este modo,

las comunidades dominadas por el picoplancton mostraron metabolismos netamente heterotróficos o equilibrados y tasas relativamente elevadas de producción de carbono orgánico disuelto en relación a la producción primaria total. Sin embargo, durante condiciones de estratificación o hundimiento, en las que dominan células de mayor tamaño, se observa un metabolismo netamente autotrófico y bajas tasas de producción de carbono orgánico disuelto en relación con la producción primaria total. En este sentido, Teira et al. (2001a) encontraron tres ambientes distintos: **1)** durante el afloramiento estival estimaron que la producción de carbono orgánico disuelto constituía el 6 % de la producción primaria total bajo condiciones autotróficas, **2)** durante la estratificación estival la producción de carbono orgánico disuelto aumentó hasta el 20% y el metabolismo se encontraba netamente equilibrado, y **3)** durante el hundimiento otoñal, la producción de carbono orgánico disuelto registró los máximos valores (~33%), mostrando una naturaleza heterotrófica (Fig. 1.11). Además, se observó una relación lineal entre las tasas de producción de carbono orgánico disuelto y particulado bajo condiciones de afloramiento, sin embargo, en ambientes oligotróficos, durante eventos de relajación y hundimiento, no se observó esta correlación, lo que sugiere diferentes procesos de liberación del carbono orgánico disuelto para cada situación (Teira et al. 2001b).

Marañón et al. (2004) presentaron por primera vez tasas de producción de carbono orgánico disuelto y particulado simultáneos durante un ciclo estacional en la Ría de Vigo. No se encontraron patrones estacionales destacables y la producción de carbono orgánico disuelto contribuyó en un 15-25% de la producción primaria total, permaneciendo constante o incluso aumentando con la profundidad. Por otro lado, la producción de carbono orgánico particulado en la columna de agua disminuyó notablemente bajo la capa superficial. En este sentido, los resultados de Marañón et al. (2004) contradicen

la idea de que la liberación de carbono orgánico disuelto ocurre preferentemente bajo condiciones de alta irradiancia y baja concentración de nutrientes. Así mismo, Varela et al. (2003) sugirieron que los procesos fisiológicos (como la exudación de carbohidratos por diatomeas) parecen ser la causa de la elevada acumulación de carbono orgánico disuelto, mientras que los procesos tróficos (como la herbivoría) son la causa más probable de la elevada liberación de nitrógeno orgánico disuelto.

Hipótesis general de trabajo:

La variabilidad espacial (ecosistemas de ría, plataforma y océano adyacente) y temporal, tanto a escala estacional (periodos de afloramiento, hundimiento y de transición) como de evento (ciclos de tensión/relajación del viento costero) tiene un efecto determinante sobre el intercambio de materiales entre los distintos ecosistemas y, en consecuencia, sobre la partición (fases disuelta y en suspensión), la composición química y la reactividad de los materiales generados (o consumidos) en dichos ecosistemas.

Objetivos:

1) El fraccionamiento durante la mineralización de la materia orgánica. La composición química (estequiometría C/N/P) y las propiedades ópticas (fluorescencia de la materia orgánica disuelta) de la materia orgánica producida, transportada o consumida en estas aguas varía tanto de costa a océano como desde las capas superficiales hasta las más profundas.

2) La partición durante la mineralización de la materia orgánica. La contribución de la materia orgánica disuelta, particuladas y en suspensión a los procesos de mineralización varía desde la costa al océano y, también, desde superficie hasta fondo.

3) El ciclo de los carbohidratos en un sistema de afloramiento costero. Los carbohidratos son el componente mayoritario del carbón orgánico biogénico producido y acumulado en las capas superiores del sistema de afloramiento del NO de la Península Ibérica. El material lábil y semilábil se puede diferenciar caracterizando los carbohidratos en mono- y polisacáridos, respectivamente.

4) La fluorescencia de la materia orgánica fluorescente usada como trazador de procesos microbianos y fotoquímicos. La fracción fluorescente de la materia orgánica disuelta es biológica y fotoquímicamente activa, de tal forma que la variabilidad espacio-temporal de ciertos fluoróforos (materiales pseudo-

húmicos y pseudo-proteicos) puede ser utilizada como trazador de procesos de producción-consumo, mineralización y fotodegradación.

Chapter 2:

Cycling of dissolved and particulate carbohydrates in a coastal upwelling system (NW Iberian Peninsula)

Chapter 2, the research work presented in this chapter is also a contribution to the paper:

M. Nieto-Cid, X. A. Álvarez-Salgado, S. Brea, F. F. Pérez. 2004. **Cycling of dissolved and particulate carbohydrates in a coastal upwelling system (NW Iberian Peninsula)**. Mar Ecol Prog Ser 283:39-54

Resumen: En este trabajo se evalúa la contribución de carbohidratos al carbono orgánico disuelto (DOC) y particulado (POC) en las aguas de plataforma del NW Ibérico entre mayo de 2001 y abril de 2002. Los carbohidratos particulados (p-CHO) representan el 26 ± 1% y 12 ± 1% de los cambios en el POC en el segmento central de la Ría de Vigo (50 m de profundidad) y en la plataforma continental (150 m de profundidad), respectivamente. La contribución de los carbohidratos disueltos (d-CHO) a los cambios en el DOC fue mayor que en el caso del material particulado: 29 ± 4% en la ría y 31 ± 4% en la plataforma. La correlación entre p-CHO y POC ($r = +0.88$, $n = 298$, $p < 0.001$) y entre d-CHO y DOC ($r = +0.82$, $n = 298$, $p < 0.001$) indican que las variaciones en los carbohidratos están ligados a los cambios en el carbono orgánico en la escala de tiempo de la frecuencia de muestreo (2 semanas). La máxima acumulación de carbohidratos sucedió durante la estación de afloramiento en la fase de 'spin down' de los episodios de afloramiento; se estimaron tasas de producción de d-CHO en la ría de ~1.5 μmol C L^{-1} d^{-1}, un orden de magnitud mayor que durante el invierno. Los monosacáridos representan entre el 30 y el 40% de los carbohidratos disueltos, sin embargo son responsables de menos del 20% de los cambios de d-CHO, indicando que la mayoría de los d-CHO formados recientemente son polisacáridos semilábiles.

Abstract: The contribution of carbohydrates to the dissolved (DOC) and suspended (POC) organic carbon pools in NW Iberian shelf waters has been assessed from May 2001 to April 2002. Particulate carbohydrates (p-CHO) represented 26 ± 1% and 12 ± 1% of the POC changes in the middle Ría de Vigo (50 m water) and the middle shelf (150 m water) respectively. The contribution of dissolved carbohydrates (d-CHO) to the DOC changes was larger: 29 ± 4% in the middle ría and 31 ± 4% in the middle shelf. The correlations between p-CHO and POC (r = +0.88, n = 298, p <0.001) and between d-CHO and DOC (r = +0.82, n = 298, p <0.001) indicate that carbohydrate changes are linked to bulk organic carbon changes at the time scale of the sampling frequency (2 weeks). Maximum carbohydrate accumulation occurred during the upwelling season at the 'spin down' phase of upwelling events; estimated rates of d-CHO production in the middle ría are ~1.5 μmol C L^{-1} d^{-1}, an order of magnitude larger than during the winter period. Although monosaccharides represent 30-40% of the bulk d-CHO, they are responsible for less than 20% of the d-CHO changes, indicating that most of the freshly produced d-CHO is semi-labile sugar polymers.

INTRODUCTION

Although marine dissolved organic matter (DOM) is one of the largest active reservoirs of organic carbon in the biosphere (Hedges 1992, 2002) and it is important for understanding the global carbon cycle and the changes in the concentration of atmospheric carbon dioxide (Siegenthaler & Sarmiento 1993), only a small portion of this pool has been already identified. The major advances have been achieved with the combination of ultrafiltration methods (Amon & Benner 1996) and nuclear magnetic resonance techniques (Benner et al. 1992, Aluwihare et al. 1997, McCarthy et al. 1997, Clark et al. 1998, Hedges et al. 2002). Carbohydrates are one of the major products of marine phytoplankton photosynthesis and represent the main part of the known fraction of organic carbon in the water column (Benner 2002, Ogawa & Tanoue 2003). According to Pakulski & Benner (1994), dissolved carbohydrate accounted for 13-46% of the dissolved organic carbon (DOC) pool in seasonal thermocline waters, with significant differences between environments: the percentage is higher in the Pacific Ocean (~30%) and the Gulf of Mexico (~23%) than in the North Atlantic (~16%). In contrast, the percentage of carbohydrates in ultrafiltered DOM (UDOM) represents from 50% (surface waters) to 25% (deep waters) by ^{13}C NMR (Benner et al. 1992), and 80 ± 4% by ^{1}H NMR (Aluwihare et al. 1997).

Particulate organic matter (POM) is a mixture of plankton and detritus with different elemental (C, H, O, N, P) and biochemical (proteins, carbohydrates, lipids, phosphorus compounds, pigments) compositions; detritus is richer in lipids and phytoplankton in proteins and carbohydrates (Ríos et al. 1998). The variability of particulate organic carbon (POC) is affected by the quality (ratio between plankton and detritus, predominance of diatoms or other autotrophs, heterotrophs,…) and the composition of the different groups. The Redfield formula ($C_{106}H_{171}O_{42}N_{16}P$) represents the average composition of the organic

tissues of marine phytoplankton (Anderson 1995, Fraga 2001), with a 23.4% (w/w) of carbohydrates, although it range from 15 to 26% for plankton net tow samples from different marine environments (Hedges et al. 2002).

Several methods have been used to determine dissolved carbohydrates until the MBTH colorimetric method was proposed by Burney & Sieburth (1977). This procedure is tedious and involves many steps. More recently, the colorimetric reagent TPTZ has been suggested (Myklestad et al. 1997). These two methods agree well, especially in filtered seawater samples (Witter & Luther III 2002). They provided concentrations much higher than those obtained by molecular separation methods such as HPLC with pulse amperometric detection (HPLC-PAD). The reasons for this divergence are not very clear yet. The numerous difficulties in carbohydrate analysis, such as the low concentrations of free monosaccharides (Pakulski & Benner 1994), their high water solubility, the lack of a light-absorbing chromophore and the presence of multiple charge states at seawater pH (neutral sugars, positively charged amino sugars and negatively charged uronic acid), are behind the multiplicity of methods and the discrepancies between them.

A limited amount of studies about the dissolved carbohydrate pool has been published over the last decade. Most of them refer to single transects sampled once (Bhosle et al. 1998, Hung et al. 2001, Witter & Luther III 2002) or twice (Pettine et al. 1999, Hung et al. 2003a) in different environments. Only one annual cycle has been presented up to day by Børsheim et al. (1999), who sampled monthly two inshore stations during two years in the Trondheimsfjord (Norway). None of these studies is devoted to oceanic or coastal upwelling areas.

Although ocean margins cover only 8% of the total ocean surface, according to different estimates they support 18-33% of the global net primary production and 27-50% of the global export production (Walsh 1991, Chavez

& Toggweiler 1995, Wollast 1998). Coastal upwelling areas are particularly productive because of the enhanced entry of nutrients from the adjacent ocean. Therefore, they are probable sites of intensified carbohydrate production.

The western coast of the Iberian Peninsula is affected by intermittent periods of upwelling (1-2 weeks, Álvarez-Salgado et al. 1999), with a marked seasonal cycle (Wooster et al. 1976). From April to October (the upwelling season) northerly winds cause Eastern North Atlantic Central Water (ENACW) to upwell over the shelf, penetrating from the bottom of the ría and enhancing the positive residual circulation pattern (Rosón et al. 1997). Transition from northerly to southerly winds occurs during the autumn (October-November). From November to March (the downwelling season), southerly winds prevail and a downwelling front develops at the slope, precluding shelf edge exchange (Castro et al. 1997). During the winter, a strong poleward flow of subtropical ENACW occurs along the slope (Haynes & Barton 1990, Álvarez-Salgado et al. 2003).

Studies of the role played by DOM in coastal upwelling systems are relatively scarce, and most of them have been conducted in the western coast of the Iberian Peninsula. These studies have confirmed that the Rías Baixas are pre-eminent sites for the synthesis of DOM (Álvarez-Salgado et al. 1999), which is exported to the adjacent shelf during upwelling events and accumulated/consumed *in situ* during relaxation/downwelling events (Álvarez-Salgado et al. 2001a). The present study, focused on the contribution of carbohydrates to the dissolved and suspended organic carbon pools, constitutes a step ahead in our knowledge of the behaviour of DOM in this coastal upwelling system. We demonstrate the importance of carbohydrates for the carbon cycling at the different stages of the seasonal cycle and approach the lability of this carbon pool through the mono- to polysaccharides ratio.

MATERIALS AND METHODS

Survey area. Figure 2.1 shows the study area, comprising the Ría de Vigo and the adjacent shelf, the two contrasting domains occupied during the present study. On one hand, the rías are characterised by a 2-layered residual circulation pattern, with an ongoing bottom current and an outgoing surface current during upwelling events and a reversal of the flow during downwelling conditions. Therefore, these large (>2.5 km^3) V-shaped embayments respond to the influence of shelf winds despite they are protected by island barriers (Gilcoto et al. 2001). In addition, continental runoff modulates also the circulation of the rías, mainly at the innermost segment, which behaves as a partially mixed estuary driven by tidal currents (average tidal range, 3 m) and river runoff. For the case of the Ría de Vigo, the main tributary is the river Oitabén-Verdugo, with an average flow of 18 $m^3 s^{-1}$ during the study period (see inset of Fig. 2.1).

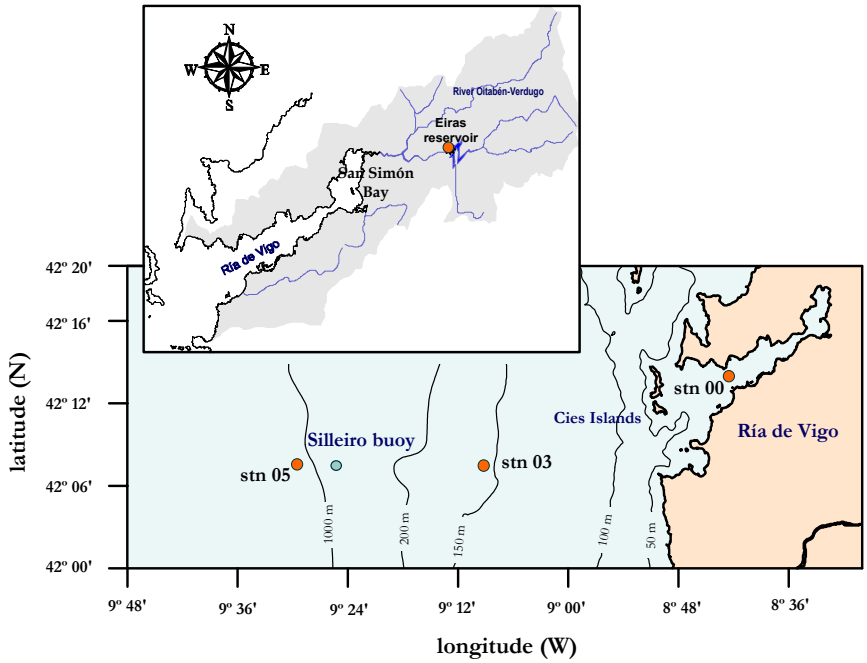

Figure 2.1 The Ría de Vigo and adjacent shelf (NW Iberian Peninsula). The three stations and the Eiras station, at the upper course of the Oitabén-Verdugo river, are shown

On the other hand, the circulation of shelf waters off the Rías Baixas is more complex; it is composed of a wind-driven along-shore current and an across-shore exchange with the adjacent ocean and the Rías Baixas. During the upwelling season, shelf surface waters are imported from the rías and the bottom waters of the rías enter from the shelf. On the contrary, during the downwelling season, a convergence front between the shelf and the rías develops. The position of that front in the along-shore direction depends on the relative strength of coastal winds and continental runoff (Álvarez-Salgado et al. 2000).

Sampling strategy. Two stations were sampled weekly aboard RV *Mytilus* from May 2001 to April 2002. The mid-shelf station (stn 03; 42º07.8'N, 9º10.2'W, 150 m deep) was occupied from 08:00 to 10:00 h GMT. Station 00 (42º13.8'N, 8º51.0'W) was located in the middle segment of the Ría de Vigo (40 m depth in low water) and it was sampled from 14:00 to 15:00 h GMT. Full-depth continuous conductivity-temperature-depth (CTD) profiles were recorded at each sampling site with a SBE 9/11 CTD device incorporated into a rosette sampler equipped with twelve 10-L Niskin bottles. Conductivity measurements were converted into practical salinity scale values (UNESCO 1985). Seawater samples were collected from 5, 25, 40, 60, 75, 100 and 150 m at stn 03, and 5, 15 and 40 m at stn 00. In addition, two samples of ENACW were taken at an oceanic station (stn 05; 42º07.8'N, 9º30.0'W, 1200 m deep), at 150 and 200 m.

Aliquots for dissolved and particulate organic matter analyses were collected in 500-mL acid-cleaned glass flasks and 5-L acid-cleaned PVC containers, respectively. Dissolved organic matter samples were filtered through precombusted (450ºC, 4 h) 47-mm ø Whatman GF/F filters in an acid-cleaned glass filtration system, under low N_2-flow pressure. Two aliquots were recovered, for organic carbon (DOC) and carbohydrates (d-CHO). Samples for

the analysis of DOC were collected in 10-mL precombusted (450ºC, 12 h) glass ampoules. After acidification with H_3PO_4 to pH < 2, the ampoules were heat-sealed and stored in the dark at 4ºC until analysis. For d-CHO, the filtrate was collected in 50-mL polyethylene containers and frozen at -20ºC until analysis. Suspended organic matter was collected under low-vacuum on precombusted (450ºC, 4 h) 25-mm ø Whatman GF/F filters for organic carbon (POC, 0.5-1.5 L of seawater) and carbohydrates (p-CHO, 250-500 mL of seawater). All filters were dried overnight and frozen (-20ºC) before analysis. Samples for DOC and POC were collected every survey (weekly periodicity), whereas d-CHO and p-CHO were taken every two surveys (fortnightly periodicity).

In addition, one station in the upper course of the river Oitabén-Verdugo was sampled regularly during the seasonal cycle (Eiras reservoir, Fig. 2.1). Samples for DOC, POC, d-CHO and p-CHO were taken with a 1.7-L Niskin bottle, adapted for riverine samples, at the surface layer. They were processed as the seawater samples.

Carbon analyses. DOC was measured with a commercial Shimadzu TOC-5000 organic carbon analyzer, working under the principle of high-temperature catalytic oxidation. After decarbonation of the sample by vigorous stirring with high-purity synthetic air for 15 min, 200 µL were injected into the vertical furnace (a quartz tube) of the analyzer, filled with a 0.5% Pt-coated Al_2O_3 catalyst at 680ºC. Quantitative production of CO_2 occurs from the DOC in the sample; and this CO_2 was measured in the Shimadzu Infrared Gas Analyzer. Three to 5 replicate injections were performed per sample and the system was standardized daily with potassium hydrogen phthalate in Milli-Q water. The concentration of DOC was determined by subtracting the average peak area from the instrument blank area and dividing by the slope of the standard curve. The system blank, obtained by frequent injection (every 5 samples) of UV-Milli-Q water, was equivalent to 5-10 µmol C L^{-1}.The precision of measurements was

1%, i.e. ±0.7 μmol C L^{-1}.Their accuracy was tested daily with the DOC reference materials provided by D. Hansell (University of Miami). We obtained an average concentration of 45.7 ± 1.6 μmol C L^{-1} (n = 26) for the deep ocean reference (Sargasso Sea deep water, 2600 m) minus blank reference materials. The nominal value provided by the reference laboratory is 44.0 ± 1.5 μmol C L^{-1}.

Measurements of POC were carried out with a Perkin Elmer 2400 CHN analyzer. Filters were packed into 30 mm tin disks and injected into a vertical quartz furnace where combustion to CO_2, N_2 and H_2O is performed at 900ºC. After separation of the gas products in a chromatographic column, a conductivity detector quantified the C, N and H content of the sample. Daily standards of acetanilide were added. The precision of the method was ±0.3 μmol L^{-1} for the case of carbon.

Carbohydrate analyses. The determination of p-CHO carbohydrates was carried out by the anthrone method (Ríos et al. 1998). It is based in the quantitative reaction of sugars with anthrone in a strongly acid medium at 90ºC, to give an intensely coloured compound. The absorption was measured at 625 nm. To avoid manipulation of a strong acid (H_2SO_4 12M), the detection of the coloured compound was performed in a segmented flow analysis (SFA) system. It was necessary to use an all-glass manifold and a pump-tube of Viton® for the sample. The system was calibrated daily with D-glucose standards. The estimated accuracy of the method is ±0.1 μmol C L^{-1}.

Dissolved mono- and polysaccharides (MCHO and PCHO) were determined by the oxidation of the free reduced sugars with 2,4,6-tripyridyl-*s*-triazine (TPTZ) followed by spectrophotometric analysis (Myklestad et al. 1997, Hung et al. 2001). Briefly, the redox reactions are the following:

$$RCHO + 2Fe(CN)_6^{3-} + 3OH^- \rightarrow RCO_2 + 2Fe(CN)_6^{4-} + 2H_2O$$

$$Fe^{3+} + Fe(CN)_6^{4-} + 2TPTZ \rightarrow Fe(CN)_6^{3-} + \mathbf{Fe(TPTZ)_2^{2+}}$$

(violet-coloured complex)

The aldehydes of the MCHO or the PCHO (after hydrolysis of glycosidic bonds) are oxidized at alkaline pH; consequently, Fe^{3+} is reduced to Fe^{2+}. Then, TPTZ is condensed with the resultant Fe^{2+} to give a violet-coloured $Fe(TPTZ)_2^{2+}$ complex, which is spectrophotometrically determined at 595 nm. Hydrolysis of PCHO was carried out at pH = 1, at 150ºC during 1 hour. Samples were acidified with HCl and, after hydrolysis, they were neutralized with NaOH. The reagents and products involved in the reactions are light sensitive; because of this, all the analytical procedure must be carrying out in the dark. Due to the large number of samples and the sensitivity of the method to ambient light, the detection of the coloured compound was run in an automated SFA system. MCHO concentrations were quantified using a daily calibration curve made from D-glucose in Milli-Q water with concentrations between +0 and +32 μmol C L^{-1}, whereas the standardization of d-CHO was made with D-glucose and soluble starch in Milli-Q water, with the same concentrations. Differences between calibration curves in Milli-Q water and seawater were negligible, as previously indicated by Witter & Luther III (2002). Quantification of MCHO and d-CHO was made by subtracting the average peak height from the blank height, and dividing by the slope of the standard curve. d-CHO were corrected for dilution during the hydrolysis step. PCHO concentrations were calculated as the difference between d-CHO and MCHO. Three replicates were measured for each sample. The estimate accuracy was ±0.6 μmol C $L^{-1}$for MCHO and ±0.7 μmol C L^{-1} for d-CHO, and the detection limit was ~2 μmol C L^{-1}. Therefore, the calculated accuracy for PCHO is ±0.9 μmol C L^{-1} ($[0.6^2 + 0.7^2]^{0.5}$).

Meteorological variables. Daily Ekman transport values ($-Q_X$, m^2s^{-1}) were calculated according to Wooster et al. (1976):

$$-Q_X = \frac{\rho_{air} \cdot C \cdot |V| \cdot V_y}{\rho_{SW} \cdot f} \quad (2.1)$$

where ρ_{air} is the density of air, 1.22 kg m^{-3} at 15ºC; C is an empirical drag coefficient (dimensionless), 1.3×10^{-3}; f is the Coriolis parameter, $9.946 \times 10^{-5} s^{-1}$ at 43º latitude; ρ_{SW} is the density of seawater, ~1025 kg m^{-3}; $|V|$ is the wind speed; and V_y is the north component of wind speed. Wind data were taken hourly from the anemometer of the SeaWatch Buoy Silleiro Meteorological Observatory at 42º07.2'N, 9º24.0'W (http://www.puertos.es). Positive values indicate upwelling and downwelling occurs when negative values are obtained.

Daily continental runoff (Q_R, m^3s^{-1}) was estimated as the sum of a function of precipitation in the drainage basin, 589 km^2 (Ríos et al. 1992), and the flow from the river Oitabén-Verdugo, regulated by the Eiras reservoir.

Regression analysis. The best-fit between any couple of variables (X, Y) was obtained minimizing the function:

$$\sum_i \left[\left(X_i - \hat{X}_i\right)^{w_X} \times \left(Y_i - \hat{Y}_i\right)^{w_Y} \right]^2 \quad (2.2)$$

where w_X and w_Y are weights for X and Y respectively, with w_X, $w_Y \geq 0$ and $w_X + w_Y = 1$. The weight factors are a function of the estimated experimental error of the measured variable (er) regarding the standard deviation (SD) of the whole set of measurements of such parameter. For a given couple of variables:

$$w_X = \left(\frac{er_X}{SD_X}\right) \Big/ \left(\frac{er_X}{SD_X} + \frac{er_Y}{SD_Y}\right); \quad w_Y = 1 - w_X \quad (2.3)$$

Any regression model can be expressed as a linear combination of two extreme categories: a) model I, which should be applied when $w_X = 0$, $w_Y = 1$ and b) model II when $w_X = w_Y = 0.5$ (Sokal and Rohlf 1995).

RESULTS

Dissolved and suspended CHO in relation to the hydrography of NW Spain

Seven hydrographic periods can be discerned on basis of the seasonal evolution of key meteorological variables such as $-Q_X$ and Q_R (Fig. 2.2a, Table 2.1) and the observed water column response (Fig. 2.2b-e). The first period, during spring and summer, was characterised by moderate upwelling-favourable winds separated by shorts intervals of wind calm. This caused marked summer stratification, with warm waters at the surface (17-19ºC) and cold waters at the bottom (13ºC). Average $-Q_X$ values indicate moderate upwelling ($-Q_X$ = 257 m^3s^{-1} km^{-1}) and reduced continental runoff (Q_R = 15 m^3s^{-1}). At the end of the summer, a strong upwelling event ($-Q_X$ = 500 $m^3s^{-1}km^{-1}$) produced a sudden cooling of the water column: temperature in the surface layer decreased up to 15-16ºC due to the uplift of ENACW (F 2.2c). During October, continental runoff was high (Q_R = 47 m^3s^{-1}) and coastal winds experienced a dramatic change in direction ($-Q_X$ = -347 $m^3s^{-1}km^{-1}$) that promoted downwelling. This downwelling produced a reversal of the residual circulation of the ría (Fig. 2.2a) with an entry of warm oceanic surface water (Fig. 2.2c,e). From 20 to 22 October strong runoff was observed (>300 m^3s^{-1}, Fig. 2.2a) that restored the positive residual circulation pattern. Transition from stratification to vertical homogenisation occurred by 20 November coinciding with enhanced Ekman transport values ($-Q_X$ = 712 $m^3s^{-1}km^{-1}$) and low continental runoff (Q_R = 10 m^3s^{-1}). At the end of the autumn and the beginning of the winter a new wind reversal ($-Q_X$ = -216 $m^3s^{-1}km^{-1}$) promoted the intrusion of the Iberian Poleward Current (IPC) on the shelf, characterised by a salinity maximum (Fig 2d) and relatively warm temperatures >14ºC (Fig. 2.2e). Continental runoff (Q_R = 13 m^3s^{-1}) was perceptible only at the innermost station, where surface salinity decreased below 34.0 (Fig. 2.3b). Maximum vertical homogenisation occurred

during the winter mixing period (by March), coinciding with positive values of $-Q_X$ (231 $m^3s^{-1}km^{-1}$) and limited runoff (Q_R = 17 m^3s^{-1}). Finally, the beginning of the spring transition from homogenisation to stratification was observed at the end of the study period, with enhanced positive values of $-Q_X$ (381 m^3s^{-1} km^{-1}), reduced Q_R (10 m^3s^{-1}) and a slight increase of surface temperature (Fig. 2.2c,e).

Table 2.1 Average offshore Ekman transport ($-Q_X$, m^2s^{-1}), continental runoff (Q_R, m^3s^{-1}), surface water flux at stn 00 (Q_{S00}, 10^3 m^3s^{-1}) and renewal rate at stn 00 (% d^{-1}) for the seven hydrographic periods identified during the sampling period. Positive values of $-Q_X$ indicates upwelling, negative values downwelling. Positive values of Q_{S00} indicates a positive residual circulation pattern and negative values a negative residual circulation pattern. For Q_{S00} and renewal rate the errors associated to the equation (2.4) are shown

	Period	Dates	$-Q_X$	Q_R	Q_{S00}	Renewal rate
1	summer strat.	15 May-21 Aug	257	15	0.8 ± 0.1	13 ± 2
2	upwelling	28 Aug-18 Sep	500	8	1.3 ± 0.1	21 ± 2
3	downwelling	25 Sep-30 Oct	-347	47	0.0 ± 0.1	2 ± 2
4	transition	6 Nov-20 Nov	712	10	1.8 ± 0.2	29 ± 3
5	IPC	27 Nov-13 Feb	-216	13	-0.3 ± 0.1	5 ± 1
6	winter mixing	20 Feb-26 Mar	231	17	0.8 ± 0.1	13 ± 2
7	spring	2 Apr-24 Apr	381	10	1.0 ± 0.1	17 ± 2
	annual cycle	**15 May-24 Apr**	**129**	**17**	**0.6 ± 0.1**	**9 ± 2**

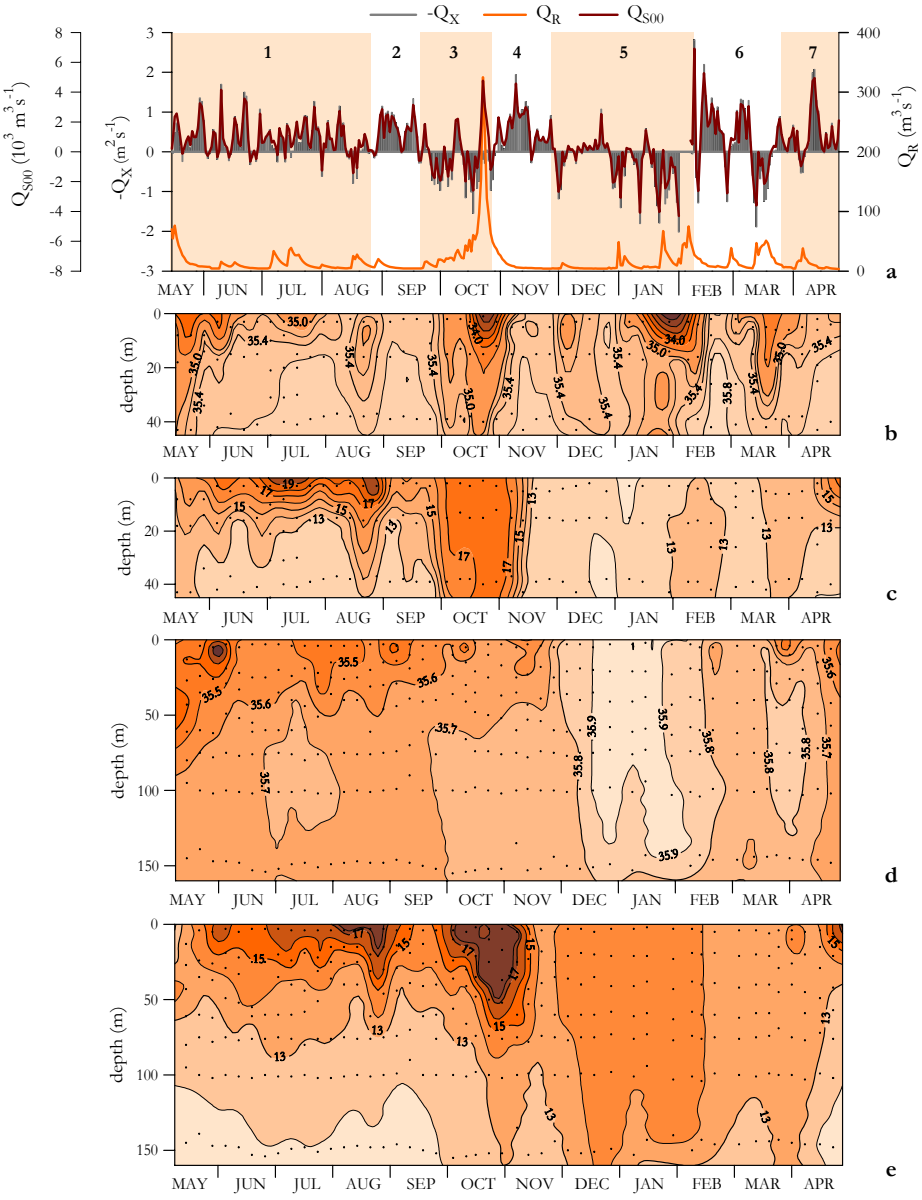

Figure 2.2 Time course of (**a**) Ekman transport, $-Q_X$ ($m^2 s^{-1}$), continental runoff, $-Q_R$ ($m^3 s^{-1}$) and surface water flux at stn 00, Q_{S00} (10^3 $m^3 s^{-1}$), (**b**) salinity at stn 00, (**c**) temperature (ºC) at stn 00, (**d**) salinity at stn 03 and (**e**) temperature (ºC) at stn 03. The seven different periods are shown in panel (**a**) and the correspondences in Table 2.1

The position of the convergence front between IPC and continental waters along the Ría de Vigo depends on the relative importance of $-Q_X$ and Q_R. Álvarez-Salgado et al. (2000) demonstrated that the residual circulation at stn 00 could be explained with these two variables by the equation:

$$Q_{S00} = 16\,(\pm 4)\cdot 10^{-3} Q_R - 2.3\,(\pm 0.2)\cdot 10^{-3} Q_X \qquad (2.4)$$

where Q_{S00} (10^3 $m^3 s^{-1}$) is the surface water flux at stn 00 (Fig. 2.2a). Considering this flux and the volume of the ría from the inner reaches to stn 00 (0.53 km^3), renewal rates were estimated for every period (Table 2.1). Under summer stratification and upwelling conditions, the residual circulation was positive (Q_{S00} = 0.8 ± 0.1 and 1.3 ± 0.1 10^3 $m^3 s^{-1}$, respectively) with large renewal rates (13 ± 2 and 21 ± 2% d^{-1}). During the downwelling period, the flux was virtually stopped (Q_{S00} = 0.0 ± 0.1 10^3 $m^3 s^{-1}$), because of enhanced runoff balancing the downwelling pattern, with a renewal of only 2 ± 2% d^{-1}. Larger renewal rates occurred during the transitional period (29 ± 3% d^{-1}). The average renewal rate for the study year was 9 ± 2% d^{-1}, and the residual circulation at stn 00 kept positive at 0.6 ± 0.1 10^3 $m^3 s^{-1}$.

At stn 00, period average concentrations of particulate organic matter, POC and p-CHO (Fig. 2.3a-b), showed maxima in surface waters during summer stratification (48 and 11.0 μM C, respectively), and minima at 15 m during the transitional and poleward periods (10 and 0.4 μM C, respectively). In the mid-shelf station (Fig. 2.3c-d) maxima were located at the surface, during upwelling events for POC (14 μM) and during summer stratification for p-CHO (1.8 μM C). Concentrations at the bottom were larger than at stn 00, suggesting the existence of a bottom nepheloid layer due to resuspension of organic rich sediments. The lowest concentrations were also found during the transitional and IPC periods. In general, there was a good agreement between POC and p-CHO distributions (r = +0.88, p < 0.001, n = 298).

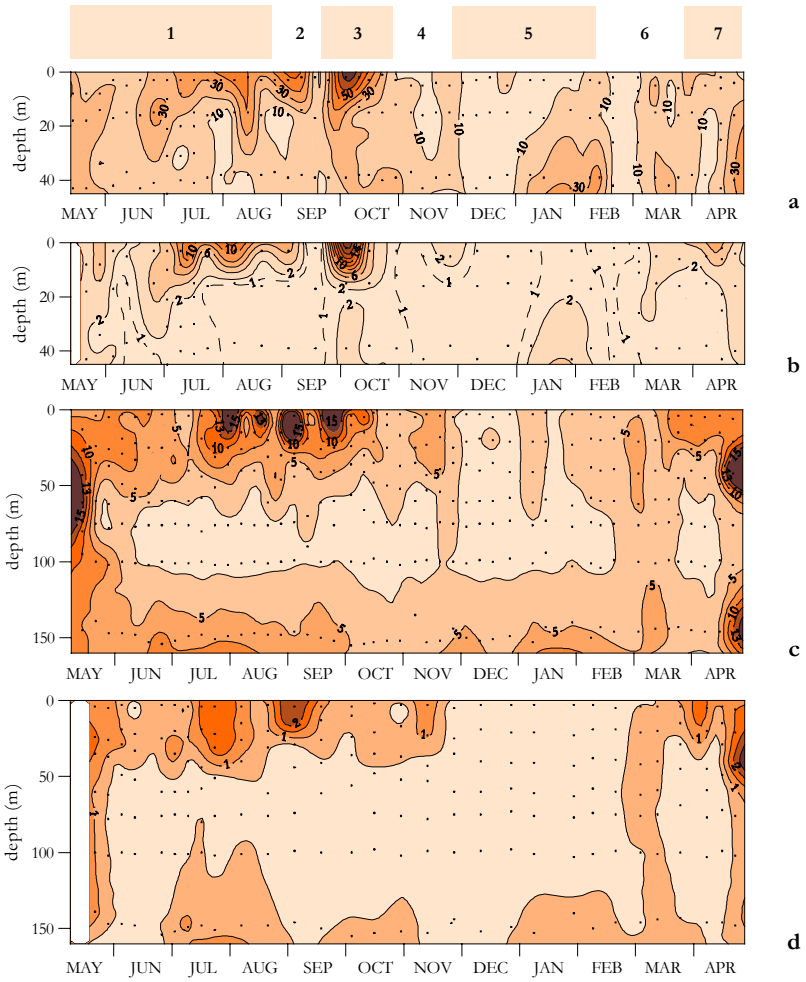

Fig. 2.3 Time course of (**a**) POC (μM) at stn 00, (**b**) p-CHO (μM C) at stn 00, (**c**) POC (μM) at stn 03 and (**d**) p-CHO (μM C) at stn 03 during the study period

Average POC and p-CHO (stn 00, Fig. 2.4a-b; stn 03, Fig. 2.5a-b) decreased monotonically with depth, although a significant rise was observed at the bottom layer ($p < 0.001$). Even concentrations at the innermost station were higher than at the outermost one, the contribution of carbohydrates to POC was similar in both of them (14 ± 6%). The average profile of the percentage of p-CHO showed a significant decrease ($p < 0.001$) with depth at stn 00 (Fig. 2.4c). At stn 03 (Fig. 2.5c) it was remarkable an absolute maximum at 75-100 m

depth. The slope of the correlation between p-CHO and POC (regression model II) was 0.26 ± 0.01 for stn 00 and 0.12 ± 0.01 for stn 03 (Table 2.2). This suggests that 26 ± 1% of the POC produced at the innermost station was p-CHO, whereas at the mid-shelf station the percentage decrease up to 12 ± 1%. The origin intercept, i.e. the fraction of p-CHO that did not covary with POC, represented the residual organic carbon that remained when p-CHO was nil. At stn 00 this residual POC was about 1.8 ± 0.2 µM C (11% of average POC at stn 00), but at stn 03 the origin intercept was not significant.

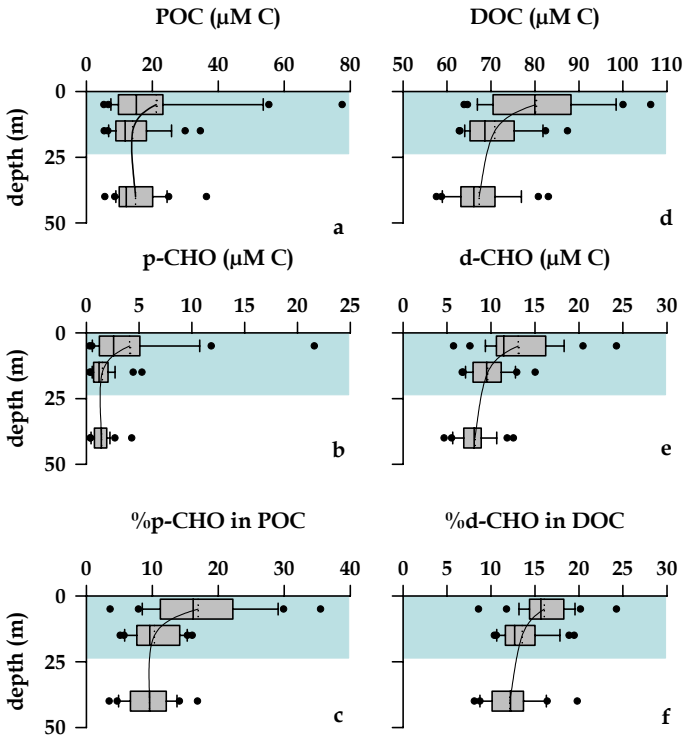

Fig. 2.4 Box and whisker plot of (**a**) POC (µM), (**b**) p-CHO (µM C), (**c**) %p-CHO in POC, (**d**) DOC (µM), (**e**) d-CHO (µM C) and (**f**) %d-CHO in DOC for the whole date set at stn 00. Fifty percent of the data are included within the limit of the boxes and the caps represent the 10th and 90th percentiles. Solid lines represent the average profiles. Shadow area symbolize the average photic layer

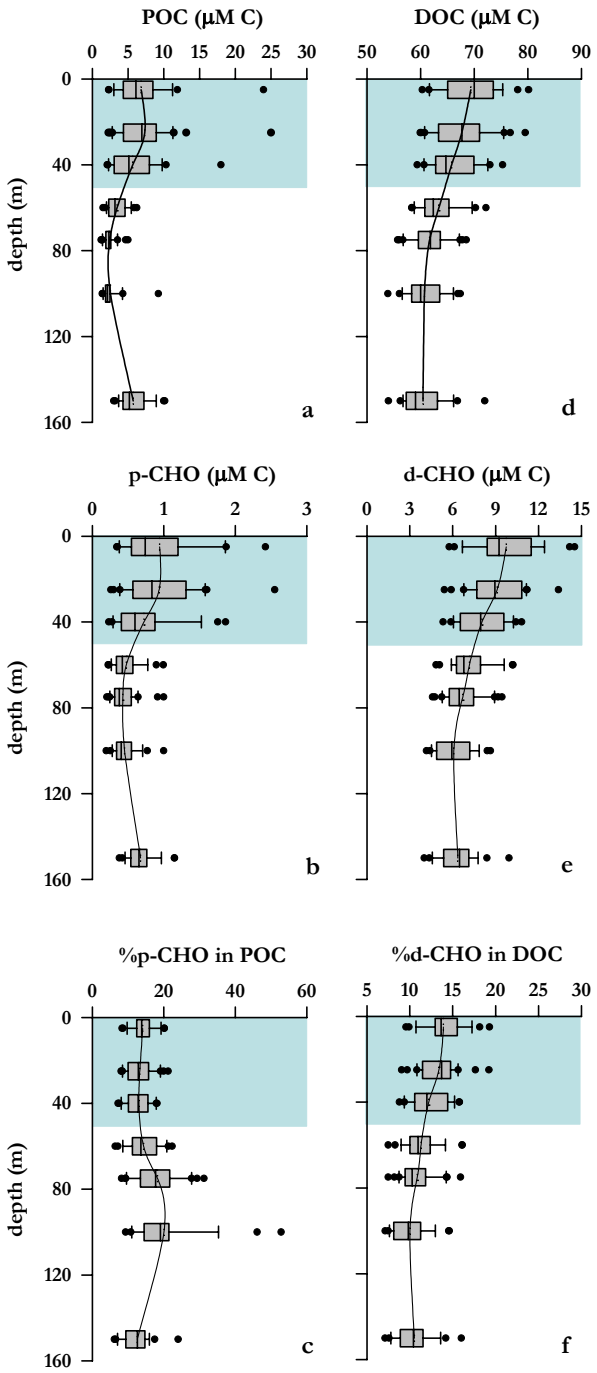

Fig. 2.5 Box and whisker plot of (**a**) POC (µM), (**b**) p-CHO (µM C), (**c**) %p-CHO in POC, (**d**) DOC (µM), (**e**) d-CHO (µM C) and (**f**) %d-CHO in DOC for the whole date set at stn 03. Fifty percent of the data are included within the limit of the boxes and the caps represent the 10th and 90th percentiles. Solid lines represent the average profiles. Shadow area symbolize the average photic layer

Surface accumulation of DOC occurred during downwelling and summer stratification periods (>90 μM C) and upwelling period (90 μM C) at stn 00, and during summer stratification, upwelling and spring periods (70-90 μM C) and downwelling period (70 μM C) at stn 03 (Fig. 2.6a,d). Relatively high average DOC values were found at 100 and 150 m in the outermost station during the IPC period. Average minima occurred in bottom waters and for the periods of transition and winter mixing. At the period of enhanced runoff in October, large concentrations were observed throughout the water column at stn 00. DOC correlated well with salinity and temperature (r = +0.77, p < 0.001, n = 298), indicating that water masses mixing was a relevant process to explain DOC distributions.

The time evolution of d-CHO was similar to DOC (r = +0.81, p < 0.001, n = 298), with surface maxima when the water column was stratified, and during the downwelling period due to the high runoff (17 and 12 μM C at stn 00 and 03, respectively), and lower values at deeper layers. This pattern was observed in PCHO too (Fig. 2.6b,e). By contrast, the distribution of MCHO (Fig. 2.6c,f) was more homogeneous and showed lower concentrations. d-CHO and PCHO correlated significantly with temperature and salinity (r = +0.69, p < 0.001, n = 298 and r = +0.67, p < 0.001, n = 298, respectively).

The average DOC and d-CHO profiles (stn 00, Fig. 2.4d-e) displayed the expected maximum values at the surface and decreased significantly with depth (p < 0.001). The same pattern was observed at stn 03 (Fig. 2.5d-e), but in this case with lower concentrations and less variability in the upper layer. Typical DOC and d-CHO values found at stn 00 vary from 80 μM and 13μM C at the surface layer and 65 μM and 8 μM C at the bottom, respectively. On average d-CHO made up 13 ± 3% of DOC, showing higher values at the surface layer that decreased significantly (p < 0.001) with depth (Fig. 2.4f, stn 00 and Fig. 2.5f, stn 03).

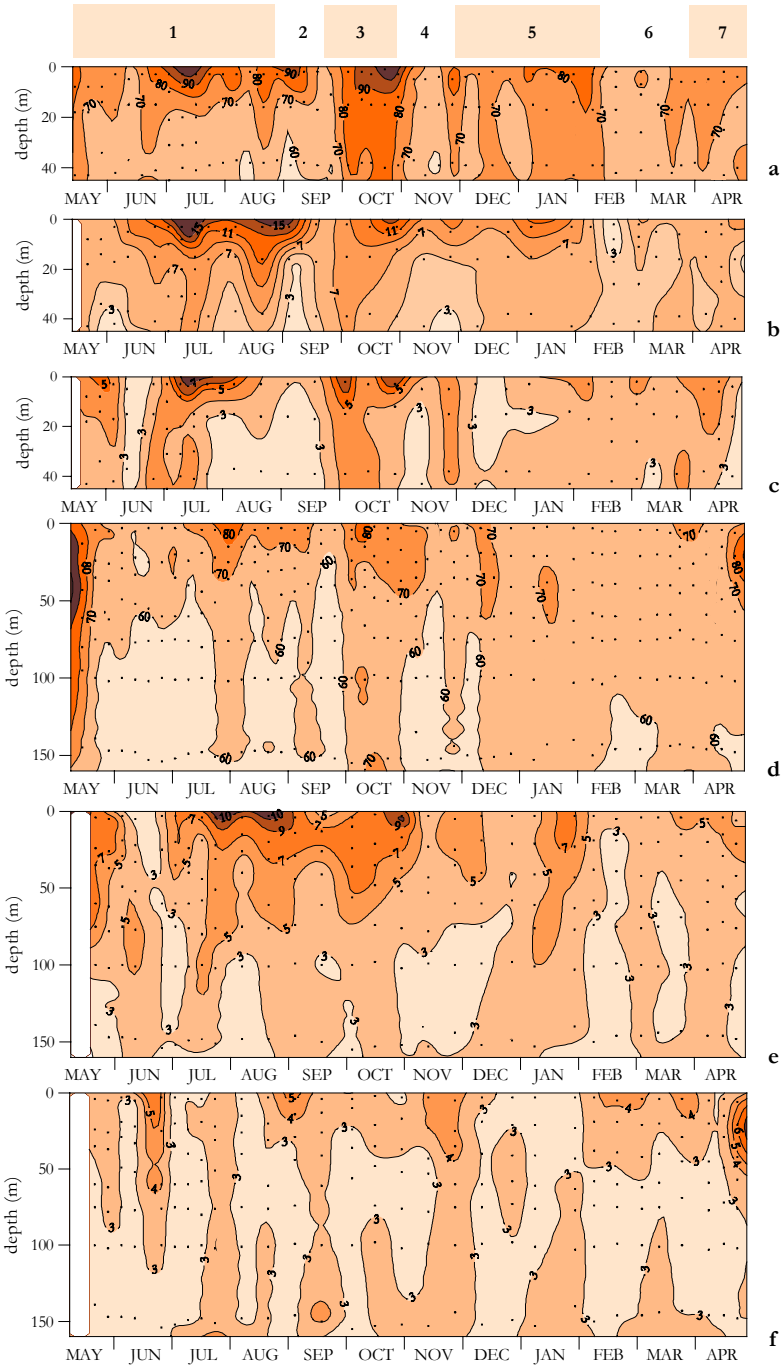

Fig. 2.6 Time course of (**a**) DOC (μM) at stn 00, (**b**) PCHO (μM C) at stn 00, (**c**) MCHO (μM C) at stn 00, (**d**) DOC (μM) at stn 03, (**e**) PCHO (μM C) at stn 03 and (**f**) MCHO (μM C) at stn 03 during the study period

Table 2.2 Selected significant ($p < 0.001$) linear regressions among physical and biogeochemical variables: particulate carbohydrates (p-CHO), particulate organic carbon (POC), dissolved carbohydrates (d-CHO), dissolved organic carbon (DOC), total carbohydrates (t-CHO), total organic carbon (TOC), dissolved polysaccharides (PCHO) and temperature (T). Numbers in brackets are the standard error of the coefficients

Variables	Equation	*r*	n
p-CHO *vs.* POC			
stn 00	p-CHO = -1.8 (±0.2) + 0.26 (±0.01) POC	+0.88	97
stn 03	p-CHO = 0.08 (±0.03) + 0.12 (±0.01) POC	+0.86	201
d-CHO *vs.* T, DOC			
stn 00	d-CHO = -16 (±4) + 0.4 (±0.1) T + 0.29 (±0.03) DOC	+0.82	97
stn 03	d-CHO = -16 (±4) + 0.3 (±0.1) T + 0.31 (±0.04) DOC	+0.71	201
TOC *vs.* T, POC			
stn 00	TOC = 22 (±6) + 3.1 (±0.5) T + 1.4 (±0.1) POC	+0.93	97
stn 03	TOC = 21 (±3) + 2.8 (±0.2) T + 1.8 (±0.1) POC	+0.86	201
t-CHO *vs.* T, p-CHO			
stn 00	t-CHO = -4 (±2) + 0.9 (±0.2) T + 1.6 (±0.1) p-CHO	+0.90	97
stn 03	t-CHO = -5 (±1) + 0.8 (±0.1) T + 4.7 (±0.5) p-CHO	+0.75	201
PCHO *vs.* d-CHO			
stn 00	PCHO = -1.8 (±0.2) + 0.82 (±0.02) d-CHO	+0.96	97
stn 03	PCHO = -1.8 (±0.2) + 0.87 (±0.02) d-CHO	+0.92	201

d-CHO variability can be explained as a linear combination of temperature and DOC (regression model I for T and combination of regression models I and II with $w_Y = 0.8$ for DOC; $r = +0.82$, $p < 0.001$ at stn 00 and $r = +0.79$, $p < 0.001$ at stn 03; Table 2.2). Figure 2.7c shows the covariation between d-CHO and DOC anomalies, calculated as: $a\,Y = Y - a_0 - a_1\,T$ (where a_0 and a_1 are the coefficients of the linear multiple regression of Y with temperature). These anomalies (*a* d-CHO from correlation of d-CHO *vs.* T in Fig. 2.7a, and *a* DOC from correlation of DOC *vs.* T in Fig. 2.7b) retained only the variability associated to the biogeochemical processes. Therefore, these multiple regressions explain the changes of dissolved carbohydrates as a function of water masses mixing (T) and biogeochemistry (DOC). The d-CHO/DOC slope, independent of water masses mixing, indicated that d-CHO represented 29 ± 4% of the net production of DOC at stn 00; this value was not significantly different from the obtained at stn 03 (31 ± 4%, Table 2.2).

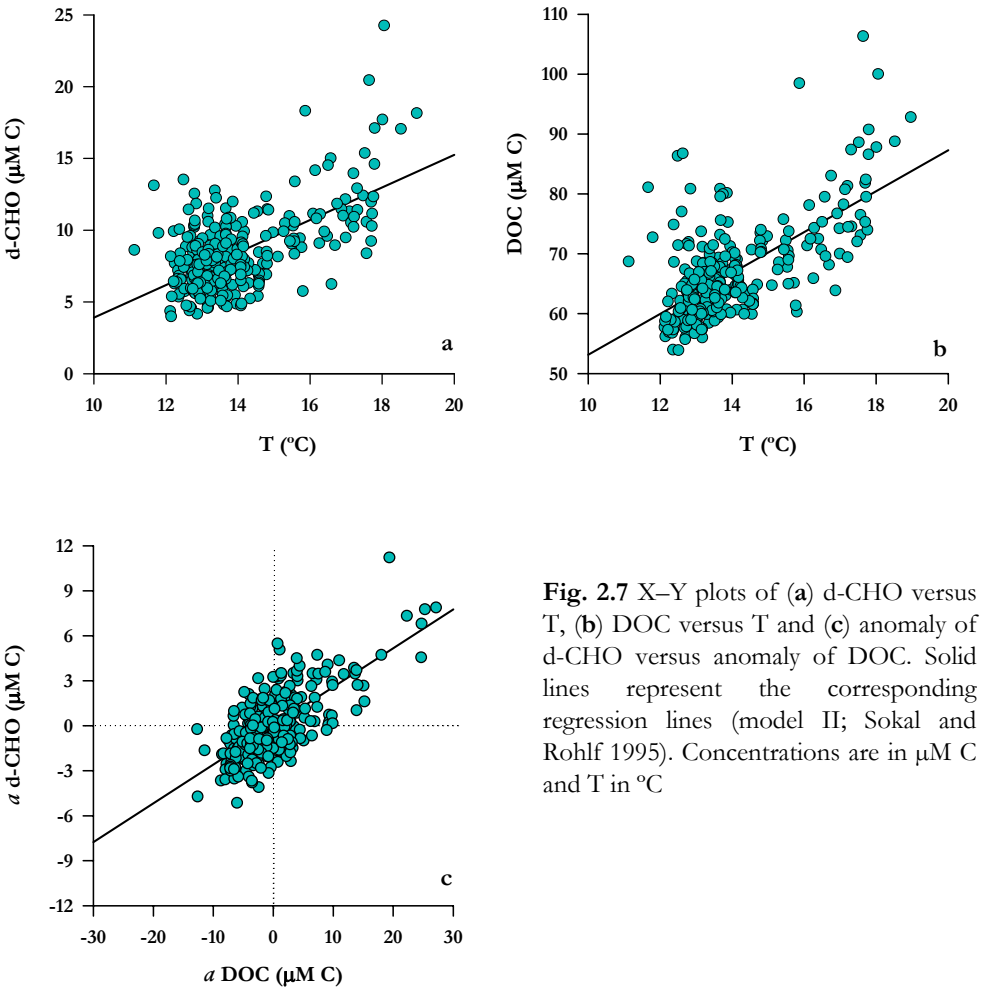

Fig. 2.7 X–Y plots of (**a**) d-CHO versus T, (**b**) DOC versus T and (**c**) anomaly of d-CHO versus anomaly of DOC. Solid lines represent the corresponding regression lines (model II; Sokal and Rohlf 1995). Concentrations are in µM C and T in ºC

A carbohydrate budget for the NW Iberian upwelling

A rough estimation of the surface carbon excess can be performed with a simple 2-endmember mixing model, one endmember being the freshwater input (F), and the other endmember the bottom water at the study site. For the case of DOC we can write:

$$\Delta DOC = DOC_S - \left(\frac{S_S}{S_B} \cdot DOC_B + \frac{S_B - S_S}{S_B} \cdot DOC_F \right) \qquad (2.5)$$

where ΔDOC is the surface DOC excess, DOC_S and S_S are the DOC and salinity at the surface layer, DOC_B and S_B are the DOC and salinity at the bottom, and DOC_F is the DOC in continental runoff. The same equation can be written for POC, p-CHO, d-CHO, PCHO and MCHO, and for the two study sites. River Oitabén-Verdugo is our freshwater endmember, considering the concentrations obtained at the Eiras reservoir (S = 0.00).

Seasonal accumulation of POC (ΔPOC) was higher at the innermost station (6.5 and 4.2 μM, respectively). The same occurred with particulate carbohydrates ($\Delta p\text{-}CHO$) with 2.5 μM C at stn 00 and 0.2 μM C at stn 03, which resulted in ~40% of POC accumulation as carbohydrates at stn 00, but just ~6% at the mid-shelf station.

As it has been pointed out before, a DOM excess was observed in surface waters as compared with bottom waters at the two sites through the study period. The average excesses for stn 00 were 10.8 μM and 4.5 μM C of DOC and d-CHO, respectively. In the case of stn 03, ΔDOC and $\Delta d\text{-}CHO$ were 8.3 μM and 2.7 μM C, respectively. The percentage of carbohydrates in this fraction was 42% for the innermost station, whereas at the mid-shelf station the value was lower (33%). The DOM accumulation depended on the hydrographic conditions; the excess was maximum during the upwelling period (18.8 μM and 7.5 μM C for DOC and d-CHO, stn 00) and minimum during the winter mixing period (1.9 μM and 0.3 μM C for DOC and d-CHO, stn 00). At stn 03 the excess was lower and less variable. The highest accumulations occurred during summer stratification and upwelling, and they were minima during the IPC period.

Calculated renewal rates for stn 00 allowed estimation of the net production of the inner Ría de Vigo. In average 1.0 μmol C L^{-1} d^{-1} of DOC and 0.4 μmol C L^{-1} d^{-1} of d-CHO, were produced. During the maximum accumulation period (upwelling) 3.9 and 1.6 μmol C L^{-1} d^{-1} of DOC and d-CHO, were net produced.

In the period of winter mixing (lower accumulation) the estimated production was only 0.3 and 0.1 μmol C L^{-1} d^{-1}.

Correlation of TOC (total organic carbon) with T and POC (regression model I for T, combination between regression models I and II with w_Y = 0.4 in stn 00 and w_Y = 0.2 in stn 03 for POC; Table 2.2) showed different results at the two study sites. Every mol of POC generated 0.4 ± 0.1 moles of DOC at stn 00 and 0.8 ± 0.1 moles at stn 03. A similar calculation for t-CHO (total carbohydrates), T and p-CHO (regression model I for T, regression model II for p-CHO in stn 03 and combination between regression models I and II with w_Y = 0.7 for p-CHO in stn 00; Table 2.2) indicated larger differences between both locations. One mol of p-CHO produced 0.6 ± 0.1 moles of d-CHO in stn 00, whereas it made 3.7 ± 0.5 moles of d-CHO at stn 03.

Mono- to polysaccharides ratio of d-CHO

The average percentage of monosaccharides in d-CHO (Fig. 2.8a-b) increased slight but significantly with depth ($p < 0.001$) at the two study sites. Similar average values were obtained for the two stations (30-40% MCHO), whereas in river samples the percentage of MCHO was higher and more variable (~50%, Fig. 2.8c). Correlation of PCHO and d-CHO (regression model II, Table 2.2) provided a slope of 0.82 ± 0.02 at stn 00 and 0.87 ± 0.02 at stn 03, which indicated that less than 20% of the d-CHO variation was due to MCHO.

The mono- to polysaccharides ratio in Δ*d-CHO* was very low in both stations: MCHO accounted for 14-18% of Δ*d-CHO*. The production rate at stn 00 was 0.1 and 0.4 μmol C $L^{-1}d^{-1}$ of MCHO and PCHO, respectively. Higher average percentages of Δ*MCHO* were found in the periods of lower DOM accumulation (during winter mixing and spring). Higher production at the innermost station occurred during the upwelling period, 0.2 and 1.5 μmol C L^{-1} d^{-1} of MCHO and PCHO, respectively.

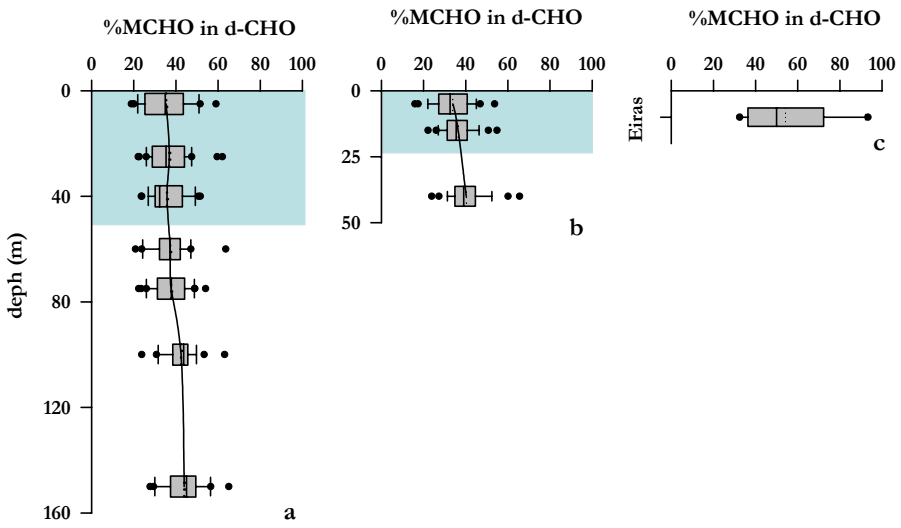

Fig. 2.8 Box and whisker plot of (**a**) %MCHO in d-CHO at stn 00, (**b**) %MCHO in d-CHO at stn 03 and (**c**) %MCHO in d-CHO at Eiras station. Fifty percent of the data are included within the limit of the boxes and the caps represent the 10th and 90th percentiles. Solid lines represent the average profiles. Shadow area symbolize the average photic layer

The freshwater endmember presented higher DOC and d-CHO concentrations than seawater samples: 91.1 and 47.9 μM C, respectively (1.1 and 3.6 times the values of the surface layer at stn 00). It is noticeable the MCHO concentration, 23.5 μM C, 5.5 times higher than at stn 00. Particulate material was also more abundant at the Eiras reservoir than at stn 00: 49.0 μM for POC (2.1 times higher) and 13.6 μM C for p-CHO (3.2 times higher).

DISCUSSION

Hydrographic control of the carbohydrates accumulation

Our results corroborate that seasonal DOC accumulation is closely connected with stratification, as it was proposed by Carlson et al. (1994) for temperate, subpolar and continental shelf regions that exhibit convective mixing and spring re-stratification. The conspicuous succession of wind stress/relaxation cycle that occur in the NW Iberian Peninsula is the reason behind the large productivity of this system and has a great importance on DOC cycling.

Nutrient entry to the photic layer takes place during the 'spin up' phase of upwelling events whereas phytoplankton growth and accumulation happens during the 'spin down' phase. DOM accumulation occurs after the bloom, accompanying phytoplankton decay. This hydrographic control of growth and accumulation of phytoplankton is a common phenomenon in coastal upwelling systems at temperate latitudes (Barber & Smith 1981, Zimmerman et al. 1987). DOC accumulation at the end of blooms, during the period of relaxation, seems to be a quite general pattern too (Kirchman et al. 1994, Norrman et al. 1995, Chen et al. 1996, Doval et al. 1997), and in this study it was demonstrated that accumulation of carbohydrates follow the same pattern. Information about seasonal accumulation of carbohydrates is scarce, but Williams (1995) found evidences for the seasonal accumulation of dissolved carbon-rich materials, from mid to late summer. This work corroborates that these substances were carbohydrates, which makes up 29-31% of the DOC changes in the water column, and 33-42% of the DOC accumulation in seasonal thermocline waters.

It was remarkable the presence at the mid shelf of slightly warm (>14ºC) and salty (>35.8) water all over the water column from December to February due to the presence of the IPC. This IPC transports to our latitudes aged and remineralised subtropical waters, with low DOC, POC, d-CHO and p-CHO concentrations. However, during the IPC period, slightly high values of organic matter were found in bottom waters of stn 03 (100 and 150 m), probably due to offshore export from the bottom ría under conditions of negative residual circulation. During winter, low and homogeneous concentrations of MOD and MOP were observed, because of reduced primary production (<0.2 g C m^{-2} d^{-1}; Álvarez-Salgado et al. 2003).

As indicated in previous studies in the Rías Baixas (Fraga & Vives 1961, Fraga 1967, Doval et al. 1997) the high concentrations of POM in bottom waters can be due to the sedimentation of phytoplankton blooms, resuspension of organic-

rich sediments or zooplankton accumulation. This bottom nepheloid layer has been recurrently observed in the Iberian upwelling (McCave & Hall 2002) and in other coastal regions (e.g. Sherwood et al. 1994). It was noticeable that p-CHO follow the same pattern that POC in the ría. However, at the middle shelf, the percentage of carbohydrate was lower at bottom than at 75-100 m. This pattern could be explained on basis of a fractionated mineralization of sinking POM, with N and P rich compound been preferentially mineralised at mid depths and carbohydrates at the bottom layers (Ríos et al. 1998).

The role of carbohydrates in the carbon balance of a marine ecosystem

The range of d-CHO concentrations at stn 00 was similar to those provided by Hung et al. (2003a) for the Gulf of Mexico (4-22 μM C) or by Witter & Luther III (2002) for the U. S. Middle Atlantic Bight (3-17 μM C). However, concentrations of d-CHO were lower at stn 03 and more similar to the oceanic values provided by Pakulski & Benner (1994).

The contribution of p-CHO to the POC pool was ~15% for both stations, a value halfway between those presented by Hung et al. (2003a) in the Gulf of Mexico (18% for 2000 and 9% for 2001). On the other hand, d-CHO accounted for 13 ± 3% of DOC, very close to the mean values provided by Pakulski & Benner (1994) for the North Atlantic Ocean (15 ± 2%) and by Børsheim et al. (1999) for the Trondheimsfjord (16 ± 2%). It was widely confirmed that the percentage is higher at the surface layers (14-16% in this study).

Correlations between p-CHO and POC give different results for both stations. At the outermost station only the 12 ± 1% of the POC produced was p-CHO and the origin intercept was nearly zero, i.e., there are not residual carbon material that remains when p-CHO is nil. Similar results were published by Hung et al. (2003a) for the Gulf of Mexico: 18 ± 1% and 8.7 ± 0.4% in 2000 and 2001, respectively, with origin intercepts not significantly different from

zero. However, the situation at stn 00 was different: the contribution of p-CHO to POC formed was higher (26 ± 1%). In addition, there was a POC pool more recalcitrant than p-CHO that accounted for 1.8 ± 0.2 μM C. These results agreed with the calculated accumulations, higher in both cases (POC and p-CHO) at the innermost station, and richer in carbohydrates. This suggests that the interior of the ría is the most productive sector, which exports particulate matter to the adjacent shelf and the ocean. The lower percentage of p-CHO at the mid shelf station pointed to the existence of degradation and sinking processes during offshore transport, especially in carbohydrates pool.

Carbohydrates in the fresh dissolved material are not significantly different between the ría and the shelf (29-31%). These values are larger than the results obtained by Hung et al. (2003a) in the Gulf of Mexico (21%), but they are similar to those proposed by Børsheim et al. (1999) in two coastal stations in the Trondheimsfjord (28-30%) and by Pettine et al. (1999) in the northern Adriatic Sea (30%). It has been demonstrated that d-CHO covaries with DOC at the time scale of the sampling frequency (2 weeks).

Average ΔDOC in the middle ría was 11 μM, but during the upwelling period this value increases up to 19 μM, similar to that provided by Doval et al (1997) for the same station during the 1995 upwelling season (21 μM). Larger percentage of carbohydrates accumulated at the innermost station: 42% as compared with 33% at the shelf station. During the upwelling event, when offshore export is the most important physical process, the percentages were more similar: 38% and 36%, respectively. Estimations of the production at the innermost station give higher values during this upwelling event (3.9 and 1.6 μmol C $L^{-1}d^{-1}$ for DOC and d-CHO, respectively), ten times larger than those calculated during winter mixing (0.3 and 0.1 μmol C $L^{-1}d^{-1}$, respectively). To our understanding no carbohydrate production data were published before. In the

case of DOC, our value is comparable with the obtained by Doval et al. (1997) for the same study area during the upwelling season (4.2 μmol C $L^{-1}d^{-1}$).

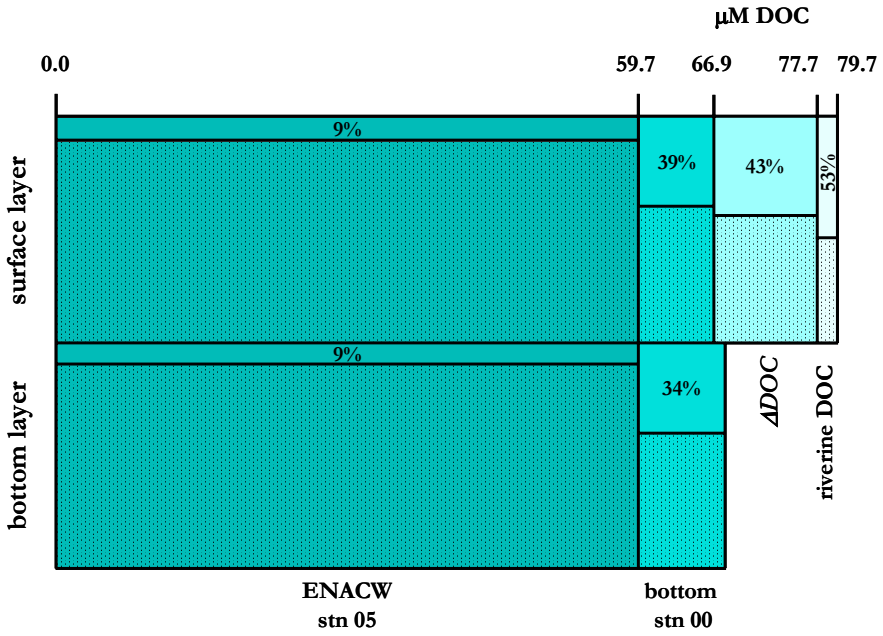

Fig. 2.9 Tentative partitioning of DOC at stn 00 in surface and bottom waters during seasonal cycle. % of d-CHO is indicated

Figure 2.9 presents a tentative partitioning of the DOC pools at stn 00 in surface and bottom waters. ENACW provides a major part of the DOC. This water mass contains minimum proportions of d-CHO (only 9% of DOC). The main d-CHO contributions are the riverine input (53% of DOC) and, especially, the new production (43%).

As it has been pointed out before, good correlations were found between TOC and POC, and t-CHO and p-CHO (Table 2.2). The slopes for both data sets give different results: one mol of POM generates more DOM at middle shelf, but differences are more notable for carbohydrates. Values are higher at outermost station because of dissolved materials are preferentially exported horizontally whereas particulate material preferentially sunk to the sediments. In addition, waters at the middle ría are mesotrophic whereas at the middle shelf

they are more oligotrophic, leading to a preferential accumulation of dissolved carbohydrates (Williams 1995).

Lability of DOM

The slight increase of the contribution of MCHO to d-CHO with depth and the average values of 30-40% observed during the study period has been described before in the literature (Pakulski and Benner 1994, Hung et al. 2001). It has also been reported in these works the nearly-uniform (~4μM C) vertical distribution of MCHO at many locations (3 ± 1 μM C in this study). Williams & Gray (1970) have hypothesised that MCHO and other low-molecular-weight organic substrates are rapidly assimilated to low concentrations by bacteria. This assumption is in accordance with the consideration of MCHO as an indicator of lability.

Percentages of MCHO in Δ*d-CHO* were much lower (14-18%) than in the bulk d-CHO (30-40%), suggesting again the preferential accumulation of semi-labile PCHO rather than labile MCHO. The percentage of accumulated MCHO increased during the periods of low accumulation, but it was not due to enhanced MCHO but depressed PCHO production. In all cases, the most productive period for both carbohydrate pools was the upwelling event.

The time course of PCHO through out the study period was similar to d-CHO and they correlate significantly. The slope of the correlations (regression model II) indicated that about 82% at stn 00 and 87% at stn 03, of the d-CHO change was due to PCHO.

Freshwater inputs have organic matter loads higher than the inner- and outermost stations, but the largest differences were found in carbohydrates. The p-CHO contribution to POC increases up to 32%, but more remarkable is the contribution of d-CHO to DOC, nearly 50% averaged during the study period. Studies carry out in estuaries indicate the major contribution of carbohydrates to the C pool of rivers (Senior & Chevolot 1991, Hung et al.

2001, Witter & Luther III 2002). The degree of polymerisation of these sugars is different from the d-CHO pool in seawater: percentages of MCHO increases in riverine waters (30-90%), in accordance with others authors as Senior & Chevolot (1991),who presented values ranging from 15 to 90% in the Elorn Estuary (Brest, France).

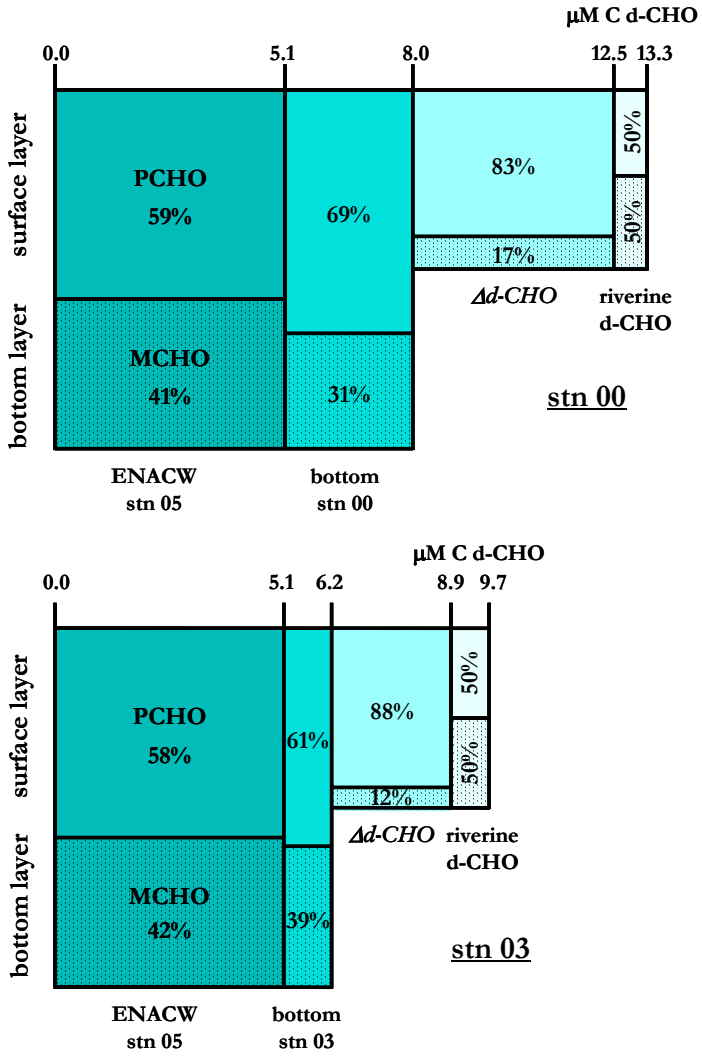

Fig. 2.10 Tentative partitioning of d-CHO at stn 00 and 03, in surface and bottom waters, during seasonal cycle. % of PCHO and MCHO are shown

Figure 2.10 presents the different dissolved carbohydrates pools calculated for the two different study sites, and the PCHO/MCHO contributions. The degree of polymerisation gives an idea of the lability of the material; semi-labile materials (81-88% of PCHO) compose d-CHO accumulations whereas riverine material is more labile (51% of PCHO). Similar proportions of MCHO were found in both sites, but with higher concentrations at the innermost station.

CONCLUSIONS

Carbohydrates in the NW Iberian coastal upwelling system follow the same seasonal pattern than the organic carbon pool, being strongly influenced by physical and biological processes. Thereby, phytoplankton growth and POM accumulation (both POC and p-CHO) was observed during the upwelling period, whereas DOM (DOC and d-CHO) accumulates during the relaxation of the upwelling pulse, when phytoplankton biomass begins to decay.

Negative residual circulation dominated during IPC period, with low values of DOM and POM except in the bottom layers at the mid shelf.

The surface excess of DOC is richer in carbohydrates than the bulk DOC. The percentage increases from 12-14% in DOC to 33-42% in Δ*DOC*, indicating that d-CHO is a main component of the freshly produced material in comparison with aged ENACW, where only 9% of DOC are d-CHO.

The surface Δ*d-CHO* presents a higher percentage of PCHO than the rest of the d-CHO pool: 80-90% of the carbohydrates excess are polysaccharides, suggesting that the material is essentially semi-labile.

Chapter 3:

DOM fluorescence, a tracer for biogeochemical processes in a coastal upwelling system (NW Iberian Peninsula)

Chapter 3, the research work presented in this chapter is also a contribution to the paper:

M. Nieto-Cid, X. A. Álvarez-Salgado, J. Gago, F. F. Pérez. 2005. **DOM fluorescence, a tracer for biogeochemical processes in a coastal upwelling system (NW Iberian Peninsula)**. Mar Ecol Prog Ser, *in press*

Resumen: La fluorescencia de la materia orgánica disuelta (FDOM) ha sido determinada por primera vez durante un ciclo estacional completo en un sistema de afloramiento costero (Ría de Vigo, NO España). Se detectaron y cuantificaron las longitudes de onda de excitación/emisión específicas para las sustancias húmicas refractarias y para los aminoácidos aromáticos lábiles. La distribución de la fluorescencia de las sustancias húmicas marinas ($FDOM_M$) correlaciona significativamente con las sales nutrientes ($r = +0.62$, $p < 0.001$) y el oxígeno disuelto ($r < -0.71$, $p < 0.001$), una vez eliminado el efecto de la mezcla de masas de agua. Esto sugiere que las sustancias húmicas son un subproducto en los procesos de mineralización de la materia orgánica en las aguas profundas de la plataforma continental. Se ha estimado que entorno a un 10% del carbono orgánico degradado en la columna de agua es transformado en sustancias húmicas, las cuales son producidas en la ría con una tasa de ~0.1 ppb QS d^{-1}. La distribución de la fluorescencia de los aminoácidos aromáticos ($FDOM_T$) correlaciona de forma significativa con la distribución de proteínas particuladas ($r > +0.57$, $p < 0.001$). $FDOM_T$ puede utilizarse como trazador de las zonas de acumulación neta de materia orgánica disuelta lábil (DOM): **1)** la capa fótica (con una tasa de ~0.5 ppb Trp d^{-1}), donde el material lábil se produce por exudación del fitoplancton y/o lisis celular; y **2)** el lecho nefeloide (con una tasa de ~0.2 ppb Trp d^{-1}), debido a un aumento *in situ* de la actividad microbiana y/o una liberación desde las aguas intersticiales del sedimento.

Abstract: Fluorescence of dissolved organic matter (FDOM) was determined for the first time during a complete seasonal cycle in a coastal upwelling system (Ría de Vigo, NW Spain). Specific excitation/emission wavelengths for the refractory humic substances and the labile aromatic amino acids were detected and quantified. The distribution of the fluorescence of marine humic substances ($FDOM_M$) correlated significantly with nutrient salts ($r = +0.62$, $p < 0.001$) and dissolved oxygen ($r < -0.71$, $p < 0.001$), after removal of the effect of water masses mixing. It suggests that humic substances are a by-product of organic matter mineralization processes in shelf bottom waters. It was estimated that about 10% of the organic carbon degraded in the water column was transformed into humic substances, which were produced in the ría at a rate of about 0.1 ppb QS d^{-1}. The distribution of the fluorescence of dissolved aromatic amino acids ($FDOM_T$) correlated significantly with the distribution of particulate proteins ($r > +0.57$, $p < 0.001$). $FDOM_T$ can be used to trace sites of net accumulation of labile DOM: **1)** the photic layer (at a rate of about 0.5 ppb Trp d^{-1}), where labile DOM is produced from phytoplankton exudation and/or lysis; and **2)** the bottom nepheloid layer (at a rate of about 0.2 ppb Trp d^{-1}), due to an *in situ* enhancement of the microbial activity and/or a release from sediment pore waters.

INTRODUCTION

Seawater dissolved organic matter (DOM) is one of the largest and least understood reservoirs of reduced carbon of the earth's surface (Hedges 1992, 2002, Hansell 2002). Most efforts to characterise DOM have been focussed on the C/N/P elemental composition, while molecular constituents have not been studied in detail. Currently, less than 30% of the molecular composition of DOM is known (Yamashita & Tanoue 2003). Although information on the elemental composition of DOM is essential to understand the origin and fate of natural organic matter, knowledge of its molecular composition is crucial to provide insights about the dynamics of the DOM pool (Ogawa & Tanoue 2003). The main problem facing the molecular characterisation of DOM stems from the low concentrations of the individual constituents in seawater, a difficulty that has been partly overcame with the improvement of ultrafiltration methods (Amon & Benner 1996). Ultrafiltration is a powerful tool in combination with nuclear magnetic resonance techniques (Benner et al. 1992, Aluwihare et al. 1997, McCarthy et al. 1997, Clark et al. 1998, Hedges et al. 2002). Nevertheless, these methods require very large samples (10^2-10^3 litres), and the physical and chemical properties of the concentrate differed from the original sample. Simple, quick and sensitive methods are still necessary to combine DOM characterisation with the requirements of hydrographic sampling.

Fluorescence spectroscopy has been used in recent decades to characterise DOM. Results from these studies have provided valuable information about the chemical nature (fluorescence functional groups) and distribution (fluorescence intensity) of DOM. In addition to simplicity, sensitivity and quickness, the small sample volume requirement is an additional attraction of this technique. It was applied first to the study of humic substances (Cabaniss & Shuman 1987, Hayase et al. 1988, Chen & Bada 1992). Coble et al. (1990)

were the pioneers in the use of excitation-emission matrices (EEM) to study DOM fluorescence. EEMs helped to allocate the two main fluorophores of natural DOM: **1)** the humic-like fluorophores, studied since the 1960's; and **2)** the protein-like fluorophores, which are due to aromatic amino acids (Mopper & Schultz 1993, Determann et al. 1996, 1998, Coble et al. 1998).

Humic substances are a heterogeneous mixture of complex high-molecular-weight biopolymers with structures still not fully understood. They constitute a significant fraction of DOM: between 30-50% of dissolved organic carbon (DOC) in natural waters (Thurman 1985). Obernosterer & Herndl (2000) observed that humic compounds comprised 15 ± 7% of DOC in the Adriatic Sea and 43 ± 7% of DOC in coastal waters of the North Sea. Although humic substances are considered a refractory DOM pool, they are microbially produced and photochemically degraded. Therefore, the fluorescence of humic compounds is a suitable parameter to study these biogeochemical processes.

The fluorescence of aromatic amino acids (tyrosine, tryptophan and phenylalanine) is a useful indicator of the dynamics of dissolved free amino acids (DFAA) in general (Yamashita & Tanoue 2003). These simple molecules are among the most labile biogenic compounds. Therefore, protein-like fluorescence can be use to study the dynamics of labile DOM.

DOM fluorescence has mainly been used in studies of estuarine mixing (Jaffé et al. 2004), photodegradation (Obernosterer & Herndl 2000, Del Vecchio & Blough 2002) or DFAA distributions (Yamashita & Tanoue 2003). Comparatively, few works comparing DOM fluorescence with DOC or nutrients distributions have been performed (Chen & Bada 1992, Hayase & Shinozuka 1995, Chen et al. 2002) and all were focused on the humic-like fluorescence.

The importance of DOM for carbon and nutrient cycles is enhanced in coastal waters, where exudation by aquatic organisms and degradation of

marine and terrestrial plant matter produce large amounts of DOM (Nagata 2000, Carlson 2002). Coastal waters support 18-33% of global net primary production and 27-50% of global export production (Walsh 1991, Chavez & Toggweiler 1995, Wollast 1998). DOM production is especially intense in coastal upwelling areas in response to nutrient fertilisation from the adjacent ocean (Hansell & Carlson 1998a, Doval et al. 1997, Álvarez-Salgado et al. 2001a). Organic matter produced in upwelling areas can experience extreme oxidising and reducing conditions (Gagosian et al. 1978).

The NW Iberian Peninsula is characterised by **1)** an upwelling season, with successive upwelling pulses separated by short intervals of calm, which favour nutrient recycling and enhance primary production (Álvarez-Salgado et al. 1999); and **2)** a second season dominated by downwelling episodes, distinguished by low primary production rates. During an upwelling event, northerly winds cause the uplift of Eastern North Atlantic Central Water (ENACW) over the shelf, which enters the rías and enhances the characteristic 2-layer circulation pattern (Rosón et al. 1997). Other conspicuous phenomena in this region are the incursion of the Iberian Poleward Current (IPC) along the slope during winter, carrying subtropical waters to these latitudes (Haynes & Barton 1990, Álvarez-Salgado et al. 2003).

Previous studies of this coastal upwelling region focused on the elemental composition of DOM (Doval et al. 1997, Álvarez-Salgado et al. 1999, 2001b). A recent study in NW Iberian shelf waters, has devoted to the molecular characterisation of DOM. In a previous article, Nieto-Cid et al. (2004), Chapter 2, studied the role of carbohydrates in the DOM cycle of this system. The aim of this work is to use DOM fluorescence to further characterise DOM during a seasonal cycle. The value of humic-like fluorophores as indicators of the humification associated with mineralization processes, and of the protein-like fluorophores as indicators of DOM lability, are the key points in this study.

MATERIALS AND METHODS

Survey area. Two domains were sampled during this study: the Rías Baixas and the adjacent shelf (Fig. 3.1). A 2-layered residual circulation pattern characterises the rías, with an ingoing bottom current and an outgoing surface current during upwelling events, and a reversal of the flow during downwelling conditions. These large (>2.5 km^3), V-shaped, embayments respond predominantly to shelf winds (Gilcoto et al. 2001, Souto et al. 2003), and, to a lesser extent, to continental runoff. For the case of the Ría de Vigo, the main tributary is the river Oitabén-Verdugo, with an average flow of 18 m^3s^{-1} during the study period.

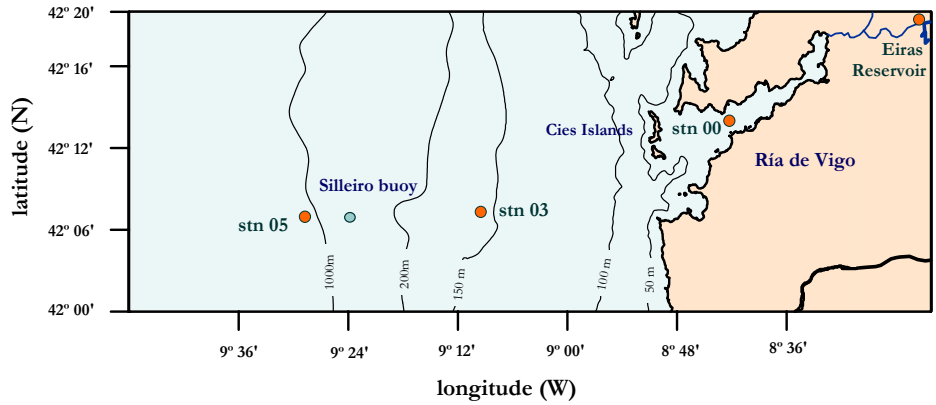

Figure 3.1 Map of the Ría de Vigo and the adjacent shelf (NW Iberian Peninsula). The positions of the three hydrographic stations and the SeaWatch buoy off Cape Silleiro are shown. The Eiras station, in the upper course of the river Oitabén-Verdugo, is also indicated

The circulation of shelf waters off the Rías Baixas is more complex; it is composed of a wind-driven long shore current and across-shore exchanges with the adjacent ocean and the rías. During the upwelling season, the rías and the shelf are coupled: shelf surface waters are imported from the rías and the bottom waters of the rías enter from the shelf. On the contrary, during the downwelling season, a convergence front develops between the shelf and the rías. The position of this front in the long shore direction depends on the

relative strength of coastal winds and continental runoff (Álvarez-Salgado et al. 2000).

Sampling strategy. Two stations were sampled weekly aboard RV Mytilus from May 2001 to April 2002: a mid-shelf station (stn 03; 42º07.8'N, 9º10.2'W; 150 m deep) and a mid-ría station (stn 00; 42º13.8'N, 8º51.0'W; 40 m depth in low water). Full-depth continuous conductivity-temperature-depth (CTD) profiles were recorded at each sampling site with a SBE 9/11 CTD device incorporated into a rosette sampler equipped with twelve 10-L Niskin bottles. Conductivity measurements were converted into practical salinity scale values (UNESCO 1985). Seawater samples were collected from 5, 25, 40, 60, 75, 100 and 150 m at stn 03, and 5, 15 and 40 m at stn 00. Samples for oxygen (O_2), nutrient salts, dissolved organic carbon and nitrogen (DOC/DON) and particulate organic carbon and nitrogen (POC/PON) analyses were collected every survey (weekly periodicity), whereas samples for DOM fluorescence (FDOM) were taken every two surveys (fortnightly periodicity).

In addition, one station in the upper course of the river Oitabén-Verdugo was sampled regularly during the seasonal cycle (Eiras reservoir, Fig. 3.1). Surface samples for DOC/DON, POC/PON, nutrients and DOM fluorescence were taken with a 1.7-L Niskin bottle. They were processed in the same way as the seawater samples.

Chemical analysis. Aliquots for dissolved and particulate organic matter analyses were collected in 500 mL acid-cleaned glass flasks and 5 L acid-cleaned PVC containers, respectively. Suspended organic matter was collected under low vacuum on precombusted (450ºC, 4 h) 25-mm ø Whatman GF/F filters for POC/PON (0.5-1.5 L of seawater filtered). All filters were dried overnight and frozen (-20ºC) before analysis.

Measurements of POC and PON were carried out with a Perkin Elmer 2400 CHN analyzer. Standards of acetanilide were run daily. The precision of the method was ±0.3 μM C and ±0.1 μM N.

Dissolved oxygen was determined by Winkler potentiometric end-point titration using a Titrino 720 analyser (Metrohm) with a precision of ±0.5 μmol kg^{-1}. The Apparent Oxygen Utilisation, AOU = O_2sat - O_2, was calculated using the algorithm proposed by Benson & Krause (UNESCO 1986) for oxygen saturation (O_2sat).

Samples for nutrient analyses were collected in 50 mL polyethylene bottles; they were kept cold (4 ºC) a few hours until analysis in the laboratory using standard segmented flow analysis (SFA) procedures. The precisions were ±0.02 μM for nitrite, ±0.1 μM for nitrate, ±0.05 μM for ammonium, ±0.02 μM for phosphate and ±0.05 μM for silicate.

DOM samples were filtered through precombusted (450ºC, 4 h) 47-mm ø Whatman GF/F filters in an acid-cleaned glass filtration system, under low N_2-flow pressure. Two aliquots were collected, for DOC/DON and DOM fluorescence.

Samples for the analysis of DOC/DON were collected in 10 mL precombusted (450ºC, 12 h) glass ampoules. After acidification with H_3PO_4 to pH < 2, the ampoules were heat-sealed and stored in the dark at 4ºC until analysis. DOC and DON were measured simultaneously with a nitrogen-specific Antek 7020 nitric oxide chemiluminescence detector, coupled in series with the carbon-specific Infrared Gas Analyser of a Shimadzu TOC-5000 organic carbon analyser (Álvarez-Salgado & Miller 1998). The system was standardized daily with a mixture of potassium hydrogen phthalate and glycine. The concentration of DOC and total dissolved nitrogen (TDN) was determined by subtracting the average peak area from the instrument blank area and dividing by the slope of the standard curve. The precision of measurements

was ±0.7 μM C for carbon and ±0.2 μM N for nitrogen. Their respective accuracies were tested daily with the DOM reference materials provided by Prof. D. Hansell (Miami University). We obtained an average concentration of 45.7 ± 1.6 μM C and 21.3 ± 0.7 μM N (n = 26) for the deep ocean reference (Sargasso Sea deep water, 2600 m) minus blank reference materials. The nominal DOC value provided by the reference laboratory is 44.0 ± 1.5 μM C; a consensus TDN value has not been set yet, but a mean value of 22.1 ± 0.8 μM N has been provided by Sharp et al. (2004) after the Lewes intercalibration exercise. DON was obtained by subtracting N_T (total inorganic nitrogen = ammonium + nitrite + nitrate) from TDN.

DOM fluorescence methodology. FDOM was measured with a Perkin Elmer LS 55 Luminescence spectrometer, equipped with a xenon discharge lamp, equivalent to 20 kW for 8 μs duration. The instrument has two monochromators that ranged between 200 and 800 nm for excitation wavelengths and between 200 and 900 nm for emission wavelengths. The detector was a red-sensitive R928 photomultiplier and a photodiode worked as reference detector. Slit widths were 10.0 nm for the excitation and emission wavelengths, and scan speed was set at 250 nm min^{-1}. Measurements were performed at a constant room temperature of 20ºC in a 1-cm quartz fluorescence cell. Milli-Q water was used as a reference for fluorescence analysis.

EEMs were performed to track the main fluorophores. These matrices were generated by combining 21 synchronous excitation-emission fluorescence spectra of the sample, obtained at a constant offset between the excitation and emission wavelengths of 10 nm. The spectra were collected starting from the highest excitation wavelength, to minimize the exposure of the sample to low-wavelength radiation and thereby minimize photodegradation. Milli-Q water EEMs were performed every day in order to correct the Raman scatter band.

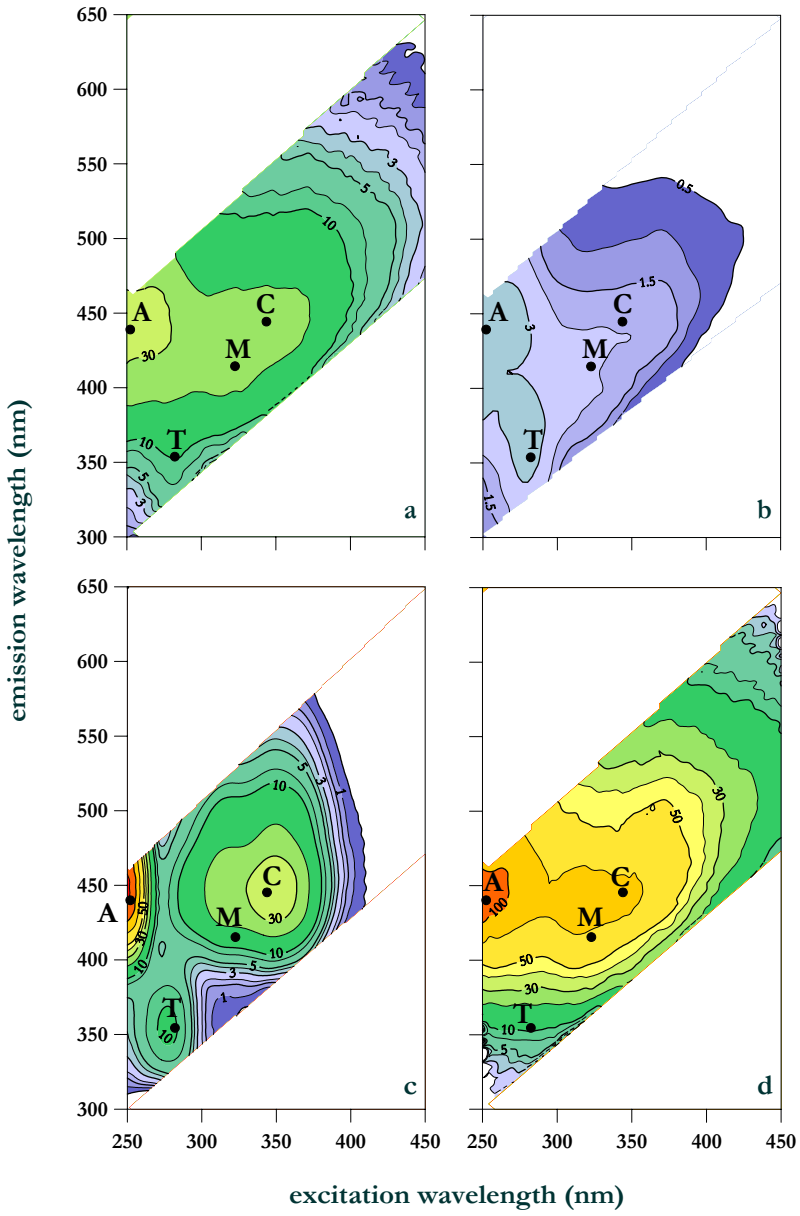

Figure 3.2 Excitation/emission matrices (EEMs) of (**a**) Oitabén-Verdugo river sample, (**b**) surface seawater sample at stn 00, (**c**) quinine sulphate (20 ppb) and tryptophan (30 ppb) in sulphuric acid 0.05 M, and (**d**) commercial fulvic acid (FA, Fredricks Research Products, Laurential Soil) 333 µM C in seawater. The Ex/Em wavelengths of the main peaks are indicated: peak A (general humic compounds), peak C (terrestrial-origin humic substances), peak M (marine-origin humic substances) and peak T (tryptophan-like fluorescence). Fluorescence intensities are reported as fluorescence units provided by the instrument

The following fluorescence peaks have been found in the EEMs of riverine and seawater samples (Fig. 3.2a-b): A, due to general humic substances (average λex/λem = 250/435 nm); C, due to terrestrial-origin humic substances (average λex/λem = 340/440 nm); M, due to marine-origin humic substances (average λex/λem = 320/410 nm); and T, due to aromatic amino acids, specifically tryptophan (average λex/λem = 280/350 nm). These peaks are consistent with those found by Coble et al. (1990), Mopper & Schultz (1993) and Coble (1996) for the λex/λem range of these EEMs. Coble (1996) and others (Mayer et al. 1999, Yamashita & Tanoue 2003) proposed another protein-like fluorophore: B, due to tyrosine (λex/λem 275/310 nm). In the present study, peak B has not been evaluated because it is strongly affected by the Raman scattering band of water and measurements were not reliable.

Previous works used only a quinine sulphate (QS) standard, valid for humic-like substances. However, this compound does not fluoresce in the region of the aromatic amino acids. Therefore, we propose a mixed standard of QS and tryptophan (Trp) in sulphuric acid 0.05 M. As shown in Fig. 3.2c, the EEM of the mixed standard cover all the FDOM peaks. Trp fluorescence and QS fluorescence do not interfere, with each other. The mixed standard remains stable for at least three months stored in the dark at 4ºC.

Due to the regularity of the Ex/Em wavelengths of the selected peaks for samples from different sites and times in the study area, we decided to carry out only discrete measurements at the selected wavelengths. Discrete DOM fluorescence analyses were executed within a few hours of sample collection. Four replicate measurements were performed for each Ex/Em wavelength. A four points standard curve was prepared daily (concentrations from +0 to +20 ppb and from +0 to +30 ppb for QS and Trp, respectively). Fluorescence of sulphuric acid 0.05 M in Milli-Q water was used as a blank. The equivalent concentration of each peak was determined by subtracting the average peak

height from the blank height, and dividing by the slope of the standard curve. Finally, although peaks A, C and M represent different humic compounds, they showed similar distributions (r = +0.95 for peak A *vs.* peak M and r = +0.98 for peak C *vs.* peak M). Therefore, only the fluorescence of peaks M ($FDOM_M$) and T ($FDOM_T$) have been used in the present work. Fluorescence units were expressed in ppb equivalents of QS (ppb QS) for $FDOM_M$ and ppb equivalents of Trp (ppb Trp) for $FDOM_T$. Note that ppb QS is identical to the quinine sulphate units (QSU) reported previously in other studies. The precisions were ±0.1 ppb QS and ±0.6 ppb Trp, respectively.

FA carbon equivalents. Assessing the contribution of humic substances to the DOC pool is not a straightforward issue, because of the highly variable composition of the two main fractions: the humic (HA) and fulvic (FA) acids. Our approach consisted of using a commercial FA (Fredricks Research Products, Laurential Soil, 38.3% C dry weight by elemental analysis) as a standard. A FA was chosen instead of a HA because FAs are the main component of marine humic substances, about 90% (Thurman 1985, Skoog 1995). The EEMs of a natural sample (Fig. 3.2a) and the commercial FA (Fig. 3.2d) compare well. The FA was dissolved in filtered (polyethersulphone 0.2 µm filters) seawater and filtered again after one week of incubation in the dark, to allow complete dissolution. Then, the fluorescence and DOC content of the standard were determined. The average ratio between DOC and $FDOM_M$, after several replicate measurements at different concentrations of the commercial FA, was 2.67 ± 0.06 µM C $(ppb\ QS)^{-1}$.

Estimation of particulate proteins and lipids. The carbon content of particulate proteins (C_{Prot}) and lipids (C_{Lip}) was estimated by subtraction of the C and N content of particulate carbohydrates (p-CHO), chlorophyll a (Chl-a) and organic phosphorus compounds (POP) from the POC and PON content of the samples, using the average chemical formula of these groups of molecules

provided by Fraga (2001). p-CHO was analysed by the anthrone method (Nieto-Cid et al. 2004, Chapter 2) with a precision of ±0.1 μM C. Chl-a was determined with a Turner Designs 10000R fluorometer after 90% acetone extraction (Yentsch & Menzel 1963); the estimated accuracy was ±0.05 μg L^{-1}. POP was analysed by $H_2SO_4/HClO_4$ digestion at 220ºC followed by the analysis of the resultant phosphate by SFA; the precision for the entire analysis was ±0.02 μM P (Álvarez-Salgado 1993).

Estimation of corrected dissolved oxygen. The dissolved oxygen concentration of the samples was referred to the oxidation state of nitrate (O_{2C}), i.e. to a hypothetical situation in which the nitrite and ammonium of the sample were oxidised to nitrate. Since 0.5 mole of oxygen are necessary to oxidize one mole of nitrite to nitrate and two moles of oxygen are required to oxidize one mole of ammonium to nitrate.

$$O_{2C} = O_2 - \frac{1}{2} \times NO_2^- - 2 \times NH_4^+ \qquad (3.1)$$

This correction allows comparison of the dissolved oxygen consumption with the N_T production independently of the inorganic nitrogen form involved in the process.

Meteorological variables. Daily Ekman transport values ($-Q_X$, $m^2 s^{-1}$) were calculated according to Wooster et al. (1976):

$$-Q_X = \frac{\rho_{air} \cdot C \cdot |V| \cdot V_y}{\rho_{SW} \cdot f} \qquad (3.2)$$

where ρ_{air} is the density of air, 1.22 kg m^{-3} at 15ºC; C is an empirical drag coefficient (dimensionless), 1.3×10^{-3}; f is the Coriolis parameter, $9.946 \times 10^{-5} s^{-1}$ at 43º latitude; ρ_{SW} is the density of seawater, ~1025 kg m^{-3}; $|V|$ is the wind speed; and V_y is the north component of wind speed. Wind data were taken hourly from the anemometer of the SeaWatch Buoy Silleiro Meteorological Observatory at 42º07.2'N, 9º24.0'W (http://www.puertos.es). Positive values

of $-Q_X$ indicate upwelling and downwelling occurs when negative values are observed.

Daily continental runoff (Q_R, m^3s^{-1}) was estimated as the sum of **1)** the flow regulated by the Eiras reservoir; and **2)** a function of the precipitation in the drainage basin not regulated by the Eiras reservoir (Ríos et al. 1992).

RESULTS

Hydrography

Seven hydrographic periods were distinguished by Nieto-Cid et al. (2004), Chapter 2, from May 2001 to April 2002. The periods were defined on the basis of the seasonal evolution of $-Q_X$ and Q_R (Fig. 3.3a) and the thermohaline structure of the water column (Fig. 3.3b-c). Briefly, the study year began during the summer stratification (period 1, 15 May-21 Aug), characterised by coastal upwelling events separated by short intervals of calm. At the end of summer, a strong upwelling event (period 2, 28 Aug-18 Sep) raised cold, organic matter-poor and nutrient-rich ENACW to the surface layer. During periods 1 and 2, the residual circulation of the Ría de Vigo was positive and characterised by low continental runoff and large renewal rates. Autumn downwelling (period 3, 25 Sep-30 Oct) was generated by predominant southerly winds, which coincided with high continental runoff. The transition from stratification to vertical homogenisation (period 4, 6 Nov-20 Nov) occurred under strong northerly winds. Then, the IPC carried subtropical surface and central waters along the shelf and promoted a reversal of the circulation pattern of the ría (period 5, 27 Nov-13 Feb). The subsequent winter mixing (period 6, 20 Feb-26 Mar) was the time of maximum vertical homogenisation and, finally, the beginning of the spring (period 7, 2 Apr-24 Apr) was characterized by the coexistence of coastal upwelling and incipient stratification.

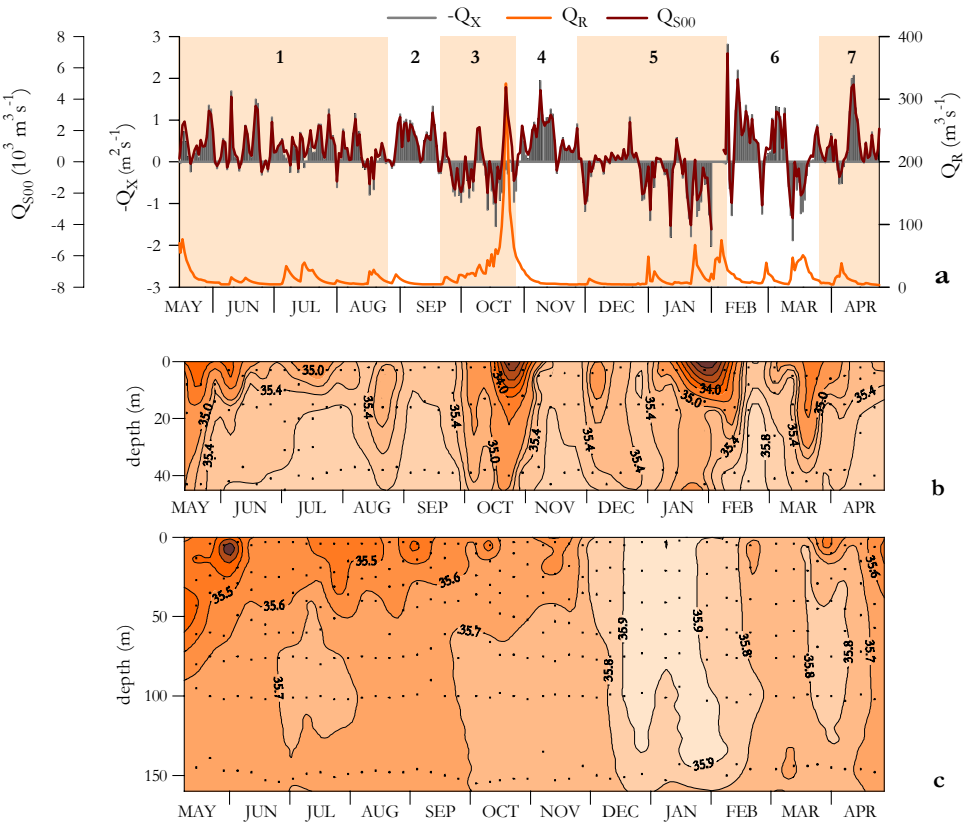

Figure 3.3 (**a**) Time course of Ekman transport, $-Q_X$ (m^2s^{-1}), continental runoff, Q_R (m^3s^{-1}) and surface water flux at stn 00, Q_{S00} (10^3 m^3s^{-1}). The different periods are shown, named from 1 to 7. Q_{S00} was calculated with the equation of Álvarez-Salgado et al. (2000): $Q_{S00} = 16\,(\pm 4)\cdot 10^{-3} Q_R - 2.3\,(\pm 0.2)\cdot 10^{-3} Q_X$. (**b**), (**c**) Time course of salinity at stn 00 and stn 03, respectively, during the study period

DOM fluorescence distributions in relation to the hydrographic conditions

This is the first study of the seasonal variability of DOM fluorescence distributions in a coastal upwelling system. Therefore, a description of the time evolution of the vertical profiles of $FDOM_M$ and $FDOM_T$ is required. Fluorescence distributions are then compared with temperature, salinity (Fig. 3.3b-c), and organic (Fig. 3.4a-b, Fig. 3.5a-b) and inorganic (Figs 3.4c-d and 3.5c-d) nitrogen distributions. The high correlations between DOC and DON

(r = +0.84, n = 434, p < 0.001) and between POC and PON (r = +0.98, n = 477, p < 0.001) ensure that comparison of DOM fluorescence with organic carbon instead of organic nitrogen produces the same results.

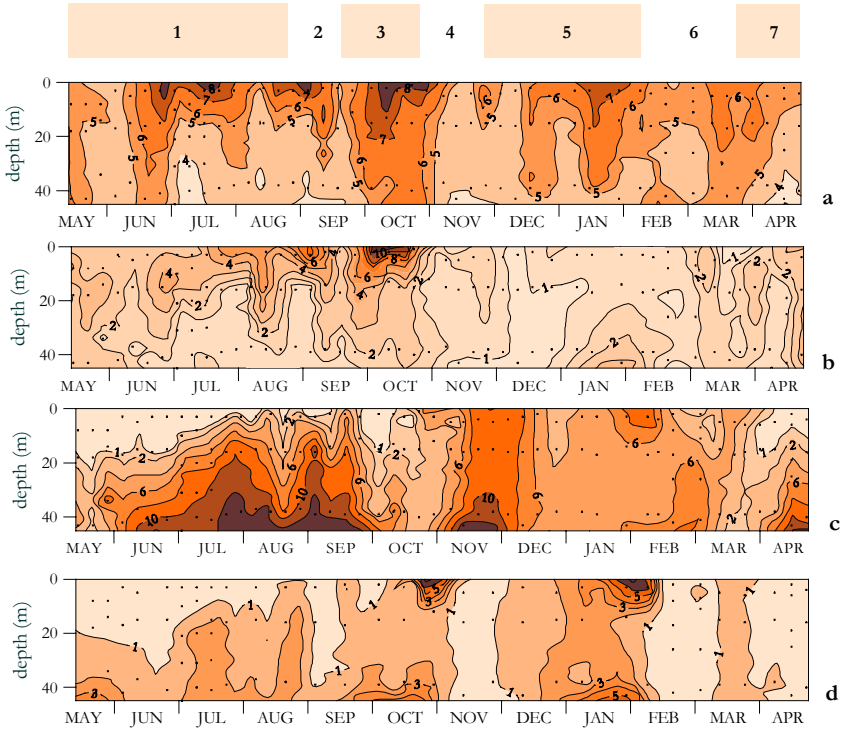

Figure 3.4 Time course of (**a**) DON (µM N), (**b**) PON (µM N), (**c**) nitrate (µM) and (**d**) ammonium (µM) at stn 00 during the study period. The different periods are shown, named from 1 to 7

The two environments sampled in this study responded differently to coastal upwelling. Therefore, it is expected that the two sites underwent different biogeochemical processes that can be traced with DOM fluorescence.

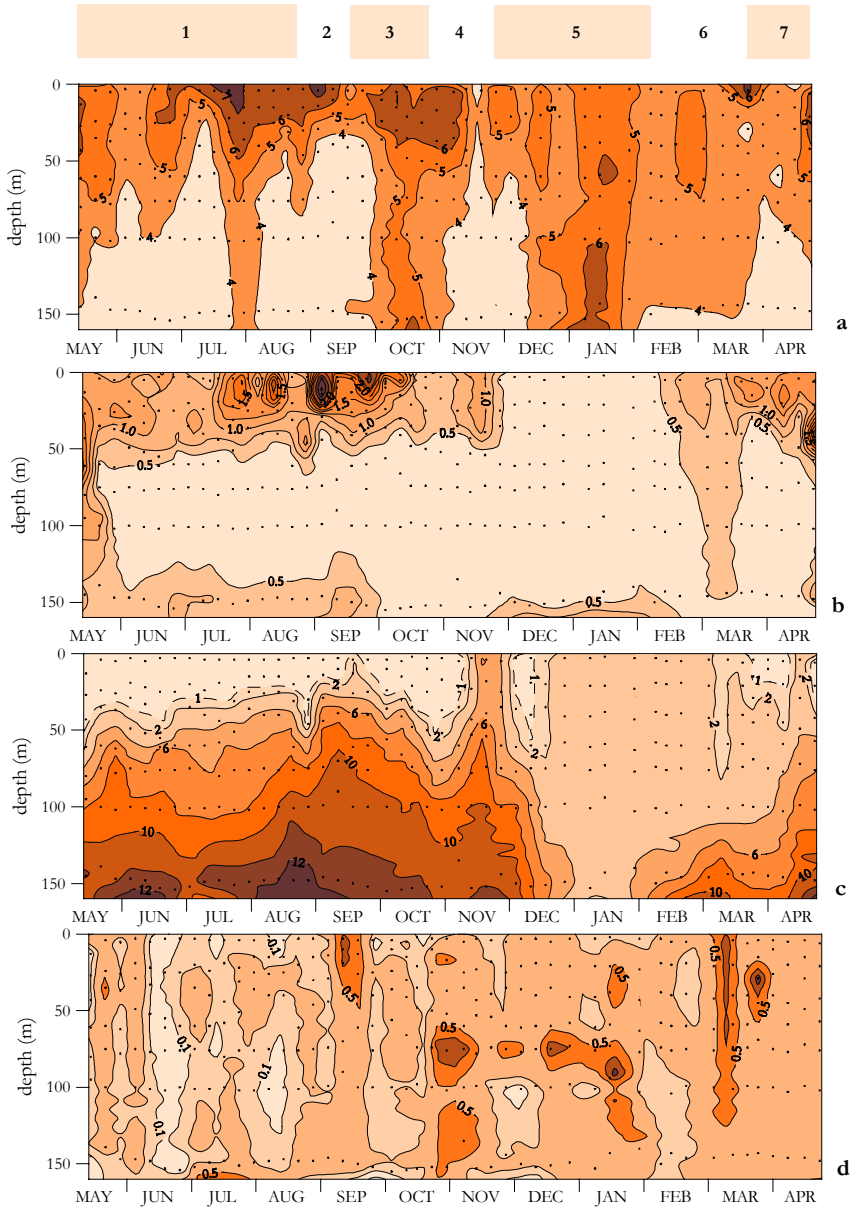

Figure 3.5 Time course of (**a**) DON (µM N), (**b**) PON (µM N), (**c**) nitrate (µM) and (**d**) ammonium (µM) at stn 03 during the study period. The different periods are shown, named from 1 to 7

Middle ría site (stn 00). Both $FDOM_M$ and $FDOM_T$ correlated significantly with temperature and salinity (r = 0.84, n = 90, $p < 0.001$ for peak M and r =

0.76, n = 90, $p < 0.001$ for peak T). Regarding the chemical parameters, $FDOM_M$ correlated significantly with DON ($r = +0.60$, n = 59, $p < 0.001$) and with ammonium ($r = +0.62$, n = 90, $p < 0.001$), and $FDOM_T$ with DON ($r = +0.73$, n = 59, $p < 0.001$), with PON ($r = +0.57$, n = 90, $p < 0.001$) and with nitrate ($r = -0.50$, n = 90, $p < 0.001$). During summer stratification (period 1) and upwelling (period 2), organic nitrogen profiles were characterised by a surface maximum and a bottom minimum (Fig. 3.4a-b), whereas inorganic nutrient profiles were opposite (Fig. 3.4c,d). These profiles are typical of the upwelling season off NW Spain. At this time, the organic nitrogen-poor and nitrate-rich ENACW rises to the surface, where production and accumulation of organic nitrogen occur in the periods of calm between successive upwelling events. $FDOM_M$ values were low in the entire water column except at the end of July (Fig. 3.6a), when a surface maximum was observed due to freshwater discharge (salinity <35.0; Fig. 3.3b). High surface concentrations of $FDOM_T$ coincided with low salinity and elevated DON and PON concentrations (Fig. 3.6b). During upwelling episodes, $FDOM_T$ levels were low throughout the water column. Downwelling (period 3) coincided with high runoff (>300 m^3s^{-1}), which produced a remarkable accumulation of DON, PON and, especially, FDOM (Fig 3.6a-b). During periods 4 to 7, $FDOM_M$ and $FDOM_T$ displayed a similar pattern, characterised by low concentrations, except from 15 Jan to 15 Feb, when high runoff occurred again (salinity <33.0; Fig. 3.3b).

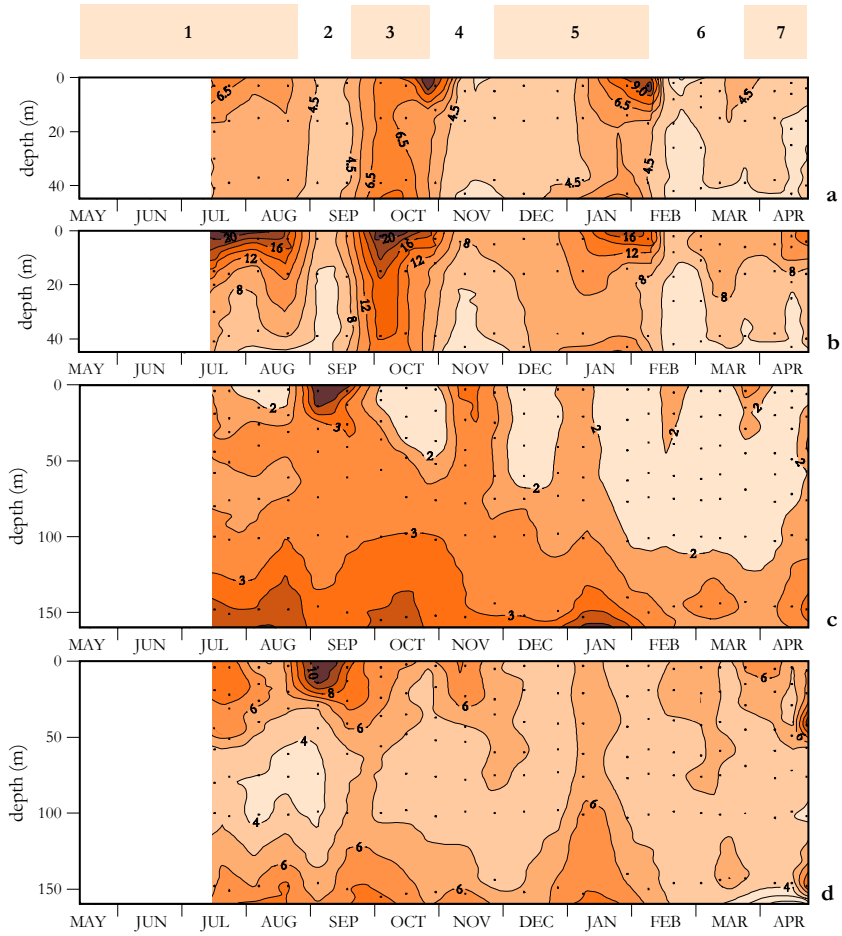

Figure 3.6 Time course of (**a**) $FDOM_M$ (ppb QS) at stn 00, (**b**) $FDOM_T$ (ppb Trp) at stn 00, (**c**) $FDOM_M$ (ppb QS) at stn 03 and (**d**) $FDOM_T$ (ppb Trp) at stn 03 during the study period. The different periods are shown, named from 1 to 7

Middle shelf site (stn 03). Multiple regressions with temperature and salinity were worst than at the middle ría, but they were still significant (r = 0.64, n = 182, p < 0.001 for $FDOM_M$ and r = 0.58, n = 182, p < 0.001 for $FDOM_T$). $FDOM_M$ only correlated significantly with nitrate (r = +0.62, n = 182, p < 0.001), whereas $FDOM_T$ correlated with PON (r = +0.73, n = 181, p < 0.001) and, to a lesser extent, with DON and nitrate (r = +0.35, n = 182, p < 0.001 and r = -0.24, n = 182, p < 0.001, respectively). Higher concentrations of DON and PON (Fig. 3.5a-b) occurred in the surface layer during the periods of

stratification (1, 2, 3 and 7), whereas, during the IPC and winter mixing periods (5 and 6), lower values were recorded. Nitrate was depleted in the photic layer and accumulated at the bottom, especially during the upwelling season (Fig. 3.5c). Just before the IPC (period 5), high nitrate levels were found throughout the water column, coinciding with a DON minimum. Ammonium concentrations were low (<0.5 μmol kg^{-1}) and patchily distributed (Fig. 3.5d). The distribution of $FDOM_M$ (Fig. 3.6c) was similar to nitrate, with low concentrations in the surface layer, except during September, and high concentrations at the bottom. On the other hand, $FDOM_T$ (Fig. 3.6d) presented a surface distribution similar to that of PON, with surface maxima during the stratification periods. Minimum DON levels occurred at the bottom, whereas in the case of PON, $FDOM_T$ and $FDOM_M$ high values were recorded because of the resuspension of organic rich sediments in the bottom nepheloid layer (BNL; Fig. 3.5b, 3.6c-d).

Box and whisker plots are a useful tool to compare average distributions of the chemical variables on the middle shelf. Figure 3.7 compares the $FDOM_T$ profile with the PON and C_{Prot} profiles, and the $FDOM_M$ profile with the N_T and $\%C_{Lip}$ profiles. Thus, $FDOM_T$ followed the distribution of fresh organic matter represented by the carbon content of proteins. In the photic layer, $FDOM_T$ was high and very variable, whilst concentrations decreased downwards. A relative maximum was observed at the BNL. In contrast, $FDOM_M$ followed the distribution of the lipids contribution to the POC pool. Average $FDOM_M$ concentration increased with depth, especially at the BNL.

The contribution of humic substances to the DOC pool was assessed using the conversion factor obtained with the commercial fulvic acid. On this basis, 6-13% of surface DOC is humic substances, increasing gradually with depth up to 11-17% at the BNL. This value was lower than at stn 00 (13-22 %).

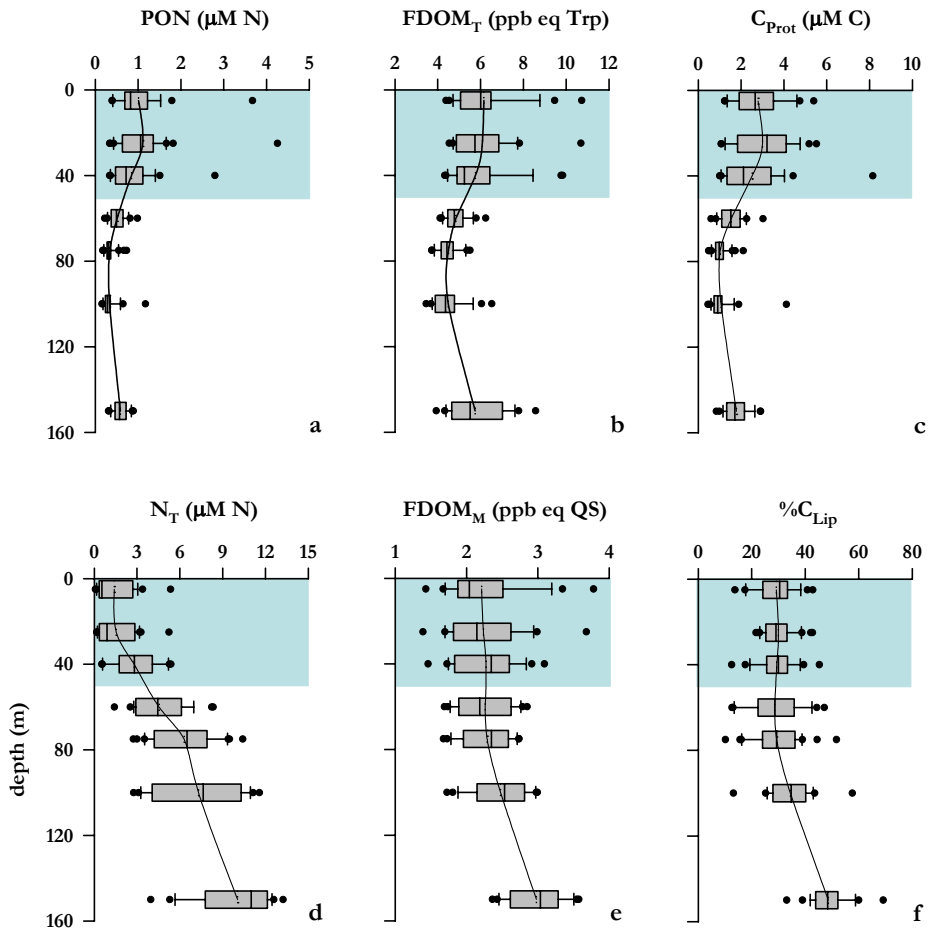

Figure 3.7 Box and whisker plot of (a) PON (µM N), (b) $FDOM_T$ (ppb Trp), (c) C_{Prot} (µM C), (d) N_T (µM N), (e) $FDOM_M$ (ppb QS) and (f) $\%C_{Lip}$ for the whole data set at stn 03. Fifty percent of the data are included within the limit of the boxes and the caps represent the 10th and 90th percentiles. Solid lines represent the average profiles

Tracing DOM production and mineralization

A regression analysis involving two conservative parameters solves a three end members mixing problem. Thus, the variation of any non-conservative parameter described by the mixing of three water masses can be estimated by means of a multiple linear regression of this parameter with salinity and temperature. This is the case for subsurface waters (AOU>0) of the NW

Iberian upwelling, where the subtropical and subpolar branches of ENACW mix with coastal waters. An anomaly (*a* Y) can be defined for each chemical parameter (Y):

$$a\,Y = Y - a_0 - a_1\,S - a_2\,T \qquad (3.3)$$

where a_0, a_1 and a_2 are the coefficients of the linear multiple regression of Y with salinity and temperature; *a* Y retains only the variability associated with the biogeochemical processes that occur in waters with AOU > 0.

Once the effect of water mass mixing was removed applying eq (3.3), both sites showed good correlations between *a* $FDOM_M$ and *a* O_{2C} (Fig. 3.8a-b; r = -0.71, n = 64, $p < 0.001$ for stn 00, and r = -0.76, n = 153, $p < 0.001$ for stn 03) and similar slopes (0.024 ± 0.003 and 0.025 ± 0.002 ppb QS $(\mu M\ O_2)^{-1}$, respectively; model II, Sokal & Rohlf 1995). Using the conversion factor of $FDOM_M$ to DOC obtained with the commercial fulvic acid, every mol of dissolved oxygen consumed would generate 0.066 ± 0.009 moles of humic carbon. Assuming a ratio of 1.42 mol O_2 $(mol\ C)^{-1}$ for the remineralization of organic matter in oxic conditions (Anderson 1995, Fraga 2001), then 9 ± 1 % of the organic carbon potentially mineralised directly to CO_2 was in fact transformed into humic substances, as a by-product of the oxidation of organic matter.

On the other hand, *a* $FDOM_T$ correlated significantly with *a* C_{Prot} (Fig. 3.8c-d; r = +0.61, n = 79, $p < 0.001$ for stn 00, and r = +0.57, n = 163, $p < 0.001$ for stn 03), i.e. the most labile organic material. In this case, the two environments showed marked differences: whereas in the middle ría the slope was 1.2 ± 0.2 ppb Trp $(\mu M\ C)^{-1}$, in the middle shelf it reduced to 0.5 ± 0.1 ppb Trp $(\mu M\ C)^{-1}$ (model II, Sokal & Rohlf 1995).

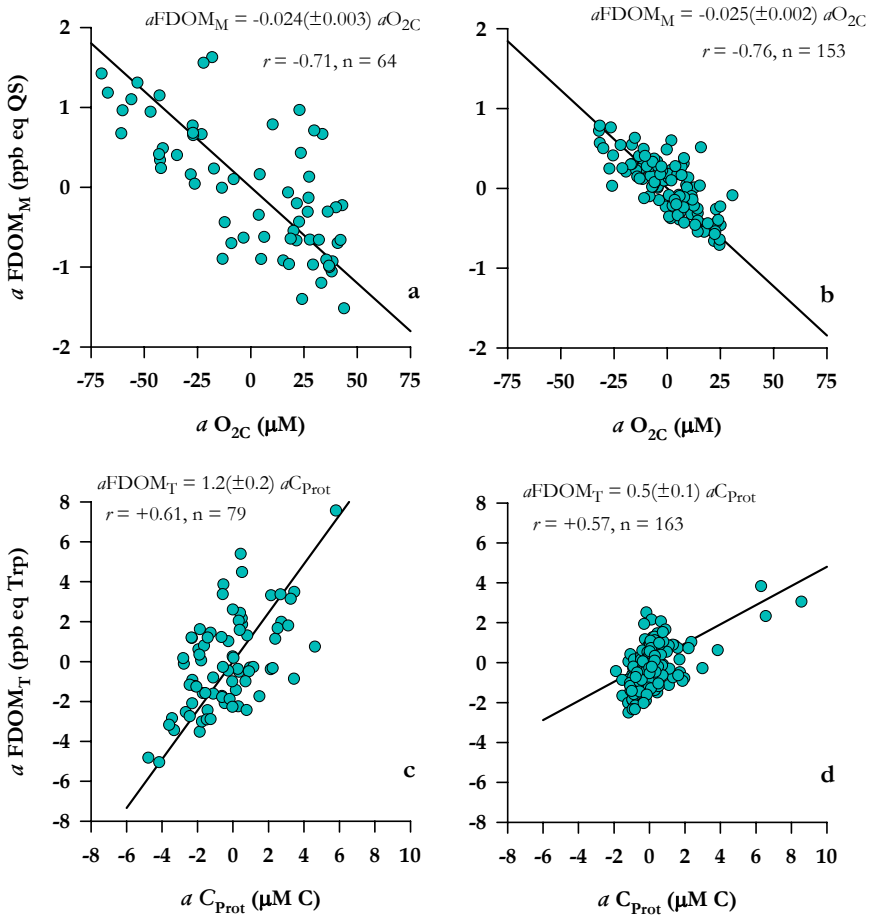

Figure 3.8 X - Y plots of (**a**) *a* $FDOM_M$ *vs. a* O_{2C} at stn 00, (**b**) *a* $FDOM_M$ *vs. a* O_{2C} at stn 03, (**c**) *a* $FDOM_T$ *vs. a* C_{Prot} at stn 00 and (**d**) *a* $FDOM_T$ *vs. a* C_{Prot} at stn 03. Solid lines represent the corresponding regression lines (model II; Sokal & Rohlf, 1995)

Seasonal accumulation

The 2-layered circulation of the Ría de Vigo (Fig. 3.9) allows us to estimate the net accumulation of organic matter at different sites using a simple mixing model. First, the net increase of FDOM in the surface layer of stns 00 or 03 can be calculated as the FDOM excess of the surface layer ($\Delta FDOM_S$) compared with the expected FDOM from the linear mixing of the freshwater and ENACW end members:

$$\Delta FDOM_S = FDOM_S - \left(\frac{S_S}{S_0} \cdot FDOM_0 + \frac{S_0 - S_S}{S_0} \cdot FDOM_F \right) \qquad (3.4)$$

where $FDOM_S$ and S_S are the FDOM and salinity of the surface layer, $FDOM_0$ and S_0 are the average FDOM and salinity of the ENACW end member, and $FDOM_F$ is the FDOM of the freshwater end member. Similar equations can be written for the two DOM fluorophores and the other chemical variables.

The ENACW end member was sampled during the same period as stn 00 and stn 03 on the continental slope off the Ría de Vigo (42º07.8'N, 9º30.0'W, 1200 m depth; stn 05 in Fig. 3.1). Although ENACW consists of two branches, a unique end member was considered in these rough calculations because the specific salinity of the ENACW upwelled each sampling date, resulting from the mixture of the subtropical and subpolar branches, was computed.

The Oitabén-Verdugo river is the freshwater endmember. The concentrations of the chemical parameters measured at the Eiras reservoir (S = 0.00) were considered. Rivers are sources of the two types of fluorophores (Mayer et al. 1999, Chen et al. 2002), but especially of humic substances. The river inputs were responsible for the surface FDOM maxima recorded under conditions of large continental runoff. This is due to the elevated inherent fluorescence of freshwater; typical values at the Eiras reservoir were 27 ppb Trp and 26 ppb QS, but differences with seawater are more apparent if FDOM/DOC ratios are compared. $FDOM_M$/DOC and $FDOM_T$/DOC ratios for seawater were 4.0-6.6 ppb QS (µmol C)$^{-1}$ and 10-14 ppb Trp (µmol C)$^{-1}$, respectively. At the Eiras reservoir, the ratios reached values of 30 ± 9 ppb QS (µmol C)$^{-1}$ and 30 ± 3 ppb Trp (µmol C)$^{-1}$. Other authors have also found an increase of the FDOM/DOC ratio with decreasing salinity (Callahan et al. 2004, Del Vecchio & Blough 2004). The seasonal cycle of the humic- and protein-like fluorophores in the freshwater end member were slightly different. $FDOM_T$ concentration was low during the spring and high during the autumn, when

continental runoff was large and high loads of labile materials of terrestrial plant origin occur. On the other hand, $FDOM_M$ was maximal in autumn and winter and decreased to minimal concentrations in spring and summer. The large contribution of terrestrial materials in autumn and the photochemical degradation of humic substances, widely reported in the literature (see Miller & Moran 1997 and Vähätalo & Wetzel 2004) and observed in the study area (Nieto-Cid et al. *submitted*, Chapter 4), are probably the reasons behind this seasonal evolution.

Second, the net increase of fluorescent DOM in the bottom layer of stn 00 or stn 03 can be estimated as the FDOM excess of the bottom sample ($\Delta FDOM_B$) compared with the expected FDOM from the linear mixing of the surface sample of stn 00 or 03 with the ENACW end member:

$$\Delta FDOM_B = FDOM_B - \left(\frac{S_0 - S_B}{S_0 - S_S} \cdot FDOM_S + \frac{S_B - S_S}{S_0 - S_S} \cdot FDOM_0 \right) \qquad (3.5)$$

where $FDOM_B$ and S_B are the FDOM and salinity at the bottom of stn 00 or stn 03. The same equation can be written for the two DOM fluorophores and the other chemical variables.

Third, the net increase of fluorescent DOM in the ría (from San Simon Bay to stn 00) and the shelf (from San Simon Bay to stn 03), can be estimated as the accumulation of FDOM in the surface sample ($\delta FDOM$) compared with the expected FDOM from the linear mixing of the surface sample of stn 00 or 03 with the bottom sample of the same station and the freshwater end member:

$$\delta FDOM = FDOM_S - \left(\frac{S_S}{S_B} \cdot FDOM_B + \frac{S_B - S_S}{S_B} \cdot FDOM_F \right) \qquad (3.6)$$

The accumulation in the outer shelf (from stn 00 to stn 03) can be estimated by subtraction of the calculation for the shelf minus the calculation for the ría.

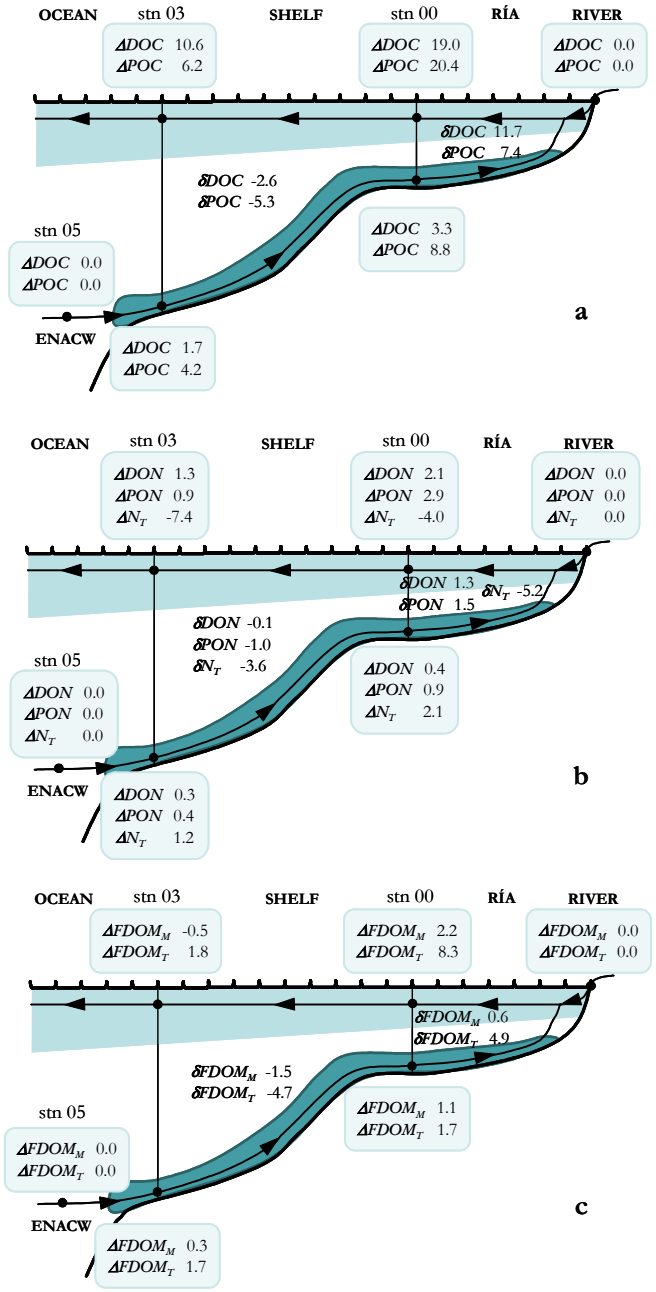

Figure 3.9 Scheme of the exchange of water between the ría, the shelf and the adjacent ocean. Δ represents surface and bottom net excesses of the chemical parameters and **δ** represents the net accumulations in the ría and the outer shelf. Plots include (**a**) DOC (μM C) and POC (μM C), (**b**) DON (μM N), PON (μM N) and N_T (μM N), and (**c**) $FDOM_M$ (ppb QS) and $FDOM_T$ (ppb Trp)

Figure 3.9 shows the net DOC, POC, DON, PON, N_T, and $FDOM_T$ excesses in the upper and bottom layers of both sites and the corresponding accumulations in the ría and the outer shelf. In general, surface and bottom values are positive for all the organic matter parameters. Only $FDOM_M$ experienced a deficit in the surface layer of stn 03. In contrast, the trends in nutrient salts were negative at the surface (net deficit) and positive at the bottom (net excess).

The N_T deficit was larger in the surface layer of the shelf, whereas the DOC, DON, POC, PON and $FDOM_T$ excesses were larger in the surface layer of the ría. For the bottom layer, larger excesses occurred in the ría for all variables except for DON and $FDOM_T$ (not significantly different in either site). Maximum surface excesses occurred in the ría during the downwelling period: ΔDOC = +38 μM C, ΔPOC = +46 μM C, ΔDON = +3.7 μM N, ΔPON = +6.9 μM N, $\Delta FDOM_M$ = +5.6 ppb QS and $\Delta FDOM_T$ = +14.1 ppb Trp.

Organic matter accumulated in the ría ($\delta FDOM > 0$) was partially consumed on the shelf ($\delta FDOM < 0$). It is possible to calculate the net production or consumption of any chemical parameter in the ría using the calculated renewal rates for each period (Table 3.1). The highest production rates of organic carbon and nitrogen occurred during the upwelling period, and coincided with maximum nutrient consumption. However, maximum $FDOM_T$ production rates took place during summer stratification (+1.3 ppb Trp d^{-1}), whereas $FDOM_M$ production rates did not show significant variations during the study year. In the bottom layer, nutrients were produced at faster rates during summer stratification and upwelling conditions (periods 1 and 2).

Table 3.1 Net production rates of DOC (µM C d^{-1}), POC (µM C d^{-1}), DON (µM N d^{-1}), PON (µM N d^{-1}), N_T (µM N d^{-1}), $FDOM_M$ (ppb eq QS d^{-1}) and $FDOM_T$ (ppb eq Trp d^{-1}) at the bottom (B) and surface (S) layer of stn 00 for the annual cycle (AC) and the main periods: summer stratification (1), upwelling (2), downwelling (3), IPC period (5), winter mixing (6), spring (7). Considering Q_{S00} and the water volume of the ría from the inner part to stn 00 (0.53 km^3), the annual average renewal rate was 9 ± 2 %d^{-1} (Nieto-Cid et al. 2004, Chapter 2)

		PERIOD						
		AC	1	2	3	5	6	7
DOC	S	**1.1**	2.2	4.2	0.3	0.4	0.5	2.0
	B	**0.3**	0.3	0.3	0.1	0.2	0.7	0.3
POC	S	**0.7**	1.7	4.5	0.5	-0.3	-0.4	0.5
	B	**0.8**	1.0	2.0	0.1	0.6	1.5	2.0
DON	S	**0.1**	0.3	0.5	0.0	0.0	0.1	0.2
	B	**0.0**	0.0	0.0	0.0	0.0	0.1	0.1
PON	S	**0.1**	0.2	0.7	0.1	0.0	0.0	0.1
	B	**0.1**	0.1	0.3	0.0	0.1	0.2	0.3
N_T	S	**-0.5**	-1.5	-1.9	0.0	0.1	-0.1	-1.3
	B	**0.2**	0.6	0.7	0.0	0.0	-0.2	0.2
$FDOM_M$	S	**0.1**	0.1	0.1	0.0	0.1	0.1	0.0
	B	**0.1**	0.2	0.2	0.0	0.0	0.1	0.2
$FDOM_T$	S	**0.5**	1.3	0.7	0.1	0.2	0.4	0.8
	B	**0.2**	0.3	0.4	0.1	0.1	0.2	0.3

In the surface layer, nutrient consumption rates correlated significantly with DON (r = -0.94, n = 7, $p < 0.001$), PON (r = -0.79, n = 7, $p < 0.05$), and $FDOM_T$ (r = -0.77, n = 7, $p < 0.05$) production rates. Nevertheless, in the bottom layer, only $FDOM_M$ production rates correlated significantly with nutrient production rates (r = +0.85, n = 7, $p < 0.01$). The contribution of humic substances to the net accumulation of DOC was larger in the bottom than in the surface (~90-15%) layer. These percentages were estimated considering the conversion factor of $FDOM_M$ to DOC obtained with the commercial fulvic acid.

DISCUSSION

DOM fluorescence as a tracer for microbial processes

As in other marine environments (Hayase et al. 1987, 1988, Chen & Bada 1992, Determann et al. 1996), $FDOM_M$ concentrations were low at the surface and increased with depth. This gradient is created by photodegradation in the surface layer and humification throughout the water column, especially at the BNL and in the sediments (Skoog et al. 1996, Burdige et al. 2004). In this sense, the good correlation between $FDOM_M$ and nutrient salts in shelf bottom waters suggests that humification was tightly coupled to mineralization, indicating that the formation of fluorescent marine humic substances goes together with the decomposition of settling particles in the water column (Hayase et al. 1987, 1988, Hayase & Shinozuka 1995). Chen & Bada (1992) suggested that the bacteria responsible for the regeneration of nutrients are simultaneously producing refractory compounds from biologically labile components.

A substantial difference between the two study sites was that $FDOM_M$ correlated better with reduced nitrogen (DON and ammonium) in the ría, and with oxidized nitrogen (nitrate) on the shelf. This suggests that humic substances are not produced during the mineralization of organic nitrogen but during the oxidation of organic carbon. Particularly, some authors point to the degradation of lipids, nitrogen-free biomolecules, as an origin for humic substances (Kieber et al. 1997). In our case, $FDOM_M$ and $\%C_{Lip}$ followed the same trend, showing lipids as one possible precursor of humic compounds.

The contributions of humic substances to the DOC pool estimated in this work (6-22%) were similar to the numbers obtained by Obernosterer & Herndl (2000) in the Adriatic Sea (15 ± 7%), and lower than in the North Sea (43 ± 7%), a marine ecosystem more affected by terrestrial contributions. The percentage of conversion of degradable organic carbon into humic substances was ~10%, either in the ría or on the shelf. This number is much higher than

the 1% obtained by Hayase & Shinozuka (1995) for mid-depth waters (300-1000 m) of the Central Equatorial Pacific. However, these authors suggested that the ratio of fluorescent organic matter to total dissolved organic substances should be much higher than 1%. In addition, the oceanic site sampled by Hayase & Shinozuka (1995) is not comparable with a coastal upwelling system, where more intense humification processes are expected. Moreover, the effect of the thermohaline parameters was eliminated from the correlation between $FDOM_M$ and oxygen in this work, but not by Hayase & Shinozuka (1995). This may also be the reason behind the low slopes of the correlations of $FDOM_M$ with nitrate, phosphate, silicate and O_{2C} on the Iberian margin (0.14 ± 0.01, 2.4 ± 0.2, 0.37 ± 0.03 and -0.026 ± 0.003 ppb QS $(\mu M)^{-1}$, respectively; model II) compared with the Central Equatorial Pacific (Hayase & Shinozuka 1995) and the North Pacific (Hayase et al. 1988).

Although $FDOM_T$ relates directly with the fluorescence of aromatic amino acids, Yamashita & Tanoue (2003) demonstrated that it could be a useful indicator of the dynamics of DFAA in general. The significant correlation with suspended proteins ($r > +0.57$, $p < 0.001$) also supports this statement. Since DFAA are liberated during phytoplankton exudation, cell autolysis and zooplankton grazing (Nagata 2000), $FDOM_T$ can be used in future studies to trace these processes, which occur preferentially in the surface layer. The accumulation of $FDOM_T$ observed in the BNL could be related to an enhancement of the *in situ* production and/or to the release of the DFAA accumulated in the pore waters of pelagic sediments (Coble 1996, Mayer et al. 1999), which exceed the rate of consumption of these labile molecules.

Production and consumption rates of fluorescent DOM

Since marine humic substances are microbiologically generated in the lower layer and photodegraded in the upper layer (Chen & Bada 1992), the net excess of $FDOM_M$ should be positive near the bottom and negative at the surface.

However, $FDOM_M$ was produced in the surface layer of the ría at an average net rate of +0.2 ppb QS d^{-1}, probably because humification processes in San Simón Bay exceed photodegradation. San Simón Bay, in the innermost part of the Ría de Vigo, is a shallow basin with an average depth of 4 m, where the ría receives most of its continental inputs. This bay is strongly affected by the tidal cycle: more than 40% of the basin sediments are exposed to the atmosphere during low tides (Gilcoto 2004). Biogenic materials entering San Simón Bay undergo strong biochemical processes, able to modify the chemical composition of the water flowing into the ría, especially due to the activity of the marine angiosperm *Zostera* (Niell 1977). The elevated pCO_2 level (>600 μatm) of the surface waters of San Simon Bay is a clear indication of the strong mineralization processes that occur there (Gago et al. 2003).

The largest excess of fluorescent DOM in the surface layer occurred during the stratification periods in the ría and the shelf, whilst the largest excess in the bottom layer was recorded during the downwelling period, in response to the reversal of the positive residual circulation pattern. Fluorescent DOM accumulates in the BNL, in agreement with the statement of Mayer et al. (1999) and Burdige et al. (2004) that sediments provide a source of protein- and humic-like fluorescence. Seasonal changes on $FDOM_T$, DOC, POC, DON and PON surface production were tied to the changes in nutrient consumption, pointing again to the close relationship between the production of $FDOM_T$ and fresh (labile) materials. However, net production of nutrients at the bottom correlated significantly only with $FDOM_M$, suggesting a coupling between mineralization and humification processes at the BNL. Despite intense mineralization processes in bottom shelf waters ($\delta N_T >> 0$), which would produce an accumulation of $FDOM_M$, the balance for the whole water column indicates a large deficit of humic-like fluorescence ($\delta FDOM_M$ = -1.5 ppb QS)

and, consequently, the importance of photodegradation of humic substances in the surface layer on the shelf.

Information on the production and accumulation of DOM in upwelling systems is scarce and practically restricted to previous studies in the NW Iberian upwelling system. Doval et al. (1997) estimated the accumulation of DOC and DON in the Ría de Vigo during the upwelling season of 1995. Their values (+21 μM C and +1.7 μM N, respectively) were similar to those obtained in this work for the upwelling period (+20 μM C and +2.2 μM N, respectively). Concomitantly, Álvarez-Salgado et al. (1999) calculated a DOC production during the upwelling season in the inner ría of +4.4 μM C d^{-1}, which is not significantly different from the +4.2 μM C d^{-1} obtained in this work. They also found that surface waters of the outer ría produced +1.3 μM C d^{-1}, whereas the shelf acted simply as a retention volume where DOM production and consumption were in equilibrium (net production = 0.0 μM C d^{-1}). The total DOC excess from the inner ría to the shelf computed by Álvarez-Salgado et al. (1999) was 8 μM C, which coincides with the number obtained in this study.

Comparison of the net accumulation of dissolved and particulate organic matter in the ría and the shelf (referred to the whole water column) produces a different view of the carbon and nitrogen cycles in NW Iberian shelf waters. Up to 40% of the net production of organic carbon and nitrogen of the inner ría was consumed on the shelf. The remaining 60% was exported to the adjacent ocean, probably in the recurrent upwelling filament off the Rías Baixas (Álvarez-Salgado et al. 2001b). Preferential consumption of the particulate fraction occurred: 70% of the POC was consumed compared with only 20% of the DOC. The reason behind this difference is the gravity sinking on the shelf of the POC exported from the rías, which experiences strong mineralization processes in the BNL. Intense nutrient mineralization in shelf bottom waters at the expense of the materials exported from the rías has been suggested by

Tenore et al. (1982), Álvarez-Salgado et al. (1997) and Prego et al. (1997). However, this is the first time that the proportion of the organic matter exported from the ría that is mineralised on the shelf has been quantified. On the other hand, DOC preferentially crosses the surface layer of the shelf to be exported to the adjacent ocean. Consequently, whereas the average DOC/POC ratio of the material accumulated in the ría was 1.6 (= 11.7/7.4; 60% DOC, 40% POC), the ratio of the material exported to the adjacent ocean was 4.3 (= (11.7-2.6)/(7.4-5.3); 80% DOC, 20% POC). The contribution of POC to the organic matter accumulated in the ría during the annual cycle was comparable with the 45% obtained by Gago et al. (2003) for the same system in 1997. However, for the case of the shelf, the 20% of POC export obtained in this study, contrasts with the 50% found by Álvarez-Salgado et al. (2001b) in the upwelling filament of the Rías Baixas, although their numbers refer exclusively to a short period in August 1998.

The C/N molar ratio of the organic matter accumulated in the ría ranges from an average of 5.0 for the particulate material to 9.0 for the dissolved material. The average C/N ratio of the products of synthesis and early degradation of marine phytoplankton is 6.7 (Anderson 1995, Fraga 2001). Therefore, the accumulated particulate material is more labile (N-richer) than the dissolved material (N-poorer). This is also in agreement with the preferential consumption of particulate material on the shelf. Although only 20% of the bulk DOC exported to the shelf was respired, this is not the case for the labile fraction of the DOM represented by $FDOM_T$: up to 95% of the DFAA exported from the ría were consumed on the shelf. Since the net average deficit of DON in shelf waters (δDON) was only -0.1 μM N, most of it was probably due to the net consumption of these DFAA. Assuming an average C/N molar ratio of 3.5 for the DFAA (Fraga 2001), it seems that only 13% of the DOC deficit on the shelf can be assigned to DFAA consumption.

The remaining 87% should be respired carbohydrates, based on the consideration that labile DOM is mainly composed of DFAA and carbohydrates (Kirchman et al. 1994, Rich et al. 1996). A decrease of $FDOM_M$ of -1.5 ppb QS is equivalent to the net photochemical degradation of 4.0 μM C of humic substances, which would be preferentially transformed into labile small organic molecules (Miller & Moran 1997).

CONCLUSIONS

It has been demonstrated that DOM fluorescence can be used as a tracer for labile DOM (DFAA) production in the surface layer and microbial decomposition processes in the bottom layer.

Fluorescence distributions suggested that humic acids and DFAA can be produced in either the surface or the bottom layer. $FDOM_T$ accumulated **1)** in the BNL, after *in situ* production by intense microbial activity and/or after release from the pore waters of the pelagic sediment; and **2)** in the photic layer, because of phytoplankton exudation or cell lysis. On the other hand, $FDOM_M$ was produced in subsurface waters by *in situ* mineralization, especially in the BNL and the sediments. The two study sites, a semi enclosed bay and an open shelf, presented the same percentage of conversion of degradable organic carbon into humic substances as a by-product of microbial oxidation processes, ~10%.

Despite photodegradation of humic substances in the surface layer, accumulation of the humic material produced in San Simon Bay occurred in the middle ría. On the contrary, photodegradation was the dominant process in the transit of surface waters of the ría to the shelf, where net consumption of humic substances was observed.

Although the literature on the photochemical degradation of humic substances is plentiful, there are no data about rates of microbial production of these macromolecules. In this work, we have found that humic substances can contribute up to 90% of the DOC excess in the BNL, an amount that demands future process orientated studies.

Chapter 4:

Microbial and photochemical reactivity of fluorescent dissolved organic matter in a coastal upwelling system

Chapter 4, the research work presented in this chapter is also a contribution to the paper:

M. Nieto-Cid, X. A. Álvarez-Salgado, F. F. Pérez. 2005. **Microbial and photochemical reactivity of fluorescent dissolved organic matter in a coastal upwelling system**. Limnol Oceanogr, *accepted*

Resumen: Se han realizado incubaciones de 24 h en luz y oscuridad en el sistema de afloramiento costero de la Ría de Vigo bajo una amplia variedad de condiciones meteorológicas y oceanográficas, donde se han observado cambios significativos en el contenido de oxígeno disuelto y en la fluorescencia de sustancias húmicas y aminoácidos aromáticos disueltos. Las tasas de respiración mostraron una correlación positiva con la producción neta de sustancias húmicas en oscuridad (r = +0.73, n = 79, p < 0.001) mostrando una pendiente de 0.027 ± 0.003 ppb QS (μmol kg^{-1} $O_2)^{-1}$, lo que sugiere la síntesis diaria de sustancias húmicas como subproducto de la respiración bacteriana de la materia orgánica disuelta. Por el contrario, el consumo de sustancias húmicas en las incubaciones con luz menos en oscuridad mostró una correlación inversa con la producción neta de estas sustancias en oscuridad (r = -0.71, n = 46, p < 0.001), indicando una rápida fotodegradación de las sustancias húmicas producidas recientemente. Incubaciones paralelas demostraron que las tasas de fotodegradación diarias y los niveles de fluorescencia húmica residual presentan una distribución estacional caracterizada por un máximo otoñal. Por último, la significativa correlación lineal entre la producción primaria bruta (Pg) y la producción neta de aminoácidos aromáticos con luz (r = +0.54, n = 46, p < 0.001) señala un rápido consumo de materiales disueltos pseudo-proteicos con una tasa media de -1.4 ± 0.2 ppb Trp d^{-1}, que se acumula en la columna de agua solo cuando Pg supera el valor de 80 ± 20 μmol $kg^{-1}d^{-1}$.

Abstract: Significant changes have been observed in the dissolved oxygen content and the fluorescence of humic substances and dissolved aromatic amino acids after 24 h light and dark incubations in the coastal upwelling system of the Ría de Vigo, under a wide variety of meteorological and oceanographic conditions. Respiration rates were positively correlated with the net production of humic substances in the dark (r = +0.73, n = 79, p < 0.001) at a net rate of 0.027 ± 0.003 ppb QS (μmol kg^{-1} $O_2)^{-1}$, suggesting a daily synthesis of marine humics as a by-product of the bacterial respiration of dissolved organic matter (DOM). On the contrary, humic substances consumption in the light minus dark incubations was inversely correlated with the net production in the dark (r = -0.71, n = 46, p < 0.001), indicating a rapid photodegradation of recently produced marine humic substances. Parallel incubation experiments demonstrated that daily photodegradation rates and residual humic fluorescence levels followed a seasonal pattern characterised by a marked autumn maximum. Finally, a significant linear correlation between the gross primary production (Pg) and the net production of aromatic amino acids in the light (r = +0.54, n = 46, p < 0.001) pointed to the quick consumption of dissolved protein-like materials at a net average rate of -1.4 ± 0.2 ppb Trp d^{-1}, which accumulates in the water column only when Pg exceeds 80 ± 20 μmol $kg^{-1}d^{-1}$.

INTRODUCTION

Marine dissolved organic matter (DOM) constitutes the main substrate for bacterioplankton growth and respiration (Azam & Cho 1987). DOM sources in estuarine and coastal waters include phytoplankton exudation, cell autolysis and grazing pressure (Nagata 2000), as well as autochthonous organic matter of terrestrial and oceanic origin (Wollast 1993, 1998). The diversity of sources produces a myriad of different compounds, with a microbial reactivity ranging from hours for the dissolved free amino acids (DFAA), monosaccharides and other labile molecules (Fuhrman 1987) to thousands of years for the most refractory humic compounds upwelled from the deep sea (Williams & Druffel 1987). The resistance of humic substances to microbial degradation contrasts with their susceptibility to photochemical decomposition (Benner & Biddanda 1998).

Fluorescence reveals as a useful, simple and quick technique to characterize and quantify two different classes of DOM: the labile DFAA (Yamashita & Tanoue 2003) and the recalcitrant humic substances (Coble et al. 1990). These two classes of compounds can be used to trace diverse biogeochemical processes such as labile organic matter production (Nieto-Cid et al. *in press*, Chapter 3), respiration (Chen & Bada 1992, Nieto-Cid et al. *in press*, Chapter 3) and photobleaching (Skoog et al. 1996, Moran et al. 2000, Del Vecchio & Blough 2002). All these processes play a key role in the accumulation, recycling and export of DOM in marine ecosystems (Carlson 2002).

The origin of dissolved labile organic matter can be autotrophic, via extracellular release (Myklestad 1995, Obernosterer & Herndl 1995) and cell lysis (Kirchman et al. 1993), or heterotrophic, via grazing losses (Storm et al. 1997). Rapid turnover maintains these compounds at nanomolar concentrations in the open ocean, but they support a large portion of the heterotrophic bacterial growth and respiration (Skoog et al. 1999). We hypothesised that the

fluorescence of dissolved aromatic amino acids ($FDOM_T$) can be used to discriminate whether the accumulation of labile DOM in the marine environment is preferentially due to anabolic (related to primary production) or catabolic (related to respiration) processes.

The origin of marine humic substances is not completely resolved. An alternative to the classical poli-phenolic and melanoidin condensation models (Hedges 1978) and the photo-oxidation of lipids (Kieber et al. 1997), is the formation of humic substances as a by-product of microbial respiration (Brophy & Carlson 1989, Tranvik 1993, Kramer & Herndl 2004). A fraction of the respired organic carbon is transformed into biologically refractory organic matter instead of CO_2 (Chen & Bada 1992, Heissenberger & Herndl 1994, Hayase & Shinozuka 1995, Ogawa et al. 2001). We hypothesized that the fluorescence of humic compounds ($FDOM_M$) can be used to trace the daily production of humic substances during microbial respiration processes.

Exposure to sunlight degrades high-molecular-weight humic substances into smaller photoproducts that are mainly removed from the DOM pool by two pathways: through direct volatilization of carbon gases (CO, CO_2, SO_2…) and through rapid bacterial utilization of labile photoproducts (Kieber et al. 1997). The relationship between photochemical and heterotrophic processes has been specifically investigated during the last decade in different environments (Lindell et al. 1995, Amon & Benner 1996, Moran & Zepp 1997, Moran et al. 2000, Obernosterer & Benner 2004, Kramer & Herndl 2004). Since photodegradation of DOM involves mainly humic substances, $FDOM_M$ is a suitable parameter to study this process. A third hypothesis to be tested in this work is that the humic material produced during bacterial respiration in the bottom layer is quickly degraded in the surface layer by photochemical processes.

Coastal upwelling systems are ideal to verify these hypotheses, since microbial activity intensifies because of the enhanced entry of nutrients from the adjacent ocean (Walsh 1991). Pelagic and benthic processes are tightly coupled due to the reduced water column depth; the organic matter produced in the photic layer is rapidly processed by microheterotrophs in the aphotic layer and the sediments, and upwelling enhances the quick rise to the surface of the products and by-products of microbial degradation.

This study was performed in the Northwest coast of the Iberian Peninsula, an area affected by a marked seasonal cycle of coastal winds (Nogueira et al. 1997). From April to October (the upwelling-favourable season), intermittent northerly winds of period 1-2 week cause Eastern North Atlantic Central Water (ENACW) to upwell over the shelf (Álvarez-Salgado et al. 1993). From November to March (the downwelling-favourable season), southerly winds prevail and a marked downwelling front develops between the Iberian Poleward Current (IPC) carrying warm and salty subtropical surface and central water to our latitudes and the coastal water (Álvarez-Salgado et al. 2000). The study site is the Ría de Vigo, one of the Rías Baixas, four large V-shaped coastal embayments in the NW Iberian shelf. These sites, which behave as an extension of the shelf, are characterised by average flushing times of about 1 wk (Rosón et al. 1999, Álvarez-Salgado et al. 2000).

MATERIAL AND METHODS

Sampling strategy. The middle segment of the coastal upwelling system of the Ría de Vigo (Fig. 4.1) was sampled about 1 hour before sunrise, twice a week, during winter (18, 21, 25 and 28 February), spring (11, 15, 18, 22 April), summer (15, 18, 22 and 26 July) and autumn (17, 19, 23, 26 September) 2002. Samples were taken with a rosette equipped with twelve 10-L PVC Niskin bottles with stainless-steel internal springs. Salinity and temperature were recorded with a SBE 9/11 conductivity-temperature-depth probe attached to

the rosette sampler. Conductivity measurements were converted into practical salinity scale values with the equation of UNESCO (1985). Water samples for the analyses of dissolved oxygen and dissolved organic matter were collected from five depths: the surface (50% Photosynthetic Available Radiation, PAR; average 2.1 ± 0.6 m), the depth of the 25% PAR (average 8 ± 2 m), the depth of the 1% PAR (average 16 ± 3 m), 27 ± 2 m and the bottom (average 41 ± 1 m).

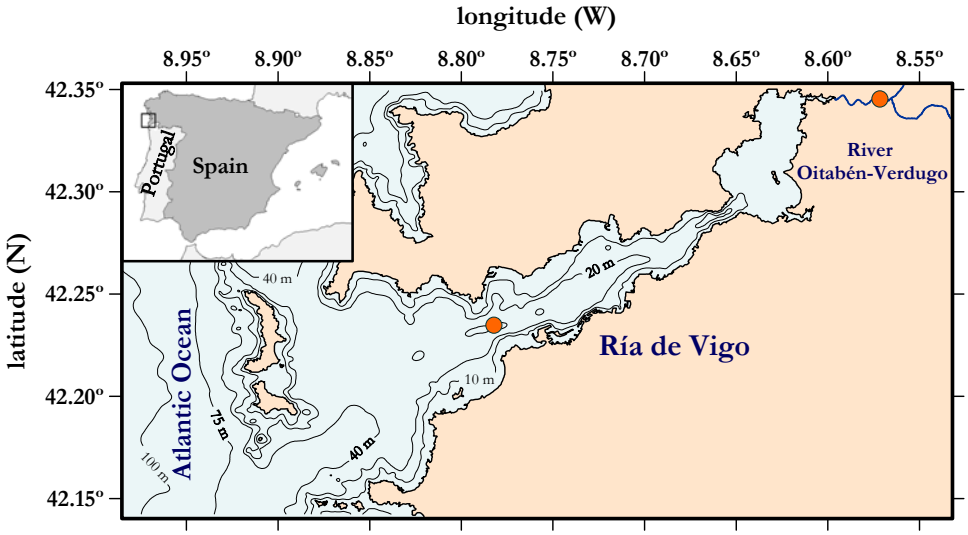

Figure 4.1 Chart showing the situation of the sampling stations (black points) in the river Oitabén-Verdugo and the Ría de Vigo (NW Spain). The 10, 20, 40, 75 and 100 m isobaths are shown

Dissolved oxygen (O_2). Samples were collected into calibrated 110 mL glass flasks. After fixation, they were kept in the dark until analysis in the laboratory, 24 h later. O_2 was determined by Winkler potentiometric end-point titration using a Titrino 720 analyser (Metrohm) with a precision of ±0.5 μmol kg^{-1}.

Dissolved organic carbon (DOC). Samples for DOM were collected into 500 mL acid-cleaned flasks and filtered through precombusted (450ºC, 4 h) 47 mm ø Whatman GF/F filters in an acid-cleaned glass filtration system, under low N_2 flow pressure. Aliquots for the analysis of DOC were collected into 10

mL precombusted (450ºC, 12 h) glass ampoules. After acidification with H_3PO_4 to pH < 2, the ampoules were heat-sealed and stored in the dark at 4ºC until analysis. DOC was measured with a Shimadzu TOC-5000 organic carbon analyzer, as described in Nieto-Cid et al. (2004). The system was standardized daily with potassium hydrogen phthalate. The concentrations of DOC were determined by subtracting the average peak area from the instrument blank area and dividing by the slope of the standard curve. The precision of measurements was ±0.7 μM C. The accuracy of the DOC analysis was tested daily with the TOC reference materials provided by D. Hansell (University of Miami). We obtained an average concentration of 45.7 ± 1.6 μM C (n = 26) for the deep ocean reference (Sargasso Sea deep water, 2600 m) minus blank reference materials. The nominal value for TOC provided by the reference laboratory is 44.0 ± 1.5 μM C.

Fluorescence of dissolved organic matter (FDOM). The DOM filtrate was measured with a Perkin Elmer LS 55 Luminescence spectrometer. The instrument was equipped with a xenon discharge lamp, equivalent to 20 kW for 8 μs duration, and a 1 cm quartz fluorescence cell. Milli-Q water was used as a reference for fluorescence analyses, and the intensity of the Raman peak was checked regularly. Discrete excitation/emission pair measurements were performed at peaks M (marine humic substances, average Ex/Em: 320 nm/410 nm; $FDOM_M$) and T (aromatic amino acids; average Ex/Em: 280 nm/350 nm; $FDOM_T$), specifically tryptophan (Coble et al. 1990; Mopper & Schultz 1993). Four replicate measurements were performed for each Ex/Em wavelength. A four points standard curve was prepared daily with a mixed standard of quinine sulphate (QS) and tryptophan (Trp) in sulphuric acid 0.05 M (Nieto-Cid et al. *in press*, Chapter 3). The equivalent concentration of every peak was determined by subtracting the average peak height from the blank height, and dividing by the slope of the standard curve. Fluorescence units were expressed in ppb

equivalents of QS (ppb QS) for $FDOM_M$ and ppb equivalents of Trp (ppb Trp) for $FDOM_T$. The precision were ±0.1 ppb QS and ±0.6 ppb Trp, respectively.

Metabolic balance of the water column. Daily photosynthetic production (Pg) and respiration (R) rates of the plankton community were estimated by the oxygen light-dark bottle method (Strickland & Parsons 1972). Samples collected in 10-L Niskin bottles were transferred to black polyethylene carboys. Five levels were sampled: 50%, 25% and 1% of surface light, and two more depths below (27 ± 2 and 41 ± 1 m). The carboys were gently shaken before sampling to prevent sedimentation of the particulate material. Series of eleven 110 mL Winkler bottles composed of triplicate initial, and quadruplicate light and dark subsamples were filled for each depth. Each series of light and dark subsamples were incubated for 24 hours (starting within one hour of the sunrise) at the original light and temperature conditions in incubators placed in the terrace of the base laboratory. Dissolved oxygen was determined by Winkler potentiometric end-point titration.

Theses incubators were also used to follow the changes in $FDOM_M$ and $FDOM_T$ under the same conditions. Series of nine 250 mL all-glass flasks compose of triplicate initial, dark and light subsamples were filled. In this case, samples were filtered before analysis through precombusted (450ºC, 4 h) 47 mm ø Whatman GF/F filters in an acid-cleaned glass filtration system, under low N_2 flow pressure. Fluorescence of initial, dark and light filtered samples was analyzed with the Perkin Elmer LS 55 spectrofluorometer.

Photodegradation of humic substances. Incubation experiments to follow the natural sunlight photodegradation of humic substances in riverine and sea (surface and bottom) water were conducted. Riverine samples were collected once a week in the Soutomaior Bridge, in the upstream limit of fresh water-seawater interface of the River Oitabén-Verdugo (Fig. 4.1). The salinity of riverine samples was <2. Surface and bottom waters of the middle ría were

incubated once a week too. Samples were filtered, first, through precombusted (450ºC, 4 h) 47 mm ø Whatman GF/F filters (nominal pore size, 1 μm), and, second, through 47 mm ø Gelman Laboratory Supor®-200 membrane filters (nominal pore size, 0.2 μm), in an acid-cleaned glass filtration system, under low N_2 flow pressure. The filtrates were collected in 250 mL quartz incubators and placed in the terrace of the base laboratory, exposed to 100% natural sunlight. $FDOM_M$ was measured several times during the incubation (0, 1, 3, 7 and 15 days).

RESULTS

The mean profile of microbial respiration rates (R) presented two significant maxima ($p < 0.005$); at the surface and bottom layers, with average values of 6.2 and 1.8 μmol kg^{-1} d^{-1}, respectively (Fig. 4.2a). The largest variability was observed in the photic layer, especially at the depth of the 25% PAR. In the case of the gross primary production (Pg), a surface maximum was observed (average 37 μmol kg^{-1} d^{-1}; Fig. 4.2b). R and Pg ranged from 0 to 15 and from 0 to 105 μmol kg^{-1} d^{-1}, respectively. These wide ranges resulted from sampling a wide variety of meteorological (coastal wind and freshwater runoff regimes) and hydrographic (stratification and homogenization regimes) conditions in the Ría de Vigo. The water-column integrated R showed a marked seasonal trend: low values during winter and spring, and significantly higher ($p < 0.001$) during the summer and autumn (Fig. 4.2c). On the contrary, the water-column integrated Pg did not show any significant seasonal pattern (Fig. 4.2d). The intra-period variability (time scale of 1/2 wk) was of the same magnitude than the inter-period variability (seasonal time scale). It is noticeable the low Pg during autumn. Average ± SD water column integrated Pg expressed in carbon units was 2.7 ± 2.1 g C m^{-2} d^{-1} if a O_2/C molar ratio of 1.4 is assumed (Anderson 1995, Fraga 2001). In average, about 40% of Pg was respired in the water column: 3/5 in the photic layer and 2/5 in the aphotic layer. The remaining

60%, the so called new or export production (Quiñones & Platt 1991), is available for export to the adjacent shelf, sinking to the sediments or be transferred to a higher trophic level. The ratio of new to total production, (Pg-R)/Pg, ranged from 0.6 to 0.8 during winter, spring and summer (autotrophic phase), but it dramatically decreased to -0.2 during autumn (heterotrophic phase). This conspicuous seasonal pattern has been throughoutly described in previous works by Moncoiffé et al. (2000) and Álvarez-Salgado et al. (2001a).

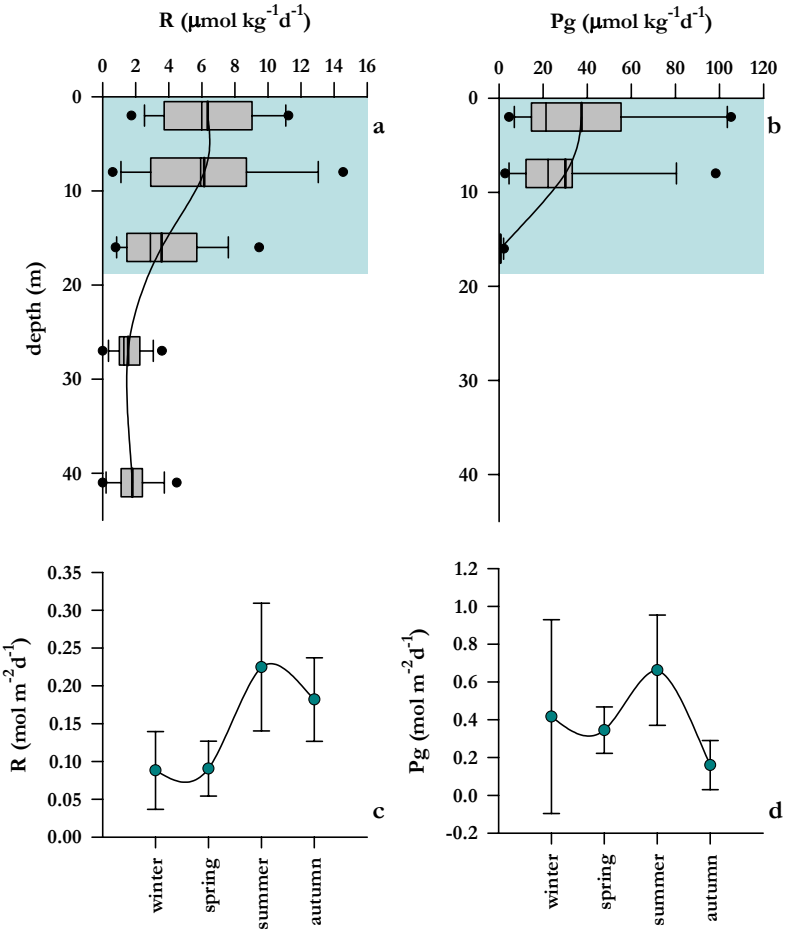

Figure 4.2 Box and whisker plot of (**a**) respiration and (**b**) gross primary production rates in the middle Ría de Vigo. Fifty percent of the data are included within the limit of the boxes and the caps represent the 10th and 90th percentiles. Solid lines represent the average profiles. Plots (**c**) and (**d**) show the average and standard deviation of the seasonal evolution of the water-column integrated respiration and gross primary production rates, respectively.

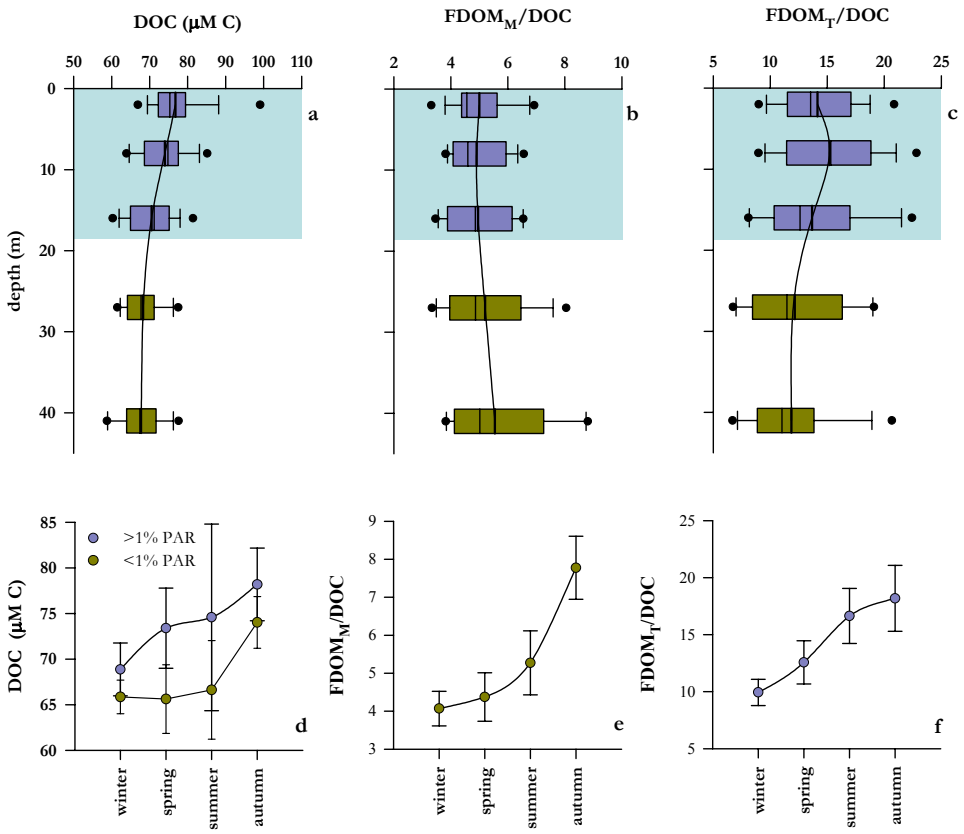

Figure 4.3 Box and whisker plot of (**a**) DOC, (**b**) $FDOM_M/DOC$ and (**c**) $FDOM_T/DOC$ profiles for the middle Ría de Vigo. Fifty percent of the data are included within the limit of the boxes and the caps represent the 10th and 90th percentiles. Solid lines represent the average profiles. Plots (**d**), (**e**) and (**f**) show the average and standard deviation of seasonal evolution of DOC, $FDOM_M/DOC$ and $FDOM_T/DOC$, respectively. ● > 1% PAR and ● < 1% PAR

The mean DOC profile showed a significant decrease with depth ($p < 0.001$) from an average surface value of 77 µM C to a bottom value of 68 µM C (Fig. 4.3a). Maximum variability occurred at the surface. This trend has been previously described by Doval et al. (1997) and Álvarez-Salgado et al. (1999). The $FDOM_M/DOC$ ratio showed a slightly, but significant, increase ($p < 0.001$) with depth, from 5.0 to 5.5 ppb QS (ppm C)$^{-1}$ (Fig. 4.3b). The $FDOM_T/DOC$ ratio presented higher values in the upper layer, with a subsurface maximum (15.2 ppb Trp (ppm C)$^{-1}$ at the 25% PAR depth), and a large variability in the

whole water column (Fig. 4.3c). DOC and $FDOM_M$/DOC displayed marked seasonal cycle in the lower layer (<1% PAR); the observed values were significantly higher ($p < 0.001$ and $p < 0.005$, respectively) during the autumn, with average values of 74.0 μM C and 7.8 ppb QS $(ppm\ C)^{-1}$, respectively (12% and 70% increase compared with the winter minimum; Fig. 4.3d, e). Seasonal variability of DOC and $FDOM_T$/DOC in the upper layer (>1% PAR) showed a similar pattern, with a significant increase ($p < 0.001$ and $p < 0.005$, respectively) from winter to autumn (78.2 μM C and 18.2 ppb Trp $(ppm\ C)^{-1}$; 8% and 39% increase compared with the winter minimum, respectively; Fig. 4.3d, f). In summary, Figure 4.3d-f indicates a seasonal accumulation of DOC with a marked enrichment in protein material in the upper layer and humic substances in the lower layer.

Microbial reactivity

The net production of humic substances measured in the dark incubations, $FDOM_M$ (dark), correlated significantly ($r = +0.73$, n = 79, $p > 0.001$) with respiration, R (Fig. 4.4a). The slope of this linear regression equation, 0.027 ± 0.003 ppb QS $(\mu mol\ kg^{-1})^{-1}$, indicates the rate of humic substances production to dissolved oxygen consumption by microbial respiration. It is noticeable the significant production of humic substances in an incubation time as short as 24 hours.

The fluorescence of aromatic amino acids measured in the dark and light incubations correlated worst with respiration and primary production rates. The only significant correlation ($r = +0.54$, n = 46, $p < 0.001$) was found between the net production obtained in the light incubations, $FDOM_T$ (light), and gross primary production, Pg (Fig. 4.4b). The slope of 0.018 ± 0.004 ppb Trp $(\mu mol\ kg^{-1})^{-1}$ indicates the rate of aromatic amino acids to dissolved oxygen production by the phytoplankton community. The origin intercept, -1.4 ± 0.2 ppb Trp d^{-1},

pointed to $FDOM_T$ consumption quicker than production, except for Pg exceeding 80 ± 20 μmol kg^{-1} d^{-1}.

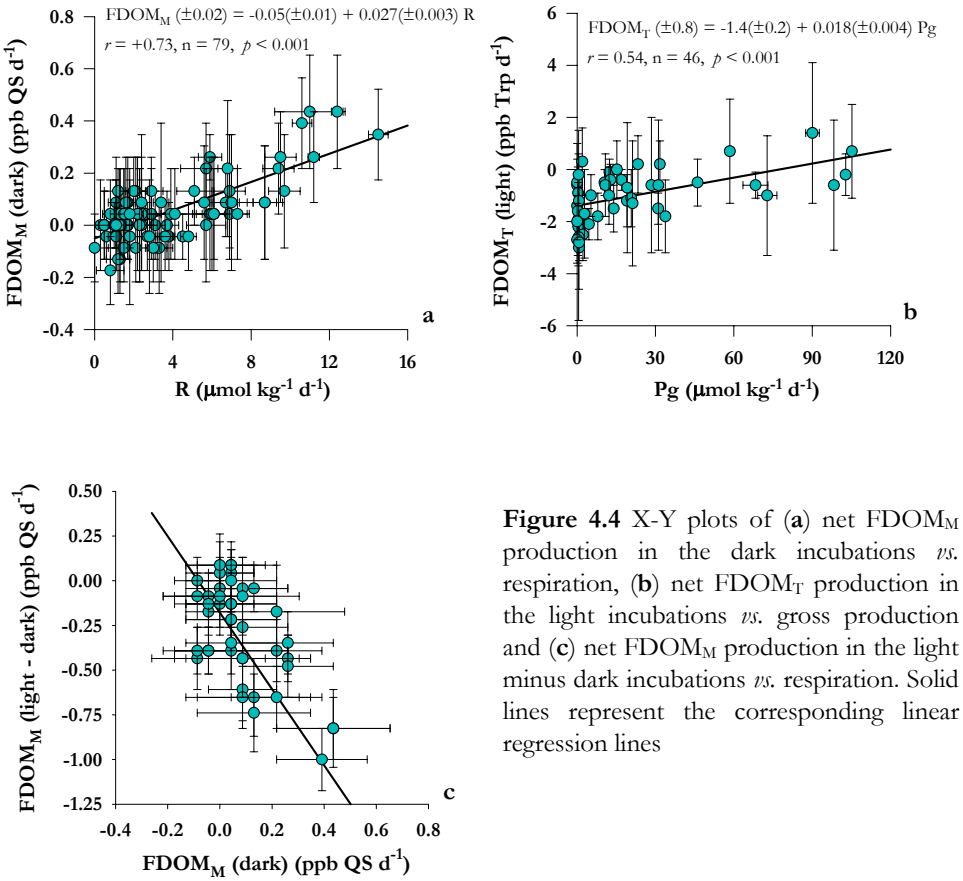

Figure 4.4 X-Y plots of (**a**) net $FDOM_M$ production in the dark incubations *vs.* respiration, (**b**) net $FDOM_T$ production in the light incubations *vs.* gross production and (**c**) net $FDOM_M$ production in the light minus dark incubations *vs.* respiration. Solid lines represent the corresponding linear regression lines

It is opportune to test if these regression parameters from an incubation bottle (10^{-1} L) could be extrapolated to the volume of a ría (10^{12} L). In order to study the relationship between dissolved oxygen and humic fluorescence in the ría after removal of the water masses mixing effect, a regression analysis involving two conservative parameters was used. The variability of any non-conservative parameter due to the mixing of the three water masses that meet in the ría (subtropical ENACW, subpolar ENACW and coastal water) can be estimated by means of a multiple linear regression of the non conservative

parameter with salinity and temperature (Nieto-Cid et al. 2004, *in press*, Chapter 2 and 3). Only samples with AOU > 0 can be used (<1% PAR, R > Pg) because S and T are conservative and O_2 is not exchanged with the atmosphere in these samples. The multiple regression of $FDOM_M$ with S, T and dissolved oxygen for sample with AOU > 0 was:

$FDOM_M$ (±0.6) = 78(±19) – 2.1(±0.5)S + 0.55(±0.08)T – 0.029(±0.003)O_{2C}

$r = 0.91$, n = 56, $p < 0.001$

The dissolved oxygen of the samples was referred to the oxidation state of nitrate (O_{2C}) to compare the oxygen consumption to the N-nutrient production independently of the nitrogen form involved in the process (Fraga 2001). Since 0.5 mol of oxygen is necessary to oxidize one mol of nitrite to nitrate and two mol of oxygen are required to oxidize one mol of ammonium to nitrate:

$$O_{2C} = O_2 - \frac{1}{2} \times NO_2^- - 2 \times NH_4^+ \qquad (4.1)$$

The resultant slope, -0.029(±0.003) ppb QS (µmol kg^{-1} $O_2)^{-1}$, is not significantly different from the incubation experiments. The opposite sign is because respiration involves the utilization of oxygen. It proves the validity of the incubation approach at the ecosystem level.

For the case of $FDOM_{T,}$ the correlation with primary production was observed in the upper layer (>1%PAR), where O_2 exchanges with atmosphere, and S and T do not behave conservatively. Therefore, validation of the incubation approach at the ecosystem level is not possible for the fluorescence of aromatic amino acids.

Photochemical reactivity

The difference between the net production of humic substances in the light and dark incubations is the material consumed by photobleaching during 1 day. A significant linear relationship (r = -0.71, n = 46, p > 0.001) was observed between the bacterial production and the photochemical consumption of humic compounds (Fig. 4.4c) in such a way that the humic material produced in

the dark, either in the aphotic layer or during the night, is rapidly photodegraded in the light.

Photobleaching experiments showed a loss of the humic-like fluorescence of the samples with the incubation time, which fitted to the exponential decay function:

$$C = (C_0 - C_f) \exp(-kt) + C_f \quad (4.2)$$

where C_0 is the initial concentration of humic compounds, C_f is the humic compounds resistant to photobleaching and k is the exponential decay constant.

The parameters of eq. 4.2 for the riverine samples in winter, spring, summer and autumn (Fig. 4.5a-d, respectively) were contrasting. It was found that the variability of C_0 and C_f followed the same pattern: they increased from a winter-spring minimum to an autumn maximum (Fig. 4.5e). The values of k suggested also a progressive increase of the decomposition rate from winter to autumn (Fig. 4.5f). Since incubations were made under natural light conditions, k depended not only on the incubation time but also on the contrasting incident light intensity, which increases from winter to autumn. Corrected k values to an average incident light are also show in Figure 4.5f; a constant decomposition rate of ~20% d^{-1}, was observed from winter to summer, followed by a 3-fold increase in autumn, when 65% of humic substances were photodegraded per day. However, the percentage of photobleached material ($(C_0-C_f)/C_0 \times 100$) was maximum in winter-spring (68%) and minimum in autumn (57%).

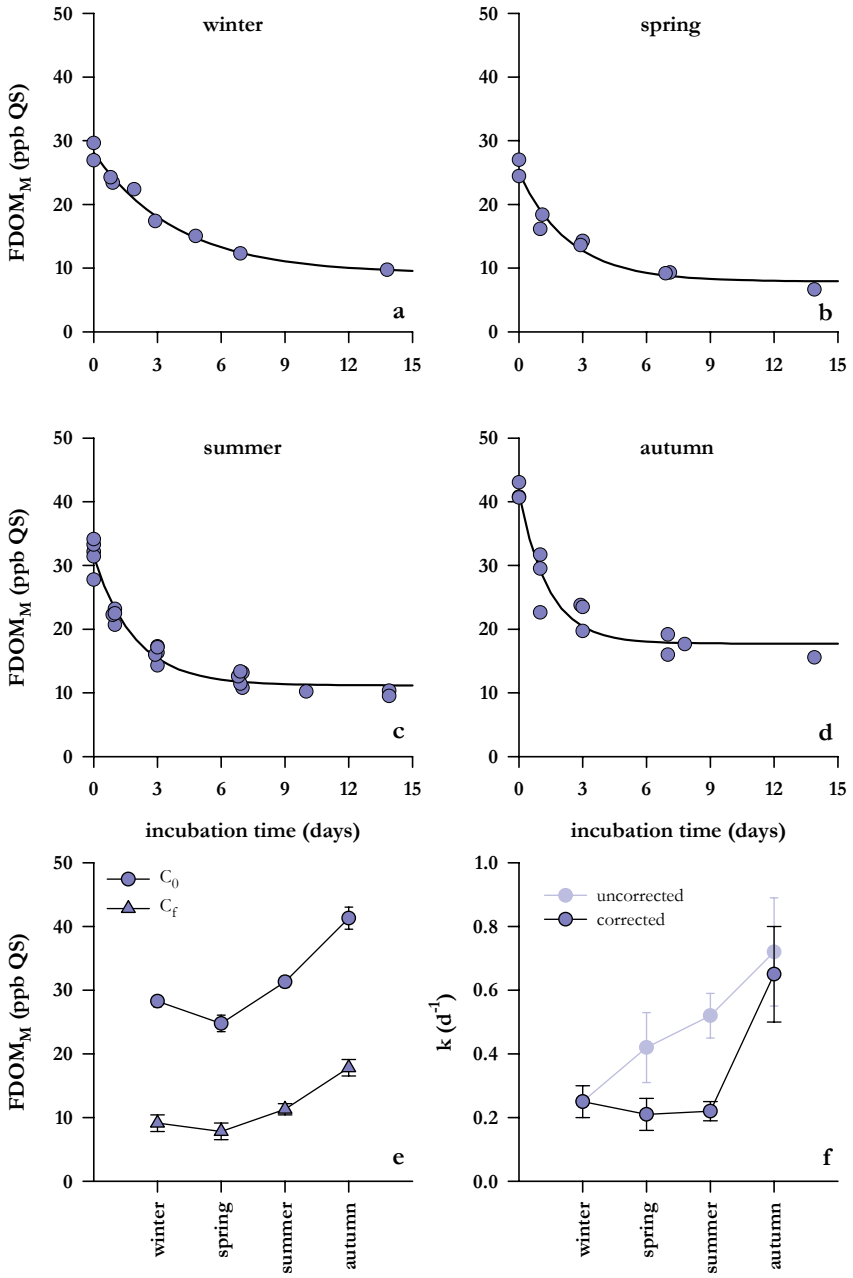

Figure 4.5 $FDOM_M$ course during the incubation time for winter (**a**), spring (**b**), summer (**c**) and autumn (**d**) riverine samples. The solid line represents the fit to an exponential decay function: $C = (C_0 - C_f) \exp(-kt) + C_f$. Seasonal variation of the estimated C_0 and C_f (**e**) and k uncorrected and corrected for incident light intensity (**f**)

Bottom and surface seawater samples from the ría displayed the same exponential decay pattern (Fig. 4.6a-d), characterised by lower initial and final concentrations (Fig. 4.6e) but with similar incident-light-corrected decomposition rates than riverine samples (Fig. 4.6f). The values of C_0, C_f and k were comparable from winter to summer, but autumn presented again the largest discrepancies: higher fluorescence and decomposition rates. It should also be noted that bottom and surface k values coincided in winter, but these values were spacing out with the increase of stratification in the water column. The decomposition rates became larger for the bottom (20 to 90% d^{-1}) than for the surface water (20 to 55% d^{-1}). Despite this, the percentage of photodegraded material during the incubations was similar at both depths. Values ranged from 44% in winter to 59% in summer for the bottom samples, whereas the percentages varied from 42% in summer to 50% in winter for the surface samples.

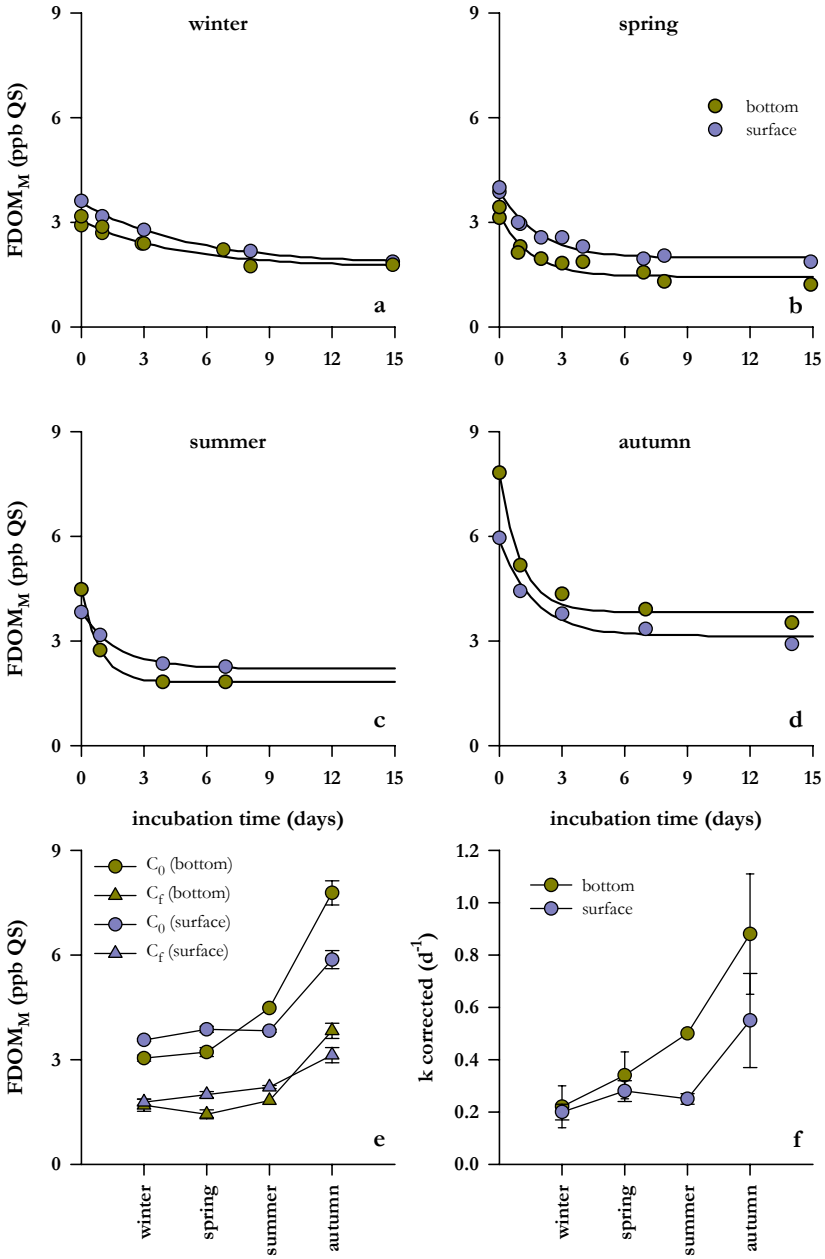

Figure 4.6 FDOM$_M$ course during the incubation time for winter (**a**), spring (**b**), summer (**c**) and autumn (**d**) seawater samples, surface (●) and bottom (●). The solid line represents the fit to the exponential decay function $C = (C_0 - C_f) \exp(-kt) + C_f$. Seasonal variation of the estimated C_0 and C_f (**e**) and k corrected for incident light intensity (**f**)

DISCUSSION

Microbial production of labile and recalcitrant DOM

A significant positive correlation has been found between the fluorescence of marine humic substances and the concentration of inorganic nutrients in the water column of different open ocean (Hayase et al. 1987, 1988, Chen & Bada 1992) and coastal marine systems (Chen & Bada 1992, Hayase & Shinozuka 1995, Nieto Cid et al. 2005, Chapter 3). All these authors concluded that marine humic substances and nutrient salts should have the same origin: the mineralization of settling organic particles. In the case of Nieto-Cid et al. (*in press*), Chapter 3, they were the first to separate the physical (water masses mixing) and biogeochemical components of the fluorescence of humic substances and nutrient salts to test a significant positive correlation between biogeochemical components. Therefore, they were all implicitly assuming that marine humic substances should be a by-product of bacterial respiration processes (Brophy & Carlson 1989, Tranvik 1993, Kramer & Hernld 2004). Other models, such as the condensation of poly phenols (Hedges 1978) or the photo-oxidation of lipids (Kieber et al. 1997) would restrict to estuaries, where poly phenols of terrestrial origin can be abundant, and the surface ocean layer, where the UV radiation is able to oxidize triglycerides and fatty acids of planktonic origin.

Net production rates of humic-like fluorophores in dark incubations of natural plankton populations have not been obtained until very recently by Yamashita & Tanoue (2004) and Kramer & Hernld (2004). In as survey of Ise Bay (Japan), former authors found that about 25% of the humic-like fluorescence intensity of surface waters was produced *in situ*. A degradation experiment using natural plankton from Ise Bay demonstrated the rapid production of humic substances in tandem with plankton degradation within the short time scale of a day in the dark. The production rate was as high as

2.97 ppb QS d^{-1} during the initial 12 hours, it reduced to 1.04 ppb QS d^{-1} during the initial 3 days, and then increased gradually at 0.07 ppb QS d^{-1}. Following a similar approach, Kramer & Herndl (2004) concentrated and resuspended in artificial seawater bacterioplankton of the coastal North Sea. They observed a steadily increase of the fluorescence of humic substances at a rate of 0.15 ± 0.03 ppb QS d^{-1} until day 9 of the incubation. Thereafter, fluorescence remained constant until the end of the experiment, on day 21.

In this work, we incubated during 1 day unaltered natural marine samples collected at different depth in the euphotic and aphotic layers of a coastal upwelling system under a wide variety of meteorological and oceanographic conditions. This confirms the results of the degradation experiment conducted by Yamashita & Tanoue (2004) in the estuarine system of Ise Bay, and by Kramer & Herndl (2004) in the coastal North Sea, consistently suggesting that *in situ* production of marine humic-like fluorophore plays an important role in the dynamics of DOM in coastal environments. Daily production rates of humic substances in the coastal upwelling system of the Ría de Vigo, <0.5 ppb QS d^{-1}, were much lower than in the experiment of Ise Bay and similar to those found in the coastal North Sea. Kramer & Herndl (2004) observed that whereas the $FMOD_M$/DOC ratio of the bacterial-derived DOM varied from 3 to 7 ppb QS (ppm C)$^{-1}$, the marine bulk DOM from the North Sea, Adriatic Sea and North Atlantic was <1.5 ppb QS (ppm C)$^{-1}$. Note that the $FMOD_M$/DOC ratio for the samples of the Ría de Vigo varied from 4 to 8 ppb QS (ppm C)$^{-1}$ (Fig. 4.3), further reinforcing the hypothesis of a bacterial origin of the humic-like fluorescence.

An added value of our work is the possibility to compare, for the first time in the literature, the daily production of marine humic-like fluorophores with the daily consumption of dissolved oxygen in the dark. Therefore, the significant positive correlation between the net production of humic substances and the

net consumption of dissolved oxygen, constitute a field evidence of the fast production of humic substances as a by-product of microbial respiration processes in the marine environment in general, and a costal upwelling system in particular. The local or universal validity of the resultant ratio of marine humic fluorescence production to dissolved oxygen consumption, 0.027 ± 0.003 ppb QS $(\mu mol\ kg^{-1})^{-1}$, has to be tested in further studies in other marine environments.

Yamashita & Tanoue (2004) also observed a continuous decrease in the fluorescence of dissolved amino acids in tandem with the production of marine humic substances during a 71 days dark incubation of the natural plankton of Ise Bay. In agreement with these authors, we obtained an average net consumption rate of protein-like fluorescence of 1.4 ± 0.2 ppb Trp d^{-1}. This rate is the origin intercept of the significant positive correlation observed between the net production of protein-like fluorophores and the net production of dissolved oxygen in the light. This relationship indicates that the production of dissolved amino acids is probably linked to phytoplankton exudation at a rate of 18 ± 4 10^{-3} ppb Trp $(\mu mol\ kg^{-1})^{-1}$ and it is rapidly consumed by bacteria, in such a way that accumulation of protein-like fluorescence after a 1 day incubation only occurs when primary production exceeds 80 ± 20 μmol O_2 kg^{-1} d^{-1}, i.e. about 0.7 ± 0.2 g C m^3 d^{-1} if a O_2/C molar ratio of 1.4 is assumed (Anderson 1995, Fraga 1991).

Bioavailability of marine humic substances by photobleaching

Photochemical processes have been identified as a potentially important mechanism for the degradation of terrestrial (e.g. Amon & Benner 1996, Opsahl & Benner 1998, Moran et al. 2000) and marine (e.g. Mopper & Zhou 1990, Benner & Biddanda 1998, Obernosterer & Herndl 2000) humic substances. Photochemical degradation of DOM is usually followed by the exponential decrease of the concentration of DOC or the absorbance of DOM

at wavelengths ranging from 350 to 450 nm during the course of incubation experiments under laboratory or natural UV light conditions. Less attention has been paid to the fluorescence technique for evaluating photodegradation rates, despite they revealed especially useful in marine systems where DOC concentrations and chromophoric DOM levels are low compared with freshwater and estuarine systems. In addition, fluorescence allows following the decomposition of specific fluorophores rather than the bulk DOM (Pullin & Cabaniss 1997). Incubations experiments to derive DOM photodegradation rates following the decrease of humic-like fluorescence under natural light conditions during short time periods (1-2 wk) are scarce in the literature. In fact, to our knowledge, only Skoog et al. (1996) carried out this type of experiment at several depths in the Baltic Sea on a single day in May 1992. They found higher photodegradation rates (0.60 to 1.25 d^{-1}) and similar percentages of photobleached material (50 to 56%) than in the Ría de Vigo for incubation times of 4 days. We observed maximum photodegradation rates during the autumn, at the time when bacterial mineralization became the dominant process either in terrestrial and marine systems (note that (Pg-R)/Pg = -0.2). Therefore, the contribution of freshly-produced terrestrial (Fig. 4.5e) and marine (Fig 4.3e and Fig. 4.6e) humic substances to DOC is maximum, although this material results to be more photosensitive or the quality, but not the intensity, of natural light enhances photodegradation (Del Vecchio & Blough 2002). Unfortunately, there are not studies following the evolution of photodegradation rates during a seasonal cycle to compare with our results.

Increased availability to bacteria of DOM exposed to natural UV light has been observed in lakes (e.g. Lindell et al. 1995, De Lange et al. 2003) and coastal waters (e.g. Miller & Moran 1997, Gustavson et al. 2000, Obernosterer & Herndl 2000). However, Tranvik & Bertilsson (2001) indicated that photochemical transformation of DOM can either reduce or enhance bacterial

utilization; whereas humic substances are predominantly transformed into labile forms, algal-derived DOM is transformed into compounds of decreased bacterial substrate quality. The same argument was used by Benner & Biddanda (1998) to explain why the effects of sunlight exposure on bacterial utilization of DOM was negative for surface samples (15-115 m) and positive for deep samples (150-1000 m) of the Gulf of Mexico. According to these authors, surface DOM was enriched in phytoplankton material, whereas the concentration of marine humic substances increased with depth. Similar conclusions have been raised by Obernosterer et al. (1999). Accordingly, Obernosterer & Benner (2004) observed that whereas photodegradation enhanced the biodegradation of terrigenous humic substances, this effect was not detected for plankton material.

In this work, we have obtained a significant negative correlation between the bacterial production and the photochemical decomposition of marine humic substances. It suggests rapid photodegradation of recently produced marine humic substances that, in turns, would enhance bacterial activity as a consequence of the transformation of marine humic substances into compounds of increased bacterial substrate quality.

Finally, we have also obtained that the humic substances of the bottom layer were photodegraded faster than the humic substances of the surface layer during the summer and autumn stratification periods. The increase of photodegradation rates with depth was also observed by Skoog et al. (1996) in the Baltic Sea. In a coastal system such as the Ría de Vigo, upwelling promotes the quick rise of bottom waters to the surface layer (Álvarez-Salgado et al., 2000) and continental inputs are quite scarce (Piedracoba et al. 2005). Therefore, the humic material of the surface layer is just the same material of the bottom layer after partial photodegradation. Although it has been previously shown that the deep sea DOM is more photoreactive than

photobleached surface material (Mopper & Zhou 1990, Mopper et al. 1991, Mopper & Kieber 2000), the time scale of the upwelling process needed to photodegrade the deep sea material is tenths to hundreds of years. On the contrary, the humic material produced during bacterial respiration in the bottom layer of the Ría de Vigo is advected to the surface layer in just 1 wk (Álvarez-Salgado et al. 2000), where intense photodegradation takes place. In this sense, Fig. 4.7, schematises the expected tightly coupling between photochemical and microbial degradation processes during an upwelling episode. Photochemical degradation of marine humics will produce gases such as CO_2 and low-molecular-weight carbonyl compounds (Mopper et al. 1991, Moran & Zepp 1997, Mopper & Kieber 2000, Kieber 2000) able to stimulate the bacterial activity of the surface layer. Therefore, the humic substances produced by the bacterial activity in the bottom layer will enhance in about 1 wk the bacterial activity of the surface layer after exposure to sunlight.

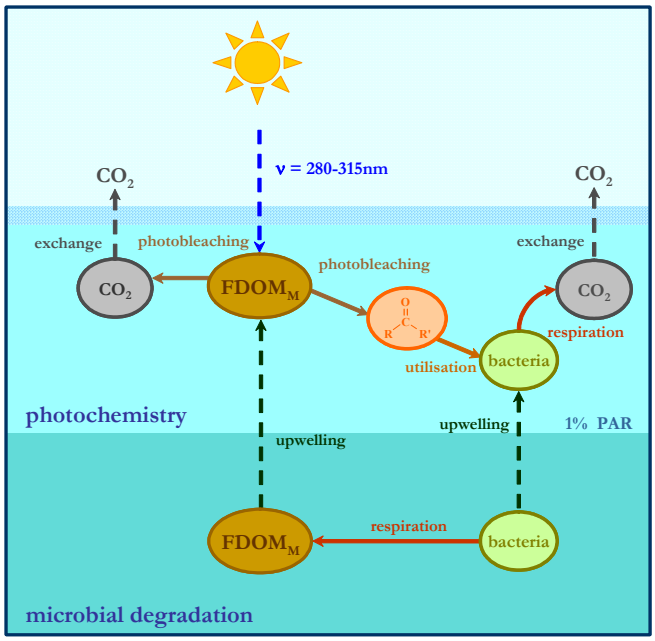

Figure 4.7. Scheme of the coupling between photochemical degradation and microbial production of humic DOM in the upper and lower layer of the coastal upwelling system of the Ría de Vigo

CONCLUSIONS

The fluorescence of humic substances and dissolved aromatic amino acids (DFAA) and the dissolved oxygen were measured in parallel 24 h light and dark incubations, for the first time in a coastal upwelling system. In one day, the system showed net production of humic substances (0.0-0.4 ppb QS d^{-1}), which were positively correlated with the respiration rates with a net ratio of 0.027 ± 0.003 ppb QS (µmol kg^{-1} O_2)$^{-1}$, suggesting a daily synthesis of marine humics as a by-product of the bacterial respiration of DOM. Consequently, the fluorescence of marine humic substances revealed as a suitable indicator of nutrient mineralization processes.

A significant linear correlation between the gross primary production and the net production of DFAA in the light, points to the quick consumption of dissolved protein-like materials at a net average rate of -1.4 ± 0.2 ppb Trp d^{-1}, which accumulates in the water column only when Pg exceeds 80 ± 20 µmol $kg^{-1}d^{-1}$. Therefore, DOM fluorescence can be used as a tracer for labile DOM (DFAA) production/consumption.

The consumption of humic substances in the light minus dark incubations was inversely correlated with the net production of humic substances in the dark, indicating a rapid photodegradation of recently produced marine humic substances as a by-product of microbial respiration. Incubation experiments demonstrated that daily photodegradation rates and residual humic fluorescence levels followed a seasonal pattern characterised by a marked autumn maximum, either in the river waters (65% photobleaching per day) or in the ría (55-90% photobleaching per day). Due to the upwelling of bottom waters, the humic material produced during bacterial respiration in the bottom layer is quickly degraded in the surface layer by photochemical processes.

Chapter 5:

Stoichiometry of the mineralization of dissolved and particulate biogenic organic matter in the NW Iberian upwelling

Chapter 5, the research work presented in this chapter is also a contribution to the paper:

X. A. Álvarez-Salgado, M. Nieto-Cid, J. Gago, S. Brea, C. G. Castro, M. D. Doval, F. F. Pérez. 2005. **Stoichiometry of the mineralization of dissolved and particulate biogenic organic matter in the NW Iberian upwelling**. J Geophys Res, *accepted*

Resumen Se ha establecido por primera vez en un sistema de afloramiento costero la composición media de los productos de degradación temprana del fitoplancton marino, tanto disueltos como particulados, utilizando un análisis de mezcla a lo largo de superficies isopícnicas combinado con un modelo estequiométrico. Un 17-18% de la materia orgánica se mineraliza en forma de material en suspensión y un 16-35% lo hace como materia disuelta. La fracción restante (50-70%) es material orgánico mineralizado probablemente a partir de grandes partículas que sedimentan rápidamente. En promedio, el material mineralizado a partir de estas partículas tiene la composición media más similar a la fórmula de Redfield. La materia orgánica disuelta presenta más de un 40% de enriquecimiento en mineralización de carbohidratos en comparación con la fórmula de Redfield. Por último, el material en suspensión está caracterizado por un enriquecimiento en mineralización de lípidos de más del 80%. Por otro lado, con respecto a la mineralización de estructuras duras, el silicio biogénico se disuelve predominantemente en el interior de la plataforma costera, donde la oxidación del carbono orgánico es más intensa y se produce un mayor depósito de diatomeas.

Abstract: The average composition of the dissolved and particulate products of early degradation of marine phytoplankton has been established for the first time in a coastal upwelling system, using a mixing analysis along isopycnal surfaces combined with a stoichiometric model. About 17-18% of the mineralised organic matter is in the form of suspended particles and 16-35% as dissolved organic matter. The missing 50-70% are probably large, fast sinking, particles. On average, the mineralised material on large particles has the closest composition to the Redfield formula. Dissolved organic matter presents >40% enrichment in carbohydrates mineralization compared with the Redfield formula. Finally, suspended particles are characterised by >80% enrichment in lipids mineralization. Regarding the mineralization of hard structures, biogenic silica dissolves predominantly in the inner shelf, where organic carbon oxidation is more intense and diatom deposition occurs preferentially.

INTRODUCTION

The composition of the products of early degradation of phytoplankton photosynthesis has been a matter of controversy over the last 50 years, after the seminal study of Redfield et al. (1963). Based on that work, Richards (1965) established an average composition of $C_{106}H_{264}O_{110}N_{16}P$. Subsequently, Anderson (1995) and Fraga et al. (1998) proposed revised formulas, $C_{106}H_{175}O_{42}N_{16}P$ and $C_{106}H_{171}O_{42}N_{16}P$ respectively, which basically corrected the overestimated H and O proportions of the original Richard's (1965) formula.

Some authors have asserted that the oxidation of biogenic organic matter in the ocean interior follows a constant with depth and basin stoichiometric model (e.g. Takahashi et al., 1985; Anderson & Sarmiento, 1994). Others considered that there is a fractionation during the mineralization of biogenic organic matter, in such a way that the most labile P- and N-rich materials are oxidized preferentially at shallower depths (e.g. Martin et al. 1987, Minster & Boulahdid 1987, Shaffer et al. 1999, Brea et al. 2004) or in the most ventilated ocean basins (Li & Peng 2002). Modifications in the quality and quantity of the sinking materials exported from the upper ocean (Pahlow & Riebesell 2000) and changes in source water type properties (Gruber et al. 2000) have also been argued to explain these inter basin differences.

Another matter of open discussion is the relative contribution of dissolved, suspended and sinking organic matter to oxygen consumption in the oceans. Some authors maintain that the oxidation of large, fast sinking, particles has to be the dominant process to keep the apparent constancy of the $-O_2/C/N/P$ ratios (Anderson & Sarmiento 1994). On the contrary, others propose fractionation during the mineralization of suspended organic matter (Copin-Montégut & Copin-Montégut 1983, Garber 1984, Martin et al. 1987, Sambrotto et al. 1993, Schneider et al. 2003). The model of Suess & Müller (1980) incorporates strong elemental fractionation of particulate organic matter (POM)

through the water column by preferential removal of N- and P-containing organic compounds. Assuming that 30% of the downward flux of biogenic materials is in the dissolved form (Yamanka & Tajika 1997), it cannot be discarded the contribution of the dissolved organic matter (DOM), with higher C/N/P ratios than POM (e.g. Clark et al. 1998, Loh & Bauer 2000, Hopkinson et al. 1997, 2002).

Biogenic matter production is enhanced in the coastal zone because of intensified nutrient fluxes from the ocean, the continents and the atmosphere (Walsh 1991). Average primary production per unit area in the coastal zone, 250 g C m^{-2} y^{-1}, is more than twice than in the open ocean, 90 g C m^{-2} y^{-1} (Wollast 1998). As a result, the mineralization of biogenic materials is also enhanced. About 83% of the ocean benthic mineralization and 87% of the burial occurs in the sediments of the coastal zone (Middelburg et al. 1993). Pelagic and benthic mineralization processes are specially intensified in coastal upwelling areas, because of the magnified entry of nutrients.

The aim of this work is to study the biochemical composition of the dissolved and particulate, soft and hard, biogenic materials mineralised in the water column of the NW Iberian upwelling system in two contrasting environments: the system of large, V-shaped embayments of Galicia (NW Spain), known as Rías Baixas (Fig. 5.1) and the adjacent open shelf. Although the rías are singular ecosystems, their large dimensions and their well-known hydrodynamic and biogeochemical behaviour make them similar to any coastal upwelling system at comparable latitudes: off Oregon (NW America) or off Chile (SW America).

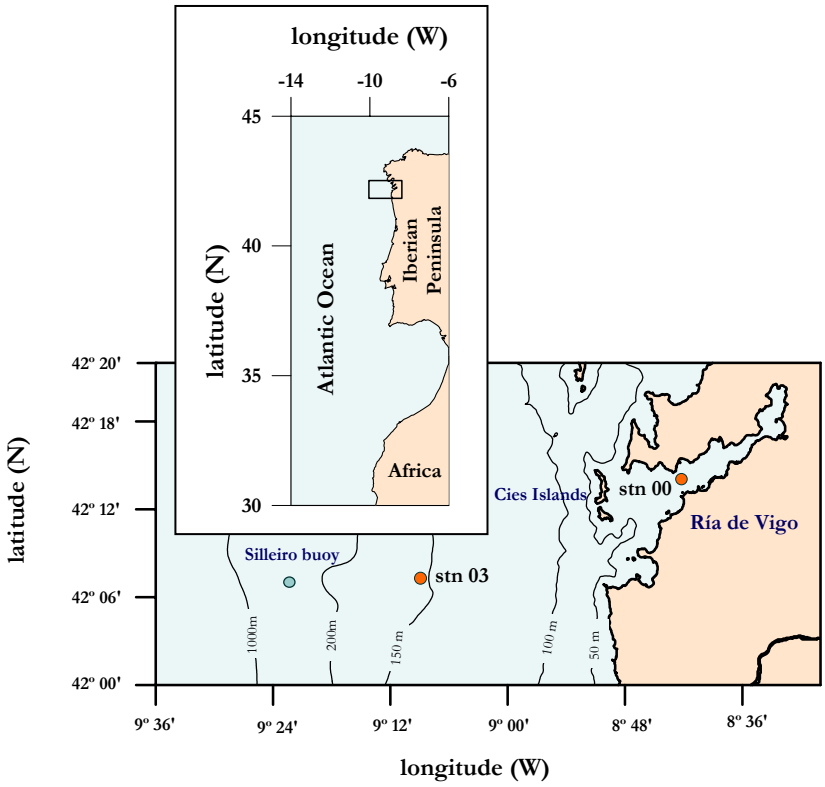

Figure 5.1 Map of the study area, the Ría de Vigo and adjacent open shelf waters. The positions of the sampling stations in the middle ría (stn 00) and the middle shelf (stn 03), as well as the Silleiro Sea Watch buoy meteorological observatory, are indicated. The isobaths of -50, -100, -150, -200 and -1000 m are also depicted

MATERIAL AND METHODS

Study area. This study is focused on the NW Iberian upwelling system (42-43ºN), at the boundary between the temperate and subpolar regimes of the Eastern North Atlantic (Fig. 5.1). Wind stress/relaxation cycles of period 1-2 wk take place from March-April to September-October, the upwelling-favourable season (Álvarez-Salgado et al. 1993). Downwelling prevails the rest of the year, favouring a reversal of the coastal circulation with the arrival of warm and salty subtropical surface and central waters to our latitudes in the form of the well defined slope Iberian Poleward Current (IPC; Álvarez Salgado et al. 2003). The winter mixing period occurs at the time of the transition from the downwelling- to the upwelling- favourable seasons.

Two contrasting environments were sampled: **1)** the Ría de Vigo, a 2.5 km^3 large V-shaped embayment which is primarily controlled by coastal winds and secondarily by continental runoff (Gilcoto et al. 2001); and **2)** the adjacent shelf, which exchanges water and materials with the rías and the open ocean and it is affected by strong alongshore currents. Both environments are connected during the upwelling season, when the surface waters of the ría are exported to the adjacent shelf and the bottom waters of the shelf enters the ría. On the contrary, during the downwelling season a convergence front develops between the subtropical IPC waters transported onshore by the Ekman transport and the waters of the ría transported offshore by the continental runoff (Álvarez-Salgado et al. 2000).

Sampling strategy. Two stations were sampled weekly from May 2001 to April 2002: stn 00 was in the middle segment of the Ría de Vigo (45 m depth) and stn 03 was in the middle shelf (150 m depth). Samples were taken with a rosette sampler equipped with twelve 10 litre PVC Niskin bottles with stainless-steel internal springs. Salinity and temperature were recorded with a SBE 9/11 conductivity-temperature-depth probe attached to the rosette sampler. Conductivity measurements were converted into practical salinity scale values with the equation of UNESCO (1985).

Samples for the analyses of dissolved oxygen, pH, total alkalinity, nutrient salts, dissolved and particulate organic carbon and nitrogen were collected from 5, 15 and 40 m in stn 00 and 5, 25, 40, 60, 75, 100 and 150 m in stn 03 with a weekly periodicity. Samples for dissolved and particulate organic phosphorus and carbohydrates were taken at the same depths but with a fortnightly periodicity.

Dissolved oxygen (O_2). It was directly collected into calibrated 110 mL glass flasks and, after fixation, they were kept in the dark until analysis in the laboratory 24 h later. O_2 was determined by Winkler potentiometric end-point

titration using a Titrino 720 analyser (Metrohm) with a precision of ±0.5 μmol kg^{-1}. The apparent oxygen utilisation, AOU = O_2sat - O_2, was calculated using the algorithm proposed by Benson & Krause (UNESCO 1986) for oxygen saturation (O_2sat).

Nutrient salts. Water samples were collected in 50-mL polyethylene bottles; they were kept cold (4ºC) until analysis in the laboratory using standard segmented flow analysis (SFA) procedures. The precisions are ±0.02 μM for nitrite, ±0.1 μM for nitrate, ±0.05 μM for ammonium, ±0.02 μM for phosphate and ±0.05 μM for silicate.

Total alkalinity (TA) and total inorganic carbon (C_T). Samples for TA and pH (total hydrogen concentration scale, 25ºC) were collected into 500 mL glass flasks and analysed within a few hours in the base laboratory. Seawater pH was measured spectrophotometrically following Clayton & Byrne (1993). The precision is ±0.003 pH units. TA was determined by titration to pH 4.4 with HCl, according to the potentiometric method of Pérez & Fraga (1987) with a precision of ±2 μmol kg^{-1}. The potential alkalinity (TA_p) was calculated following Fraga & Álvarez-Salgado (2004):

$$TA_p = TA - NH_4^- + 0.93 \times NO_2^- + NO_3^- + \\ + 0.08 \times \left(NH_4^+ + NO_2^- + NO_3^-\right) + 0.23 \times HPO_4^{2-} \qquad (5.1)$$

Total inorganic carbon (C_T) was calculated from pH and TA with the carbonic and boric acid dissociation constants of Lueker et al. (2000). The estimated precision of this calculation is ±3 μmol kg^{-1}.

Dissolved organic carbon (DOC) and nitrogen (DON). Samples were taken into 500 mL acid-cleaned flasks and filtered through precombusted (450ºC, 4 h) 47 mm ø Whatman GF/F filters in an acid-cleaned glass filtration system, under low N_2 flow pressure. Aliquots for the analysis of DOC/DON were collected into 10 mL precombusted (450ºC, 12 h) glass ampoules. After acidification with H_3PO_4 to pH < 2, the ampoules were heat-sealed and stored

in the dark at 4ºC until analysis. DOC and DON were measured simultaneously with a nitrogen-specific Antek 7020 nitric oxide chemiluminescence detector, coupled in series with the carbon-specific Infrared Gas Analyser of a Shimadzu TOC-5000 organic carbon analyser (Álvarez-Salgado & Miller 1998). The precision is ±0.7 μM C for carbon and ±0.2 μM N for nitrogen. Their respective accuracies were tested daily with the TOC/TDN reference materials provided by Prof. D. Hansell (Univ. of Miami). We obtained an average concentration of 45.7 ± 1.6 μM C and 21.3 ± 0.7 μM N (n = 26) for the deep ocean reference (Sargasso Sea deep water, 2600 m) minus blank reference materials. The nominal value for TOC provided by the reference laboratory is 44.0 ± 1.5 μM C; a consensus TDN value has not been supplied yet, but a mean ± SD value of 22.1 ± 0.8 μM N for four High Temperature Catalytic Oxidation (HTCO) systems and 21.4 μM N for one persulphate oxidation method has been provided by Sharp et al. (2004) as a result of the Lewes intercalibration exercise. DON was obtained by subtracting N_T (total inorganic nitrogen =ammonium + nitrite + nitrate) from TDN.

Dissolved organic phosphorus (DOP). Samples were taken and filtered as indicated for DOC/DON. The filtrate was collected into 50 mL polyethylene containers and frozen at -20ºC until analysis. It was measured by the SFA system for phosphate, after oxidation with $Na_2S_2O_8$/borax and UV radiation (Armstrong et al. 1966). Only the organic mono-phosphoric esters are analysed because poly-phosphates are resistant to this oxidation procedure. Daily calibrations with phosphate, phenyl phosphate and adenosine 5'-monophosphate (AMP) in seawater were carried out. Standards of AMP were determined in order to calculate the mono-phosphoric esters recovery (~80%). The precision of the method is ±0.04 μM P.

Dissolved mono- and polysaccharides (MCHO and PCHO). Sampling and storage procedures are identical than for DOP samples. MCHO and

PCHO were determined by the oxidation of the free reduced sugars with 2,4,6-tripyridyl-s-triazine (TPTZ) followed by spectrophotometric detection at 595 nm (Myklestad et al. 1997, Hung et al. 2001). The system was standardised daily with D-glucose. The precision is ±0.6 μM C for MCHO and ±0.7 μM C for d-CHO, and the detection limit was ~2 μM C. See Nieto-Cid et al. (2004), Chapter 2, for further details.

Particulate organic carbon and nitrogen (POC and PON). Suspended organic matter was collected under low vacuum on precombusted (450ºC, 4 h) 25-mm ø Whatman GF/F filters (POC/PON, 0.5-1.5 L of seawater). All filters were dried overnight and frozen (-20ºC) before analysis. Measurements of POC and PON were carried out with a Perkin Elmer 2400 CHN analyser. An acetanilide standard was used daily. The precision of the method is ±0.3 μM C and ±0.1 μM N.

Particulate organic phosphorus (POP). It was determined by $H_2SO_4/HClO_4$ digestion at 220ºC of the particulate material collected from 250-500 mL of seawater on Whatman GF/F filters. The phosphoric acid resultant from the digestion was analysed with the SFA method for phosphate. The precision is ±0.02 μM P.

Particulate carbohydrates (p-CHO). About 250-500 mL of seawater were filtered and stored as indicated for POC, PON and POP. p-CHO was determined by the anthrone method (Ríos et al. 1998). It is based in the quantitative reaction of sugars with anthrone in a strongly acid medium at 90ºC, to give an intensely coloured compound. The absorption was measured at 625 nm. The system was calibrated daily with D-glucose. The precision of the method is ±0.1 μM C

Chlorophyll (Chl a). Between 100 and 200 mL of seawater were filtered through GF/F filters and frozen (-20ºC) before analysis. Chl a was determined

with a Turner Designs 10000R fluorometer after 90% acetone extraction (Yentsch & Menzel 1963). The precision is ±0.05 mg m^{-3}.

RESULTS AND DISCUSSION

Hydrography of NW Iberian shelf waters

Figure 5.2 identifies the seven hydrographic periods defined by Nieto-Cid et al. (2004), Chapter 2, during the sampling period, on basis of the meteorological conditions (offshore Ekman transport, $-Q_X$; continental runoff Q_R) and the water column response (salinity and temperature):

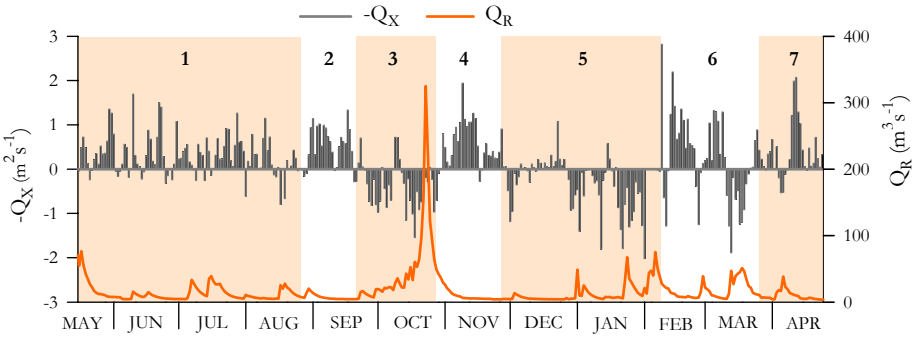

Figure 5.2 Seasonal evolution of the offshore Ekman transport ($-Q_X$) calculated with wind data provided by the Silleiro Sea Watch buoy (http://www.puertos.es). The freshwater discharge to the Ría the Vigo (Q_R) is also shown

Period 1 (15 May-21 Aug) : spring and summer upwelling events separated by short intervals of wind calm, which cause a marked thermal stratification with warm waters in the surface layer and cold and salty upwelled Eastern North Atlantic Central water (ENACW) in the bottom (Fig. 5.3a,b). Strong gradients of the chemical variables are observed, with high O_2 and low N_T, TA_P, and SiO_4 levels in seasonal thermocline waters and low O_2 and high N_T , TA_P and SiO_4 in shelf bottom waters (Fig. 5.3c,d and 5.4a,b). Accumulations of DOC, d-CHO, POC and p-CHO in the surface layer were observed during the periods of wind calm (Fig. 5.5). Maximum primary production rates in the study area are commonly observed in association with this succession of wind stress-relaxation events: Arístegui et al. (2005) have proposed an average value of 2.5 g

C m^{-2} d^{-1} during the upwelling season off NW Spain. It contrasted with the low organic matter content of upwelled ENACW (<60 µM DOC, <5 µM d-CHO, <2.5 µM POC and < 0.5 µM p-CHO), except at the bottom nepheloid layer, where POC values >5 µM-C were commonly observed.

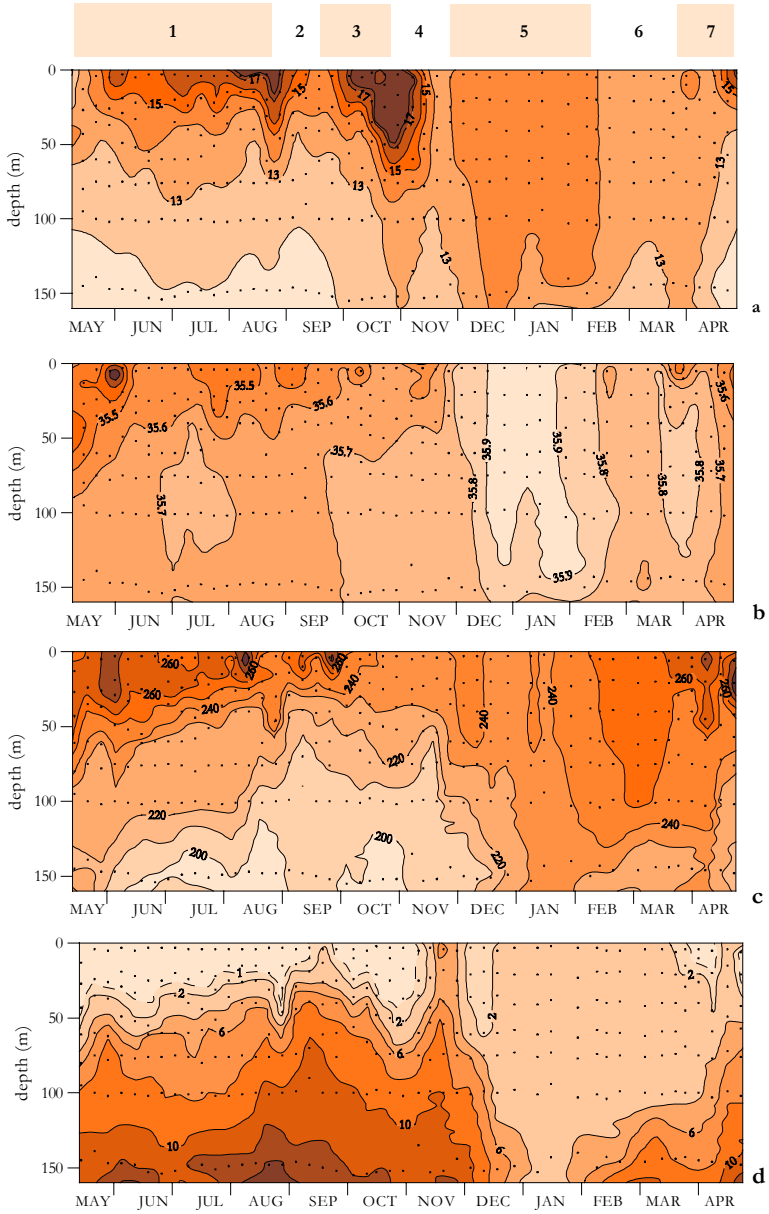

Figure 5.3 Seasonal evolution of (**a**) temperature (ºC), (**b**) salinity (pss), (**c**) dissolved oxygen (µmol kg^{-1}) and (**d**) total inorganic nitrogen (µmol kg^{-1}) at stn 03

Period 2 (28 Aug-18 Sep): late summer strong upwelling event, which produced the sudden uplift of the cold, salty, oxygen and organic matter poor and nutrient- and TA_p-rich ENACW to the surface layer, where temperatures <15ºC were recorded.

Period 3 (25 Sep-30 Oct): autumn downwelling, forced by the predominant southerly winds and low continental runoff (Fig. 5.2), provoked the entry of warm (> 17ºC), oxygen- and organic matter-rich and nutrient- and TA_p-poor oceanic surface water.

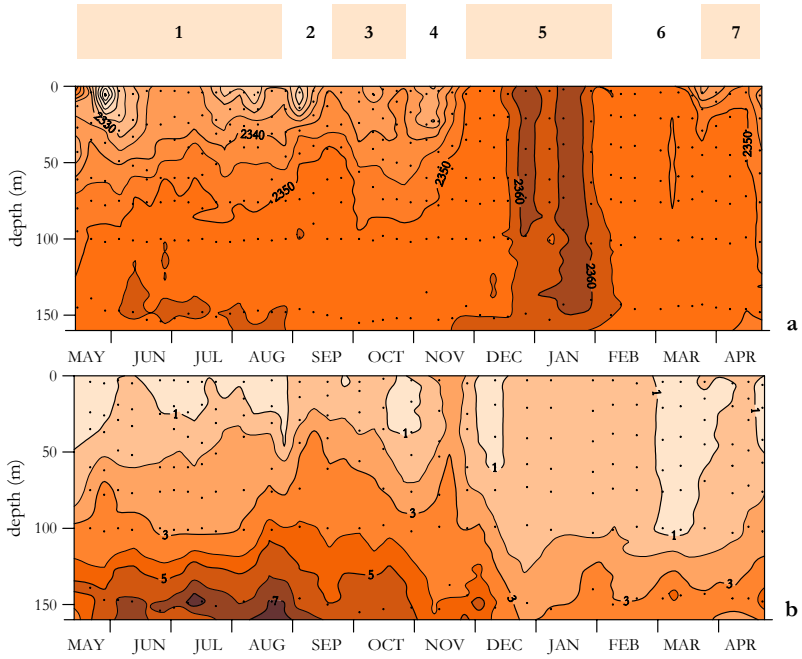

Figure 5.4 Seasonal evolution of (**a**) potential alkalinity (μeq kg^{-1}) and (**b**) silicate (μmol kg^{-1}) at stn 03

Period 4 (6 Nov-20 Nov): transition from stratification to vertical homogenisation enhanced by strong northerly winds (Fig. 5.2).

Period 5 (27 Nov-13 Feb): arrival of the IPC carrying warm and salty subtropical surface and central waters (Fig. 5.3a,b) to our latitudes, producing a strong impact in the water column: N_T levels remained <1 μM throughout the

water column (Fig. 5.3d) and dissolved and particulate organic matter reached minimum levels (Fig. 5.5).

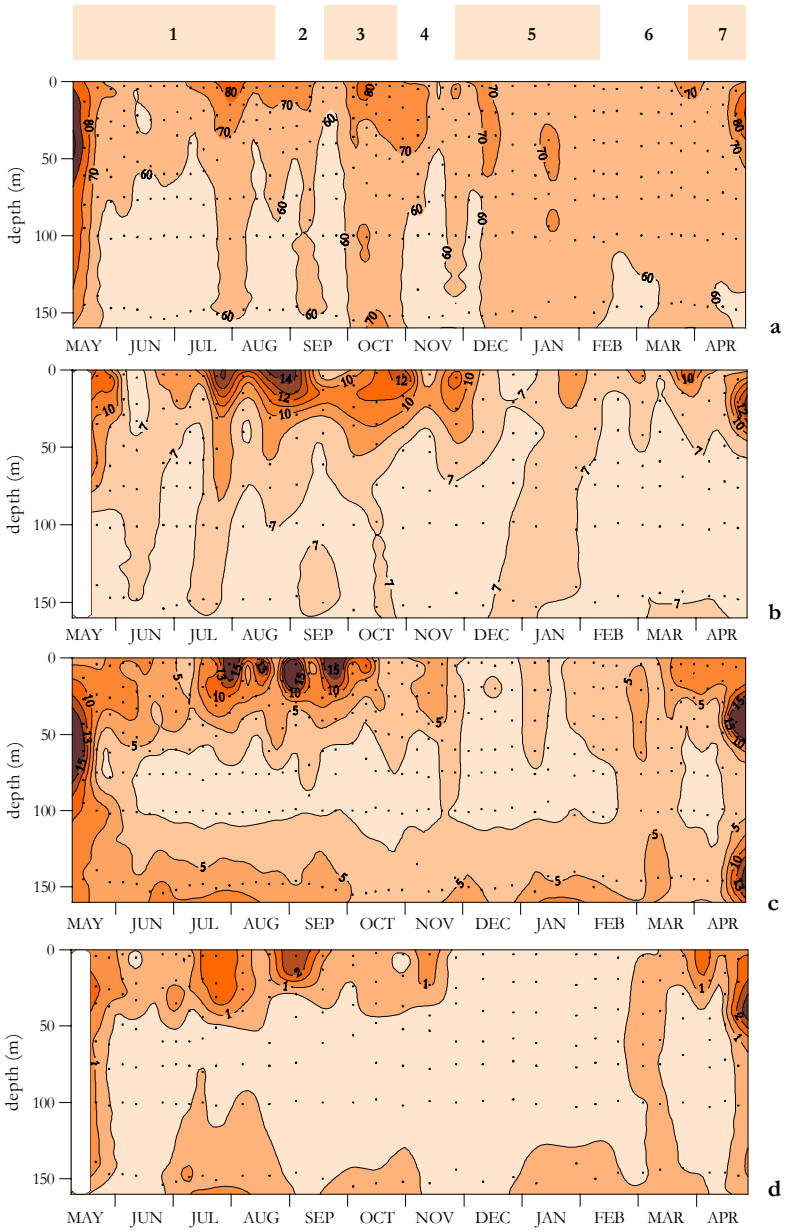

Figure 5.5 Seasonal evolution of (**a**) dissolved organic carbon (µM C), (**b**) dissolved carbohydrates (µM C), (**c**) suspended organic carbon (µM C) and (**d**) suspended carbohydrates (µM C) at stn 03

Period 6 (20 Feb-26 Mar): winter mixing, the period of maximum vertical homogenisation, when ventilation of the water column occurred (Fig. 5.3c) and organic matter levels remained very low (Fig. 5.5) because of the low primary production rates (<0.2 g C m^{-2} d^{-1}; Álvarez-Salgado et al. 2003).

Period 7 (2 Apr-24 Apr): incipient spring stratification under dominant upwelling- favourable winds (Fig. 5.2), which produced a surface accumulation of dissolved and particulate organic materials (Fig. 5.5) in the first spring bloom peak of the season.

Figure 5.5 shows the seasonal evolution of the DOC, d-CHO, POC and p-CHO profiles at the mid shelf station. DON and DOP are significantly correlated with DOC: r = +0.78 for DOC *vs.* DON (n = 284, p < 0.001) and r = +0.41 for DOC *vs.* DOP (n = 160, p < 0.001). PON and POP also correlate significantly with POC: r = +0.95 for POC *vs.* PON (n = 325, p < 0.001) and r = +0.90 for POC *vs.* POP (n = 213, p < 0.001). In addition, d-CHO correlates with DOC (r = +0.70, n = 208, p < 0.001) and p-CHO with POC (r = +0.87, n = 215, p < 0.001).

Despite the correlations referred above, average profiles of the DOC/DON, POC/PON, DOC/DOP and POC/POP molar ratios (Fig. 5.6a-d) exhibit a conspicuous vertical structure, characterised by a general increase with depth: the C/N/P ratios of the bottom samples are significantly different for the C/N/P ratios of the surface samples at p < 0.001 either for the dissolved or the particulate materials. This is consistent with previous results obtained from marginal seas and open ocean waters (Williams et al. 1980, Hopkinson et al. 1997, Sanders & Jickells 2000, Hung et al. 2003b) and can be explained by the preferential oxidation of organic nitrogen and phosphorus compounds at shallower levels in the water column (Suess & Müller 1980, Shaffer et al. 1999). The elemental C/N/P ratios of DOM are greater than the Redfield ratios, ranging from average C/N values of 12.6 in the surface layer to 14.5 in the

bottom layer, and average C/P of 615 in the surface layer to 1090 in the bottom layer. It should be noticed again that the method for the determination of DOP is only able to analyse monophosphoric esters. By contrast, the elemental C/N/P ratios of POM are much closer to the Redfield values: from 6.8 and 100 for C/N and C/P in the surface layer to 9.5 and 140 in the bottom layer.

Stoichiometry of the mineralization in coastal and shelf waters of NW Spain

Chemical data of waters below the upper mixed layer (AOU > 0) were analysed along isopycnal surfaces to obtain respiratory ratios. Subsurface waters of the NW Iberian upwelling consists of a mixing of the subtropical and subpolar branches of ENACW with ENACW modified in the surface layer by heat exchange with the atmosphere and continental runoff from the Rías Baixas (Álvarez-Salgado et al. 1997). Four isopycnal ranges (σ_0) were defined: 26.7-26.8, 26.8-26.9, 26.9-27.0 and 27.0-27.1. Samples with AOU > 0 and σ_0 < 26.7 were discarded, to minimise the ENACW samples affected by continental runoff/heat exchange with the atmosphere. For each isopycnal range, an anomaly (ΔY) can be defined for each nutrient (Y):

$$\Delta Y = Y - a_0 - a_1 \times S - a_2 \times T \qquad (5.2)$$

where a_0, a_1 and a_2 are the coefficients of the linear multiple regression of Y with salinity and temperature. ΔY retains only the variability associated to the biogeochemical processes that occur within a given isopycnal range, *i.e.* the decomposition of organic matter and the dissolution of calcareous and siliceous structures.

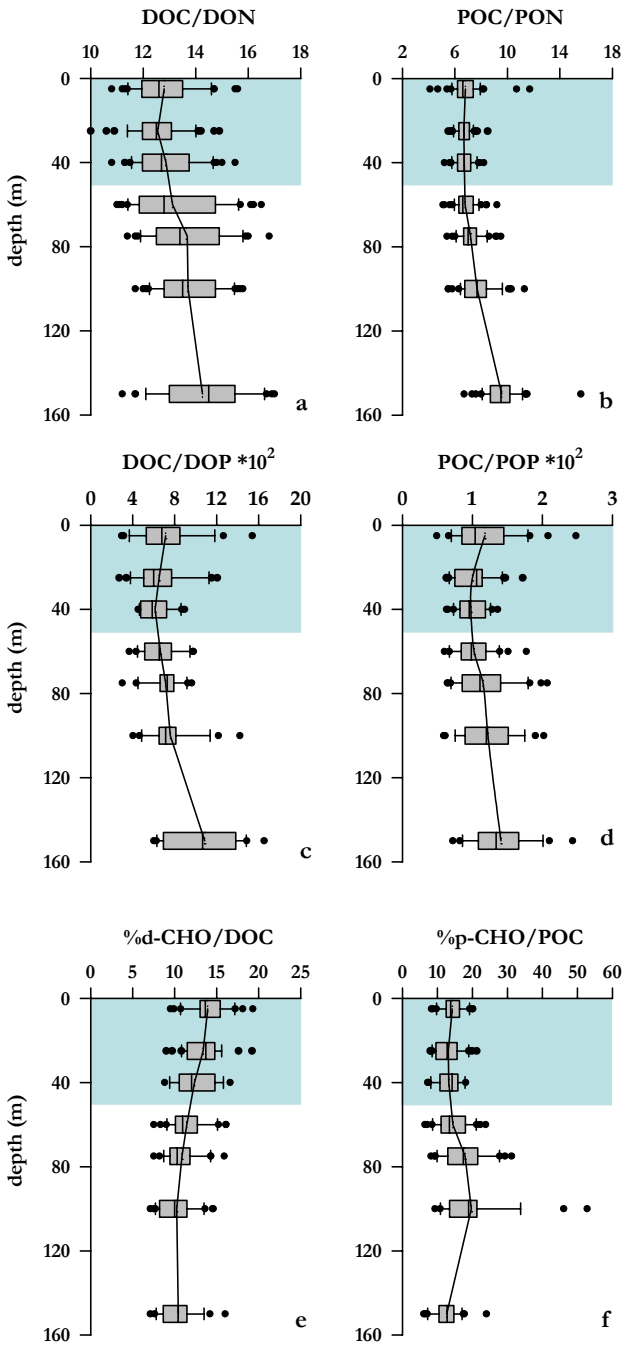

Figure 5.6 Box-Whisker plot of (**a**) DOC/DON, (**b**) POC/PON, (**c**) DOC/DOP, (**d**) POC/POP, (**e**) d-CHO/DOC and (**f**) p-CHO/POC molar ratios. Fifty percent of the data are included within the limit of the boxes and the caps represent the 10th and 90th percentiles. Solid lines represent the average profiles

Table 5.1 presents a selection of the results obtained analysing the linear correlation between pair of anomalies of the chemical variables measured during this study for the mid ría (stn 00) and mid shelf (stn 03) sites for the four isopycnal ranges collectively. The best fit between any pair of nutrient anomalies (ΔX, ΔY) was obtained minimizing the function:

$$\sum_i \left[\left(\Delta X_i - \Delta \hat{X}_i \right)^{w_X} \times \left(\Delta Y_i - \Delta \hat{Y}_i \right)^{w_Y} \right]^2 \qquad (5.3)$$

where $\Delta \hat{X}_i$ and $\Delta \hat{Y}$ are the expected values of ΔX and ΔY from the linear regression equation respectively, i.e. $\Delta \hat{Y} = m \times \Delta X_i$ and $\Delta \hat{X}_i = \Delta Y_i / m$, with m being the slope of the correlation between ΔX and ΔY; w_X and w_Y are weights for variables X and Y respectively, with w_X, $w_Y \geq 0$ and $w_X + w_Y = 1$. The weight factors were estimated as a function of the precision of the analytical determination of the variable (er) compared with the standard deviation of the set of measurements of that variable for water samples with AOU > 0 (SD). For a given couple of variables X and Y:

$$w_X = \left(\frac{er_X}{SD_X} \right) / \left(\frac{er_X}{SD_X} + \frac{er_Y}{SD_Y} \right) \qquad (5.4)$$

Minimising eq. (5.3) considering the weight factor of eq. (5.4) ensures that the slopes of the linear regression equations account for the relative precision (er/SD) of the pairs of nutrient anomalies that are correlated each time. The function to minimise is:

$$\sum_i \left[\left(\Delta X_i - \frac{\Delta Y_i}{m} \right)^{w_X} \cdot \left(\Delta Y_i - m \cdot \Delta X_i \right)^{w_Y} \right]^2 = \left(\frac{1}{m} \right)^{2 \cdot w_X} \cdot \sum_i \left(\Delta Y_i - m \cdot \Delta X_i \right)^2 \qquad (5.5)$$

In addition, the resulting value of the slope (m) which makes eq (5.5) minimum is:

$$m = \frac{1 - 2 \cdot w_X}{2 - 2 \cdot w_X} \cdot \frac{\sum_i \Delta X_i \cdot \Delta Y_i}{\sum_i \Delta X_i^2} + \tag{5.6}$$

$$+ \frac{\sqrt{\left((1 - 2 \cdot w_X) \cdot \sum_i \Delta X_i \cdot \Delta Y_i\right)^2 + 4 \cdot w_X \cdot (1 - w_X) \cdot \sum_i \Delta X_i^2 \cdot \sum_i \Delta Y_i^2}}{2 \cdot (1 - w_X) \cdot \sum_i \Delta X_i^2}$$

Therefore, m is an intermediate case between: **1)** the slope of a Type I regression (which should be applied when $w_X = 0$, $w_Y = 1$), $m = \sum_i (\Delta X_i \times \Delta Y_i) / \sum_i \Delta X_i^2$ and **2)** the slope of a Type II regression (which should be applied when $w_X = w_Y = 0.5$), $m = \sqrt{\sum_i \Delta Y_i^2 / \sum_i \Delta X_i^2}$ (Sokal & Rolf 1995). Table 5.1 summarizes also the values of w_X for the corresponding X/Y pairs.

Table 5.1 Regression coefficient (*r*), slope and standard error of the slope of the correlation between selected pairs of nutrient anomalies for samples with $\sigma_0 > 26.8$ at stations 00 and 03. The value of w_X (see eq 5.4) is also included

ΔY/ΔX	stn 00			stn 03			w_X
	r	slope	error	*r*	slope	error	
$\Delta O_2/\Delta C_T$	-0.96	1.22	±0.05	-0.93	1.29	±0.03	0.88
$\Delta O_2/\Delta N_T$	-0.90	10.7	±0.6	-0.92	8.1	±0.2	0.65
$\Delta O_2/\Delta P$	-0.93	148	±7	-0.93	130	±4	0.73
$\Delta N/\Delta SiO_4$	0.91	1.1	±0.1	0.83	1.8	±0.1	0.39
$\Delta SiO_4/\Delta CaCO_3$	0.63	2.4	±0.4	0.45	1.6	±0.2	0.95
$\Delta CaCO_3/\Delta Corg$	0.64	0.05	±0.02	0.53	0.07	±0.01	0.22
ΔDOC/ΔDON	0.60	6.8	±0.9	0.61	7.9	±0.6	0.66
ΔDOC/ΔDOP	0.40	116	±22	0.28	156	±16	0.79
Δd-CHO/ΔDOC	0.46	32%	±10%	0.41	27%	±6%	0.19
ΔPOC/ΔPON	0.91	7.6	±0.4	0.93	7.8	±0.2	0.72
ΔPOC/ΔPOP	0.73	87	±10	0.89	92	±4	0.84
Δp-CHO/ΔPOC	0.60	9%	±2%	0.74	10%	±1%	0.25
$\Delta DOC/\Delta C_T$	-0.36	14%	±5%	-0.16	36%	±17%	0.55
$\Delta DON/\Delta N_T$	-0.40	19%	±6%	-0.23	30%	±10%	0.14
$\Delta DOP/\Delta PO_4$	-0.20	7%	±7%	-0.42	18%	±4%	0.11

Specially remarkable in Table 5.1 are the high correlations found between ΔO_2, ΔC_T, ΔN_T, ΔP and ΔSiO_4, either in the ría or the shelf. The correlations

are also significant between the anomalies of the dissolved and the particulate organic materials. These nutrient anomalies can be converted into proportions of carbohydrates (Cho), lipids (Lip), proteins (Prt), photosynthetic pigments (Chl) and phosphorus compounds (Pho). Table 5.2 summarizes the average composition of these groups of biomolecules and the relative contribution of each group to the average composition of marine phytoplankton proposed by Fraga et al. (1998).

Considering the chemical formulas in Table 5.2, the following set of five mass balance equations can be written for the suspended organic material:

$$\Delta C = 139 \times \Delta Prt + 17 \times \Delta Cho + 53 \times \Delta Lip + 45 \times \Delta Pho + 46 \times \Delta Chl \quad (5.7)$$

$$\Delta H = 217 \times \Delta Prt + 28 \times \Delta Cho + 89 \times \Delta Lip + 76 \times \Delta Pho + 52 \times \Delta Chl \quad (5.8)$$

$$\Delta O = 45 \times \Delta Prt + 14 \times \Delta Cho + 6 \times \Delta Lip + 31 \times \Delta Pho + 5 \times \Delta Chl \quad (5.9)$$

$$\Delta N = 39 \times \Delta Prt + 12 \times \Delta Pho + 4 \times \Delta Chl \quad (5.10)$$

$$\Delta P = 5 \times \Delta Pho \quad (5.11)$$

Since suspended C, N, P, Cho and Chl have been measured, the system can be solved to obtain the average chemical formula and the proportions of the different biomolecules.

The same set of equations can be used for the case of the dissolved organic nutrients assuming that the dissolved organic matter that is oxidized in subsurface waters of the NW Iberian Peninsula is essentially composed of the most labile materials, *i.e.* the same biomolecules than the suspended organic material. These results were also obtained by Hopkinson et al. (2002) in the Middle Atlantic Bight and, in our case, it is supported by the reduced flushing time of shelf waters of the NW Iberian shelf, 1-2 wk (Rosón et al. 1999), and corroborated also by the low $\Delta C/\Delta N/\Delta P$ ratios of DOM (Table 5.1). Another necessary assumption is that $\Delta Chl = 0$ for dissolved organic matter, which is very reasonable since the porphyrin groups of the chlorophylls are among the most resistant biomolecules in nature (McCarthy et al. 1997).

Table 5.2 Chemical composition of the main organic products of synthesis and early degradation of marine phytoplankton according to Fraga et al. (1998). Percentages (in weight) of each group correspond to the average composition of marine phytoplankton

	chemical formula	% (w/w)
phosphorus compounds	$C_{45}H_{76}O_{31}N_{12}P_5$	12.1
pigments	$C_{46}H_{52}O_5N_4Mg$	2.0
proteins	$C_{138}H_{217}O_{45}N_{39}S$	45.7
carbohydrates	$C_6H_{10}O_5$	22.7
lipids	$C_{53}H_{89}O_6$	17.5
average composition	$C_{106}H_{171}O_{41}N_{16}P$	100.0

For the case of the dissolved inorganic nutrients, the chemical composition of the oxidized material and the proportions of the different biomolecules are calculated from the O_2, C_T, N_T and HPO_4^{2-} anomalies. Equations describing the mineralization of proteins, carbohydrates, lipids and phosphorus compounds can be written:

$$C_{138}H_{217}O_{45}N_{39}S + 220\ O_2 + 179\ OH^- \longrightarrow \longrightarrow 138\ HCO_3^- + 39\ NO_3^- + SO_4^{2-} + 129\ H_2O \quad (5.12)$$

$$C_6H_{10}O_5 + 6\ O_2 + 6\ OH^- \longrightarrow 6\ HCO_3^- + 5\ H_2O \quad (5.13)$$

$$C_{53}H_{89}O_6 + 72.25\ O_2 + 53\ OH^- \longrightarrow 53\ HCO_3^- + 44.5\ H_2O \quad (5.14)$$

$$C_{45}H_{76}O_{31}N_{12}P_5 + 69.75\ O_2 + 67\ OH^- \longrightarrow \longrightarrow 45\ HCO_3^- + 12\ NO_3^- + 5\ HPO_4^{2-} + 46.5\ H_2O \quad (5.15)$$

Consequently, the corresponding linear system of mass balance equations is:

$$\Delta O_2 = 220 \times \Delta Prt + 6 \times \Delta Cho + 72.25 \times \Delta Lip + 69.75 \times \Delta Pho \quad (5.16)$$

$$\Delta C_T = -138 \times \Delta Prt - 6 \times \Delta Cho - 53 \times \Delta Lip - 45 \times \Delta Pho \quad (5.17)$$

$$\Delta N_T = -39 \times \Delta Prt - 12 \times \Delta Pho \quad (5.18)$$

$$\Delta P = -5 \times \Delta Pho \quad (5.19)$$

Dissolved oxygen consumption in equations (5.12)-(5.15) is referred to the oxidation state of nitrate. However, ammonium and nitrite are relatively abundant in NW Iberian shelf waters. Since 0.5 mol of oxygen are necessary to oxidize one mol of nitrite to nitrate and two mol of oxygen are required to oxidize one mol of ammonium to nitrate, the following oxygen correction has to be applied (Ríos et al. 1989):

$$O_{2C} = O_2 - 0.5 \times NO_2^- - 2 \times NH_4^+ \quad (5.20)$$

In addition, inorganic carbon is produced during the degradation of organic matter and calcareous ($CaCO_3$) structures. Since equations (5.12)-(5.15) refer only to the oxidation of organic carbon, the influence of the precipitation-dissolution of $CaCO_3$ must be corrected from C_T variability (C_{TC}):

$$C_{TC} = C_T - \frac{1}{2} \times TA_P \quad (5.21)$$

TA_P also allow us to estimate the dissolution of calcareous structures ($\Delta CaCO_3$)

$$\Delta CaCO_3 = -\frac{1}{2} \times \Delta TA_P \quad (5.22)$$

Introducing the nutrient ratios of Table 5.1 in equations (5.7)-(5.11) and (5.16)-(5.19) it is possible to obtain the average biochemical composition of the organic and inorganic materials mineralised in bottom waters of the ría and the shelf of the NW Iberian upwelling system during a complete seasonal cycle. The R_C ratio ($=-\Delta O_2/\Delta C_T$) cannot be directly used because it is affected by the dissolution of anthropogenic CO_2. Therefore, we tested the whole range of

possible R_C values. It varies from 1.00 (100% carbohydrates) to 1.59 (100% proteins). Following Anderson (1995), we arbitrarily established that only the R_C values that produce a percentage >5% for carbohydrates and lipids would be valid. Results are shown in Table 5.3; it ranges from 1.28 to 1.45 in the ría and from 1.39 to 1.49 in the shelf. Note that the calculated R_C values are 1.22 and 1.29 for the ría and the shelf, respectively (Table 5.1), *i.e.* out of the permitted range. Table 5.3 also shows the biochemical composition of the materials mineralised as obtained from the inorganic nutrients, the DOM and the POM anomalies.

Table 5.3 Average chemical composition of the products of early degradation of marine phytoplankton photosynthesis as obtained from inorganic nutrients, dissolved organic matter and suspended organic matter. R_C in mol O_2 (mol C)$^{-1}$, phosphorus compounds, proteins, lipids and carbohydrates in % (w/w).

		stn 00		stn 03	
Nutrients	**R_C**	**1.28**	**1.45**	**1.39**	**1.49**
	Phosphorus compounds	10.0	13.8	12.7	15.1
	Proteins	33.4	46.1	50.4	59.9
	Lipids	5.1	35.0	5.1	20.0
	Carbohydrates	51.5	5.0	31.9	5.1
DOM	**R_C**	**1.36**		**1.36**	
	Phosphorus compounds	10.4		8.2	
	Proteins	44.6		41.1	
	Lipids	8.8		18.2	
	Carbohydrates	36.3		32.4	
POM	**R_C**	**1.43**		**1.42**	
	Phosphorus compounds	15.8		14.9	
	Proteins	41.1		40.8	
	Lipids	31.6		31.4	
	Carbohydrates	11.5		12.9	

The results presented in this table also allow us to write the following biochemical reactions for the decomposition of the biogenic material:

Mid ría, from nutrients anomalies (using an average R_C = 1.37)

$$(C_{108}H_{176}O_{46}N_{14}P)(SiO_2)_{13}(CaCO_3)_5 + 146.5\ O_2 + 57\ H_2O \longrightarrow \rightarrow 113\ HCO_3^- + 14\ NO_3^- + HPO_4^{2-} + 13\ H_4SiO_4 + 5\ Ca^{2+} + 124\ H^+ \quad (5.23)$$

Mid ría, from DOM anomalies

$$C_{116}H_{186}O_{55}N_{17}P + 157.5\ O_2 + 33\ H_2O \longrightarrow \rightarrow 116\ HCO_3^- + 17\ NO_3^- + HPO_4^{2-} + 135\ H^+ \quad (5.24)$$

Mid ría, from POM anomalies

$$C_{87}H_{141}O_{27}N_{11}P + 123.75\ O_2 + 23.5\ H_2O \longrightarrow \rightarrow 87\ HCO_3^- + 11\ NO_3^- + HPO_4^{2-} + 100\ H^+ \quad (5.25)$$

Mid shelf, from nutrients anomalies (using an average R_C = 1.44)

$$(C_{91}H_{145}O_{36}N_{16}P)(SiO_2)_9(CaCO_3)_6 + 129\ O_2 + 49\ H_2O \longrightarrow \rightarrow 97\ HCO_3^- + 16\ NO_3^- + HPO_4^{2-} + 9\ H_4SiO_4 + 6\ Ca^{2+} + 109\ H^+ \quad (5.26)$$

Mid shelf, from DOM anomalies

$$C_{156}H_{251}O_{65}N_{20}P + 212.5\ O_2 + 42\ H_2O \longrightarrow \rightarrow 156\ HCO_3^- + 20\ NO_3^- + HPO_4^{2-} + 178\ H^+ \quad (5.27)$$

Mid shelf, from POM anomalies

$$C_{92}H_{149}O_{29}N_{12}P + 131\ O_2\ 25\ H_2O \longrightarrow \rightarrow 92\ HCO_3^- + 12\ NO_3^- + HPO_4^{2-} + 106\ H^+ \quad (5.28)$$

Mineralization of organic biomolecules

Sinking, suspended and dissolved organic matter have different gravity properties, they cycle differently in the ocean, and they have different elemental ratios (e.g. Loh & Bauer 2000, Hopkinson et al. 1997, 2002). Comparison of the standard deviation of the calculated ΔC_{TC}, ΔDOC and ΔPOC values at stns 00 (25.6, 4.0 and 4.3 μM C, respectively) and 03 (10.0, 3.5 and 1.8 μM C, respectively), yielded that the average contribution of DOC and POC to the

mineralization of organic carbon was about 30% in the mid ría (1/2 DOC, 1/2 POC) and 50% (2/3 DOC, 1/3 POC) in the mid shelf. Therefore, the biochemical reactions obtained from the nutrient anomalies (eq. 5.23 and 5.26) contain a fraction that was missing in the DOM and POM analyses (50-70 % of the total). This missing fraction is probably composed of the products of degradation of large, fast sinking, organic materials not collected in the POC analysis (representative for particles in the 1-200 μm size range).

Remarkable differences were found between the average composition of the dissolved, suspended and missing sinking organic materials that are mineralised in the waters below the upper mixed layer of the NW Iberian upwelling system. Regarding the dissolved material, there are not remarkable differences between the mid ría and mid shelf sites and the most conspicuous characteristic of this material is that carbohydrates are preferentially consumed (32-36%; Table 5.3) as compared with a material of Redfield composition (22.7%; Table 5.2). As for the case of the dissolved material, the composition of the oxidized suspended organic matter did not differ between the ría and the shelf ($p < 0.05$), but in this case lipids are preferentially oxidized: 31% (Table 5.3) as compared with 17.5% for a material of Redfield composition (Table 5.2). Finally, assuming average R_C values of 1.37 and 1.44 for the mid ría and mid shelf stations respectively, it results that the missing sinking material mineralised experiences a preferential consumption of carbohydrates in the mid ría (31% as compared with 22.7% in Table 5.2) and of proteins in the mid shelf (55% as compared with 45% in Table 5.2).

Hopkinson et al. (2002) were able to differentiate between labile and recalcitrant materials in the mesotrophic Middle Atlantic Bight. The C/N/P ratios of the labile material were similar to the values obtained in the NW Iberian Peninsula and indicate that the stoichiometry of DOM mineralization is similar to that for particles (Garber 1984). The study of Hopkinson et al. (2002)

showed that DOP was more labile than DON and DON more than DOC. This result was also observed by Lucea et al. (2003) in a different environment: the oligotrophic NW Mediterranean. They both confirmed previous conclusions reached by Jackson & Williams (1985) and Hopkinson et al. (1997) about preferential mineralization of phosphorus. Abell et al. (2000) merit an special mention since they were able to differentiate the organic matter mineralization in upper thermocline waters of the subtropical (oligotrophic) and temperate (mesotrophic) North Pacific Ocean: DOC+POC mineralization exhibited a C/N molar ratio of 30 ± 10 in the subtropical and 8 ± 1 in the temperate North Pacific. Hung et al. (2003b) obtained a C/N molar ratio of DOM mineralization of 8.4 and an N/P molar ratio of 19 in the East China Sea, suggesting that they are due to the recently produced fractions. Therefore, there is a body of evidence in the literature supporting the fact that the labile dissolved organic material consumed in mesotrophic environments, especially in coastal areas, has a composition similar to the suspended and sinking organic particles.

Since most experimental work on remineralization of nutrients from particulate and dissolved organic matter has dealt with laboratory decomposition studies, this work is likely the first estimation in the field of the molecular composition of the mineralised dissolved organic matter in a coastal environment. This type of analysis is more accurate than the estimation of mineralization ratios based on the vertical profiles of the bulk C/N/P ratios of DOM and POM as those of Figure 5.6, because DOM and POM concentrations can contain refractory components and preformed contributions.

Mineralization of siliceous and calcareous structures

The ratio between soft and hard biogenic material decomposition rates varies with depth in the oceans. Since the upper ocean is $CaCO_3$ over saturated

(Takahashi et al. 1981, Broecker & Peng 1982), carbon regeneration at that level is predominantly due to the oxidation of organic carbon (Honjo et al. 1982, Honjo & Manganini 1993). However, a recent review of the global carbonate budget showed evidences that 60-80% of the biogenic $CaCO_3$ dissolves in the upper 1000 m, above the lysocline, as a result of biological mediation (Milliman et al. 1999). In deeper layers, the dissolution of hard structures predominates because of the increased pressure, decreased temperature and longer residence times (Broecker & Peng 1982). These authors, using the Geochemical Ocean Section Study (GEOSECS) dataset, estimated a $\Delta Ca/\Delta Corg$ ratio of ~0.1 for the permanent thermocline and ~0.5 for deep waters. Takahashi et al. (1985) obtained a $\Delta Ca/\Delta Corg$ ratio of 0.05 for the upper and 0.08 for the lower permanent thermocline of the North Atlantic. Finally, Ríos et al. (1995) found a $\Delta Ca/\Delta Corg$ ratio of 0.08 for the upper 2300 m and 0.52 for deeper waters of the Eastern North Atlantic Ocean.

A $\Delta Ca/\Delta Corg$ ratio of 0.05 ± 0.02 was estimated for shelf subsurface waters of the NW Iberian upwelling system (Table 5.1). This value is within the range mentioned for the upper thermocline waters. A similar $\Delta Ca/\Delta Corg$ value of 0.07 ± 0.01 was calculated for the subsurface waters of the Ría de Vigo. The water column below the mixed layer is always supersaturated with respect to calcite and aragonite (312 ± 42% and 200 ± 28%, respectively). Therefore, $CaCO_3$ dissolution should occur preferentially at or near the top of sediments (Archer et al. 1989). The high organic matter content of the sediment, either in the rías (Vilas et al. 2005) or the inner shelf (Lopez-Jamar et al. 1992), creates an environment where the dissolution of $CaCO_3$ is favoured by strong acidification. In fact, the sediments inside the rías are characterised by low proportions of $CaCO_3$ where the organic matter content is high (Vilas et al. 2005).

Regarding biogenic silica, it is also exported to the deep ocean as sinking particles, where dissolution occurs. As for the case of $CaCO_3$, most of the silica dissolution takes place below the main thermocline. The high covariation between alkalinity and silicate profiles in open ocean deep waters (Brewer et al. 1995, Broecker & Peng 1982, Ríos et al. 1995) is probably due to the biologically mediated dissolution of these hard structures in the microenvironments created by marine snow, zooplankton guts, etc. According to Milliman et al. (1999) and Tréguer et al. (1995), the open ocean $CaCO_3$ and opal decomposition rates in the water column are $47 \cdot 10^{12}$ mol y^{-1} and $91 \cdot 10^{12}$ mol y^{-1} respectively. Therefore, a mean $\Delta Si/\Delta Ca$ molar decomposition ratio of ~2 can be proposed. For the North Atlantic, an average $\Delta Si/\Delta Ca$ ratio for the whole water column of 1.4 was calculated by Pérez et al. (2002). According to Berger & Herguera (1992), a $\Delta Si/\Delta Ca$ ratio of 1.4 is expected for an area with a mean organic carbon flux of 10 mmol m^{-2} d^{-1}, which is in close agreement with their productivity value for the Eastern North Atlantic Ocean (Martin et al. 1993). Lower $\Delta Si/\Delta Ca$ ratios, around 1.05, were measured in sediment traps deployed at the North Atlantic Bloom Experiment (NABE) site below 3100 m (Newton et al. 1994).

In this study, the $\Delta Si/\Delta Ca$ ratio was variable, with a value of 2.4 ± 0.4 in the Ría de Vigo and 1.6 ± 0.2 in the shelf (Table 5.1). The latter value is in close agreement with that found at the NABE site. As observed in the open ocean (Berger & Herguera 1992), the $\Delta Si/\Delta Ca$ ratio increases as the organic matter flux increases; this is, it increases from the shelf to the ría. Along the middle shelf of the NW Iberian Peninsula, Alvarez-Salgado et al. (1997) found a large silicate accumulation in bottom waters due to rapid opal dissolution. Opal dissolution was high compared with organic matter decomposition: the $\Delta N/\Delta Si$ molar ratio in the ría (1.1 ± 0.1) is about half than in the shelf, (1.8 ± 0.1; Table 5.1). In this sense, maximum percentages of opal and diatom valve

numbers in sediments were recorded in the main channel of the Ría de Vigo (Prego et al. 1995), suggesting a strong downward flux of diatom frustules there.

Contribution of DOM to nutrient mineralization in the NW Iberian upwelling

A huge effort has been made over the last decade by marine biogeochemists to understand the role played by DOM in carbon, nitrogen and phosphorus cycles in the oceans. Most of this knowledge has been reviewed in a recent book edited by Hansell & Carlson (2002).

One of the key questions to answer is the true contribution of DOM to the apparent oxygen utilization of subsurface ocean waters. According to the results of the biogeochemical general circulation model of Yamanka & Tajika (1997), ~70% of the biogenic organic matter exported from the surface (<100m) to the central (100-500 m) waters of the World Ocean are sinking particles. The remaining ~30% is in the dissolved form. DOM below 1000 m is extremely refractory, confirming that recycling times of this pool range from years to thousands of years (Hansell & Carlson 1998b) and that oxygen consumption is almost exclusively due to large sinking particles (Jahnke 1996).

The analysis of the standard deviation of calculated ΔC_{TC}, ΔDOC and ΔPOC values on the previous section estimated that from 16% to 35% of the organic carbon regenerated in bottom waters of the ría and the shelf, respectively, was in the dissolved form. The increase in the offshore direction is consistent with the larger particle fluxes recorded within the rías (Varela et al. 2004) than over the shelf (Olli et al. 2001). It is also remarkable the low correlation between DOC and C_{TC} anomalies (lower than -0.36), which confirms the general statement that the variability observed in the AOU of the oceans is mainly linked to the flux of large sinking organic particles (Anderson & Sarmiento 1994). DON/N_T and DOP/PO_4 anomalies reproduced the same pattern

observed for DOC/C_{TC}: the contribution of dissolved organic matter to the mineralization of organic nitrogen and phosphorus increased from the ría to the shelf, ranging from 15% to 40%, and the correlation coefficients were also very low, ranging from -0.20 to -0.42. In the continental shelf of Georges Bank, a region of nearly constant upwelling of nutrient rich deep water that can be compared with the NW Iberian shelf, Hopkinson et al. (1997) obtained that 19% and 15% of the mineralized N and P that accumulates in deeper water is due to dissolved organic matter mineralization. In open ocean waters of the North Pacific, DON contributed from 10% to 25% to the mineralised nitrate in deep waters according to different estimates (Jakson & Williams 1985, Maita & Yanada 1990, Koike & Tupas 1993). As indicated in the previous section, Abell et al. (2000) differentiated the organic matter mineralization in upper thermocline waters of the subtropical (oligotrophic) and temperate (mesotrophic) North Pacific Ocean: total organic carbon contributed 70% to organic mater mineralization in the subtropical North Pacific and only 20% in the temperate North Pacific.

CONCLUSIONS

Four main conclusions can be extracted from this work about the mineralization of biogenic materials in a coastal upwelling system:

More than 50% of the oxygen consumption in shelf subsurface waters is due to the mineralization of large, fast sinking organic matter, 17-18% to suspended organic matter and 16-35 % to dissolved organic matter.

The products of early degradation of the sinking, suspended and dissolved organic matter can be expressed as a linear combination of the main groups of biomolecules: lipids, carbohydrates, proteins and phosphorus compounds.

Proteins are preferentially oxidized in the sinking organic matter, carbohydrates in the dissolved organic matter and lipids in the suspended organic matter, as compared with the average Redfield formula.

SiO_2 is preferentially dissolved in the middle ría.

Chapter 6:

Local remineralization patterns in the mesopelagic zone of the Eastern North Atlantic off the NW Iberian Peninsula

Chapter 6, the research work presented in this chapter is also a contribution to the paper:

C. G. Castro, M. Nieto-Cid, X. A. Álvarez-Salgado et al. 2005. **Local remineralization patterns in the mesopelagic zone of the Eastern North Atlantic off the NW Iberian Peninsula**. Deep-Sea Res I, *submitted*

Resumen: Entre mayo 2001 y abril 2002, se ha muestreado, con una frecuencia semanal, una estación en la zona de transición costera en el límite de la plataforma en el NO Ibérico, centrándose en el análisis a corta escala de las condiciones oceanográficas en el dominio del Agua Central del Atlántico Nororiental (ENACW) en el margen ibérico. En este masa de agua se han distinguido tres capas, definidas por isopícnas: capa superior ($\sigma < 26.95$), capa media ($26.95 > \sigma < 27.10$) y capa inferior ($\sigma > 27.10$). Se observó una correlación significativa entre las anomalías de nitrógeno (DON) y carbono orgánico disuelto (DOC) para las tres capas. Sin embargo, la relación anomalía de DON *vs.* anomalía de nitrógeno inorgánico sólo es significativa en la capa de ENACW menos profunda, donde el DON es mineralizado preferentemente sobre el DOC, explicando el ~17% de la mineralización de la materia orgánica. El comportamiento observado en los niveles más profundos puede ser ocasionado por la solubilización de las partículas en sedimentación, ya que en estas profundidades este proceso puede ser favorecido frente a la mineralización. Se ha observado un fraccionamiento de la mineralización de la materia orgánica entre las capas superior e inferior de la ENACW, lo que sugiere una remineralización preferencial de compuestos de N y P. Por otro lado, las anomalías de la fluorescencia húmica y del nitrato correlacionan en todo el rango de ENACW, indicando la producción de sustancias húmicas como subproducto de la degradación microbiana de la materia orgánica.

Abstract: One station situated at the coastal transition zone in the NW Iberian shelf-break was sampled on weekly frequency between May 2001 and April 2002, in order to study, on this short time scale, the oceanographic conditions of the Eastern North Atlantic Central Water (ENACW) domain off the NW Iberian Peninsula. Three different layers were defined by density: upper ($\sigma < 26.95$), middle ($26.95 > \sigma < 27.10$) and lower ($\sigma > 27.10$). There existed a significant correlation between dissolved organic nitrogen (ΔDON) and carbon (ΔDOC) anomalies for whole water column, however, ΔDON *vs.* inorganic nitrogen anomaly only was significant at the shallower ENACW layer, where DON is preferentially mineralised over DOC, accounting for ~17% of organic matter mineralization. The behaviour observed in the two deeper levels would respond to the solubilization of fast sinking particles, as with depth, the rate of this process is much larger than that of mineralization. Fractionation of organic matter mineralization was observed between the upper and lower layers of ENACW, pointing to a preferential remineralization of nitrogen and phosphorus rich organic matter in the mesopelagic layer occupied by ENACW. On the other hand, humic fluorescence and nitrate anomalies correlate significant and directly through the whole ENACW depth range, pointing to the production of dissolved humic substances as a by-product of the microbial degradation processes of biogenic organic matter. The average rate of this process is 0.18 ± 0.01 ppb QS $(\mu M\ N)^{-1}$ in the upper ENACW layer, decreasing down to 0.11 ± 0.05 ppb QS $(\mu M\ N)^{-1}$ in the lower ENACW layer.

INTRODUCTION

The mesopelagic or twilight zone, located between the base of the euphotic zone and 1000 m, plays an important role in the ocean mineralization-respiration processes. Arising importance of the mesopelagic layer is its contribution to the metabolic state of the ocean, defined as the balance between *in situ* primary production and total respiration (Smith & Hollibaugh 1993), and its repercussion in the global carbon cycle (Arístegui et al 2002, 2003, Del Giorgio & Duarte 2002, Karl et al 2003, Hansell et al. 2004). Del Giorgio & Duarte (2002) estimated a total respiration in the mesopelagic layer of ~ 24.5 Gt C yr^{-1}, which represents about 37% of the total respiration of the open ocean (see their table 1). However, these authors also state that there is an extremely large uncertainty (minimum 35%) in the above estimate as respiration measurements below the euphotic zone are rarely done due to the lack of sufficiently sensitive techniques to measure mineralization rates in the mesopelagic layer. Concerning about this lack and the importance of remineralization processes in the mesopelagic layer, emerging programs as IMBER (Integrated Marine Biogeochemistry and Ecosystem Research) and OCTET (Ocean Carbon Transport, Exchanges and Transformations) are going to dedicate part of the future efforts to develop new methodologies.

The mesopelagic layer has been considered as the largest "heterotrophic digester" of the oceans (Benner 2000). The nature and extension of the transformation and remineralization of organic matter through the mesopelagic layer affects the quantity and stoichiometry of materials delivered to the deep sea and seafloor. On the other hand, the mesopelagic layer is also critical for the input of nutrients into the euphotic zone and its subsequent control on the primary production of the system.

In this sense, especially sensible zones to the mesopelagic biogeochemical processes are the regions of formation of modal waters, where thermocline

subsurface waters are transferred into the euphotic zone on a year basis. Nutrients and dissolved organic matter (DOM) concentrations of the newly-formed modal waters depend on the concentrations of the subsurface thermocline waters just before the winter mixing and, consequently, on the mineralization processes that have occurred in the mesopelagic layer. This is the case for the Eastern North Atlantic Central (ENACW) waters, the main subsurface modal waters in the ventilated thermocline of the Eastern North Atlantic.

In this line, this work try to have a first view of the temporal variability of the mineralization patterns in the core of ENACW, which is the main source of nutrients to the NW Iberian upwelling system.

Based on the thermohaline properties, Fiúza (1984) discerned two vintages of ENACW: central waters with temperatures <13°C (ENACW of subpolar origin; $ENACW_{SP}$) and ENACW with temperatures >13°C (ENACW of subtropical origin; $ENACW_{ST}$). $ENACW_{SP}$ is formed north of ~43°N with winter mixed layer depths between 400-600 m and high nutrient concentrations (nitrate concentrations between 3 and 10 μmol kg^{-1} at the time of formation; Castro 1997, Pérez et al. 2005). Once formed $ENACW_{SP}$ subducts and it is conveyed southward as part of the anticyclonic circulation of the subtropical gyre (McCartney & Talley 1982). The subtropical vintage of ENACW is formed south of 40°N in shallower winter mixed layers (~200 meters deep) and lower nutrient levels (nitrate concentrations between 0.5 and 2 μmol kg^{-1}). $ENACW_{ST}$ is transported northward by the Portugal Coastal Under Current (PCUC) during the upwelling season and by the Portugal Coastal Counter Current (PCCC) during the rest of the year (Álvarez-Salgado et al. 1993, Castro et al. 1997).

Previous studies have been focused on the mineralization processes of ENACW over the shelf (Álvarez-Salgado et al. 1993, 1997, *accepted*). From these

studies, we know that ENACW is gaining mineralised nutrient as the upwelling season progresses and that nutrient enrichment is more intensified on the Galician west coast, off the Rías Baixas (Fig. 6.1), than on the northern coast. This intensification on the west coast is caused by a longer residence time of the upwelled water and a higher input of particulate organic matter outwelled from the Rías Baixas (Álvarez-Salgado et al. 1997). In fact, this stronger nutrient enrichment due to remineralization on the west shelf is able to buffer the difference on nutrient concentrations between $ENACW_{SP}$, which usually upwells on the north coast, and $ENACW_{ST}$, upwelling on the west coast, in such a way that the potential primary production controlled by upwelled nutrient levels is similar for the two regions. On the oceanic domain, Pérez et al. (1993, 2001) studied the remineralization patterns of the water masses in this eastern boundary, with data collected on a series of hydrographic cruises carried out between 1982 and 1993. These authors were mainly focused on studying the spatial remineralization patterns and their relationship with the mixing and displacement of water masses in the region.

The aim of this manuscript is to have a first view of the temporal variability of the mineralization patterns in the mesopelagic layer of the Eastern North Atlantic, based on the chemical data collected with a weekly frequency in a station off the NW Iberian Peninsula between May 2001 and April 2002.

MATERIAL AND METHODS

A transect from the coast to 85 km off the NW Iberian coast (Fig. 6.1) was sampled on weekly frequency between May 2001 and April 2002, in the framework of the DYBAGA project. The aim of this project was to study on this short time scale the oceanographic conditions off the NW Iberian Peninsula. The basis for this manuscript is the hydrographic data collected at the most offshore station (stn 05), which corresponds to the oceanic reference

for analysing the processes and hydrographic conditions over the shelf and inside the Ría de Vigo.

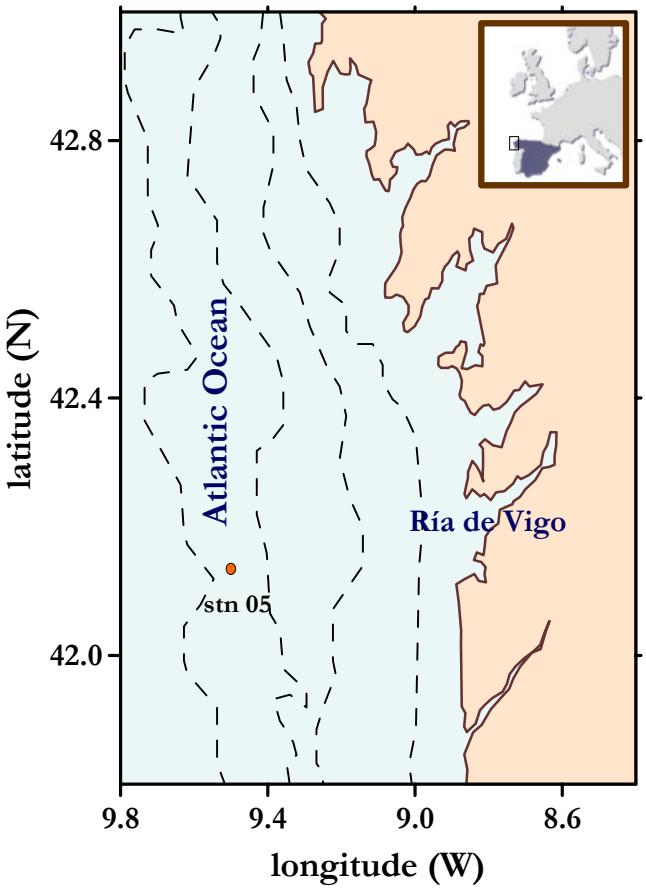

Figure 6.1 Map of the study area, shelf breakwaters of the NW Iberian upwelling system. The position of the sampling station is indicated. The isobaths of 50, 100, 150, 200 and 1000 m are depicted

A total of 47 surveys were carried out on board of RV *Mytilus* but unfortunately due to bad weather conditions we were not able to achieve the sampling of stn 05 in two occasions (November 7th, 2001 and April 2nd, 2002). Conductivity, temperature and pressure (CTD) were measured with a SBE 9/11 CTD probe incorporated into a rosette sampler with 10-L PVC Niskin bottles. Salinity was calculated from conductivity measurements using the equation of UNESCO (1985). Samples for the analysis of dissolved oxygen, total alkalinity,

pH, nutrient salts, dissolved organic carbon and nitrogen and fluorescence of dissolved humic substances were collected at 15 different depths in the water column from the surface to the upper core of Mediterranean Water with a more intense sampling at ENACW depths.

Dissolved oxygen was determined by Winkler potentiometric titration. The estimated analytical error was ±1 μmol kg^{-1}. Total alkalinity was determined by potentiometric titration with HCl to a final pH of 4.4 (Pérez & Fraga 1987). The analytical error was ±2 μmolkg^{-1}. The measurements of pH were analysed spectrophotometrically following Clayton & Byrne (1993). Total inorganic carbon (C_T) was estimated from pH and total alkalinity using the carbonic system equations with the carbonic and boric acid dissociation constants of Lueker et al. (2000). Nutrient samples were determined by segmented flow analysis with Alpkem Autoanalyzers following Hansen & Grasshoff (1983) with some improvements (Mouriño & Fraga 1985). The analytical errors were ±0.02 μM for nitrite, ±0.05 μM for nitrate, ammonium and silicate and ±0.01 μM for phosphate. Dissolved organic carbon (DOC) and nitrogen (DON) were measured simultaneously with a nitrogen-specific Antek 7020 nitric oxide chemiluminescence detector, coupled in series with the carbon-specific Infrared Gas Analyser of a Shimadzu TOC-5000 organic carbon analyzer (Álvarez-Salgado & Miller 1998). The analytical errors were ±1 μM for DOC and ±0.2 μM for DON.

The fluorescence of dissolved humic substances ($FDOM_M$) was measured with a Perkin Elmer LS 55 Luminescence spectrometer working with a xenon discharge lamp, equivalent to 20 kW for 8 μs duration, and a 1-cm quartz fluorescence cell. Milli-Q water was used as a reference for fluorescence analysis, and the intensity of the Raman peak was checked several times every working day. Discrete FDOM analyses were executed within few hours after sample collection at Ex/Em wavelength 320/410 nm. Four replicated were

performed. A four point standard curve was prepared daily with quinine sulphate (QS) in sulphuric acid 0.05M. The equivalent concentration of every peak was determined by subtracting the average peak height from the blank height, and dividing by the slope of the standard curve. Fluorescence units were expressed in ppb equivalents of QS (ppb QS) with an analytical error of ±0.1 ppb QS. For more details, see Nieto-Cid et al. (*in press*), Chapter 3.

The Brunt-Väisälä frequency (N^2; Millard et al. 1990) is commonly used for evaluating the stability of the water column, $N^2 = (g/\rho) \cdot (\partial\rho/\partial z)$, where g is gravity, ρ is density and z is depth. The average N^2 integrated over the water column can be calculated as:

$$N^2 = g/Z \cdot \ln(\rho_b/\rho_s) \qquad (6.1)$$

where Z is the water depth, ρ_s is surface density and ρ_b is bottom density.

STOICHIOMETRIC MODEL

Separation of physical and biogeochemical components of the distribution of chemical parameters

As we mentioned before, ENACW off the NW Iberian Peninsula occupies the water column from a salinity maximum at 50-100 meters depth, characteristic of the saltier and warmer portions of $ENACW_{ST}$, to a salinity minimum at 450-500 m depth, characteristic of the fresher and colder portions of $ENACW_{SP}$. Thus, ENACW can be defined by two straight θ/S lines, i.e. three end members (Fig. 6.2; Castro et al. 1998).

A three end member mixing problem can be solved by means of a linear regression analysis involving two conservative variables, salinity and potential temperature. An anomaly (ΔY) can be defined for each chemical parameter (Y):

$$\Delta Y = Y - a_0 - a_1 \times S - a_2 \times T \qquad (6.2)$$

where a_0, a_1 and a_2 are the coefficients of the linear multiple regression of Y with salinity and temperature. ΔY retains only the variability associated to the

biogeochemical processes *i.e.* the decomposition of organic matter and the dissolution of calcareous and siliceous structures.

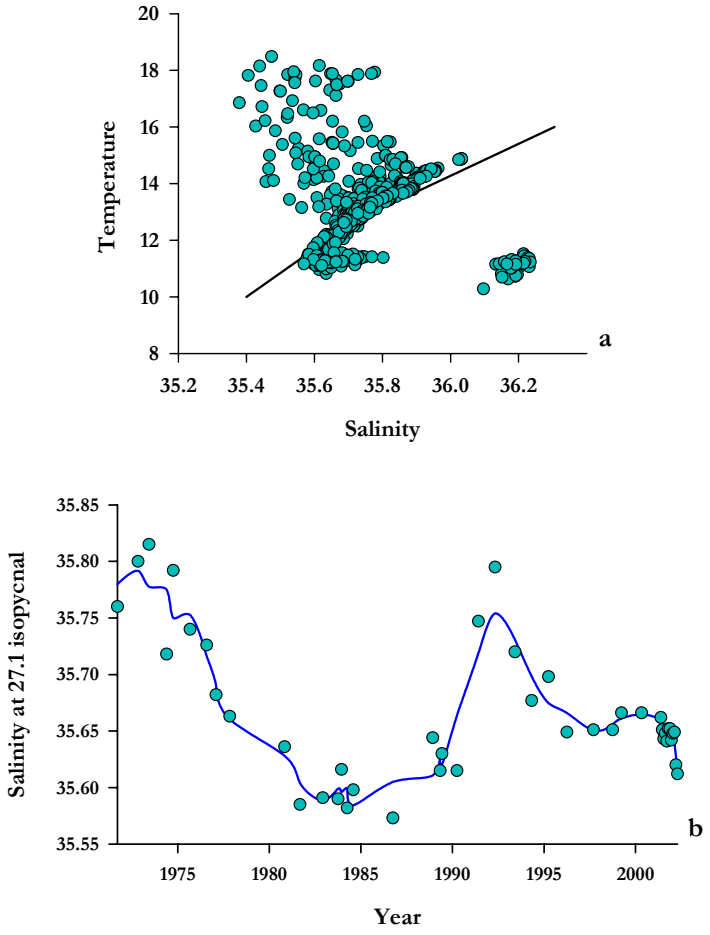

Figure 6.2 (**a**) Temperature *vs.* salinity diagram for all the water samples collected during the DYBAGA project at stn 05 since May 2001 until May 2002. Black solid line is the reference line defined by Fiúza (1984) for ENACW. (**b**) Interannual variability of salinity on the isopycnal level 27.1 kg m^{-3} by Pérez et al. (2000) updated with salinity values at stn 05 during the study period

Regression analysis of nutrient anomalies

The best fit between any couple of nutrient anomalies (ΔX, ΔY) was obtained minimizing the function:

$$\sum_i \left[\left(\Delta X_i - \Delta \hat{X}_i \right)^{W_X} \times \left(\Delta Y_i - \Delta \hat{Y}_i \right)^{W_Y} \right]^2 \qquad (6.3)$$

where $\Delta \hat{X}_i$ and $\Delta \hat{Y}$ are the expected values of ΔX and ΔY from the linear regression equation respectively, i.e. $\Delta \hat{Y} = m \times \Delta X_i$ and $\Delta \hat{X}_i = \Delta Y_i / m$, with m being the slope of the correlation between ΔX and ΔY; w_X and w_Y are weights for variables X and Y respectively, with w_X, $w_Y \geq 0$ and $w_X + w_Y = 1$. The weight factors were estimated as a function of the precision of the analytical determination of the variable (er) compared with the standard deviation of the set of measurements of that variable for water samples with AOU > 0 (SD). For a given couple of variables X and Y:

$$w_X = \left(\frac{er_X}{SD_X} \right) \Big/ \left(\frac{er_X}{SD_X} + \frac{er_Y}{SD_Y} \right) \qquad (6.4)$$

Minimising eq. (6.3) considering the weight factor of eq. (6.4) ensures that the slopes of the linear regression equations account for the relative precision (er/SD) of the pairs of nutrient anomalies that are correlated each time. Combining and rearranging eqs. (6.3) and (6.4), it results that the function to minimise is:

$$\sum_i \left[\left(\Delta X_i - \frac{\Delta Y_i}{m} \right)^{W_X} \cdot \left(\Delta Y_i - m \cdot \Delta X_i \right)^{W_Y} \right]^2 = \left(\frac{1}{m} \right)^{2 \cdot W_X} \cdot \sum_i \left(\Delta Y_i - m \cdot \Delta X_i \right)^2 \qquad (6.5)$$

In addition, the value of the slope (m) that makes eq (6.5) minimum is:

$$m = \frac{1-2\cdot w_X}{2-2\cdot w_X}\cdot\frac{\sum_i \Delta X_i\cdot\Delta Y_i}{\sum_i \Delta X_i^{\,2}} + \tag{6.6}$$

$$+\frac{\sqrt{\left((1-2\cdot w_X)\cdot\sum_i \Delta X_i\cdot\Delta Y_i\right)^2 + 4\cdot w_X\cdot(1-w_X)\cdot\sum_i \Delta X_i^{\,2}\cdot\sum_i \Delta Y_i^{\,2}}}{2\cdot(1-w_X)\cdot\sum_i \Delta X_i^{\,2}}$$

Therefore, m is an intermediate case between: **1)** the slope of a Type I regression (which should be applied when $w_X = 0$, $w_Y = 1$), $m = \sum_i(\Delta X_i \times \Delta Y_i)/\sum_i \Delta X_i^{\,2}$ and **2)** the slope of a Type II regression (which should be applied when $w_X = w_Y = 0.5$), $m = \sqrt{\sum_i \Delta Y_i^{\,2}/\sum_i \Delta X_i^{\,2}}$ (Sokal & Rolf 1995). Table 6.1 summarizes the values of er/SD for all the study variables at the different isopycnal layers.

Conversion of nutrient anomalies into the chemical composition of biogenic materials

Fraga (2001) reviewed in detail the average composition of phytoplankton carbohydrates (Cho), lipids (Lip), proteins (Prt), pigments (Chl) and phosphorus compounds (Pho). Table 6.2 summarizes the average composition of these groups of biomolecules. This table also contains the relative contribution of each group to the average composition of marine phytoplankton.

Table 6.1 Ratio of the analytical error of the chemical variables (er) and the standard deviation of their anomalies (SD) for ENACW samples in the NW Iberian shelf break. Dimensionless

Variable	$\frac{er}{SD}$		
	Upper ($\sigma_0 < 26.95$)	**Middle ($26.95 < \sigma_0 < 27.10$)**	**Lower ($\sigma_0 > 27.10$)**
ΔO_{2C}	0.04	0.08	0.11
ΔC_{TC}	0.21	0.38	0.21
ΔN_T	0.06	0.11	0.18
ΔP	0.21	0.37	0.52
ΔSi	0.08	0.16	0.18
ΔCa	4.10	3.86	3.79
ΔDOC	0.34	0.33	0.35
ΔDON	0.33	0.28	0.29
$\Delta FDOM_M$	0.83	1.43	2.25

Table 6.2 Chemical composition of the main organic products of synthesis and early degradation of marine phytoplankton according to Fraga et al. (1998). Percentages (in weight) of each group correspond to the average composition of marine phytoplankton

	chemical formula	**% (w/w)**
phosphorus compounds	$C_{45}H_{76}O_{31}N_{12}P_5$	12.1
pigments	$C_{46}H_{52}O_5N_4Mg$	2.0
proteins	$C_{138}H_{217}O_{45}N_{39}S$	45.7
carbohydrates	$C_6H_{10}O_5$	22.7
lipids	$C_{53}H_{89}O_6$	17.5
average composition	$C_{106}H_{171}O_{41}N_{16}P$	100.0

Considering the chemical formulas in Table 6.2, the chemical composition of the oxidized material and the proportions of the different biomolecules can be calculated from the O_2, C_T, NO_3 and HPO_4^{2-} anomalies. NO_2^- and NH_4^+ levels in ENACW are <0.1 and <0.2 μmol kg^{-1}, respectively. Equations describing the mineralization of proteins, carbohydrates, lipids and phosphorus compounds can be written:

$$C_{138}H_{217}O_{45}N_{39}S + 220\ O_2 + 179\ OH^- \longrightarrow \longrightarrow 138\ HCO_3^- + 39\ NO_3^- + SO_4^{2-} + 129\ H_2O \quad (6.7)$$

$$C_6H_{10}O_5 + 6\ O_2 + 6\ OH^- \longrightarrow 6\ HCO_3^- + 5\ H_2O \quad (6.8)$$

$$C_{53}H_{89}O_6 + 72.25\ O_2 + 53\ OH^- \longrightarrow 53\ HCO_3^- + 44.5\ H_2O \quad (6.9)$$

$$C_{45}H_{76}O_{31}N_{12}P_5 + 69.75\ O_2 + 67\ OH^- \longrightarrow \longrightarrow 45\ HCO_3^- + 12\ NO_3^- + 5\ HPO_4^{2-} + 46.5\ H_2O \quad (6.10)$$

Consequently, the corresponding linear system of mass balance equations is:

$$\Delta O_2 = 220 \times \Delta Prt + 6 \times \Delta Cho + 72.25 \times \Delta Lip + 69.75 \times \Delta Pho \quad (6.11)$$

$$\Delta C_T = -138 \times \Delta Prt - 6 \times \Delta Cho - 53 \times \Delta Lip - 45 \times \Delta Pho \quad (6.12)$$

$$\Delta N_T = -39 \times \Delta Prt - 12 \times \Delta Pho \quad (6.13)$$

$$\Delta P = -5 \times \Delta Pho \quad (6.14)$$

Inorganic carbon is consumed during the degradation of organic matter and calcareous ($CaCO_3$) structures. Since equations (6.7)-(6.10) refer only to the oxidation of organic carbon, the influence of the precipitation/dissolution of $CaCO_3$ must be corrected from C_T variability (C_{TC}):

$$C_{TC} = C_T - \frac{1}{2} \times TA_P \quad (6.15)$$

Where TA_P is the potential alkalinity, calculated following Fraga & Álvarez-Salgado (2005):

$$TA_P = TA - NH_4^- + 0.93 \times NO_2^- + NO_3^- + \\ + 0.08 \times \left(NH_4^+ + NO_2^- + NO_3^-\right) + 0.23 \times HPO_4^{2-} \quad (6.16)$$

RESULTS AND DISCUSSION

Temporal variability

Based on the wind regime (offshore Ekman transport, $-Q_X$; continental runoff Q_R) and on the structure of the water column (N^2), we have identified seven different periods between May 2001 and the end of April 2002 (Fig. 6.3). The period between May 15th and August 21st, was characterized by short pulses of northerly winds. In spite of its recurrence, these northerly winds were not strong enough to disrupt the thermal stratification of the upper 100 m of the water column (period 1 in Fig. 6.3), with the exception of the intense and prolonged northerly winds episode between August 21st and September 22nd which provoked the decrease of the water column stratification (about $1 \cdot 10^5$ s^{-2} in N^2; period 2 in Fig. 6.3).

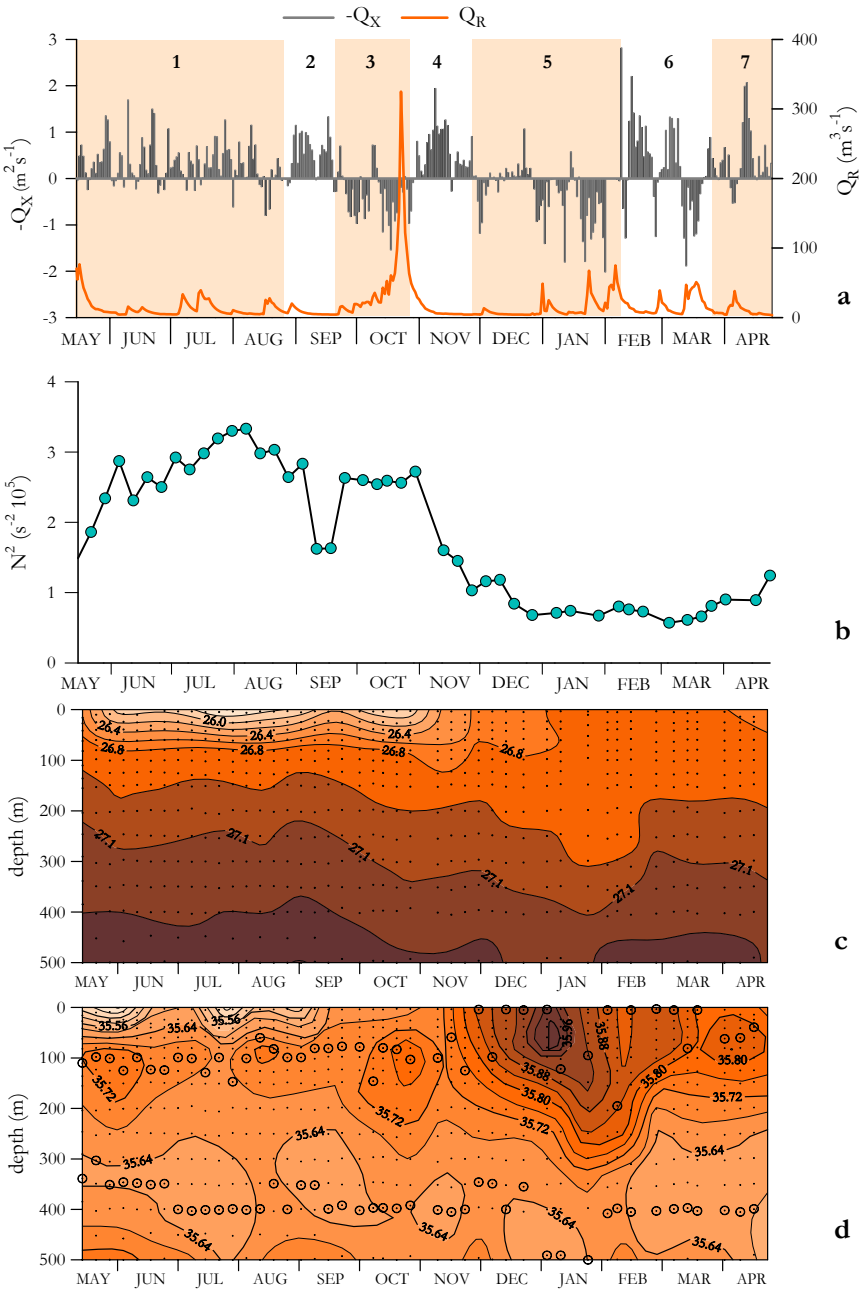

Figure 6.3 Time course of (**a**) Ekman transport ($-Q_X$; m^2s^{-1}) calculated with wind data provided by the SeaWatch Buoy Meteorological Observatory (http://www.puertos.es) and continental runoff (Q_R; m^3s^{-1}), (**b**) frequency of Brunt-Väisälä (N^2; s^{-2}), (**c**) density and (**d**) salinity. The seven different periods are shown in panel (**a**). The open circles on plot (**d**) correspond to the upper and lower limit of ENACW

From September 22nd, there was a wind reversal and relatively high southerly winds begun to prevail, but water column stratification was still high until October 30th, probably due to an intense continental runoff from the Rías Baixas, which was able to establish a salinity gradient and maintain a relatively strong stratified water column in the upper meters. After that, there was a sharp decrease of water column stratification in November. Since November 29th, the prevailing southerly winds favoured the presence of even saltier waters with maximum salinity values as high as 35.9. The period from the beginning of February until mid-March, corresponds to the winter mixing, with salinity values slightly fresher than during the previous periods. Winter mixed layer depths varied between 100 and 200 m, with maximum deepening at the beginning of February.

During the study period, ENACW occupied water column depths between 100 and 400 m (delimited by white circles on the time evolution of salinity; Fig. 6.3d), being even shallower during the autumn and winter seasons. We have observed the presence of the two branches of ENACW of subpolar and subtropical origins at station 5 during the entire year, as we can see in the temperature-salinity (TS) diagram for all the water samples collected at this location (Fig. 6.2). Here, ENACW is clearly recognised by the cluster of points with a linear TS relationship varying between a salinity minimum of 35.58 (~11.34°C) and a maximum of 36.02 (~14.85°C). These thermohaline characteristics are very similar to those previously described by Fiúza (1984) for this water mass and represented by a straight line on the TS diagram. Pérez et al. (2000) studied the inter annual variability of salinity on the isopycnal 27.1 kg m^{-3}, as representative of ENACW, and its relationship with the North Atlantic Oscillation (NAO). They found a close coupling between salinity at 27.1 kg m^{-3} isopycnal and NAO with low salinity associated to low NAO index reflecting weak westerly winds and increasing precipitation over southern Europe. We

have updated their time series and added the monthly salinity averages at 27.1 kg m^{-3} isopycnal for station 5 during the study period. Our data follow the trend of the previous five years, corresponding to low salinities, though they were not as low as during the previous minimum phase among 1980-87 (35.591 ± 0.014).

In the same way, our results also support the seasonal cycle of stratification/homogenisation in the PCCC waters established by Álvarez-Salgado et al. (2003) based only on seven cruises off the Galician Coast. The temporal evolution of the salinity maximum of the upper limit of ENACW tracks the evolution of the core of the PCCC. During the upwelling season (May 15th until September 22nd), a well-defined subsurface salinity maximum, corresponding to the ENACW upper limit, was maintained beneath the seasonal thermocline. This salinity maximum clearly defines the core of the poleward current conveying $ENACW_{ST}$. This core was characterized by salinity values of 35.65-35.75, nitrate levels between 4-8 μM, DON between 4-5 μM and fluorescence ~2.5 ppb QS (Fig. 6.3 and 6.4). After the transitional period to low stratification (October 30th until November 29th, 2001), the upper limit of ENACW surfaced and it reached much higher salinity values. Thus, we observed the presence of $ENACW_{ST}$ as saltier as 35.94 conveyed northward by the PCCC. These volumes of $ENACW_{ST}$ were also characterized by low nitrate concentrations (< 3 μM) and relatively high concentrations of DOM (DON > 4.5 μM and DOC > 62 μM; distribution not shown) and fluorescence of ~2.0 ppb QS. During the subsequent winter mixing, the salinity maximum of ENACW upper limit decreased (~0.06) though remained high (ΔS = 35.88-35.82). The recently formed $ENACW_{ST}$ was enriched in inorganic nutrients and $FDOM_M$ and presented relatively low DON and DOC concentrations (Fig. 6.3 and 6.4). Regarding the salinity minimum of the lower limit of ENACW, it was about the isopycnal level of 27.17 kg m^{-3} at approximately 350-400 m, except

during the winter mixing period, when ENACW lower limit deepened to ~500 m.

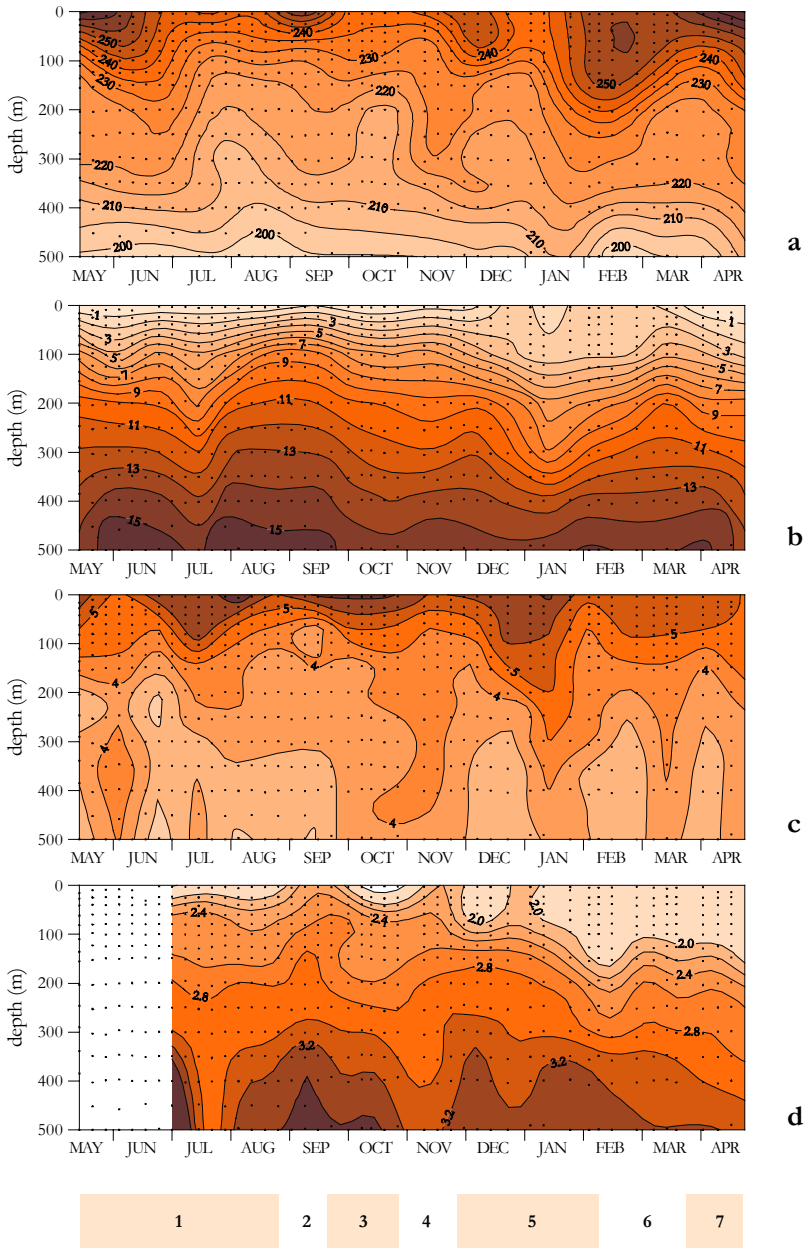

Figure 6.4 Time course of (**a**) oxygen (µM), (**b**) nitrate (µM), (**c**) dissolved organic nitrogen (µM) and (**d**) fluorescence of dissolved humic substances (ppb QS) for the study period

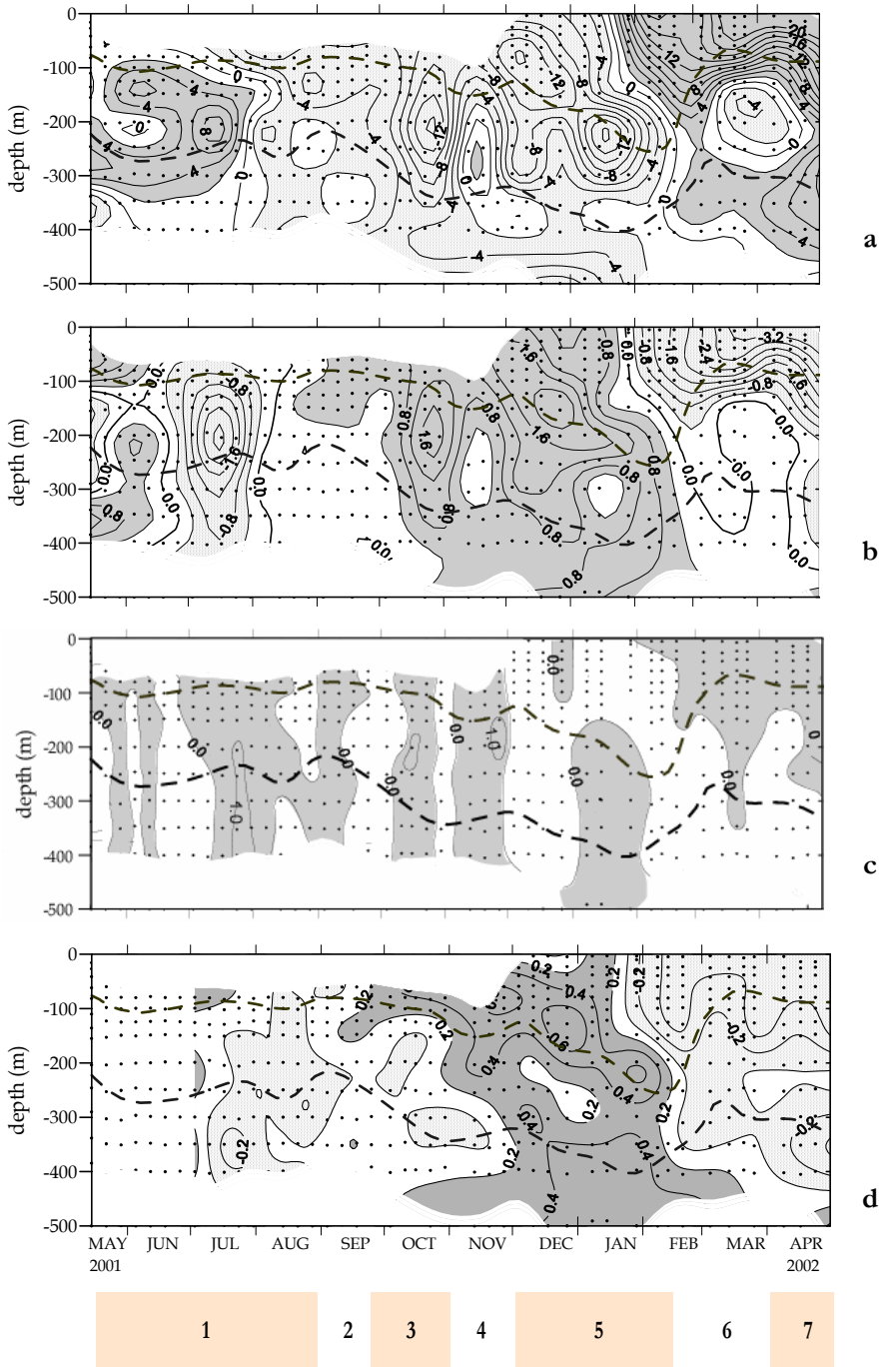

Figure 6.5 Time course of the anomalies for (**a**) oxygen (µM), (**b**) nitrate (µM), (**c**) dissolved organic nitrogen (µM) and (**d**) fluorescence of dissolved humic substances (ppb QS) for the study period

Seasonal pattern of mineralization

The high frequency sampling carried out, allows us to study the temporal trend of nutrient enrichment due to remineralization processes in the ENACW domain during an entire year. The temporal evolution of oxygen, nitrate, DON and $FDOM_M$ followed a similar trend and strongly correlated with temperature ($r > 0.70$; $p < 0.001$ for the four cases) due to mixing of different modes of ENACW. The residual variability not explained by the thermohaline properties corresponds to the aging that ENACW experienced due to biogeochemical or ventilation processes, as we discuss below. Fig. 6.5 represents the oxygen, nitrate, DON and $FDOM_M$ anomalies of ENACW waters for the study period. Positive nutrient anomaly (negative oxygen anomaly) is associated with higher than average nutrient concentration for this water parcel associated with enrichment due to mineralization of organic matter. Negative nutrient anomaly corresponds with lower than the average nutrient concentration for the study region and they can be associated with ventilation processes.

The temporal distributions of oxygen and nitrate anomalies are very similar ($r = -0.90$; $p < 0.001$) and suggest a seasonal pattern modulated by remineralization-ventilation processes in the domain of ENACW. As the upwelling season progressed, we observed an aging of the subsurface waters. Thus, oxygen anomalies decreased (nitrate anomalies increased) between May 15th and September 18th, reflecting the decomposition of organic matter formed during the productive spring and summer seasons. However, the most negative oxygen anomalies (highest nitrate enrichment) were recorded during the autumn (September 25th and November 27th), associated with $ENACW_{ST}$ conveyed northward in the PCUC/PCCC. The situation dramatically changed during the winter, when maximum ventilation occurred and the recently formed ENACW was characterized by high oxygen and low nitrate levels compared with the average. The lowest oxygen anomalies were observed at the sea surface

in contrast with the vertical structure of the anomalies during the previous periods, when the extreme anomalies were located at the base of the nutricline. This tendency was still observed during the subsequent spring bloom.

The temporal distribution of DON anomalies does not follow such a clear seasonal pattern. The only striking feature was the high positive DON anomalies observed at the beginning of the winter mixing period and the positive values for the subsequent spring period. For the previous periods, this distribution of DON anomalies seems to respond to short-time events of DON enrichment in the entire water column, *i.e.* there is a homogenised distribution of DON anomaly for the entire water column.

Finally, the temporal distribution of $FDOM_M$ anomalies presents the same trend as oxygen and nitrate. Until September, with the progress of the upwelling season, fluorescence anomalies increased. Maximum anomalies were also reached in winter, following the 26.95 isopycnal (at the base of the pycnocline) where metabolic processes were high. The lowest anomalies were observed at the sea surface at the end of winter and at the beginning of spring, in relation with high oxygen and low nitrate anomalies.

Fractionation of mineralization in the ENACW domain

One issue to test is if there is a fractionation of organic matter mineralization in the water column. Fractionation has important consequences for the global carbon cycle. The amount and depth at which dissolved inorganic carbon is released from mineralization determines the strength of the biological pump for drawdown of the atmospheric CO_2 (Shaffer et al. 1999).

With this aim, we have 'vertically' divided the domain of ENACW in three isopycnal ranges and study the remineralization ratios obtained from the correlations of the anomalies of the chemical variables for each density interval. The upper level extends from the shallow salinity maximum to the 26.95 isopycnal, density horizon of maximum nutrient and oxygen anomaly, and

corresponds to $ENACW_{ST}$. The lower level extends from the 27.10 isopycnal to the deep salinity minimum and corresponds to $ENACW_{SP}$. Waters at intermediate density values constitutes the middle layer.

In Table 6.3**,** we present the results. The low $\Delta O_2/\Delta P$ and $\Delta O_2/\Delta NO_3$ ratios relative to the classical Redfield ratios, suggests the preferential remineralization of protein rich organic matter, as we discuss below based on the biochemical composition. For the same region, Álvarez-Salgado et al. (2003) obtained $\Delta O_2/\Delta C_{TC}/\Delta N/\Delta P$ remineralization ratios of 113±3/108±12/16.7±0.6/1 for ENACW between densities of 26.6 and 27.2, based on a series of seven cruises carried out between 1983 and 1998. Similar to our results, these molar ratios point to a preferential remineralization of protein rich organic matter.

Table 6.3 Regression coefficient (*r*), slope and standard error of the slope of the correlation between selected pairs of nutrient anomalies for samples of the upper, middle and lower levels of ENACW off NW Spain. ns = no significant

	Upper ($\sigma_0 < 26.95$)			**Middle** ($26.95 < \sigma_0 < 27.10$)			**Lower** ($\sigma_0 > 27.10$)		
	r	**slope**	**error**	***r***	**slope**	**error**	***r***	**slope**	**error**
$\Delta O_2/\Delta C_{TC}$	-0.957	-1.22	0.04	-0.877	-1.34	0.06	-0.750	-1.4	0.2
$\Delta O_2/\Delta N_T$	-0.958	-7	0.2	-0.78	-6.7	0.4	-0.597	-8.9	1.2
$\Delta O_2/\Delta P$	-0.933	-125	5	-0.805	-139	8	-0.650	-154	18
$\Delta DOC/\Delta DON$	0.250	6	3	0.465	5	1	0.468	5	2
$\Delta DON/\Delta N_T$	-0.430	-0.17	0.04	-0.228	ns	ns	0.114	ns	ns
$\Delta Ca/\Delta Corg$	0.708	0.07	0.01	0.226	0.07	0.02	0.353	0.14	0.04
$\Delta Si/\Delta Ca$	0.697	1.2	0.1	0.166	1.1	0.5	0.213	1.1	0.5
$\Delta N/\Delta Si$	0.868	2.8	0.1	0.707	3.1	0.2	0.429	2.2	0.5
$\Delta FDOM_M/\Delta NO_3$	0.885	0.18	0.01	0.616	0.13	0.02	0.385	0.11	0.05

The biochemical composition of the mineralised organic matter can be obtained from these O_2/C/N/P molar ratios by solving the determined system of linear equations (6.11)-(6.14) and it is summarised in Table 6.4. It should be noted that the $\Delta O_2/\Delta C_{TC}$ ratio cannot be directly used because it is affected by the differential dissolution of anthropogenic CO_2 throughout the seasonal

cycle. Therefore, we tested the range of $\Delta O_2/\Delta C_{TC}$ values that produce at least 5% mineralization of lipids and carbohydrates (Anderson 1995). It ranges from 1.47 to 1.51 in the upper, 1.50 to 1.52 in the middle and 1.35 to 1.47 in the lower layer. The latter is the only layer where the expected and observed $\Delta O_2/\Delta C_{TC}$ values (1.4 ± 0.2) coincided, because it is less affected by the penetration of anthropogenic carbon.

Table 6.4 Average chemical composition (phosphorus compounds, proteins, lipids and carbohydrates) of the products of early degradation of marine phytoplankton photosynthesis as obtained from inorganic nutrients, in % (w/w)

	Upper ($\sigma_0 < 26.95$)	**Middle** ($26.95 < \sigma_0 < 27.10$)	**Lower** ($\sigma_0 > 27.10$)	**Redfield**
Pho	14.7 ± 0.7	13.4 ± 0.4	12 ± 2	12
Prt	67 ± 3	72 ± 2	51 ± 8	47.1
Cho	11 ± 8	8 ± 5	22± 25	24.4
Lip	8 ± 4	7 ± 2	15 ± 14	16.5
Formula	$C_{84}H_{133}O_{32}N_{18}P$	$C_{92}H_{146}O_{34}N_{21}P$	$C_{109}H_{175}O_{44}N_{17}P$	$C_{106}H_{171}O_{44}N_{16}P$

In the upper and middle layers the average biochemical composition is richer in N (Prt) and P (Pho) compounds (>80%) and poor in carbon (Cho and Lip) compounds (<20%) than Redfield's mean (58 and 40% respectively; see Table 6.4). On the other hand, biochemical composition of the lower layer is comparable to Redfield's values, the contribution of Prt + Pho decreases to 63%, whereas the percentage of Lip + Cho increases to 37%. In this sense, our results corroborate the study of Li & Peng (2002), who found a systematic decrease in protein content of remineralised organic matter from the North Atlantic to the North Pacific, following the conveyor belt circulation (see their table 3). Also Brea et al. (2004), analysing the nutrient remineralization ratios in the Eastern South Atlantic, found that proteins were mineralized preferably

over other compounds in the domain of South Atlantic Central Waters, while for deeper water masses there was a decrease in the protein proportion.

The comparison of the mineralization and biochemical composition for the three layers show a preferential remineralization of protein and phosphorus compounds in the upper and middle layers and of carbohydrates and lipids in the lower layer, and it constitute a vertical fractionation in the domain of ENACW. Thus, we can suggest that in our region, the two branches of ENACW present different ratios of organic matter mineralization. Previous works (Castro et al. 1998, Thomas et al. 2002) also looking at stoichiometric ratios from chemical data, did indicate the same vertical fractionation in the Eastern North Atlantic between water column depths above and below the main thermocline. These authors found a higher released of nutrients over inorganic carbon in the upper layer. Likewise, Minster & Boulahdid (1987), revisiting the method of Takahashi et al. (1985), estimated the Redfield ratios along several isopycnals in the North Atlantic and found no fractionation of organic matter remineralization for the two shallower levels (27.0 and 27.2); however they found a decrease in the $\Delta O_2/\Delta P$ for deeper levels (27.4 and 27.8).

There are not many manuscripts dealing with shallow mineralization processes and basically all of them are focused on the oligotrophic subtropical gyres of the North Pacific and North Atlantic oceans (Jenkins & Goldman 1985, Sarmiento et al. 1990, Emerson & Hayward 1995, Abell et al. 2000). For the North Pacific Subtropical Gyre, Emerson & Hayward (1995) described the presence of subsurface waters with negative preformed nitrate, which suspect is due to the oxidation of DOM rich in carbon. Subsequently, Abell et al. (2000) corroborated this hypothesis based on DOM data, and found a different mineralization regime for central waters that outcrop inside the gyre and those outcropping just north of it. Along isopycnals that outcrop inside the gyre the C:N mineralization ratio is 30 ± 10, due to the oxidation of an excess of labile

DOC produced by nitrogen fixing organisms while for deeper isopycnals the C:N ratio is 8 ± 1. By comparison with this situation, we should hypothesize a different mineralization pattern for $ENACW_{ST}$ and $ENACW_{SP}$ taking into account their different oceanographic regime, the same as the above result.

Likewise, we do not observe an increasing ratio of ΔDOC:ΔDON as should be expected considering a preferential mineralization of nitrogen over carbon, as reported for other regions (Hopkinson et al. 1997, 2005, Loh & Bauer 2000, Hung et al. 2003b). In fact, the C:N molar ratio of the dissolved organic matter fraction is low for the three layers (Table 6.3) and similar to the classical Redfield ratio of 6.6, suggesting the mineralization of relatively labile dissolved organic matter.

Mineralization of siliceous and calcareous structures

During the whole period, the calcite saturation profile varies from 3.5 times in subsurface waters to 2.5 at 500 meter. Since the upper ocean is $CaCO_3$ over saturated (Takahashi et al. 1981, Broecker & Peng 1982), carbon regeneration at that level is predominantly due to the oxidation of organic carbon (Honjo et al. 1982, Honjo & Manganini 1993). Millimam et al. (1999) showed in a review of the global carbonate budget that 60-80% of the biogenic $CaCO_3$ dissolves in the upper 1000 m, above the lysocline, as a result of biological mediation in special microambient as snow aggregates and invertebrate guts. The ratio between soft and hard biogenic material decomposition rates varies with depth in the oceans (Broecker & Peng 1982). These authors, using the Geochemical Ocean Section Study (GEOSECS) dataset, estimated a ΔCa/ΔCorg molar ratio of ~0.1 for the permanent thermocline and ~0.5 for deep waters. Several authors obtained a ΔCa/ΔCorg molar ratio of 0.05 for the upper and 0.08 for the lower permanent thermocline of the North Atlantic (Takahashi et al. 1985, Ríos et al. 1995). Recently, for the Eastern North Atlantic Ocean, Pérez et al. (2002) fit the vertical profile of the ΔCa/ΔCorg ratio to a polynomial depth

function that varies from 0.05 in the upper layer to 0.55 in deep waters. The vertical variation of ΔCa/ΔCorg ratio from 0.07 ± 0.01 in the upper level to 0.14 ± 0.04 in the lower level (Table 6.3) fits very well with this vertical pattern. The low value in the upper layer is in agreement with those found in the middle and the innermost part of the NW Iberian shelf by Álvarez-Salgado et al. (*accepted*), Chapter 5.

Biogenic silica also dissolved in the deep ocean as sinking particles falling from the photic layer. Most of the silica dissolution takes place below the main thermocline. The high covariation between alkalinity and silicate profiles in open ocean deep waters (Brewer et al. 1995, Broecker & Peng 1982, Ríos et al. 1995) is probably due to the biologically mediated dissolution of these hard structures in the microenvironments created by marine snow, zooplankton guts, etc. A mean ΔSi/ΔCa molar decomposition ratio of ~2 can be proposed according to the open ocean $CaCO_3$ and opal decomposition rates in the water column (Milliman et al. 1999, Tréguer et al. 1995). For the North Atlantic, Pérez et al. (2002) calculated an average ΔSi/ΔCa ratio for the whole water column of 1.4. According to Berger & Herguera (1992), a ΔSi/ΔCa ratio of 1.4 is expected for an area with a mean organic carbon flux of 10 mmol $m^{-2}d^{-1}$, which is in close agreement with the productivity of the Eastern North Atlantic Ocean (Martin et al. 1993). Lower ΔSi/ΔCa ratios, around 1.05, were measured in sediment traps deployed at the North Atlantic Bloom Experiment (NABE) site below 3100 m (Newton et al. 1994). In this study, the ΔSi/ΔCa molar ratio presented a constant with depth ratio of 1.1 (Table 6.3), which fits well with the oceanic values and with those find by Álvarez-Salgado et al. (*accepted*), Chapter 5, in the adjacent NW Iberian shelf. The ΔSi/ΔCa values of 2.4 ± 0.4 in the Ría de Vigo and 1.6 ± 0.2 in the shelf go in agreement with the ΔSi/ΔCa value of 1.1 at the shelf break, following the expected seaward decreases of organic matter flux.

Opal dissolution was high compared with organic matter decomposition: the ΔN/ΔSi molar ratios show a vertical variability from 2.8 ± 0.1 in the upper level to 2.2 ± 0.5 in the lower level (Table 6.3). This vertical gradient suggests a relative increase of opal dissolution with depth in the ENACW, which is in agreement with an increase of the dissolution of biogenic silica in deeper water. On the other hand, these values fit with the seaward increase of ΔN/ΔSi from the inner NW Iberian shelf. Álvarez-Salgado et al. (*accepted*), Chapter 5, give ΔN/ΔSi molar ratios of 1.1 ± 0.1 in the Ría of Vigo and 1.8 ± 0.1 in the middle shelf. Assuming a theoretic ΔN/ΔSi ratio of ~1 for diatoms (Brzezinski 1985), it results that diatoms represents from 90% in the Ría de Vigo to 35% in the upper layer at shelf break of the mineralised biogenic matter. The percentage increases to 45% in the lower layer.

Contribution of DOM to mineralization in the domain of central waters

Another important question is to know how much is the contribution of DOM to remineralization of organic matter in the domain of ENACW. We have estimated this contribution based on the slope of ΔDON *vs.* ΔN_T (Table 6.3) and ΔDOC *vs.* ΔC_{CT}. A significant correlation was obtained between ΔDON *vs.* ΔN_T only at the shallower isopycnal level (σ < 26.95 kg m^{-3}) and no correlation for the other levels. For ΔDOC *vs.* ΔC_{CT} we did not find any correlation for any of the three levels. On the other hand, a significant correlation (Table 6.3) was observed between ΔDOC *vs.* ΔDON for the three levels, being even higher for the two deepest levels. From these results, it is suggested that DON accounted for ~17% of organic matter remineralization at the shallower ENACW level (σ <26.95 kg m^{-3}). At this level, there is a preferential remineralization of nitrogen *vs.* carbon, as the lack of correlation between ΔDOC *vs.* ΔC_{CT} points. However, neither DON nor DOC contributes significantly to organic matter remineralization for the densest levels of ENACW, nevertheless there are still significant correlations between ΔDOC *vs.*

ΔDON with low slopes (6 ± 3, 5 ± 1, 5 ± 2 for upper, middle and lower layers, respectively), pointing to relatively young (high reactive; "labile" or "semilabile") DOM material (Hopkinson et al. 2005). Based on the temporal distribution of DON anomalies (Fig. 6.4c), we suggest that the export of relatively reactive DOM is due to the leaking of DOM from sinking organic matter. That is, the observed plumes of DOM anomalies can be explained under the scenario described by Azam & Long (2001) where bacteria attracted to the sinking organic particles solubilize these particles, converting sinking organic matter into DOM in such a way that the rate of solubilization is much higher than mineralization.

The contribution of DON to mineralization processes (~17%) for shallower ENACW (σ < 26.95) is lower than values obtained on the ría and shelf during the same study period (19-30%; Álvarez-Salgado et al. *accepted*, Chapter 5). On the continental shelf of George Bank, where also upwelling of nutrient-rich deep waters occurs, Hopkinson et al. (1997) estimated that ~19% of remineralised N in the entire water column is derived from the export and decomposition of DOM. Only Abell et al. (2000) analysed the contribution of total organic carbon (TOC) and nitrogen (TON) to organic matter oxidation at different isopycnal levels for a southern transect in the eastern subtropical North Pacific. They observed a situation completely different to that previously describe for the NW Iberian upwelling system. These authors found that for isopycnals outcropping in the subtropical gyre, TOC and TON contribute to 70% and 20% respectively. In contrast, along isopycnals that outcrop to the north of the gyre, both TOC and TON contribute to 30% to organic matter remineralization. They explained this preferential remineralization of TOC relative to TON based on the excess of labile TOC produced during nitrogen fixation in the Subtropical region. In addition, Arístegui et al. (2002) estimated

that the DOC flux supports ~10% of the respiration in the dark ocean on the basis of the relation between DOC and apparent oxygen utilization.

The potential of the fluorescence of dissolved organic matter to trace mineralization processes in the central waters domain

The contribution of humic substances to the DOC pool was assessed using the conversion factor of 2.67 ± 0.06 μM C (ppb QS)$^{-1}$ obtained with a commercial fulvic acid (Nieto-Cid et al. *in press*, Chapter 3). On this basis, 9 ± 2% of DOC in ENACW upper layer was humic substances, increasing to 12 ± 1% and 14 ± 1% in middle and lower layers, respectively. These numbers are in the range of those provided by Obernosterer & Herndl (2000) in the Adriatic Sea (15 ± 7%), but considerably lower than those proposed for the same authors in the North Sea (43 ± 7%), due to the higher terrestrial contributions in the later ecosystem.

Mineralization processes involve an increase in the concentration of nutrients, oxygen and carbonate, linked to a decrease in organic matter. It was confirmed that these changes go accompanied by an increase in $FDOM_M$ (Chen & Bada 1992, Hayase & Shinozuka 1995, Wedborg et al. 1998, Nieto-Cid et al. *in press*, *submitted*, Chapter 3-4). Comparison of $FDOM_M$ and NO_3 anomalies (Table 6.3) indicates that dissolved humic substances are produced during the microbial degradation of biogenic organic matter at an average rate of 0.18 ± 0.01, 0.13 ± 0.02 and 0.11 ± 0.05 ppb QS (μM N)$^{-1}$ at the upper, middle and lower ENACW layers. $\Delta FDOM_M/\Delta O_2$ ratios ranged from -0.026 in the <26.95 to -0.012 ppb QS (μM O_2)$^{-1}$ in the >27.1 layer. These values are in the range of those found in the NW Iberian shelf 0.14 ± 0.01 ppb QS (μM N)$^{-1}$ and -0.026 ± 0.003 ppb QS (μM O_2)$^{-1}$, (Nieto-Cid et al. *in press*, Chapter 3) and the Ría de Vigo, -0.029 ± 0.003 ppb QS (μM O_2)$^{-1}$, (Nieto-Cid et al. *submitted*, Chapter 4). Likewise, these values are similar to those reported by Hayase et al. (1987) in Tokyo Bay (0.09 ppb QS (μM N)$^{-1}$). It is interesting to note that the $\Delta FDOM_M/\Delta O_2$ rate

calculated for the ENACW upper layer is the same that the rate of production of humic substances by bacterial respiration (0.027 ± 0.003 ppb QS (μM O_2)$^{-1}$) obtained by Nieto-Cid et al. (*submitted*), Chapter 4, after 24 h hours dark incubations.

CONCLUSIONS

The high spatio-temporal resolution of the data collected during the DYBAGA project allows us to resolve the variability of local aging of ENACW on a yearly basis. The analysis of the anomalies of nutrients, fluorescence, oxygen and inorganic carbon indicates that there is a seasonal aging with an increasing (decreasing) on nutrients, fluorescence and inorganic carbon (oxygen) during the summer upwelling, reaching maximum (minimum) values during autumn, associated with the mineralization of biogenic material exported from the euphotic zone after the productive upwelling period. Afterwards, the situation changes dramatically, and we have obtained minimum (maximum) anomalies on nutrients, fluorescence and inorganic carbon (oxygen) due to winter mixing. Even the distribution of DON anomalies, which responded to short time scale events during the previous months, presented a clear signal for this period. Thus, it can be considered that there is a biogeochemical reset of the system during the winter mixing.

For our time series data, DOM concentration anomalies were homogenously vertical distributed in the domain of ENACW. Taking into account that we do not observe any correlation between DOM anomalies and inorganic variable anomalies, except for ΔDON *vs.* ΔN_T for ENACW < 26.95 kg m^{-3}, and that there is a significant correlation between ΔDON *vs.* ΔDOC for the three layers, we suggest that this pattern responds to the solubilization of fast sinking particles where the rate of solubilization is much larger than mineralization. For the shallower ENACW layer (σ < 26.95 kg m^{-3}), DON is preferentially mineralised over DOC, accounting for ~17% of organic matter mineralization at this level.

Based on the stoichiometry ratios derived from the nutrient, oxygen and inorganic carbon concentrations, fractionation of organic matter mineralization was observed between the upper and lower layers of ENACW. In the

mesopelagic layer occupied by ENACW, there is a preferential remineralization of nitrogen and phosphorus rich organic matter.

$FDOM_M$ and NO_3 anomalies correlate significant and directly through the whole ENACW depth range. This good correlation points to the production of dissolved humic substances as a by-product of the microbial degradation processes of biogenic organic matter. The average rate of this process is 0.18 ± 0.01 ppb QS $(\mu M\ N)^{-1}$ in the upper ENACW layer (<26.95), decreasing down to 0.11 ± 0.05 ppb QS $(\mu M\ N)^{-1}$ in the lower ENACW layer (>27.1).

Chapter 7:

Summary and general conclusions

SUMMARY AND GENERAL CONCLUSIONS

Current knowledge on the role played by dissolved organic matter (DOM) in coastal upwelling systems is still scarce, and mainly restricted to the NW Iberian margin. An intensive hydrographic sampling was conducted in the area from May 2001 to April 2002. Three stations were occupied once a week, representative for the three contrasting environments existing in the NW Iberian upwelling system: **1)** the highly productive, large (>2.5 km^2), and V shaped coastal embayments known as "Rías Baixas"; **2)** the adjacent open shelf waters; and **3)** the coastal transition zone at the NW Iberian shelf-break.

C, N and P in dissolved, particulate organic and inorganic forms were determined at selected depths in the three study sites. In addition, dissolved mono- and polysaccharide concentrations and the fluorescence of protein-like and humic substances were also intensively measured to characterise labile (monosaccharides, dissolved free amino acids), semi-labile (polysaccharides) and refractory (humic substances) DOM pools.

The NW Iberian margin is occupied by the subtropical and subpolar branches of Eastern North Atlantic Central Water (ENACW), modified at the surface layer by continental runoff and heat exchange with the atmosphere. Combination of an inverse water masses analysis, able to separate the physical from the biogeochemical components of the measured variables in the ENACW domain, with a stoichiometric model allowed us to study the spatial and temporal patterns of nutrient mineralization, i.e. the contribution of the different organic matter pools (dissolved, suspended and sinking) to the microbial respiration and the biochemical composition of the mineralised organic matter.

In addition, a process-oriented short-time-scale (1/2 wk frequency) study was conducted in the coastal embayment of the Ría de Vigo during winter, spring,

summer and autumn 2002 in order to quantify the rates of microbial and photochemical reactivity of DOM.

1. **The DOM pool contributes significantly to oxygen consumption in the ENACW domain of the NW Iberian margin**

Three layers were defined in the ENACW domain at the NW Iberian shelf-break: the upper 150 m ($\sigma < 26.95$), the middle 150-300 m ($26.95 < \sigma < 27.10$) and the lower 300-500 m ($\sigma > 27.10$). The contribution of DOM to nutrient mineralization is only significant in the upper 150 m, accounting for 17 ± 4% of the nitrogen mineralization. Downwards, the solubilization of fast sinking particles is getting more importance, generating solubilization rates higher than mineralization in the lower layers. The contribution of DOM to oxygen consumption in ENACW increases significantly on the shelf, from 20 to 30%. In these waters, about 20% of the regenerated inorganic nutrients are due to the mineralization of suspended organic matter and more than 50% to the mineralization of large, fast sinking particles. The C/N molar ratio of the mineralised DOM in the ENACW domain of the shelf-break (6 ± 2) is similar to the values observed at the shelf (7.3 ± 0.7) and rías (6.3 ± 0.8). It is noticeable that these ratios are not significantly different from the ratio of the products of synthesis and early degradation of marine phytoplankton.

2. **Fractionation during organic matter mineralization in the NW Iberian margin**

The biochemical composition of the products of early degradation of dissolved, suspended and sinking organic matter has been approached by introducing the biogeochemical component of an inverse water masses analysis into a stoichiometric model. As a result, C, N and P anomalies due to mineralization were converted into proteins, lipids, phosphorus compounds and carbohydrate anomalies. In the ENACW domain, fractionation during the mineralization of biogenic materials occurs, with N and P compounds being

preferentially consumed, as compared with the Redfield formula, in the upper layer, and C compounds (carbohydrates and lipids) in the lower layer. Over the shelf, proteins are preferentially oxidized in the sinking organic matter pool, carbohydrates in the dissolved organic matter pool and lipids in the suspended organic matter pool, as compared again with the Redfield formula.

3. Carbohydrates, a main carbon pool in the NW Iberian margin

Carbohydrate changes are linked to bulk organic carbon changes within the time scale of the sampling frequency (2 wk; $r > +0.82$, n = 298, $p < 0.001$). The contribution of dissolved carbohydrates to the dissolved organic carbon (DOC) changes is about 30% in the shelf and the ría. The surface DOC excess is richer in carbohydrates than the bulk DOC, this percentage increasing from 12-14% in the bulk DOC to 30-40% in the DOC excess, indicating that dissolved carbohydrates are a main component of the freshly produced material in comparison with aged ENACW, where only 9% of DOC are dissolved carbohydrates. The carbohydrate excess at the surface layer presentes a higher percentage of polysaccharides than the bulk carbohydrates pool: 80-90% of the carbohydrates excess are polysaccharides, suggesting that the material accumulated in the surface layer is essentially semi-labile. The average flushing time of the Ría de Vigo, 11 days, is compatible with the accumulation of semi-labile material in the surface layer.

4. Dynamics of dissolved aromatic amino acids

The fluorescence of dissolved free amino acids (DFAA) and dissolved oxygen were measured in parallel 24 h light and dark incubations, for the first time in a coastal upwelling system. A significant linear correlation between the gross primary production (Pg) and the net production of DFAA in the light, points to the quick consumption of dissolved protein-like materials at a net average rate of -1.4 ± 0.2 ppb Trp d^{-1}, which accumulates in the water column only when Pg exceeds 80 ± 20 μmol $kg^{-1}d^{-1}$. Therefore, DOM fluorescence can

be used as a tracer for labile DOM (DFAA) production/consumption. Fluorescence distributions indicate that DFAA can be produced either in the surface, as demonstrated by the incubation experiments, or at the bottom layer. Protein-like fluorescence accumulated **1)** in the photic layer, because of phytoplankton exudation or cell lysis; and **2)** in the bottom nepheloid layer (BNL), after *in situ* production by intense microbial activity and/or after release from the pore waters of the pelagic sediment. The contribution of DFAA fluorescence to the DOC pool ($FDOM_T$/DOC) in the upper layers of the ría follows a seasonal pattern, increasing significantly from a winter minimum to an autumn maximum.

5. Production of humic substances as a by-product of microbial oxidation processes

Significant changes have been observed in the dissolved oxygen content and the fluorescence of humic substances after 24 h dark incubations in the coastal upwelling system of the Ría de Vigo. In one day, the system showed net production of humic substances (0.0-0.4 ppb QS d^{-1}), which were positively correlated with the respiration rates with a net ratio of 0.027 ± 0.003 ppb QS ($\mu mol\ kg^{-1}\ O_2$)$^{-1}$, suggesting a daily synthesis of marine humics as a by-product of the bacterial respiration of DOM. Consequently, the fluorescence of marine humic substances revealed as a suitable indicator of nutrient mineralization processes. The three distinct environments sampled during this study presented similar $\Delta FDOM_M/\Delta O_2$ ratios as the incubation experiments: -0.024 ± 0.003, -0.025 ± 0.002 and -0.019 ± 0.007 ppb QS ($\mu mol\ kg^{-1}\ O_2$)$^{-1}$ from the Ría de Vigo, the open shelf and the shelf-break. About 10% of the degraded organic carbon is converted into humic substances as a by-product of microbial oxidation processes in the three study sites. Thus, DOM fluorescence can be used as a tracer for microbial decomposition processes. Fluorescence distributions suggest that humic acids are produced in subsurface

waters by *in situ* mineralization, especially in the BNL and the sediments. In this work, we found that humic substances contribute up to 90% of the DOC excess in the BNL, an amount that demands future process orientated studies. The contribution of humic fluorescence to the DOC pool ($FDOM_M$/DOC) in the lower layer of the ría followed the same seasonal pattern than the $FDOM_T$/DOC ratio in the upper layer: increasing significantly from a winter minimum to an autumn maximum.

6. Seasonality of the photodegradation of humic substances

The consumption of humic substances in the light minus dark incubations was inversely correlated with the net production of humic substances in the dark, indicating a rapid photodegradation of recently produced marine humic substances as a by-product of microbial respiration. Incubation experiments demonstrated that daily photodegradation rates and residual humic fluorescence levels followed a seasonal pattern characterised by a marked autumn maximum, either in the river waters (65% photobleaching per day) or in the ría (90 and 55% photobleaching per day in bottom and surface waters, respectively). It is noticeable that the bottom seawater, enriched in marine humic substances, is photodegraded faster than the surface seawater and the riverine water. Fluorescence distributions suggest that humic acids are photodegraded in the upper layer by the sunlight. Due to the upwelling of bottom waters, the humic material produced during bacterial respiration in the bottom layer is quickly degraded in the surface layer by photochemical processes. Despite these processes, in the middle ría was accumulated the humic material produced in the inner ría (San Simón Bay, site where strong mineralization processes promote higher humification processes that exceed photodegradation). On the contrary, photodegradation is the dominant process in the transit of the ría surface waters towards the shelf, where net consumption of humic substances is observed.

CONCLUSIONES (en castellano)

El conocimiento actual del papel que juega la materia orgánica disuelta en los sistemas de afloramiento costero es aún exiguo, y restringido mayoritariamente al margen NO Ibérico. Un muestreo hidrográfico intensivo fue realizado en esta zona desde mayo 2001 hasta abril 2002. Se muestrearon semanalmente tres estaciones, representativas de los tres diferentes ambientes que existen en el sistema de afloramiento del NO Ibérico: **1)** los amplios (>2.5 km^2) entrantes costeros en forma de V, altamente productivos, y conocidos como "Rías Baixas"; **2)** la plataforma costera adyacente; y **3)** la zona costera de transición del borde de la plataforma del NO Ibérico.

C, N y P, en sus formas disueltas y particuladas, orgánicas e inorgánicas, fueron determinadas en profundidades fijas en los tres lugares de estudio. Al mismo tiempo se han medido concentraciones de mono- y polisacáridos y la fluorescencia de sustancias pseudo-proteicas y pseudo-húmicas, con el objetivo de caracterizar la materia orgánica lábil (monosacáridos, aminoácidos libres), semilábil (polisacáridos) y refractaria (sustancias húmicas).

En el margen del NO Ibérico se encuentran dos ramas del Agua Central Atlántica Nororiental (ENACW) que son modificadas en superficie por los aportes continentales y el intercambio de calor con la atmósfera. La combinación de un análisis inverso de masas de agua, capaz de separar las componentes física y biogeoquímica de las variables medidas en el dominio del ENACW, con un modelo estequiométrico nos ha permitido estudiar los patrones espaciales y temporales de la mineralización de nutrientes, i.e., la contribución de los distintos grupos de materia orgánica disuelta (disuelto, en suspensión y en sedimentación) a la respiración microbiana de la materia orgánica mineralizada.

Como complemento se ha realizado un estudio orientado a procesos de corta escala (frecuencia de 1/2 semana) en la Ría de Vigo durante el invierno,

primavera, verano y otoño 2002, buscando la cuantificación de las tasas de reactividad microbiana y fotoquímica de la materia orgánica disuelta.

1. **La materia orgánica disuelta contribuye significativamente al consumo de oxígeno en el dominio de las aguas centrales en el margen NO Ibérico**

   Se han definido tres capas en el dominio de las aguas centrales: la primera abarca los 150 m superiores ($\sigma < 26.95$), la segunda entre 150 y 300 m ($26.95 < \sigma < 27.10$) y la tercera entre 300 y 500 m ($\sigma > 27.10$). La contribución de la materia orgánica disuelta a la mineralización de nutrientes es significativa solo en los primeros 150 m, contribuyendo al 17 ± 4% de la mineralización de nitrógeno. En las capas inferiores la solubilización de las partículas en sedimentación adquiere mayor importancia, generando tasas de solubilización mayores que las de mineralización. Sin embargo el aporte de la materia orgánica disuelta al consumo de oxígeno en las aguas centrales aumenta significativamente en la plataforma costera, donde adquiere valores del 20 al 30%. En esta masa de agua, alrededor de un 20% de los nutrientes inorgánicos regenerados son debidos a la mineralización de la materia orgánica en suspensión y más de un 50% a la mineralización de las grandes partículas en sedimentación. Por otro lado, la relación C/N de la materia orgánica disuelta mineralizada en el dominio de las aguas centrales del borde de plataforma (6 ± 2) es similar a los valores observados en la plataforma (7.3 ± 0.7) y en la ría (6.3 ± 0.8). Estas relaciones no son significativamente distintas de la relación C/N de los productos de síntesis y degradación temprana del fitoplancton marino.

2. **Fraccionamiento durante la mineralización de la materia orgánica en el margen NO Ibérico**

   Se ha estimado la composición bioquímica de los productos de degradación temprana de la materia orgánica disuelta, en suspensión y en rápida sedimentación con la implementación de un análisis inverso de masas de agua y

un modelo estequiométrico. Como resultado, las anomalías de C, N y P debidas a la mineralización fueron convertidas en anomalías de proteínas, lípidos, compuestos de fósforo y carbohidratos. Así, en el dominio de las aguas centrales existe un fraccionamiento durante la mineralización de los materiales biogénicos, siendo los compuestos de N y P consumidos preferentemente, i.e., en comparación con la fórmula de Redfield, en la capa superficial, y los compuestos de C (carbohidratos y lípidos) en las capas más profundas. A lo largo de la plataforma las proteínas son preferentemente oxidadas en el material orgánico en sedimentación, los carbohidratos en el material orgánico disuelto y los lípidos en el material orgánico en suspensión, comparándolos de nuevo con los valores de la fórmula de Redfield.

3. Carbohidratos, un importante componente de carbono en el margen del NO Ibérico

Los cambios en la concentración de carbohidratos están acoplados a los cambios en el conjunto total del carbono orgánico en la escala de tiempo de la frecuencia de muestreo (2 semanas; $r > +0.82$, n = 298, $p < 0.001$). Así, aproximadamente el 30% de los cambios observados en el carbono orgánico disuelto es debido a los carbohidratos disueltos. Por otro lado, la acumulación superficial de carbono orgánico disuelto está especialmente enriquecida en carbohidratos, incrementándose el porcentaje de azúcares de un 12-14% a un 30-40%, lo que indica que los carbohidratos disueltos son el componente principal del material recientemente producido en comparación con las envejecidas aguas centrales, donde solo el 9% del carbono orgánico disuelto son carbohidratos disueltos. El exceso superficial de carbohidratos presenta, además, una mayor contribución de polisacáridos (80-90%), lo que sugiere que este material es esencialmente semilábil. Además, el tiempo medio de renovación del agua de la Ría de Vigo, 11 días, lo que totalmente compatible con la acumulación de material semilábil en la superficie.

4. Ciclo de los aminoácidos aromáticos disueltos

Se midieron paralelamente, en incubaciones de 24 h (luz y oscuridad), y por primera vez en un sistema de afloramiento costero, la fluorescencia de los aminoácidos disueltos y el oxígeno disuelto. Los resultados mostraron una correlación lineal significativa entre la producción primaria bruta y la producción neta de aminoácidos disueltos en la luz, lo que indica un rápido consumo de los materiales pseudo-proteicos a una tasa media de -1.4 ± 0.2 ppb Trp d^{-1}, que solo se acumulan en la columna de agua cuando la producción primaria bruta es superior a 80 ± 20 µmol $kg^{-1}d^{-1}$. Por lo tanto, la fluorescencia de la materia orgánica disuelta puede ser usada como un trazador de producción y/o consumo de materia orgánica lábil. Las distribuciones de esta fluorescencia indican que los aminoácidos disueltos pueden ser producidos tanto en la superficie, como se ha demostrado en los experimentos de incubación, como en el fondo. La fluorescencia pseudo-proteica es así acumulada **1)** en la capa fótica, debido a la exudación del fitoplancton o a la lisis celular; y **2)** en el lecho nefeloide, debido a una producción *in situ* por una intensa actividad microbiana y/o a la liberación desde las aguas intersticiales de los sedimentos pelágicos. La contribución de la fluorescencia de los aminoácidos disueltos al conjunto del carbono orgánico disuelto en la capa superficial de la ría presenta un patrón estacional, aumentando significativamente desde un mínimo invernal a un máximo otoñal.

5. Producción de sustancias húmicas como subproducto de los procesos de oxidación microbiana

Se han observado cambios significativos en el contenido de oxígeno disuelto y en la fluorescencia de las sustancias húmicas al cabo de incubaciones de 24 h en oscuridad en el sistema de afloramiento costero de la Ría de Vigo. En un día el sistema mostró una producción neta de sustancias húmicas (0.0-0.4 ppb QS d^{-1}), la cual correlaciona con las tasas de respiración, con una relación de 0.027

± 0.003 ppb QS (µmol kg^{-1} $O_2)^{-1}$, sugiriendo la síntesis diaria de sustancias húmicas como subproducto de la respiración bacteriana de la materia orgánica disuelta. Así, la fluorescencia de estos compuestos constituye un indicador adecuado de los procesos de mineralización de nutrientes. Las correlaciones de las anomalías de fluorescencia de sustancias húmicas y oxígeno de los tres ambientes muestreados durante este estudio mostraron pendientes similares a las de los experimentos de incubación: -0.024 ± 0.003, -0.025 ± 0.002 y -0.019 ± 0.007 ppb QS (µmol kg^{-1} $O_2)^{-1}$ para Ría de Vigo, la plataforma costera y el borde de plataforma, respectivamente. Alrededor de un 10% del carbono orgánico disuelto mineralizado es convertido en sustancias húmicas como subproducto de los procesos de oxidación microbiana. En consecuencia, la fluorescencia de las sustancias húmicas puede utilizarse como trazador de procesos de descomposición microbiana. Las distribuciones de esta fluorescencia sugieren que los compuestos húmicos son producidos en la columna de agua por mineralización *in situ*, especialmente en los sedimentos y en el lecho nefeloide, donde las sustancias húmicas contribuyen en más de un 90% del carbono orgánico disuelto acumulado. La distribución de la contribución de la fluorescencia húmica al carbono orgánico disuelto en las capas profundas de la ría presenta un incremento significativo desde el invierno al otoño.

6. Patrón estacional de la fotodegradación de las sustancias húmicas

El consumo neto de sustancias húmicas en las incubaciones de luz menos las de oscuridad correlaciona inversamente con la producción neta de sustancias húmicas en oscuridad, sugiriendo una rápida fotodegradación de las sustancias húmicas formadas recientemente como subproductos de la respiración microbiana. Las incubaciones demuestran que las tasas de fotodegradación y los niveles de fluorescencia residual presentan un patrón estacional caracterizado por un marcado máximo otoñal, tanto en muestras de río (65%

de material fotodegradado por día) como en muestras de la ría (90 y 55% de material fotodegradado por día en aguas de fondo y de superficie, respectivamente). Es significativo el hecho de que las aguas del fondo de la ría, enriquecidas en sustancias húmicas marinas, se fotodegradan más rápidamente que las aguas de superficie de la ría y el río. Las distribuciones de fluorescencia húmica sugieren que los ácidos húmicos son fotodegradados en la superficie por la luz solar. El afloramiento de las aguas más profundas de la ría provoca que el material producido durante la respiración bacteriana en el fondo sea rápidamente fotodegradado en la superficie mediante procesos fotoquímicos. A pesar de estos procesos, en el medio de la ría se observa la acumulación del material húmico producido en el interior de la ría (en la bahía de San Simón, donde ocurren intensos procesos de mineralización que conllevan procesos de humificación más intensos que los de fotodegradación). Por el contrario, los procesos fotoquímicos son los dominantes en el transito desde la superficie de la ría hasta la plataforma, donde se observa un consumo neto de sustancias húmicas.

Chapter 8:

Literature cited

Abell J, Emerson S, Renaud P (2000) Distributions of TOP, TON and TOC in the North Pacific subtropical gyre: implications for nutrient supply in the surface ocean and remineralisation in the upper thermocline. J Mar Res 58:203-222

Aluwihare LI, Repeta DJ, Chen RF (1997) A major biopolymeric component to dissolve organic carbon in sea water. Nature 387:166-169

Aluwihare LI, Repeta DJ, Pantoja S, Johnson CG (2005) Two chemically distinct pools of organic nitrogen accumulate in the ocean. Science 308:1007-1010

Álvarez-Salgado XA (1993) Transporte e balance bioxeoquímico do nitróxeno na Ría de Arousa. PhD Thesis. University of Santiago de Compostela, 194 pp

Álvarez-Salgado XA, Rosón G, Pérez FF, Pazos Y (1993) Hydrographic variability off the Rías Baixas (NW Spain) during the upwelling season. J Geophys Res 98:14447-14455

Álvarez-Salgado XA, Rosón G, Pérez FF, Figueiras FG, Pazos Y (1996a) Nitrogen cycling in an estuarine upwelling system, the Ríade Arousa (NW Spain). I. Short-time-scale patterns of hydrodynamic and biogeochemical circulation. Mar Ecol Progr Ser 135:259-273

Álvarez-Salgado XA, Rosón G, Pérez FF, Figueiras FG, Ríos AF (1996b) Nitrogen cycling in an estuarine upwelling system, the Ríade Arousa (NW Spain). II. Spatial differences in the short-time-scale evolution of fluxes and net budgets. Mar Ecol Progr Ser 135:275-288

Álvarez-Salgado XA, Castro CG, Pérez FF, Fraga F (1997) Nutrient mineralization patterns in shelf waters of the Western Iberian upwelling. Cont Shelf Res 17:1247-1270

Álvarez-Salgado XA, Miller AEJ (1998). Simultaneous determination of dissolved organic carbon and total dissolved nitrogen in seawater by high temperature catalytic oxidation: conditions for precise shipboard measurements. Mar Chem 62: 325-333

Álvarez-Salgado XA, Doval MD, Pérez FF (1999) Dissolved organic matter in shelf waters off the Ría de Vigo (NW Iberian upwelling system). J Mar Sys 18:383-394

Álvarez-Salgado XA, Gago J, Míguez BM, Gilcoto M, Pérez FF (2000) Surface waters of the NW Iberian margin: upwelling on the shelf versus outwelling of upwelled waters from the Rías Baixas. Est Coast Shelf Sci 51:821-837

Álvarez-Salgado XA, Gago J, Míguez BM, Pérez FF (2001a) Net ecosystem production of dissolved organic carbon in a coastal upwelling system: the Ría de Vigo, Iberian margin of the North Atlantic. Limnol Oceanogr 46:135-147

Álvarez-Salgado XA, Doval MD, Borges AV, Joint I, Frankignoulle M, Woodward EMS, Figueiras FG (2001b) Off-shelf fluxes of labile materials by an upwelling filament in the NW Iberian Upwelling System. Prog Oceanogr 51:321-337

Álvarez-Salgado XA, Figueiras FG, Pérez FF, Groom S, Nogueira E, Borges AV, Chou L, Castro CG, Moncoiffé G, Ríos AF, Miller AEJ, Frankignoulle M, Savidge G, Wollast R (2003) The Portugal coastal counter current off NW Spain: new insights on its biogeochemical variability. Prog Oceanogr 56:281-321

Álvarez-Salgado XA, Nieto-Cid M, Gago J, Brea S, Castro CG, Doval MD, Pérez FF. Stoichiometry of the mineralization of dissolved and particulate biogenic organic matter in the NW Iberian upwelling. J Geophys Res, *accepted*. Chapter 5 in this thesis

Amon RMW, Benner R (1996) Bacterial utilization of different size classes of dissolved organic matter. Limnol Oceanogr 41:41-51

Anderson LA (1995) On the hydrogen and oxygen content of marine phytoplankton. Deep-Sea Res Part I 42:1675-1680

Anderson LA, Sarmiento JL (1994) Redfield ratios of remineralization determined by nutrient data analysis. Global Biogeochem Cycles 8:65-80

Antia AN (2005) Particle-associated disolved elemental fluyes: revising the stoichiometry of mixed layer export. Biogeosciences Discussions 2:275-302

Archer D, Emerson S, Reimers CE (1989) Dissolution of calcite in deep-sea sediments: pH and O_2 microelectrode results. Geochim Cosmochim Acta 53:2831-2845

Arístegui J, Duarte CM, Agustí S, Doval M, Álvarez-Salgado XA, Hansell DA (2002) Disolved organic carbon support of respiration in the dark ocean. Science 298:1967

Arístegui J, Agustí S, Duarte CM (2003) Respiration in the dark ocean. Geophys Res Lett 30:1041, doi 10.1029/2002GL016227

Arístegui J, Álvarez-Salgado XA, Barton ED, Figueiras FG, Hernández-León S, Roy C, Santos AMP (2005) Oceanography and Fisheries of the Canary Current/Iberian Region of the Eastern North Atlantic. In: Brink KH, Robinson AR (eds) The Sea, volume 14. John Wiley & Sons, New York, p 877-931

Armstrong FAJ, Williams PM, Strickland JDH (1966) Photo-oxidation of organic matter in sea water by ultraviolet radiation, analytical and other applications. Nature 211:481-483

Azam F, Fenchel T, Field JG, Gray JS, Meyer-Reil LA, Thingstad TF (1983) The ecological role of water-column microbes in the sea. Mar Ecol Progr Ser 10:257-263

Azam F, Cho BC (1987) Bacterial utilization of organic matter in the sea. In: Symposium of the Society for General Microbiology. 4.1. Ecology of Microbial Communities. University Press, Cambridge

Azam F, Long RA (2001) Sea snow microcosms. Nature 414:495-498

Barber RT, Smith RL (1981) Coastal upwelling ecosystems. In: Longhurst AR (ed) Analysis of marine systems. Academic Press, San Diego, p 31-68

Benner R (2000) Missing pieces of the ocean carbon cycle puzzle. OCTEC Workshop Report (March 7-10, 2000) www. msrc.sunysb.edu/octet

Benner R (2002) Chemical composition and reactivity. In: Hansell DA, Carlson CA (eds) Biogeochemistry of Marine Dissolved Organic Matter. Academic Press, San Diego, p 59-90

Benner R, Pakulski JD, McCarthy M, Hedges JI, Hatcher PG (1992) Bulk chemical characteristics of dissolved organic matter in the ocean. Science 255:1561-1564

Benner R, Biddanda B (1998) Photochemical transformations of surface and deep marine dissolved organic matter: effects on bacterial growth. Limnol Oceanogr 43: 1373-1378

Berger WH, Herguera JC (1992) Reading the sedimentary record of the ocean's productivity. In: Falkowski PG Woodhead AD (eds) Primary Productivity and Biogeochemical Cycles in the Sea. Plenum Press, New York

Bhosle NB, Bhaskar PV, Ramachandran S (1998) Abundance of dissolved polysaccharides in the oxygen minimum layer of the Northern Indian Ocean. Mar Chem 63:171-182

Bode A, Varela M, Canle M, González N (2001) Dissolved and particulate organic nitrogen in shelf waters of northern Spain during spring. Mar Ecol Progr Ser 214:43-54

Bode A, Barquero S, Gonzalez N, Álvarez-Osorio T, Varela M (2004a) Contribution of heterotrophic plankton to nitrogen regeneration in the upwelling ecosystem of A Coruña (NW Spain). J Plank Res 26:11-28

Bode A, Varela MM, Teira E, Fernández E, González N, Varela M (2004b) Planktonic carbon and nitrogen cycling off northwest Spain: variations in production of particulate and dissolved organic pools. Aquat Microb Ecol 37:95-107

Børsheim KY, Myklestad SM, Sneli, JA (1999) Monthly profiles of DOC, mono- and polysaccharides at two locations in the Trondheimsfjord (Norway) during two years. Mar Chem 63:255-272

Brea S, Álvarez-Salgado XA, Álvarez M, Pérez FF, Mémery L, Mercier H, Messias MJ (2004) Nutrient mineralization rates and ratios in the Eastern South Atlantic. J Geophys Res 109:doi 10.1029/2003JC002051

Brewer PG, Glover DM, Goyet C, Shafer DK (1995) The pH of the North Atlantic Ocean: Improvements to the global model for sound absorption in seawater. J Geophys Res 100: 8761-8776

Broecker WS, Peng TH (1982) Tracers in the Sea. Lamont Doherty Earth Observatory, Palisades, New York, 690 pp

Bronk DA (2002) Dynamics of DON. In: Hansell DA, Carlson CA (eds) Biogeochemistry of Marine Dissolved Organic Matter. Academic Press, San Diego, p 153-247

Brophy JE, Carlson DJ (1989) Production of biologically refractory dissolved organic carbon by natural seawater microbial populations. Deep-Sea Res II 36: 497-508

Brzezinski MA (1985) The Si:C:N ratio of marine diatoms: interspecific variability and the effect of some environmental variables. J Phycol 21:347-357

Burdige DJ, Kline SW, Chen W (2004) Fluorescent dissolved organic matter in marine sediment pore waters. Mar Chem 89:289-311

Burney CM, Sieburth JM (1977) Dissolved carbohydrates in seawater: II. A spectrophotometric procedure for total carbohydrate analysis and polysaccharide estimation. Mar Chem 5:15-28

Cabaniss SE, Shuman MS (1987) Synchronous fluorescence spectra of natural waters: tracing sources of dissolved organic matter. Mar Chem 21:37-50

Callahan J, Dai M, Chen RF, Li X, Lu Z, Huang W (2004) Distribution of dissolved organic matter in the Pearl River Estuary, China. Mar Chem 89:211-224

Carlson CA (2002) Production and removal processes. In: Hansell DA, Carlson CA (eds) Biogeochemistry of Marine Dissolved Organic Matter. Academic Press, San Diego, p 91-151

Carlson CA, Ducklow HW, Michaels AF (1994) Annual flux of dissolved organic carbon from the euphotic zone in the northwestern Sargasso Sea. Nature 371:405-408

Castro CG (1997) Caracterización química del agua subsuperficial del Atlántico Nororiental y su modificación por procesos biogeoquimicos. Ph.D. Thesis, University of Santiago, Spain, 244 pp

Castro CG, Álvarez-Salgado XA, Figueiras FG, Pérez FF, Fraga F (1997) Transient hydrographic and chemical conditions affecting microplankton populations in the coastal transition zone of the Iberian upwelling system (NW Spain) in September 1986. J Mar Res 55:321-352

Castro CG, Pérez FF, Holley SE, Ríos AF (1998) Chemical characterisation and modelling of water masses in the Northeast Atlantic. Progr Oceanogr 41:249-279

Chavez FP, Toggweiler JR (1995) Physical estimates of global new production: the upwelling contribution. In: Summerhayes CP, Emeis KC, Angel MV,

Smith RL, Zeitzschel B (eds) Upwelling in the ocean. Modern processes and ancient records. Wiley and sons, New York, p 13-32

Chen RF, Bada JL (1992) The fluorescence of dissolved organic matter in seawater. Mar Chem 37:191-221

Chen RF, Fry B, Hopkinson CS, Repeta DJ, Peltzer ET (1996) Dissolved organic carbon on Georges Bank. Cont Shelf Res 19:409-420

Chen RF, Zhang Y, Vlahos P, Rudnick SM (2002) The fluorescence of dissolved organic matter in the Mid-Atlantic Bight. Deep-Sea Res II 49:4439-4459

Cherrier J, Bauer JE, Druffel ERM (1996) Utilization and turnover of labile dissolved organic matter by bacterial heterotrophs in eastern north Pacific surface waters. Mar Ecol Progr Ser 139:267-279

Clark LL, Ingall ED, Benner R (1998) Marine phosphorus is selectively remineralized. Nature 393:426

Clayton TD, Byrne RH (1993) Spectrophotometric seawater pH measurements: total hydrogen ion concentration scale concentration scale calibration of m-cresol purple and at-sea results. Deep-Sea Res I 40:2115-2129

Coble PG (1996) Characterization of marine and terrestrial DOM in seawater using excitation-emission matrix spectroscopy. Mar Chem 51:325-346

Coble PG, Green SA, Blough NV, Gagosian RB (1990) Characterization of dissolved organic matter in the Black Sea by fluorescence spectroscopy. Nature 348:432-435

Coble PG, Del Castillo CE, Avril B (1998) Distribution and optical properties of CDOM in the Arabian Sea during the 1995 Southwest Monsoon. Deep-Sea Res II 45:2195-2223

Cole JJ, Findlay S, Pace ML (1988) Bacterial production in fresh and saltwater ecosystems: A cross-system overview. Mar Ecol Prog Ser 43:1-10

Copin-Montégut C, Copin-Montégut G (1983) Stoichiometry of carbon, nitrogen, and phosphorus in marine particulate matter. Deep-Sea Res II 30:31-46

Copin-Montégut G, Avril B (1993) Vertical distribution and temporal variation of dissolved organic carbon in the north-western Mediterranean sea. Deep-Sea Res II 40:1963-1972

De Lange HJ, Morris DP, Williamson CE (2003) Solar ultraviolet photodegradation of DOC may stimulate freshwater food webs. J Plankton Res 25: 111-117

Del Giorgio PA, Duarte CM (2002) Respiration in the open ocean. Nature 420:379-384

Del Vecchio R, Blough NV (2002) Photobleaching of chromophoric dissolved organic matter in natural waters: kinetics and modelling. Mar Chem 78:231-253

Del Vecchio R, Blough NV (2004) Spatial and seasonal distribution of chromophoric dissolved organic matter and dissolved organic carbon in the Middle Atlantic Bight. Mar Chem 89:169-187

Determann S, Reuter R, Willkomm R (1996) Fluorescent matter in the eastern Atlantic Ocean. Part 2: vertical profiles and relation to water masses. Deep-Sea Res I 43:345-360

Determann S, Lobbes JM, Reuter R, Rullkötter J (1998) Ultraviolet fluorescence excitation and emission spectroscopy of marine algae and bacteria. Mar Chem 62:137-156

Doval MD, Álvarez-Salgado XA, Pérez FF (1997) Dissolved organic matter in a temperate embayment affected by coastal upwelling. Mar Ecol Prog Ser 157:21-37

Duce RA, Liss PS, Merrill JT, Atlas EL, Buat-Menard P, Hicks BB, Miller JM, Prospero JM, Arimoto R, Church TM, Ellis W, Galloway JN, Hansen L,

Jickells TD, Knap AH, Reinhardt KH, Schneider B, Soudine A, Tokos JJ, Tsunogai S, Wollast R, Zhou M (1991) The atmospheric input of trace species to the World Ocean. Global Biogeochem Cycles 5:193-259

Emerson S, Hayward TL (1995) Chemical tracers of biological processes in shallow waters of North Pacific: Preformed nitrate distributions. J Mar Res 53:499-513

Eppley RW, Peterson BJ (1979) Particulate organic matter flux and planktonic new production in the deep ocean. Nature 282:677-680

Falkowski P, Scholes RJ, Boyle E, Canadell J, Canfield D, Elser J, Gruber N, Hibbard K, Högberg P, Linder S, Mackenczie FT, Moore III B, Pedersen T, Rosenthal Y, Seitzinger S, Smetacek V, Steffen, W. (2000) The Global Carbon Cycle: A Test of Our Knowledge of Earth as a System. Science 290:291-296

Fiúza AFG (1984) Hidrologia e dinâmica das águas costeiras de Portugal. Ph.D. Thesis, University of Lisbon, Portugal, 294 pp

Fraga F (1967) Hidrografía de la Ría de Vigo 1962, con especial referencia a los compuestos de nitrógeno. Invest Pesq (Spain) 31:145-259

Fraga F (2001) Phytoplanktonic biomass synthesis: application to deviations from Redfield stoichiometry. Sci Mar 65:153-169

Fraga F, Vives F (1961) La descomposición de la material orgánica nitrogenada en el mar. Invest Pesq (Spain) 19:65-79

Fraga F, Ríos AF, Pérez FF, Figueiras FG (1998) Theoretical limits of oxygen:carbon and oxygen:nitrogen ratios during photosynthesis and mineralization of organic matter in the sea. Sci Mar 62:161-168

Fraga F, Álvarez-Salgado XA (2005) On the variation of alkalinity during the photosynthesis of phytoplankton. Ciencias Marinas, *submitted*

Fuhrman JA (1987) Close coupling between release and uptake of dissolved free amino acids in seawater studied by an isotope dilution approach. Mar Ecol Prog Ser 37: 45-52

Gago J, Gilcoto M, Pérez FF, Ríos AF (2003) Short-term variability of fCO_2 in seawater and air-sea CO_2 fluxes in a coastal upwelling system (Ría de Vigo, NW Spain). Mar Chem 80:247-264

Gagosian RB, Ahmed SI, Farrington JW, Lee RF, Mantoura RFC, Nelson KH, Packard TT, Reinhart Jr KL (1978) Future research problems in marine organic Chemistry. Mar Chem 6:375-382

Garber JH (1984) Laboratory study of nitrogen and phosphorus remineralization during the decomposition of coastal plankton and seston. Est Coast Shelf Sci 18:685-702

Gazeau F, Smith SV, Gentili B, Frankignoulle M, Gattuso JP (2004) The European coastal zone: characterization and first assesment of ecosystem metabolism. Est Coast Shelf Sci 60:673-694

Gilcoto M (2004) El campo termohalino como trazador de la dinámica de la Ría de Vigo y su acoplamiento meteorológico. PhD Thesis. University of Vigo, 211 pp

Gilcoto M, Álvarez-Salgado XA, Pérez FF (2001) Computing optimum estuarine residual fluxes with (OERFIM) a multiparameter inverse method: application to the Ría de Vigo (NW Spain). J Geophys Res 106:31303-31318

Gruber N, Keller K, Key RM (2000) What story is told by oceanic tracer concentrations?. Science 290:455-456

Gustavson K, Garde K, Wängberg SA, Selmer JS (2000) Influence of UV-B radiation on bacterial activity in coastal waters. J Plankton Res 22: 1501-1511

Hansell DA (2002) DOC in the Global Ocean Carbon Cycle. In: Hansell DA, Carlson CA (eds) Biogeochemistry of Marine Dissolved Organic Matter. Academic Press, San Diego, p 685-715

Hansell DA, Carlson CA (1998a) Net community production of dissolved organic carbon. Global Biogeochem Cycles 12:443-453

Hansell DA, Carlson CA (1998b) Deep-ocean gradients in the concentration of dissolved organic carbon. Nature 395:263-266

Hansell DA, Carlson CA (2001) Biogeochemistry of total organic carbon and nitrogen in the Sargasso Sea: control by convective overturn. Deep-Sea Res II 48:1649-1667

Hansell DA, Carlson CA (2002) Biogeochemistry of marine dissolved organic matter. Academic Press, San Diego, 2002

Hansell D, Ducklow H, Macdonald AM, Baringer MO (2004) Metabolic poise in the North Atlantic Ocean diagnosed from organic matter transports. Limnol Oceanogr 49:1084-1094

Hansen HP, Grasshoff K (1983). Automated chemical analysis. In: Grasshoff K, Ehrhadt M, Kremling K (eds) Methods of seawater analysis. Verlag Chemie, Wheinheim, p 347-395

Hayase K, Yamamoto M, Nakazawa I, Tsubota H, (1987) Behaviour of natural fluorescence in Sagami Bay and Tokyo Bay, Japan - Vertical and lateral distributions. Mar Chem 20:265-276

Hayase K, Tsubota H, Sunada I (1988) Vertical distribution of fluorescence organic matter in the North Pacific. Mar Chem 25:373-381

Hayase K, Shinozuka N (1995) Vertical distribution of fluorescent organic matter along with AOU and nutrients in the equatorial Central Pacific. Mar Chem 48:283-290

Haynes R, Barton ED (1990) A poleward flow along the Atlantic coast of the Iberian Peninsula. J Geophys Res 95:11425-11441

Hedges JI (1978) The formation and clay mineral reactions of melanoidins. Geochim. Cosmochim Acta 42: 69-76

Hedges JI (1992) Global biogeochemical cycles: progress and problems. Mar Chem 39:67-93

Hedges JI (2002) Why dissolved organics matter. In: Hansell DA, Carlson CA (eds) Biogeochemistry of Marine Dissolved Organic Matter. Academic Press, San Diego, p 1-33

Hedges JI, Baldock JA, Gélinas Y, Lee C, Peterson ML, Wakeham SG (2002) The biochemical and elemental compositions of marine plankton: a NMR perspective. Mar Chem 78:47-63

Heissenberger A, Herndl GJ (1994) Formation of high molecular weight material by free-living marine bacteria. Mar Ecol Prog Ser 111: 129-135

Honjo S, Manganini SJ, Cole JJ (1982) Sedimentation of biogenic matter in the deep ocean. Deep-Sea Res I 29:609-625

Honjo S, Manganini SJ (1993) Annual biogenic particle fluxes to the interior of the North Atlantic Ocean studied at 34ºN 21ºW. Deep-Sea Res 40:587-607

Hopkinson Jr CS, Fry B, Nolin AM (1997) Stoichiometry of dissolved organic matter dynamics on the continental shelf of the northeastern U.S.A. Cont Shelf Res 17:473-489

Hopkinson Jr CS, Vallino JJ, Nolin A (2002) Decomposition of dissolved organic matter from the continental margin. Deep-Sea Res II 49:4461-4478

Hopkinson Jr CS, Vallino JJ (2005) Efficient export of carbon to the deep ocean through dissolved organic matter. Nature 433:142-145

Hung CC, Tang D, Warnken KW, Santschi PH (2001) Distribution of carbohydrates, including uronic acids, in estuarine waters of Galveston Bay. Mar Chem 73:305-318

Hung CC, Guo L, Santschi PH, Alvarado-Quiroz N, Haye JM (2003a) Distributions of carbohydrate species in the Gulf of Mexico. Mar Chem 81:119-135

Hung JJ, Chen CH, Gong GC, Sheu DD, Shiah FK (2003b) Distributions, stoichiometric patterns and cross-shelf exports of dissolved organic matter in the East China Sea. Deep-Sea Res 50:1127-1145

Jackson GA, Williams PM (1985) Importance of dissolved organic nitrogen and phosphorus to biological nutrient cycling. Deep-Sea Res II 32:223-235

Jaffé R, Boyer JN, Lu X, Maie N, Yang C, Scully NM, Mock S (2004) Source characterization of dissolved organic matter in a subtropical mangrove-dominated estuary by fluorescence analysis. Mar Chem 84:195-210

Jahnke RA (1996) The global ocean flux of particulate organic carbon: areal distribution and magnitude. Global Biogeochem Cycles 10:71-88

Jenkins WJ, Goldman JC (1985) Seasonal oxygen cycling and primary production in the Sargasso Sea. J Mar Res 43:465-491

Karl DM, Laws EA, Morris P, Williams PJleB, Emerson S (2003) Metabolic balance of the open sea. Nature 426:32

Keil RG, Kirchman DL (1999) Utilization of dissolved protein and amino acids in the northern Sargasso Sea. Aquat Microb Ecol 18:293-300

Kieber DJ (2000) Photochemical production of biological substrates. In: de Mora SJ, Demers S, Vernet M (eds) The Effects of UV Radiation in the Marine Environment. Cambridge University Press, Cambridge, p 130-148

Kieber RJ, Hydro LH, Seaton PJ (1997) Photooxidation of triglycerides and fatty acids in seawater: Implication toward the formation of marine humic substances. Limnol Oceanogr 42:1454-1462

Kirchman DL (2000) Uptake and regeneration of inorganic nutrients by marin heterotrophic bacteria. In: Kirchman DL (ed) Microbial Ecology of the Oceans. Wiley, New York, p 261-288

Kirchman DL, Lancelot C, Fasham M, Legendre L, Radach G, Scott M (1993) Dissolved organic matter in biogeochemical models of the ocean. In: Evans GT, Fasham MJR (eds) Towards a Model of Ocean Biogeochemical processes. Springer-Verlag, Berlin, p. 209-225

Kirchman DL, Ducklow HW, McCarthy JJ, Garside C (1994) Biomass and nitrogen uptake by heterotrophic bacteria during the spring phytoplankton bloom in the North Atlantic Ocean. Deep-Sea Res 41:879-895

Klump JV, Martens CS (1983) Benthic nitrogen regeneration. In: Carpenter EJ, Capone FG (eds) Nitrogen in the Marine Environment. Academic Press, New York, p 411-457

Knauer GA (1993) Productivity and new production of the oceanic system. In: Wollast R, MacKenzie FT Chou I (eds) Interactions of C, N, P and S Biogeochemical Cycles and global change. Springer Verlag, p 211-231

Koike I, Tupas L (1993) Total dissolved nitrogen in the Northern North Pacific assessed by a high-temperature combustion method. Mar Chem 41:209-214

Kramer GD, Herndl G (2004) Photo- and bioreactivity of chromophoric dissolved organic matter produced by marine bacterioplankton. Aquat Microb Ecol 36: 239-246

Leboulanger C, Oriol L, Jupin H, Descolas-Gros C (1997) Diel variability of glycolate in the eastern tropical Atlantic ocean. Deep-Sea Res II 44:2131-2139

Legendre L, Le Févre J (1995) Microbial food webs and the export of biogenic carbon in oceans. Aquat Microb Ecol 9:69-77

Li YH, TH Peng (2002) Latitudinal change of remineralization ratios in the oceans and its implication for nutrient cycles. Global Biogeochem Cycles 16:doi 10.1029/2001GB001828

Lindell MJ, Graneli W, Tranvik LJ (1995) Enhanced bacterial growth in response to photochemical transformation of dissolved organic matter. Limnol Oceanogr 40: 195-199

Loh AN, Bauer JE (2000) Distribution, partitioning and fluxes of dissolved and particulate organic C, N and P in the eastern North Pacific and Southern Oceans. Deep-Sea Res II 47:2287-2316

López-Jamar E, Cal RM, González G, Hanson RB, Rey J, Santiago G, Tenore KR (1992) Upwelling and outwelling effects on the benthic regime of the continental shelf off Galicia, NW Spain. J Mar Res 50:465-488

Lucea A, Duarte CM, Agustí S, Sondergaard M (2003) Nutrient (N, P and Si) and carbon partitioning in the stratified NW Mediterranean. J Sea Res 49:157-170

Lueker TJ, Dickson AG, Keeling CD (2000) Ocean pCO_2 calculated from dissolved inorganic carbon, alkalinity and equations for K_1 and K_2: validations based on laboratory measurements of CO_2 in gas and seawater at equilibrium. Mar Chem 70:105-119

Maita Y, Yanada M (1990) Vertical distribution of total dissolved nitrogen and dissolved organic nitrogen in seawater. Geochem J 24:245-254

Marañón E, Cermeño P, Fernández E, Rodríguez J, Zabala L (2004) Significance and mechanisms of photosyntetic production of dissolved organic carbon in a coastal eutrophic ecosystem. Limnol Oceanogr 49:1652-1666

Martin JH, Knauer GA, Karl DM, Broenkow WW (1987) VERTEX: carbon cycling in the northeast Pacific. Deep-Sea Res II 34:267-285

Martin JH, Fitzwater SE, Gordon RM, Hunter CN, Tanner SJ (1993) Iron, primary production and carbon-nitrogen flux studies during the JGOFS North Atlantic Bloom Experiment. Deep-Sea Res II 40:641-653

Mayer LM, Schick LL, Loder III TC (1999) Dissolved protein fluorescence in two Maine estuaries. Mar Chem 64:171-179

McCarthy M, Pratum T, Hedges J, Benner R (1997) Chemical composite of dissolved organic nitrogen in the ocean. Nature 390:150-154

McCartney MS, Talley LD (1982) The subpolar mode water of the North Atlantic Ocean. J Phys Oceanogr 12:1169-1188

McCave IN, Hall IR (2002) Turbidity of waters over the Northwest Iberian continental margin. Prog Oceanogr 52:299-313

Middleburg JJ, Vlug T, Van der Nat FJW (1993) Organic matter mineralization in marine systems. Global Planet Change 8:47-58

Millard RC, Owens WB, Fofonoff NP (1990) On the calculation of the Brunt-Väisälä frequency. Deep-Sea Res II 37:167-181

Miller WL, Moran MA (1997) Interaction of photochemical and microbial processes in the degradation of refractory dissolved organic matter from a coastal marine environment. Limnol Oceanogr 42:1317-1324

Milliman JD, Troy PJ, Bach WM, Adams AK, Li YH, Mackenzie FT (1999) Biologically mediated dissolution of calcium carbonate above the chemical lysocline?. Deep-Sea Res I 46:1653-1669

Minster JF, Boulahdid M (1987) Redfield ratios along isopycnal surfaces– a complementary study. Deep-Sea Res 34:1981-2003

Moncoiffé G, Álvarez-Salgado XA, Figueiras FG, Savidge G (2000) Seasonal and short-time-scale dynamics of microplankton community production and respiration in an inshore upwelling system. Mar Ecol Prog Ser 196: 111-126

Mopper K, Zhou X (1990) Hydroxyl radical photoproduction in the sea and its potential impact on marine processes. Science 250: 661-664

Mopper K, Zhou X, Kieber RJ, Kieber DJ, Sikorski RJ, Jones RD (1991) Photochemical degradation of dissolved organic carbon and its impact on the oceanic carbon cycle. Nature 353: 60-62

Mopper K, Schultz CA (1993) Fluorescence as a possible tool for studying the nature and the water column distribution of DOC components. Mar Chem 41:229-238

Mopper K, Kieber DJ (2000) Marine photochemistry and its impact on carbon cycling. In: de Mora SJ, Demers S, Vernet M (eds) The effects of UV Radiation in the Marine Environment. Cambridge University Press, Cambridge, p 101-129

Moran MA, Zepp RG (1997) Role of photoreactions in the formation of biologically labile compounds from dissolved organic matter. Limnol Oceanogr 42: 1307-1316

Moran MA, Sheldon WM, Zepp RG (2000) Carbon loss and optical property changes during long-term photochemical and biological degradation of estuarine dissolved organic matter. Limnol Oceanogr 45:1254-1264

Mouriño C, Fraga F (1985) Determinación de nitratos en agua de mar. Invest Pesq (Spain) 49:81-96

Myklestad SM (1995) Release of extracellular products by phytoplankton with special emphasis on polysaccharides. Sci Total Environ 165: 155-164

Myklestad SM, Skanoy E, Hestmann S (1997) A sensitive and rapid method for analysis of dissolved mono- and polysaccharides in seawater. Mar Chem 56:279-286

Nagata T (2000) Production mechanisms of dissolved organic matter. In: Kirchman DL (ed) Microbial Ecology of the Oceans. Wiley, New York, p 121-152

Newton PP, Lampitt RS, Jickells TD, King P, Boutle C (1994) Temporal and spatial variability of biogenic particle fluxes during the JGOFS Northeast Atlantic process studies at 47ºN, 20ºW. Deep-sea Res 41:1617-1642

Niell FX (1977) Distribución y zonación de las algas bentónicas en la facies rocosa del sistema intermareal de las rías bajas gallegas. Invest Pesq 41, 219-237

Nieto-Cid M, Álvarez-Salgado XA, Brea S, Pérez FF (2004) Cycling of dissolved and particulate carbohydrates in a coastal upwelling system (NW Iberian Peninsula). Mar Ecol Prog Ser, 283:39-54. Chapter 2 in this thesis

Nieto-Cid M, Álvarez-Salgado XA, Gago J, Pérez FF DOM fluorescence, a tracer for biogeochemical processes in a coastal upwelling system (NW Iberian Peninsula). Mar Ecol Prog Ser, *in press*. Chapter 3 in this thesis

Nieto-Cid M, Álvarez-Salgado XA, Pérez FF. Microbial and photochemical reactivity of fluorescent dissolved organic matter in a coastal upwelling system. Limnol Oceanogr, *submitted*. Chapter 4 in this thesis

Nogueira E, Pérez FF, Ríos AF (1997) Seasonal patterns and long-term trends in an estuarine upwelling ecosystem (Ría de Vigo, NW Spain). Est Coast Shelf Sci 44: 285-300

Norrman B, Zweifel UL, Hopkinson CS Jr, Fry B (1995) Production and utilization of dissolved organic carbon during an experimental diatom bloom. Limnol Oceanogr 40:898-907

Obernosterer I, Herndl GJ (1995) Phytoplankton extracellular release and bacterial growth: dependence on the inorganic N:P ratio. Mar Ecol Prog Ser 116: 247-257

Obernosterer I, Reitner B, Herndl GJ (1999) Contrasting effects of solar radiation on dissolved organic matter and its bioavailability to marine bacterioplankton. Limnol Oceanogr 44: 1645-1654

Obernosterer I, Herndl GJ (2000) Differences in the optical and biological reactivity of the humic and non humic dissolved organic carbon component in two contrasting coastal marine environments. Limnol Oceanogr 45:1120-1129

Obernosterer I, Benner R (2004) Competition between biological and photochemical processes in the mineralization of dissolved organic carbon. Limnol Oceanogr 49: 117-124

Ogawa H, Amagai Y, Koike I, Kaiser K, Benner R (2001) Production of refractory dissolved organic matter by bacteria. Science 292: 917-920

Ogawa H, Tanoue E (2003) Dissolved organic matter in oceanic waters. J Oceanogr 59:129-147

Olli K, Wexels Riser C, Wassmann P, Ratlova T, Arashkevich E, Pasternak A (2001) Vertical flux of biogenic matter during a Lagrangian study off the NW Spanish continental margin. Prog Oceanogr 51:443-466

Opsahl S, Benner R (1998) Photochemical reactivity of dissolved lignin in river and ocean waters. Limnol Oceanogr 43: 1297-1304

Pahlow M, Riebesell U (2000) Temporal trends in deep ocean Redfield ratios. Science 287:831-833

Pakulski JD, Benner R (1994) Abundance and distribution of carbohydrates in the ocean. Limnol Oceanogr, 39:930-940

Pérez FF, Fraga F (1987) A precise and rapid analytical procedure for alkalinity determination. Mar Chem 21:169-182

Pérez FF, Mouriño C, Fraga F, Ríos AF (1993) Displacement of water masses and remineralization rates off the Iberian Peninsula by nutrient anomalies. J Mar Res 51:869-892

Pérez FF, Pollard RT, Read JF, Valencia V, Cabanas JM, Ríos AF (2000) Climatological coupling of the thermohaline decadal changes in Central Water of the Eastern North Atlantic. Sci Mar 64:347-353

Pérez FF, Castro CG, Álvarez-Salgado XA, Ríos AF (2001) Coupling between the Iberian basin-scale circulation and the Portugal boundary current system: a chemical study. Deep-Sea Res I 48:1519-1533

Pérez FF, Álvarez M, Ríos AF (2002) Improvements on the back-calculation technique for estimating anthropogenic CO_2. Deep-Sea Res I 49:859-875

Pérez FF, Castro CG, Ríos AF, Fraga F (2005) Chemical properties of the deep winter mixed layer in the Northeast Atlantic (40-47ºN). J Mar Sys 54:115-125

Pettine M, Patrolecco L, Manganelli M, Capri S, Farrace MG (1999). Seasonal variations of dissolved organic matter in the northern Adriatic Sea. Mar Chem 64:153-169

Piedracoba S, Álvarez-Salgado XA, Rosón G, Herrera JL (2005) Short-timescale termohaline variability and residual circulation in the central segment of the coastal upwelling system of the Ría de Vigo (northwest Spain) during four contrasting periods. J Geophys Res 110:doi 10.1029/2004JC002556

Prego R, Bao R, Howland R (1995) The biogeochemical cycling of dissolved silicate in a Galician Ria. Ophelia 42:301-318

Prego R, Bao R, Vidal JR (1997) Upwelling influence on the Galician coast: silicate in shelf water and underlying surface sediments. Cont Shelf Res 17:307-318

Pullin MJ, Cabaniss SE (1997). Physicochemical variations in DOM-synchronous fluorescence: implications for mixing studies. Limnol Oceanogr 42: 1766-1773

Quiñones RA, Platt T (1991) The relationship between the f-ratio and the P:R ratio in the pelagic ecosystem. Limnol Oceanogr 36: 211-213

Redfield AC, Ketchum BK, Richards FA (1963) The influence of organisms on the composition of sea-water. In: Hill MN (ed) The Sea. Wiley, New York, p 26-77

Rich JH, Ducklow HW, Kirchman DL (1996) Concentrations and uptake of neutral monosaccharides along 140ºW in the equatorial Pacific: contribution of glucose to heterotrophic bacterial activity and the DOM flux. Limnol Oceanogr 41:595-604

Richards FA, Anoxic basins and fjord. In: Riley JP, Skirrow G (eds) Chemical Oceanography, Vol. 1., Academic Press, New York, p. 611-645

Ríos AF, Fraga F, Pérez FF (1989) Estimation of coefficients for the calculation of "NO", "PO" and "CO", starting from the elemental composition of natural phytoplankton. Sci Mar 53:779-784

Ríos AF, Anderson TR, Pérez FF (1991) The carbonic system distribution and fluxes in the NE Atlantic during Spring 1991. Prog Oceanogr 35:295-314

Ríos AF, Nombela MA, Pérez FF, Rosón G, Fraga F (1992) Calculation of runoff to an estuary. Ría de Vigo. Sci Mar 56:29-33

Ríos AF, Anderson TR, Pérez FF (1995) The carbonic system distribution and fluxes in the NE Atlantic during Spring 1991. Progr Oceanogr 55:295-314

Ríos AF, Fraga F, Pérez FF, Figueiras FG (1998) Chemical composition of phytoplankton and Particulate Organic Matter in the Ría de Vigo. Sci Mar 62:257-271

Rosón G, Álvarez-Salgado XA, Pérez FF (1997) A non stationary box model to determine residual fluxes in a partially mixed estuary, based on both thermohaline properties. Application to the Ría de Arousa (NW Spain). Est Coast Shelf Sci 44:249-262

Rosón G, Álvarez-Salgado XA, Pérez FF (1999) Carbon cycling in a large coastal embayment, affected by wind-driven upwelling: short-time-scale variability and spatial differences. Mar Ecol Prog Ser 176: 215-230

Sambrotto RN, Savidge G, Robinson C, Boyd P, Takahashi T, Karl DM, Langdon C, Chipman D, Marra J, Codispoti L (1993) Elevated consumption of carbon relative to nitrogen in the surface ocean. Nature 363:248-250

Sanders R, Jickells T (2000) Total organic nutrients in Drake Passage. Deep-Sea Res II 47:997-1014

Sarmiento JL, Thiele G, Key RM, Moore WS (1990) Oxygen and Nitrate New Production and remineralization in the North Atlantic Subtropical gyre. J Geophys Res 95:18303-18315

Schimel D, Alves D, Enting I, Heimann M, Joos F, Raynaud D, Wigley T, Prather M, Derwent R, Ehhalt D, Fraser P, Sanhueza E, Zhou X, Jonas P, Charlson R, Rodhe H, Sadasivan S, Shine KP, Fouquart Y, Ramaswamy V, Solomon S, Srinivasan J, Albritton D, Isaksen I, Lal M, Wuebbles D (1996) Radiative forcing of climate change. In: Houghton JT, Meira Filho LG, Callander BA, Harris A, Kattenberg A, Maskell K (eds) Climate change 1995: The science of climate change. University Press, Cambridge, p 65-132

Schneider B, Schlitzer R, Fischer G, Nöthing EM (2003) Depth-dependent elemental compositions of particulate organic matter (POM) in the Ocean. Global Biogeochem Cycles 17:doi 10.1029/2002GB001871

Senior W, Chevolot L (1991) Studies of dissolved carbohydrates (or carbohydrate-like substances) in an estuarine environment. Mar Chem 32:19-35

Shaffer G, Bendtsen J, Ulloa O (1999) Fractionation during remineralization of organic matter in the ocean. Deep-Sea Res 46:185-204

Sharp JH, Carlson CA, Peltzer ET, Castle-Ward DM, Savidge KB, Rinker KR (2002) Final dissolved organic carbon broad community intercalibration and preliminary use of DOC reference materials. Mar Chem 77:239-253

Sharp JH, Beauregard AY, Burdige D, Cauwet G, Curless SE, Lauck R, Nagel K, Ogawa H, Parker AE, Primm O, Pujo-Pay M, Savidge WB, Seitzinger S, Spyres G, Styles R (2004) A direct instrument comparison for measurement of total dissolved nitrogen in seawater. Mar Chem 84:181-193

Sherwood CR, Butman B, Cacchione DA, Drake DE, Gross TF, Sternberg RW, Wiberg PL, Williams AJ (1994) Sediment-transport events on the northern California continental shelf during the 1990-1991 STRESS experiment. Cont Shelf Res 14:1063-1099

Siegenthaler U, Sarmiento JL (1993) Atmospheric carbon dioxide and the ocean. Nature, 365:119-125

Skoog A (1995) Organic carbon and humic substances in the marine environment. PhD Thesis. University of Göteborg and Chalmers University of Technology, 55 pp

Skoog A, Wedborg M, Fogelqvist E (1996) Photobleaching of fluorescence and the organic carbon concentration in a coastal environment. Mar Chem 55:333-345

Skoog A, Biddanda B, Benner R (1999) Bacterial utilization of dissolved glucose in the upper water column of the Gulf of Mexico. Limnol Oceanogr 44: 1625-1633

Smith SV, Hollibaugh JT (1993) Coastal metabolism and the oceanic organic carbon balance. Rev Geophys 31:75-89

Sokal FF, Rohlf FJ (1995) Biometry: the principles and practice of statistics in biological research. Freeman and Co, New York, 887 pp

Souto C, Gilcoto M, Fariña-Busto L, Pérez FF (2003) Modelling the residual circulation of a coastal embayment affected by wind-driven upwelling: Circulation of the Ría de Vigo (NW Spain). J Geophys Res 108:3340-3357

Storm SL, Benner R, Ziegler S, Dagg MJ (1997) Planktonic grazers are potentially important source of marine dissolved organic carbon. Limnol Oceanogr 42: 1364-1374

Strickland JDH, Parsons TR (1972) A practical handbook of seawater analysis. 2nd ed Bull Fish Res Bd Can 167

Suess E, Müller PJ (1980) Productivity, sedimentation rate and sedimentary organic matter in the oceans. II. Elemental fractionation. In: Proceedings of the C.N.R.S. Symposium on the Benthic Boundary Layer. Marseille, France, p 17-26

Sugimura Y, Suzuki Y (1988) A high-temperature catalytic oxidation method for the determination of non-volatile dissolved organic carbon in seawater by direct injection of a liquid sample. Mar Chem 24:105-132

Sunda WG (1995) The influence of nonliving organic matter on the availability and cycling of plant nutrients in seawater. In: Zepp RG, Sonntag C (eds) Role of nonliving organic matter in the Earth's carbon cycle. John Wiley and Sons Ltd., New York, p 191-207

Suzuki Y (1993) On the measurement of DOC and DON in seawater. Mar Chem 41:287-288

Suzuki Y, Sugimura Y, Itoh T (1985) A catalytic oxidation method for the determination of total nitrogen dissolved in sea water. Mar Chem 16:83-97

Takahashi T, Broecker WS, Brainbridge AE (1981) The alkalinity and total carbon dioxide concentration in the world ocean. In: Bolin B (ed)

Carbon Cycle Modelling, SCOPE col. 16. John Wiley, New York, p 271-286

Takahashi T, Broecker WS, Langer S (1985) Redfield ratio based on chemical data from isopycnal surfaces. J Geophys Res 90:6907-6924

Teira E, Serret P, Fernández E (2001a) Phytoplankton size-structure, particulate and dissolved organic carbon production and oxygen fluxes through microbial communities in the NW Iberian coastal transition zone. Mar Ecol Progr Ser 219:65-83

Teira E, Pazó MJ, Serret P, Fernández E (2001b) Dissolved organic carbon production by microbial populations in the Atlantic Ocean. Limnol Oceanogr 46:1370-1377

Teira E, Abalde J, Álvarez-Ossorio MT, Bode A, Cariño C, Cid A, Fernández E, González N, Lorenzo J, Valencia J, Varela M (2003) Plankton carbon budget in a coastal wind-driven upwelling station off A Coruña (NW Iberian Peninsula). Mar Ecol Progr Ser 265:31-43

Tenore KR, Boyer LF, Cal RM, García-Fernández C, González N, González-Gurriaran E, Hanson RB, Iglesias J, From M, López-Jamar E, McClain J, Pamatmat MM, Pérez A, Rhoads DC, Santiago GD, Tietjen J, Westrich J, Windom HL (1982) Coastal upwelling in the Rías Bajas, NW Spain: contrasting the benthic regimes in the Rías of Arosa and Muros. J Mar Res 40:701-772

Thomas CJ, Blair NE, Alperin MJ, DeMaster DJ, Jahnke RA, Martens CS, Mayer L (2002) Organic carbon deposition on the North Carolina continental shelf slope off Cape Hatteras (USA). Deep-Sea Research II 49:4687-4709

Thurman EM (1985) Organic geochemistry of natural waters. Chapter 10: Aquatic humic substances. Martinus Nijhoff/Dr W. Junk Publishers, Dordrecht, p 273-361

Tranvik LJ (1993) Microbial transformation of labile dissolved organic matter into humic-like matter in seawater. FEMS Microbiol Ecol 12: 177-183

Tranvik LJ, Bertilsson S (2001) Contrasting effects of solar UV radiation on dissolved organic sources for bacterial growth. Ecol Lett 4: 458-463

Tréguer P, Nelson DM, van Bennekom AJ, DeMaster DJ, Laynaert A, Quéguiner B (1995) The silicate balance in the world ocean: a reestimate. Science 268:375-379

UNESCO (1985) The international system of units (SI) in oceanography. UNESCO Tech Pap Mar Sci 45

UNESCO (1986) Progress on oceanographic tables and standards 1983-1986. Work and recommendations of UNESCO/SCOR/ICES/IAPSO Joint panel. UNESCO Tech Pap Mar Sci 50

Vähätalo AV, Wetzel RG (2004) Photochemical and microbial decomposition of chromophoric dissolved organic matter during long (months-years) exposures. Mar Chem 89:313-326

Varela M, Prego R, Pazos Y (2004) Vertical biogenic particle flux in a western Galician ria (NW Iberian Peninsula). Mar Ecol Prog Ser 269:17-24

Varela MM, Barquero S, Bode A, Fernández E, González N, Teira E, Varela M (2003) Microplanktonic regeneration of ammonium and dissolved organic nitrogen in the upwelling area of the NW of Spain: relationships with dissolved organic carbon production and phytoplankton size-structure. J Plank Res 25:719-736

Vilas F, Bernabeu AM, Méndez G (2005) Sediment distribution pattern in the Rias Baixas (NW Spain): main facies and hydrodynamic dependence. J Mar Sys 54:261-276

Walsh JJ (1991) Importance of continental margins in the marine biochemical cycling of carbon and nitrogen. Nature 359:53-55

Wedborg M, Hoppema M, Skoog A (1998) On the relation between organic and inorganic carbon in the Weddell Sea. J Mar Sys 17: 59-76

Williams PJleB, Grey RW (1970) Heterotrophic utilization of dissolved organic compounds in the sea. 2. Observations on the response of heterotrophic marine populations to abrupt increases in amino acid concentration. J Mar Biol Assoc UK 50:871-881

Williams PJleB (1995) Evidence for the seasonal accumulation of carbon-rich dissolved organic material, its scale in comparison with changes in particular material and the consequential effect on net C/N assimilation ratios. Mar Chem 51:17-29

Williams PM, Carlucci A, Olson R (1980) A deep profile of some biologically important properties in the central North Pacific gyre. Oceanol Acta 3:471-476

Williams PM, Druffel ERM (1987) Radiocarbon in dissolved organic matter in the central North Pacific Ocean. Nature 330: 246-248

Witter AE, Luther III GW (2002) Spectrophotometric measurement of seawater carbohydrate concentrations in neritic and oceanic waters from the U. S. Middle Atlantic Bight and the Delaware estuary. Mar Chem 77:143-156

Wollast R (1993) Interactions of carbon and nitrogen cycles in the coastal zone. In: Wollast R, Mackenzie FT, Chou L (eds) Interaction of C,N,P and S biochemical cycles and global change. Springer-Verlag, Heidelberg, p. 195-210

Wollast R (1998) Evaluation and comparison of the global carbon cycle in the coastal zone and in the open ocean. In: Brink KH, Robinson AR (eds) The Sea, Vol. 10. John Wiley and sons, New York, p 213-252

Wong CS, Hirai S (1997) Ocean storage of Carbon Dioxide: A review of Ocean Carbonate and CO2 Hydrate Chemistry. IEA Greenhouse Gas R&D Programme, Cheltenham, U.K.

Wooster WS, Bakun A, McClain DR (1976) The seasonal upwelling cycle along the eastern boundary of the North Atlantic. J Mar Res 34:131-141

Yamanaka Y, Tajika E (1997) Role of dissolved organic matter in the marine biogeochemical cycle: studies using an ocean biogeochemical general circulation model. Global Biogeochem Cycles 11:599-612

Yamashita Y, Tanoue E (2003) Chemical characterization of protein-like fluorophores in DOM in relation to aromatic amino acids. Mar Chem 82:255-271

Yamashita Y, Tanoue E (2004) In situ production of chromophoric dissolved organic matter in coastal environments. Geophys Res Lett 31:doi 10.1029/2004GL019734

Yentsch CS, Menzel DW (1963) A method for the determination of phytoplankton chlorophyll and phaeophytin by fluorescence. Deep-Sea Res Oceanogr Abstr 10:221-231

Zimmerman RC, Kremer JN, Dugdale RC (1987) Acceleration of nutrient uptake by phytoplankton in a coastal upwelling ecosystem: a modelling analysis. Limnol Oceanogr 40:299-305